This electronic thesis or dissertation has been downloaded from the King's Research Portal at https://kclpure.kcl.ac.uk/portal/



Investigating histone deacetylase four in sensory neurons

Crow, Megan

Awarding institution:
King's College London

The copyright of this thesis rests with the author and no quotation from it or information derived from it may be published without proper acknowledgement.

END USER LICENCE AGREEMENT



Unless another licence is stated on the immediately following page this work is licensed

under a Creative Commons Attribution-NonCommercial-NoDerivatives 4.0 International

licence. https://creativecommons.org/licenses/by-nc-nd/4.0/

You are free to copy, distribute and transmit the work

Under the following conditions:

- Attribution: You must attribute the work in the manner specified by the author (but not in any way that suggests that they endorse you or your use of the work).
- Non Commercial: You may not use this work for commercial purposes.
- No Derivative Works - You may not alter, transform, or build upon this work.

Any of these conditions can be waived if you receive permission from the author. Your fair dealings and other rights are in no way affected by the above.

Take down policy

If you believe that this document breaches copyright please contact librarypure@kcl.ac.uk providing details, and we will remove access to the work immediately and investigate your claim.

Download date: 08. Oct. 2023

INVESTIGATING HISTONE DEACETYLASE FOUR IN SENSORY NEURONS

Megan Crow

Presented for the degree of Doctor of Philosophy at King's College London

2014

Abstract

Histone deacetylase inhibitors are analgesic in preclinical pain models but the contribution of specific histone deacetylases (HDACs) to pain states remains unclear. HDAC4 is a transcriptional co-repressor that has previously been linked to aberrant nociception and synaptic plasticity. The aim of this project was to investigate the role of HDAC4 *in vivo* using the Cre-loxP system to conditionally delete HDAC4 from primary sensory neurons and characterize transcriptional and behavioural outcomes in models of pain and peripheral nerve regeneration.

To do this I established two novel HDAC4 conditional knockout strains that enabled investigation of HDAC4 in both sensory neuron development and in adult sensory processing. In both strains, loss of HDAC4 was associated with altered expression of the gene encoding the transient receptor potential cation channel member A1 (*Trpa1*) and the voltage-gated calcium channel subunit α2δ-1 (*Cacna2d1*) in naïve ganglia. Bioinformatics analysis indicated that HDAC4 may bind *Cacna2d1* directly. Furthermore, across many injury paradigms I found that HDAC4 conditional knockouts expressed lower levels of calcitonin-related polypeptide alpha (*Calca*) and the gene encoding the high-affinity nerve growth factor receptor (*Ntrk1*). While peripheral expression of HDAC4 was not required for sensory neuron differentiation, peripheral nerve regeneration or for the development of mechanical hypersensitivity in neuropathic pain models, I found highly reproducible and significant attenuation of thermal hypersensitivity in models of chronic inflammation. This was associated with significantly reduced mRNA expression of the transient receptor potential cation channel member V1 (*Trpv1*) and reduced capsaicin sensitivity *in vitro*, possibly as a result of aberrant nerve growth factor signaling.

HDAC inhibitors and other drugs that target chromatin modifying and transcriptional regulatory proteins are already being used clinically to treat cancer. Work to characterize the function of these molecules in diverse systems will provide a rational basis for the broader application of these therapies.

Table of Contents

Abstract **2**

Table of Contents **3**

Table of Figures **7**

Table of Tables **11**

Acknowledgements **16**

1 Introduction **17**

1.1 Development of the dorsal root ganglia **18**

1.1.1 Differentiation of sensory neurons 18

1.1.2 Neurotrophic factor receptors specify neuronal subtypes of the DRG 20

1.2 Sensory transduction **22**

1.2.1 Molecular transducers of external stimuli 23

1.2.2 Propagating the receptor potential 26

1.3 Response to injury **26**

1.3.1 Inflammation and peripheral sensitization 27

1.3.2 Signaling pathways and transcriptional regulation 27

1.3.3 Nerve injury 30

1.4 Epigenetics **32**

1.5 HDAC4 ..... **35**

1.5.1 Molecular mechanisms of HDAC4 37

1.5.2 HDAC4 in neurons 42

1.6 Summary and aims **44**

2 Methods **45**

2.1 Animals **45**

2.1.1 Genotyping 46

2.1.2 Tamoxifen Dosing 47

2.1.3 Inflammatory pain models 48

2.1.4 Neuropathic pain models 48

2.1.5 Sciatic crush model of peripheral nerve regeneration 48

2.2 Behaviour **49**

2.2.1 Rotarod 49

2.2.2 Von Frey Test 49

2.2.3 Hargreaves Test 49

2.2.4 Tail flick 50

2.2.5 Hot Plate 50

2.2.6 Randall-Selitto Test 50

2.2.7 Sciatic Functional Index 51

2.2.8 Pinprick Assay 51

2.3 Molecular Biology **51**

2.3.1 DRG dissections 51
2.3.2 RNA extraction 52
2.3.3 Real-time quantitative PCR (RT-qPCR) 52
2.3.4 TaqMan Low-Density RT-qPCR Array Cards 53
2.3.5 Microarray 54
2.3.6 Protein extraction 54
2.3.7 Western Blotting 54
2.4 Tissue culture 55

2.4.1 Dissociated dorsal root ganglion culture 55
2.5 Fluorescence microscopy 55

2.5.1 Sample Preparation 55
2.5.2 Immunocytochemistry 56
2.5.3 Microscopy and Image Analysis 56
2.5.4 Calcium Imaging 57
2.6 Statistical analysis and experimental design 57

3 Generation and characterization of HDAC4 mutant mice 59
3.1 Introduction 59

3.2 Aims 64

3.3 Methods 64

3.4 Results 65

3.4.1 Generation of HDAC4$^{Nav1.8}$ conditional knockouts 65
3.4.2 Functional effects of HDAC4 knockout in $Na_v1.8$-positive sensory neurons 71
3.4.3 Advillin CreERT2 conditional knockout 77
3.4.4 Functional effects of HDAC4 deletion in adult sensory neurons 79
3.4.5 Is there a consistent effect of HDAC4 deletion on sensory neuron transcription? Comparing transcription data from HDAC4$^{Nav1.8}$ and HDAC4^{Adv} cKOs 83
3.5 Discussion 86

3.5.1 $Na_v1.8$ Cre and Advillin CreERT2 successfully recombine floxed HDAC4 86
3.5.2 HDAC4 is not required for sensory neuron development 87
3.5.3 HDAC4 may be required for *Cacna2d1* and *Trpa1* expression in uninjured sensory neurons 88
3.5.4 HDAC4 regulates transcriptional responses after injury 89

4 HDAC4 and Regeneration 92
4.1 Introduction 92

4.2 Aims 94

4.3 Methods 94

4.4 Results 95

4.4.1 Pilot data indicate that HDAC4 may be involved in functional recovery following peripheral nerve injury, via an ATF3-dependent transcriptional mechanism 95
4.4.2 HDAC4 does not affect neurite outgrowth *in vitro*, or regeneration of epidermal nerve fibres after peripheral nerve injury 98
4.4.3 HDAC4 cKOs have similar ATF3 protein expression after sciatic nerve transection 101
4.4.4 *Atf3* mRNA is not differentially regulated in HDAC4^{Adv} cKO after sciatic nerve transection 102
4.4.5 HDAC4 is not required for sensory recovery after peripheral nerve injury 103
4.5 Discussion 104

5 HDAC4 and Nociception 108
5.1 Introduction 108

5.2 Aims....112

5.3 Methods....113

5.4 Results 113

5.4.1 Baseline sensory behaviour and acute nociception are unaffected by HDAC4 deletion 113
5.4.2 Mechanical hypersensitivity after nerve injury does not require HDAC4 expression from the $Na_v1.8$ population of sensory neurons 118
5.4.3 HDAC4 is dispensable for the development of mechanical hypersensitivity in the d4T model 121
5.4.4 Loss of HDAC4 alters responses to inflammation 122
Discussion 129

5.4.5 Peripheral expression of HDAC4 is not required for most pain modalities 129
5.4.6 Loss of HDAC4 is associated with altered transcriptional regulation in inflammatory states, and reduced sensitivity to capsaicin *in vitro* 131
5.4.7 Thermal hypersensitivity is attenuated in HDAC4 cKOs in a model of chronic inflammatory pain, but not after nerve injury or acute inflammation....132

6 General Discussion.... 136

Appendix 1: Bioinformatics analysis of HDAC4 expression and function 140
6.1 Introduction 140

6.2 Aims....140

6.3 Results 141

6.3.1 Characterising *Hdac* mRNA expression in the DRG and spinal cord ...141
6.3.2 Localising *Hdac4* expression using the Allen Brain Atlas 143
6.3.3 Using published chromatin immunoprecipitation and next generation sequencing data (ChIP-Seq) to investigate HDAC4 function....145

6.3.4 Bioinformatics analysis of HDAC4 targets using publicly available microarray and ChIP-Seq data reveals three conserved HDAC4 target genes 149
6.3.5 Pathway analysis of putative HDAC4 targets confirms known functions of the protein 152
6.3.6 Network analysis of both experimentally validated and predicted HDAC4 targets identifies HDAC4 and NGF as upstream regulators and NF-Kappa B proteins as possible intermediaries 153
6.4 Discussion 155

6.4.1 Expression data shows *Hdac4* mRNA in DRG and spinal cord 155
6.4.2 "Conserved" HDAC4 targets include *Cacna2d1*, an important pain gene 156
6.4.3 Network analysis confirms known functions of HDAC4 in tissue development, morphology and cell-to-cell signaling, and suggests a role for NF-Kappa B interactions in mediating transcriptional effects 157

Appendix 2: Bioinformatics analysis parameters 181

Appendix 3: GPAT output file from ChIP-Seq analysis..... 184

Appendix 4: Gene expression data 200

Table of Figures

Figure 1 - Sensory neuron differentiation, adapted from Lallemend and Ernfors 2012 19

Figure 2 - Signaling cascades in peripheral sensitization 28

Figure 3 - Commonly dysregulated transcripts in pain are associated with immune function and synaptic transmission, among others. Adapted from LaCroix-Fralish *et al.,* 2011 32

Figure 4 - Schematic representation of chromatin structure and key epigenetic processes involved in gene expression 34

Figure 5 – Classification of the HDAC family HDACs are grouped based on sequence homology to yeast proteins. Class I HDACs (a) are similar to yeast Rpd3 whereas class II HDACs (b) show homology to yeast Hda1. Binding motifs to MEF2 are represented in green and other motifs and phosphorylable serines are represented in blue. (DAC, deacetylase domain). Figure adapted from Yang and Seto, 2008. 36

Figure 6 – Nucleo-cytoplasmic shuttling of HDAC4 41

Figure 7 – General workflow to generate germline chimeras from gene-targeted embryonic stem cells, adapted from (Capecchi, 2005) 60

Figure 8 - By Mendel's laws, the original strain loses 50% of its genomic content with each cross to a pure inbred strain.....66

Figure 9 - Breeding Scheme, HDAC4$^{Nav1.8}$ cKO.....67

Figure 10 – Genotyping scheme and representative results 68

Figure 11 – Cre driven from the $Na_v1.8$ promoter successfully causes deletion of floxed HDAC4 in the DRG.....70

Figure 12 – There is no difference in the proportion of TrkA positive neurons or cell size in HDAC4$^{Nav1.8}$ cKOs compared to littermate controls 71

Figure 13 - HDAC4 is not required for sensory neuron differentiation 73

Figure 14 – HDAC4 has a limited effect on gene expression in naïve sensory neurons 75
Figure 15 - Loss of HDAC4 results in altered transcriptional regulation following acute dissociation of DRG neurons 76
Figure 16 - Validation of HDAC4^{Adv} conditional deletion 78
Figure 17 - Class IIa HDACs are upregulated following HDAC4 deletion 79
Figure 18 - Knockout of HDAC4 from adult DRG results in altered gene expression 80
Figure 19 – After peripheral nerve injury multiple genes trend toward differential expression between HDAC4^{Adv} cKOs and littermates 81
Figure 20 - *Cacna2d1* and *Trpa1* trend toward differential expression in both strains of HDAC4 cKOs. 84
Figure 21 - HDAC4 cKO have altered transcriptional responses to injury 85
Figure 22 – After peripheral nerve injury, *Atf3* is less upregulated in HDAC4$^{Nav1.8}$ cKO DRG samples compared to littermate controls 93
Figure 23 - Regeneration-associated genes are induced after sciatic nerve transection 96
Figure 24 – A trend toward delayed sensory recovery was observed in HDAC4$^{Nav1.8}$ cKOs after sciatic nerve crush 97
Figure 25 - Neurite outgrowth is not impaired in HDAC4$^{Nav1.8}$ cKOs 99
Figure 26 – HDAC4$^{Nav1.8}$ cKOs have similar epidermal innervation after sciatic nerve crush when compared to littermate controls 100
Figure 27 - ATF3 protein expression is not different between HDAC4$^{Nav1.8}$ cKOs and littermates 24 hours after nerve injury 102
Figure 28 - *Atf3* is not differentially expressed in HDAC4^{Adv} cKOs after sciatic nerve injury 103

Figure 29 - No difference in sensory recovery was observed in a second behavioural experiment 103
Figure 30 - HDAC4 expression in $Na_v1.8$ positive neurons is not required for baseline mechano- or thermo-sensation or acute nociception 114
Figure 31 - HDAC4 cKO in adult sensory neurons does not affect acute nociception or sensory perception 116
Figure 32 - Noxious mechanical and cold sensing are impaired after tamoxifen treatment 117
Figure 33 - *Sst* and *Calca* are differentially expressed in both strains of HDAC4 cKO after nerve injury 119
Figure 34 - $HDAC4^{Nav1.8}$ cKOs develop mechanical and thermal hypersensitivity after partial sciatic nerve ligation 120
Figure 35 - D4T results in mechanical hypersensitivity that does not require peripheral expression of HDAC4 122
Figure 36 - HDAC4 cKO have differential gene expression after inflammatory stimulation 123
Figure 37 - Fewer $HDAC4^{Nav1.8}$ cKO DRG neurons respond to capsaicin 124
Figure 38 - HDAC4 is not required for thermal hypersensitivity in the carrageenan model of acute inflammatory pain 125
Figure 39 - HDAC4 is required for thermal hypersensitivity after CFA 126
Figure 40 - HDAC4 is not required for mechanical hypersensitivity after CFA 127
Figure 41 - Known HDAC4 targets are transcriptionally dysregulated after CFA 128
Figure 42 - HDAC mRNA expression profiles in mouse and rat DRG and spinal cord 142
Figure 43 - *Hdac4* mRNA is expressed in all DRG sensory neurons at P4 144

Figure 44 - Bioinformatics analysis of published HDAC4 ChIP-Seq data, partial chromosome 16 alignment.....147
Figure 45 – Venn Diagram from genevenn.sourceforge.net.....150
Figure 46 - HDAC4 and putative targets show similar tissue expression profiles, figure adapted from BioGPS.org.....151
Figure 47 - Example of results from Ingenuity Pathway Analysis.....153
Figure 48 - Ingenuity Pathway Analysis Network.....154

Table of Tables

Table 1 - HDAC4 interacting proteins 38

Table 2 - Sexes of animals used in each study 45

Table 3 - Genotyping primers 46

Table 4 - RT-qPCR primers 53

Table 5 - Quantification of subpopulation markers 72

Table 6 - Multivariate analysis confirms that HDAC4 is required for transcriptional regulation of NGF-associated genes 76

Table 7 - List of studies used for transcription 'meta-analysis'.....83

Table 8 - Top ranked gene expression changes, naïve and SNT contra.....84

Table 9 - Top ranked gene expression changes after nerve injury, by unadjusted p-value. FC are calculated against $HDAC4^{fl/fl}$ ipsilateral controls. 118

Table 10 - Sample of GPAT output - Overlapping Peaks on Chromosome 10.....148

Table 11 - Bowtie Alignment Parameters 181

Table 12 - MACS peak-finding parameters.....183

Table 13 – $HDAC4^{Nav1.8}$ *in vitro* injury model, 50 ng/mL NGF (Study 1).....200

Table 14 - $HDAC4^{Nav1.8}$ naive gene expression (Study 2) 203

Table 15 - $HDAC4^{Nav1.8}$ D28 partial sciatic nerve ligation (Study 2). Expression values are normalized to wildtype naïve controls.....207

Table 16 - $HDAC4^{Adv}$ naive gene expression (Study 3) 210

Table 17 - $HDAC4^{Adv}$ 24 hours after sciatic nerve transection (Study 3). Values are normalized to wildtype naïve controls. 213

Table 18 - $HDAC4^{Adv}$ D15 CFA gene expression (Study 4) 216

LIST OF ABBREVIATIONS

AC	adenylyl cyclase
AEA	anandamide
ANOVA	analysis of variance
ASIC	acid-sensing ion channel
ATF3	activating transcription factor 3
ATM	ataxia telangiectasia
AUC	area under the curve
BAC	bacterial artificial chromosome
BCL2	B-cell lymphoma 2
BDNF	brain-derived neurotrophic factor
BK	bradykinin
Cacna2d1	calcium channel, voltage-dependent, alpha 2/delta subunit
Calca	calcitonin-related polypeptide alpha
CaMK	calcium/calmodulin-dependent protein kinase
cAMP	cyclic AMP
CAP2	adenylyl cyclase-associated protein 2
CB	cannabinoid
cDNA	complementary DNA
CFA	complete Freund's adjuvant
CGRP	calcitonin-gene related peptide
ChIP	chromatin immunoprecipitation
cKO	conditional knockout
coREST	co-repressor for the RE1 transcription factor
COX2	cyclooxygenase 2
CREB	cAMP response element binding protein
D4T	2′,3′-didehydro-3′-deoxythymidine
DRG	dorsal root ganglion/a (used interchangeably)
EGF	epidermal growth factor

ERK	extracellular signal-related kinase
ES	embryonic stem cell
et al	et alia (latin: and others)
FC	fold change
fl/fl	homozygous floxed
GDNF	glial-derived trophic factor
GFL	glial-derived trophic factor family ligands
GO	gene ontology
HAT	histone acetyltransferase
HDAC	histone deacetylase
HDACi	histone deacetylase inhibitor
$HDAC4^{Adv}$	HDAC4 Advillin-CreERT2 conditional knockout
$HDAC4^{Nav1.8}$	HDAC4 Nav1.8-Cre conditional knockout
HGF	hepatocyte growth factor
Hsp27	heat shock protein 27
IB4	isolectin B4
i.p.	intraperitoneal
i.v.	intravenous
JAK/STAT	janus kinase/signal transducer and activator of transcription
JNK	cJun terminal kinase
L3	dorsal root gangion of the 3^{rd} lumbar segment
KAT	lysine acetyltransferase
KCl	potassium chloride
KCNK	two-pore domain potassium channel family
KDAC	lysine deacetylase
MAPK	MAP kinases
MEF2	myocyte enhancer factor 2
MRGPR	mas-related G-protein coupled receptor
mRNA	messenger RNA
Na_v	voltage-gated sodium channel

NARTI	nucleoside analogue anti-retrovirals
NF200	neurofilament 200
NFKB	nuclear factor kappa-light-chain-enhancer of activated B cells
NGF	nerve growth factor
NGN1	neurogenin 1
NGS	next-generation sequencing
NSAID	non-steroidal anti-inflammatory drug
NT3	neurotrophin-3
NTKR	neurotrophic tyrosine kinase receptor
Ntrk1	neurotrophic tyrosine kinase receptor 1
OE	over-expression
Oprm1	mu-opioid receptor
P2rx3	purinoreceptor 3
Palmd	palmdelphin
PBS	phosphate buffered saline
PCA	principle component analysis
PCR	polymerase chain reaction
PFA	paraformaldehyde
PKA	protein kinase A
PKC	protein kinase C
PP2A	protein phosphatase 2A
PSL	partial sciatic nerve ligation
Ptgs2	prostaglandin-endoperoxide synthase 2
PTM	post-translational modification
PWL	paw withdrawal latency
PWT	paw withdrawal threshold
PVDF	polyvinylidene fluoride
RM	repeated measures
RPM	revolutions per minute
RT-qPCR	real-time quantitative polymerase chain reaction

RUNX	runt related transcription factor
SDS-PAGE	sodium dodecylsulfate polyacrylamide gel electrophoresis
Seq	next generation sequencing
Snap25	synaptosomal-associated protein 25
SNT	sciatic nerve transection
Sprr1a	small proline-rich protein 1A
SST	somatostatin
TRP	transient receptor potential cation channel
TTX-R	tetrodotoxin-resistant
Vglut1	vesicular glutamate transporter 1
wt	wildtype (used interchangeably with $HDAC4^{fl/fl}$)

Acknowledgements

I'm still not sure how I managed to do this, but I would like to thank all of the people who have made it possible.

First and foremost, I would like to thank Mac for the opportunity to grow and learn so much over the past four years. Thank you for being a great mentor and for providing me with the motto of my PhD project: hope springs eternal!

Thank you to Fran, Thanos, Hannes and Katalin for always helping me to problem solve, both in and out of the lab.

Thanks to Nikita, Tom, Sean, Fede, Matt, Natalie, Clive, John Grist, Andy, Nick, the BSU staff, John Chesson and all the other lab members, past and present, who have helped with my experiments and have been great company over lunch or a pint (or a few!)

Thank you to Viv, Caroline and Tina for being so friendly and helpful through all the administrative hiccups along the way.

Thank you to my friends: Brenna, Lia, Steph, Gaby, Jack, David, Adi, Chris and Kira for keeping me fed, laughing, dancing, singing and otherwise sane and happy.

Finally, I need to thank my family: Jess, Dan, Jake, Mom and Dad, I could not have made it this far without your completely unshakeable love and support. Thank you for always being there for me and believing that I could do this.

1 Introduction

We have evolved to engage with the world in which we find ourselves. Our senses, refined over many millennia, are tuned to the frequencies of light and sound, the vibrations and textures and smells appropriate for our survival.

Aristotle proposed that we have five senses: vision, hearing, taste, olfaction and touch. Today that list has expanded to incorporate nociception, itch, thermosensation and proprioception. All of these sensory systems rely on similar organizational properties. The neuronal patterns that underlie them encode modality, location, intensity and duration via relay systems. They employ specialized receptors to transform outside signals into electrical impulses, and it is the sum of all of these signals, in combination with motivational and emotional processing, that give rise to a percept. How the binding of the individual inputs occurs is still beyond the understanding of neuroscience, but for the past century scientists have made great advances characterizing the properties of the sensory receptors, their relays, and the ways in which they can be modulated. In this chapter I will give an overview of the development, physiology and anatomy of dorsal root ganglion sensory neurons, which are responsible for transducing touch, proprioception, thermosensation, itch and nociception. Later I will go on to discuss the molecular and cellular biology of these neurons, and the ways in which different molecular pathways are altered in pathological states such as inflammation and after nerve injury. Finally, I will touch on the novel field of epigenetics and discuss how epigenetic mechanisms may be involved in these processes, with a focus on the putative role of histone deacetylase four (HDAC4).

1.1 Development of the dorsal root ganglia

All neuronal tissue derives from the ectoderm, the top layer of tissue formed early in embryonic development (Kandel et al., 2000). The ectoderm develops into the neural plate, a specialized structure which, in a series of steps, folds in on itself to form the neural tube. The cells continue to proliferate in an asymmetric way, forming the telencephalon, mesencephalon and the rhombencephalon, which are the embryonic origins of the brain, midbrain/pons and spinal cord, respectively. Sensory neuron and glial precursors migrate from the dorsal neural tube to form the neural crest (Marmigere and Ernfors, 2007). Subsequently the cell bodies cluster into ganglia, and their axons extend to their peripheral targets.

1.1.1 Differentiation of sensory neurons

Throughout the nervous system, development begins with over-proliferation of cells and synaptic connections, followed by apoptosis and pruning of excess neurons and synapses. This is also the case for sensory neurons of the dorsal root ganglia (DRG). Axon guidance proceeds via combinations of chemical and physical signals that promote pathfinding to end organs (Dickson, 2002). A limiting amount of growth factors are released from peripheral targets, and upon innervation, growth factors bind to their cognate receptors, causing phosphorylation and the initiation of downstream signaling pathways that inhibit programmed cell death via the B-cell lymphoma 2 protein (BCL2) and caspases (Levi-Montalcini and Cohen, 1956; Smith, 2001). The sensitivity of the innervating cells to different growth factors, in concert with intrinsic factors that govern their responses to downstream signaling pathways, progressively specifies different subtypes of DRG neurons (Figure 1).

On a population level, DRG neurons can be broken into two main subtypes: large light cells, and small dark cells (Lawson and Biscoe, 1979), which go on to specify

light touch/proprioceptive neurons and small, primarily nociceptive neurons, respectively. These two subtypes are distinct from the moment of neurogenesis (Frank and Sanes, 1991). Exit from the cell cycle requires the expression of neurogenin transcription factors (NGN1 and NGN2), and early specification of neuronal fate is governed by the transcription factors SOX10, KROX20, FOXS1, BRN3A and ISLET1 (for review see Marmigere and Ernfors, 2007).

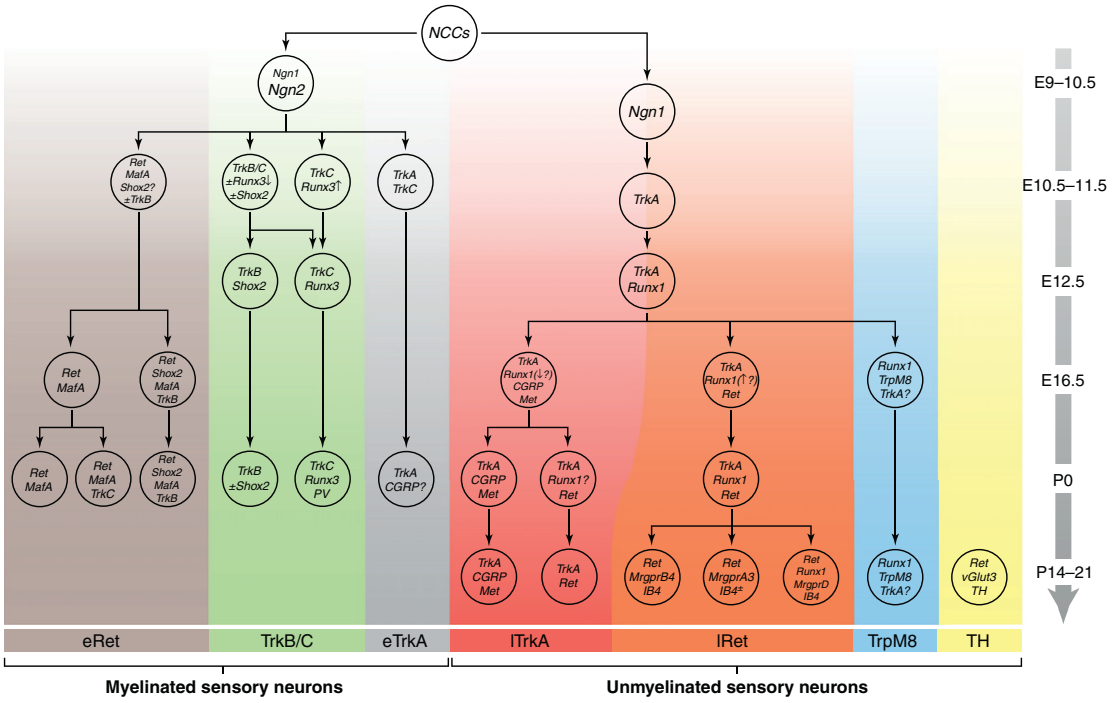


Figure 1 - Sensory neuron differentiation, adapted from Lallemend and Ernfors 2012
The cell lineages described in the mouse are outlined in different colours, with the stage of development indicated on the right hand side of the figure, E = embryonic, P = postnatal. NCC = neural crest cells, the origin of all DRG sensory neurons. Three main lineages of myelinated sensory neurons have been described, the early Ret expressing (eRet), the TrkB/C and the early TrkA lineage. The unmyelinated neurons are broken into four populations: the late TrkA (lTrkA), late Ret expressing (lRet), TRPM8 expressing and tyrosine hydroxylase (TH) expressing subtypes. The embryonic origin of the TH neurons is unknown, which is why it appears unconnected to the others. Many questions remain regarding the cues for sensory neuron development, and question marks indicate lineages that remain to be clarified with fate-mapping studies.

1.1.2 Neurotrophic factor receptors specify neuronal subtypes of the DRG

Several classes of neurotrophic factor receptors are expressed in the DRG, some of which are critical for development of sensory neuron subpopulations. These include the neurotrophic tyrosine kinase receptor (NTKR) family members, TrkA, TrkB and TrkC, and the receptor kinases Met and Ret. TrkA is preferentially activated by nerve growth factor (NGF), TrkB responds to brain-derived neurotrophic factor (BDNF) and TrkC responds to neurotrophin-3 (NT3). Met is the receptor for hepatocyte growth factor (HGF) and Ret activation is coupled to glial-derived trophic factor (GDNF) family ligand (GFLs) signaling. The precise timing and expression of these receptors is critical for appropriate peripheral innervation, cell survival and to specify the molecular and physiological characteristics of the different sensory neuron types, for example by regulating the expression of channels that can transduce specific stimuli. Importantly, growth factors, particularly NGF, can elicit nociception in adulthood, and blocking them has emerged as an important novel strategy for pain relief in the clinic, although poorly misunderstood side-effects have slowed the wide-spread application of these therapies (FDA, 2012; Lane et al., 2010; Pezet and McMahon, 2006). Understanding the molecular cues that regulate growth factor signaling, and an in-depth characterization of the cell populations that respond to NGF will be critical for this to be of use.

The majority of anatomical studies to characterize distribution of Trk receptors have been performed in lumbar ganglia of the rat and mouse, which largely innervate cutaneous tissues. It must be noted, therefore, that these findings may not fully describe ganglia that innervate viscera or muscles (McMahon et al., 1994). Broadly speaking, TrkB and TrkC are the primary growth factor receptors expressed in large light neurons, though a small subset of peptidergic large neurons also express TrkA.

This population is characterized by fast conduction velocities, large myelinated fibres and transduces proprioceptive and light touch information from the periphery. Its diversification relies on RUNX3, a runt-domain transcription factor, alongside the MAF and SHOX transcription factors (Lallemend and Ernfors, 2012).

Conversely, TrkA signaling is essential for the survival and development of small, unmyelinated sensory neurons, which transmit information about pain, itch and temperature (Snider, 1994). Two main classes of small neurons are formed through multiple stages of development, the calcitonin-gene related peptide (CGRP)-positive (peptidergic) population, and the isolectin B4 (IB4)-positive (non-peptidergic) population, although other sub-classes have also been identified.

A different set of transcription factors is responsible for the development of these small cell populations. Expression of NGN1 first specifies differentiation of small neurons, after the first wave of neurogenesis occurs in the neural crest (Ma et al., 1999). Neurons then begin to express the NGF receptor TrkA and the transcription factor RUNX1 (Ma et al., 1999). Upon target innervation half of the neurons will switch to become GDNF sensitive, progressively losing TrkA and CGRP expression and upregulating Ret, forming the non-peptidergic subpopulation (Luo et al., 2007; Molliver, 1997; Yoshikawa et al., 2007). The other half will continue to express TrkA and CGRP, a proportion of which will further differentiate to form an HGF-sensitive population (Gascon et al., 2010). Further specification of neurons continues in the early postnatal period, with non-peptidergic neurons preferentially expressing different Mas-related G-protein coupled (MRGPR) receptors (Liu et al., 2008; Molliver, 1997; Samad et al., 2010).

The differential reliance on growth factors and transcription factors implies that these populations of neurons may have selective activation patterns, with implications for

the generation of pain (Snider and McMahon, 1998). In the following sections, I will discuss how these populations may encode sensory information.

1.2 Sensory transduction

In 1822 Magendie first ascribed sensory function to the dorsal roots of the spinal cord. Since then scientists have continued to refine and expand upon our understanding of the transduction of outside signals to form percepts.

Early studies of sensory perception supported the idea of a “labeled line” encoding of sensory stimulation: a single fibre fired to encode a single stimulus. Evidence for this came from Blix, Von Frey and others in the second half of the nineteenth century, who demonstrated that different areas of the skin were sensitive to different types of stimulation. Von Frey proposed that labeled lines had distinct anatomical structures, which was true in the case of light touch and pressure, but could not be demonstrated for the different nociceptive stimuli. This was the primary argument of Weddell, Adrian, Nafe and others who instead proposed a “pattern theory” of sensory encoding, in which any stimulus was thought to activate any nerve, and the quality of the stimulus was determined by the pattern of activation. Evidence from nerve recordings refuted this, as it was discovered that nerves responded to very specific stimuli, although these experiments also demonstrated that there was not always a one-to-one relationship between nerve activation and perception. Today, a modified version of the Gate Theory of Melzack and Wall, called the population-coding hypothesis is argued to be the most accurate description to account for these varied data: specific sense information is encoded by labeled lines that engage in “cross-talk” in the periphery. This is then translated into central activation patterns in the spinal cord that are recognized by higher cortical centres, giving rise to sensory perception (Ma, 2012). It must be noted that this theory does not fully account for all

aspects of sensation; visceral pain, for example, may be more accurately described by the pattern theory (Cervero and Laird, 1999).

In order to detect the wide range of stimuli, cutaneous somatosensory receptors form a diverse array of nerve endings that are finely tuned to respond to particular modalities. Touch and proprioceptive information are primarily relayed via large, Aβ afferents innervating Merkel cells, Meissner's corpuscles, Pacinian corpuscles and Raffini endings. Nociception and thermosensation are detected by thinly myelinated Aδ fibres and unmyelinated C fibres that terminate in the epidermis as free nerve endings. In addition, a class of "silent nociceptors" exists, that are normally unresponsive to mechanical stimulation unless they are first sensitized by inflammatory mediators (Lynn and Carpenter 1982, Meyer 1991).

The modality specificity of each of these receptors relies on the selective expression of channels and receptors that transduce external stimuli into ionic currents and action potential generation. Over the past few decades, great strides have been made in identifying channels and receptors with selective activation properties (Basbaum et al., 2009), for example the transient receptor potential (TRP) ion channels that are required for sensing a variety of stimulants including heat, protons and toxins, and the MRGPR class of G-protein coupled receptors, some of which respond selectively to pruritogens like chloroquine, a malaria treatment that commonly evokes itch as a side-effect (Liu et al., 2009). In the following section I will discuss some of the key molecules and general principles of the molecular basis of sensory transduction.

1.2.1 Molecular transducers of external stimuli

Capsaicin, the ingredient in chili peppers that gives them their kick, was the basis of the discovery of the first somatosensory TRP channel to be identified, TRPV1

(Caterina, 1997). TRPV1 is a ligand-gated ion channel and upon binding of capsaicin, the channel opens and allows an influx of cations, leading to depolarization. Because capsaicin administration feels 'hot', it was postulated that TRPV1 may also be involved in heat sensing, and indeed it is: it can be activated by increases in temperature, with an activation threshold of ~43ºC (Basbaum et al., 2009). Approximately thirty other members of the TRP family have been identified, a number of which have been shown to have some role in thermosensation through both heterologous expression and knockout studies, notably TRPM8, the menthol receptor, that is involved in cold sensing (Bautista et al., 2007; Colburn et al., 2007; Dhaka et al., 2007). The precise distribution of these receptors and their individual contributions to thermosensation is an area of active enquiry.

Mechanosensation has proven much more difficult to study due to inherent technical challenges, including a dearth of *in vivo* assays to study different aspects of somatosensation in model animals, and a lack of molecular markers for assigning currents to particular cell types when measured by patch clamp *in vitro* (Basbaum et al., 2009). A number of candidate mammalian mechanotransducers have been proposed based on homology with mechanosensitive channels in model organisms, including the TRP channel TRPA1, the acid-sensing ion channels (ASICs), and the Piezo proteins (PIEZO1 and PIEZO2). To date, the evidence regarding TRPs and ASICs is conflicting, and neither family has been shown conclusively to have an essential role in mechanotransduction, though both have been implicated in hypersensitivity in pathological conditions (Delmas et al., 2011). In contrast, the Piezo proteins, and more recently the delayed-rectifier voltage-gated potassium channel $K_v1.1$, have been convincingly shown to be mechanosensitive and can confer mechanosensivity when heterologously expressed in cell lines (Coste et al., 2010; Hao et al., 2013). PIEZO2 is expressed in the DRG, and siRNA against it can

inhibit rapidly adapting currents in response to mechanical stimulation, implying that it may play a role in non-nociceptive mechanosensation. $K_v1.1$, on the other hand, appears to be more important in regulating the firing rate of Aβ rapidly adapting mechanoreceptors and the firing threshold of C-high threshold mechanoreceptors, potentially implicating it in noxious mechanosensation.

Other proteins have also been shown to influence touch sensitivity through a modulatory role in sensory neurons, for example members of the two-pore domain (KCNK) potassium channel subfamily and the integral membrane protein Stomatin which may alter excitability of sensory neurons rather than having a role in mechanosensation *per se* (Delmas et al., 2011). Mechanical allodynia, the perception of an innocuous stimulus as painful, and hyperalgesia, a heightened response to a painful stimulus are hallmarks of many chronic pain states, and understanding the molecular pathways that underlie them may provide new avenues for treatment (Wood and Eijkelkamp, 2012). The identification of cutaneous mechanotransducers is an area of ongoing research, and remains one of the key challenges in the field of somatosensation and pain.

Chemosensation refers to the process by which sensory receptors respond to chemical irritants. These may arise from endogenous sources, such as histamine and bradykinin that are released from damaged tissues after injury, or from the external environment. Alongside their function as mechano- and thermosensitive channels, TRP channels have also been shown to play a critical role in chemosensation, particularly TRPA1, the receptor for the pungent ingredients in mustard and garlic, isothyocyanates and thiosulfinates (Bautista et al., 2006). TRPA1 channels can respond to structurally diverse stimuli that are capable of crossing the membrane to covalently modify cysteine residues on the intracellular side of the channel. Because chemical irritants can result in sensitization of sensory neurons to

subsequent input, this positions TRPA1 as a potentially important molecule at the interface between acute and chronic nociception.

1.2.2 Propagating the receptor potential

The activation of mechano- thermo- and chemosensitive channels results in the influx of depolarizing cations, generating what is known as the receptor potential. The receptor potential activates voltage-sensitive channels in the membrane to further depolarize the terminal and cause an action potential to travel to the cell body. Many different voltage-gated sodium, potassium and calcium channels have been identified on sensory neuron terminals, some of which have been shown to be critical for modality-specific sensation, for example the voltage-gated sodium channel $Na_v1.7$, is required for nociception but not for light touch and proprioception (Nassar et al., 2004). Selective antagonists for this channel may have therapeutic potential in the treatment of chronic pain.

Voltage-sensitive calcium channels play a key role in the release of neurotransmitters and neuropeptides from both central and peripheral terminals of DRG sensory neurons (Basbaum et al., 2009). They are heteromeric proteins, composed of the α1 pore-forming subunit along with various combinations of α2δ, α2β and α2γ subunits that modulate their activity. The α2δ subunit, encoded by the *Cacna2d1* gene, has been shown to be important in regulating the kinetics of channel activation and inactivation, as well as the current density. They are the primary targets of gabapentinoids used to treat epilepsy and neuropathic pain (Field et al., 2006).

1.3 Response to injury

Tissue injury results in changes to sensory neuron activity via direct stimulation of afferents as well as indirect mechanisms involving the release of mediators from non-neuronal cells (McMahon, 2013). The modification and alternate transcriptional

regulation of sensory receptors and channels are critical for appropriate behavioural responses to allow for tissue healing. These mechanisms may also be engaged to produce persistent pain in the absence of overt tissue injury. Deeper understanding of these mechanisms may help to identify novel therapeutic targets for patients. Here I will discuss changes to sensory neuron function that emerge as a result of inflammation and nerve injury, respectively.

1.3.1 Inflammation and peripheral sensitization

Two thousand years ago, Celsus described the four classical signs of inflammation: *rubor* (redness), *tumor* (swelling), *calor* (heat) and *dolor* (pain). These signs result from the activation of many different cell types at the site of injury that release a wide variety of signaling factors, including bradykinin, ATP, neurotransmitters, neuropeptides, neurotrophins, and cytokines, collectively known as “inflammatory soup” (McMahon, 2013). Some of these factors can bind to receptors on nociceptors, and directly enhance the excitability of the nerve fibre. This process is called peripheral sensitisation, and it is characterized by a decrease in response threshold, an increased response to suprathreshold stimuli and spontaneous activity, corresponding to the experience of hyperalgesia. In the following sections, I will discuss some of the key molecules involved in peripheral sensitization, and the downstream signaling pathways they engage to produce this altered activity.

1.3.2 Signaling pathways and transcriptional regulation

Many overlapping mechanisms contribute to the phenomenon of peripheral sensitization, including post-translational modification of chemo- and thermosensitive receptors and voltage-gated channels, as well as more long-term changes in excitability resulting from transcriptional dysregulation (Figure 2). One of the best-characterized mediators is the growth factor, NGF. Although required for sensory

neuron survival during development, in the adult, peripheral NGF administration is acutely nociceptive, and blocking NGF or its high-affinity receptor, TrkA, have been shown to be potently analgesic (Pezet and McMahon, 2006). Upon release, NGF binds to TrkA as a dimer, leading to auto-phosphorylation of the internal side of the receptor. The phosphorylation of the TrkA receptor can have direct effects on other receptors in the membrane, for example it can transactivate TRPV1, enhancing capsaicin sensitivity (Chuang et al., 2001). Alternatively, NGF may have more long-term effects through the action of intracellular signalling cascades, or by retrograde transport to the cell soma (Pezet and McMahon, 2006).

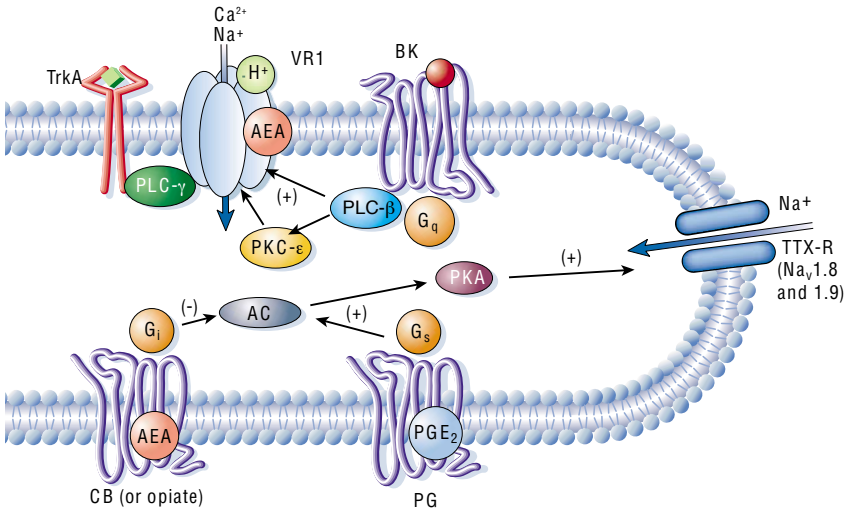


Figure 2 - Signaling cascades in peripheral sensitization
Activation of nociceptors by inflammatory soup components such as bradykinin (BK), protons (H+), prostaglandin (PG) and NGF leads to the activation of downstream signaling pathways that enhance excitability by sensitizing textrodotoxin-resistant (TTX-R) voltage-gated sodium channels. Hypersensitivity to heat can be induced by direct sensitization of TRPV1 (VR1) by binding of H+ or anandamide (AEA), or through the action of NGF and BK binding their own receptors to induce phospholipase-C signaling (PLC) which stimulates PKC-epsilon, enhancing TRPV1 responses. PG binding to the PGE2 receptor also contributes to sensitization by coupling to Gs proteins that increase adenylyl cyclase (AC) and activate protein kinase A (PKA) phosphorylation of TTX-R channels. This can be opposed by cannabinoids (CBs) or opiates acting through Gi coupled GPCRs, contributing to peripherally-mediated analgesia. Adapted from Julius and Basbaum, 2001.

The cyclic AMP (cAMP)-dependent protein kinases PKA and PKCε as well as the MAP kinases (MAPK) have all been implicated as downstream effectors of NGF sensitization. Both PKA and PKCε sensitize neurons by altering the activity of

tetrodotoxin-resistant voltage-gated sodium currents (Gold et al., 1998; Khasar et al., 1999) and may also contribute to TRPV1 sensitization via direct phosphorylation (Srinivasan et al., 2008) (Figure 2). Both the p38 MAPK and the extracellular signal-related kinase (ERK) are phosphorylated by nociceptive stimulation, and blocking them has been shown to be analgesic (Dai et al., 2002; Ji et al., 2002; Obata et al., 2004). p38 activation has been shown to depend on NGF, and is required for NGF-induced thermal hypersensitivity and TRPV1 protein upregulation (Ji et al., 2002).

Sensitization of TRPs and voltage-gated sodium channels leads increased channel opening and influx of calcium ions, which act on downstream signalling pathways to induce transcriptional changes. One transcription factor that has been implicated in peripheral sensitization is the cAMP response element binding protein (CREB) (Nakanishi et al., 2010). CREB regulates the expression of many neuropeptides, including CGRP, which is rapidly induced by inflammation (Nahin and Byers, 1994). Other signalling pathways, such as the janus kinase/signal transducer and activator of transcription (JAK/STAT) pathway, as well as the cJun N-terminal kinase (JNK) and nuclear factor kappa-light-chain-enhancer of activated B cells (NFKB) family members have also been implicated in inflammation-associated hypersensitivity (Han et al., 2001; Igwe, 2005; Inoue et al., 2006; Tamura et al., 2005), and may contribute to altered transcriptional regulation. For example, Igwe demonstrated that inhibition of the p65 subunit of NFKB could block the expression of cyclooxygenase two (COX2), the major target of non-steroidal anti-inflammatory drugs (NSAIDs) and a known pain mediator (Igwe, 2005).

Though a number of studies have demonstrated transcriptional changes of individual targets in inflammatory pain models, including upregulation of the genes encoding CGRP and BDNF (Lindsay and Harmar, 1989; Michael et al., 1997), there are

surprisingly few studies that have characterized the transcriptional profile of primary sensory neurons using high-throughput techniques (Chang et al., 2010; Yang et al., 2007). Instead, more focus has been placed on describing changes in the spinal cord, as the site of central sensitization, and on immune cells (Donate et al., 2013; Geranton et al., 2007; Ren et al., 2005; Rodriguez Parkitna et al., 2006; Victoratos et al., 1997; Yukhananov and Kissin, 2008). The study by Yang *et al* only found one target, the chemokine *Ccl2*, that has since replicated across many different pain models (LaCroix-Fralish et al., 2011). Using cut-off criteria of unadjusted p value <0.05 and fold change >1.5 over naïve, the more recent study by Chang *et al* identified 235 differentially regulated oligo probes, of which 140 had been annotated, and represented individual genes. Overall there was a trend for upregulation of genes associated with neuronal growth and survival, and downregulation of inflammation-associated genes. Two recent studies have indicated that drugs that are capable of altering chromatin architecture, and may thus impact transcription, can be analgesic in inflammatory pain models (Bai et al., 2010; Zhang et al., 2011). Further work on chromatin remodeling may give rise to new insights about the underlying mechanisms of peripheral sensitization, as will be discussed in the section on epigenetics below.

1.3.3 Nerve injury

After traumatic injury to a peripheral nerve, the affected cell bodies undergo drastic changes to gene and protein expression, and display altered morphology: cell bodies appear swollen, Nissl bodies dissolve and the nucleus is displaced. The distal nerve undergoes the process of Wallerian degeneration, while the proximal end forms a growth cone and begins the process of regeneration and remyelination. The capacity to regenerate is unique to the peripheral nervous system, owing in part to the permissive milieu created by the injury site (Makwana and Raivich, 2005). Functional

recovery depends both on the severity and location of the injury. Unrepaired lacerating injuries (neurotmesis) have the worst outcomes due to misrouting of regenerating fibres, whereas injuries that do not disrupt the nerve sheath (axonotmesis) are more likely to regenerate appropriately along their original path.

There are three main signals that are thought to underlie the phenotypic changes to the primary sensory neuron cell bodies and their subsequent regenerative capacity: 1 – rapid influxes of calcium which result from electrical stimulation of the nerve upon injury; 2 – retrograde transport of factors, such as cytokines, from the injury site; and, 3 – loss of tonic neurotrophic factor signaling (Patodia and Raivich, 2012). All of these signals may result in transcriptional changes, as outlined in the previous section.

Unlike the inflammation field, the DRG transcriptome has been extensively characterized following nerve injury (Bonilla et al., 2002; Costigan et al., 2002; Hammer et al., 2010; Levin et al., 2008; Valder et al., 2003; Vega-Avelaira et al., 2009; Wang et al., 2002; Xiao et al., 2002), and it is clear that transcriptional mechanisms are important for various aspects of the response to injury, for example by enhancing the production of cytoskeletal proteins to achieve regeneration (recently reviewed by (Patodia and Raivich, 2012)). Some work has been done to try to identify commonly occurring transcriptional events, for example the 'meta-analysis' published by LaCroix-Fralish *et al* (LaCroix-Fralish et al., 2011) which looked for commonly dysregulated transcripts in twenty microarray datasets from multiple tissues and pain models. This group identified 79 genes that were altered in at least four studies. Interestingly, this list was enriched for genes associated with immune function and synaptic transmission, indicating that these processes may be involved across a wide variety of pain states (LaCroix-Fralish et al., 2011).

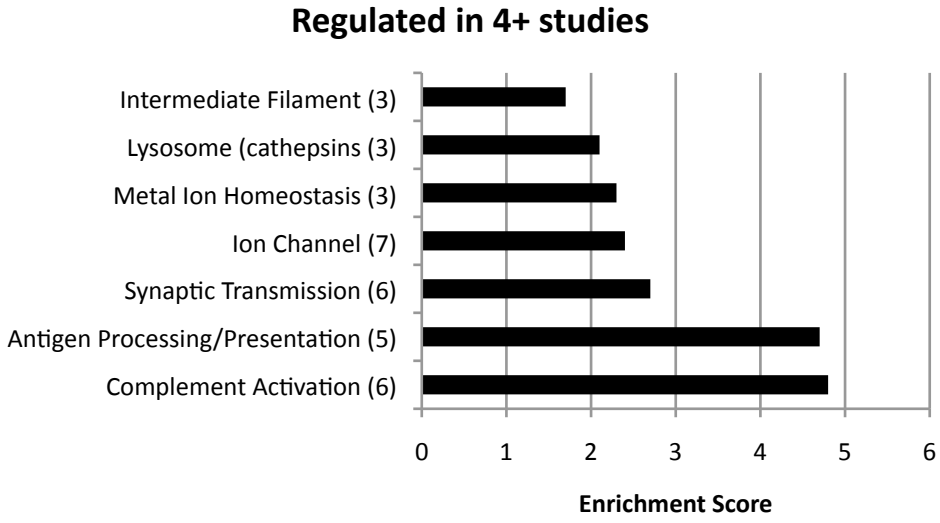


Figure 3 - Commonly dysregulated transcripts in pain are associated with immune function and synaptic transmission, among others. Adapted from LaCroix-Fralish *et al.,* 2011

Many transcription factors have been implicated in mediating these changes, including cJUN and CREB, but the extent to which these transcription factors engage epigenetic modification of chromatin to exert their effects is only beginning to be explored. For example, one recent study looked at the activity of the RE-1 site transcription factor (REST) following nerve injury, and found that two genes with RE-1 binding sites, *Scn9a* and *Oprm1,* bound to REST after injury and were downregulated, which was associated with reduced histone H3 acetylation around the RE-1 motifs (Uchida et al., 2010). In the following section, I will introduce the field of epigenetics, and discuss how a deeper understanding of the molecules involved in modulating chromatin, for example through histone deacetylation, may provide new avenues for the treatment of diseases associated with long-term transcriptional dysregulation.

1.4 Epigenetics

Transcriptional regulation is critical for appropriate cellular responses to external stimulation. With the increasing availability of high-throughput transcriptional profiling

the massive scale and influence of transcriptional change in disease states has been recognized, leading to further investigations into the mechanisms that underlie and maintain these changes. Epigenetic mechanisms, such as covalent DNA- and histone post-translational modifications, may provide the missing link as they are dynamic, responding readily to external cues; instructive for transcription; and potentially long-lasting (Allis et al., 2007). Exploring these mechanisms may lead to novel approaches to treating disease (Arrowsmith et al., 2012; Crow et al., 2013).

Epigenetics is a field with a convoluted history, due in part to the simultaneous use of the word to describe two different things. In the nineteen-fifties, the word epigenetics was defined by Waddington as the study of "causal mechanisms" through which "the genes of the genotype bring about phenotypic events"; Nanney used it to explain his observation that cells of the same genotype could have different phenotypes that persisted for many generations (Haig, 2004). Today, epigenetics refers to the study of alterations to gene function that cannot be explained by DNA sequence (Allis et al., 2007). There are several molecular mechanisms that contribute to epigenetic gene regulation including ATP-dependent chromatin remodeling, covalent modifications of DNA and histone proteins and exchange of histone variants. Historically, research in this area has focused on dividing cells and mitotic/meiotic heritability, but in recent years there has been much interest in studying epigenetic processes within the post-mitotic environment of the nervous system (Day and Sweatt, 2011; Maze et al., 2013). Particular attention has been paid to the role of histone post-translational modifications and I will discuss this in greater detail below.

In the nucleus DNA is tightly associated with histones to form chromatin, the substrate for epigenetic processes to regulate gene expression. The repeating unit of chromatin is the nucleosome, which is composed of 147 base pairs of superhelical DNA wrapped around a core of eight histone proteins (two copies each of H2A, H2B

H3 and H4). To date, more than 350 chromatin modifying proteins have been identified which are capable of changing the physical interactions between DNA and histones or can result in gene regulation by recruiting transcriptional machinery (Kouzarides, 2007). Chromatin modifying proteins are commonly broken down into writers (that add modifications), readers (that respond to modifications and translate them into different actions) and erasers (that take away modifications). These three divisions can be further sub-divided by the specific modification (e.g. lysine acetylation vs. lysine methylation) that they write, read or erase (Figure 4).

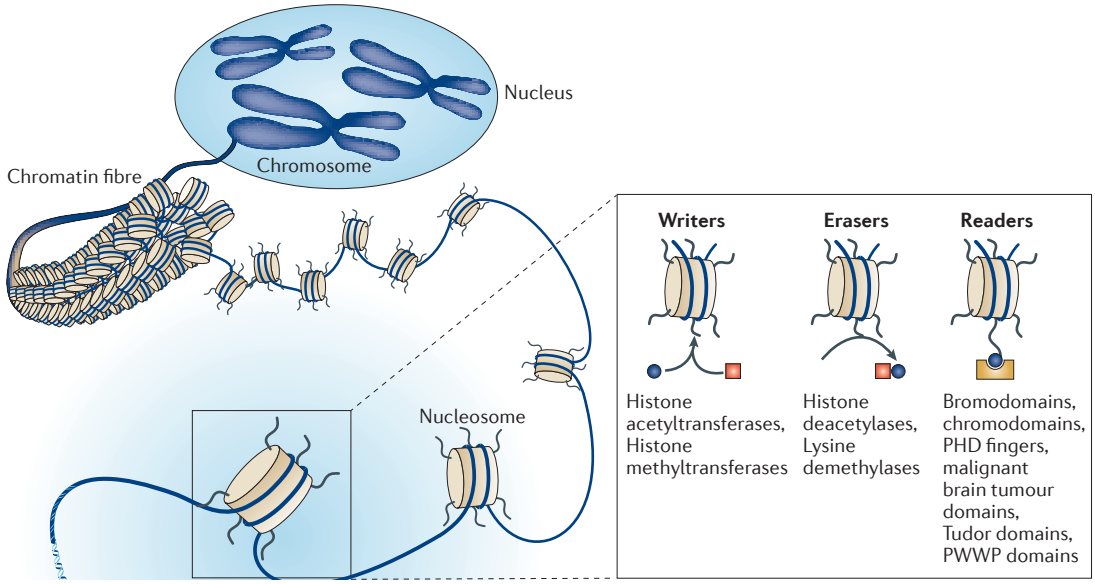


Figure 4 - Schematic representation of chromatin structure and key epigenetic processes involved in gene expression
DNA is packaged into chromatin by wrapping around histones, forming a repeating subunit called a nucleosome. Histones are subject to post-translational modifications (PTMs) that alter their association with DNA, for example acetylation of terminal lysine residues reduces chromatin compaction, which can enhance accessibility to RNA polymerase. There is no one-to-one relationship between histone marks and transcriptional status, which suggets that gene expression is mediated by a combination of PTMs. Chromatin modifying protein families are illustrated on the right. 'Writers' deposit marks onto histones, whereas 'erasers' remove them. Marks are recognized by 'readers' that contain specific protein-binding domains, e.g. plant homeodomains (PHDs) or bromodomains. Figure adapted from Arrowsmith *et al.,* 2012.

Although the genome is studded with histone modifications or 'marks', many of them appear to be poorly predictive of transcriptional status on their own, leading to the idea of the 'histone code' or 'language'. By this schema it is thought that the combinatorial effect of multiple histone modifications defines the transcriptional status

of a particular gene (Fischle et al., 2003; Lee et al., 2010). Although we are a long way away from understanding what these marks do on a genome-wide basis, the use of drugs to inactivate various classes of chromatin modifying proteins and the study of individual targets has been informative, implicating these marks and the enzymes responsible for them in diverse biological processes, from differentiation and proliferation to neurodegeneration and pain (Szyf, 2009).

In our lab, we became interested in epigenetic mechanisms after a post-doctoral fellow (Dr. Franziska Denk) discovered that intrathecal treatment with histone deacetylase inhibitors could be analgesic in two rat models of painful peripheral neuropathy (Denk et al., 2013). Although this behavioural effect was very reproducible, the potential mechanisms underlying this were far from obvious, as the role of histone deacetylases in primary sensory and second-order interneurons was completely unknown. My project has its origins in exploring histone deacetylases but we quickly focused on a specific member of the histone deacetylase family, HDAC4, as evidence from the literature suggested it may have a role in mediating sensory behaviour (Rajan et al., 2009; Williams et al., 2010). In the following sections I will discuss this in greater detail.

1.5 HDAC4

Lysine acetylation is a reversible process, mediated by the opposing actions of lysine acetyltransferases (HATs or KATs) and lysine deacetylases (HDACs or KDACs) to transfer an acetyl moiety from acetyl-coenzyme A to the epsilon-amino group of a lysine residue. Although this modification was discovered on histones in the 1960s, its functional implications only began to be appreciated from the nineteen-nineties when Allis's lab provided direct evidence that histone acetylation was connected to the control of gene expression (Brownell et al., 1996). Although originally thought to

be restricted to histones, it is now appreciated that acetylation affects many different proteins, with wide-ranging implications for cell function (Glozak et al., 2005).

The first lysine deacetylases were identified in 1996 (Rundlett et al., 1996). Following this, many other proteins were discovered that also had deacetylase activity, and they were classed according to sequence homology to the yeast deacetylases Rpd3, Hda1 and Sir2 (Figure 5). In the mouse, HDACs are divided into four classes: class I, which are homologous to Rpd3 contains HDAC1, -2, 3, and -8; class II, related to Hda1 contains HDAC4, -5, -6, -7, -9 and -10, but is further subdivided into classes IIa and IIb based on phylogenetic analysis; class III, or Sirtuins, which are NAD+ dependent rather than zinc-dependent enzymes; and class IV, which contains HDAC11 (Haberland et al., 2009).

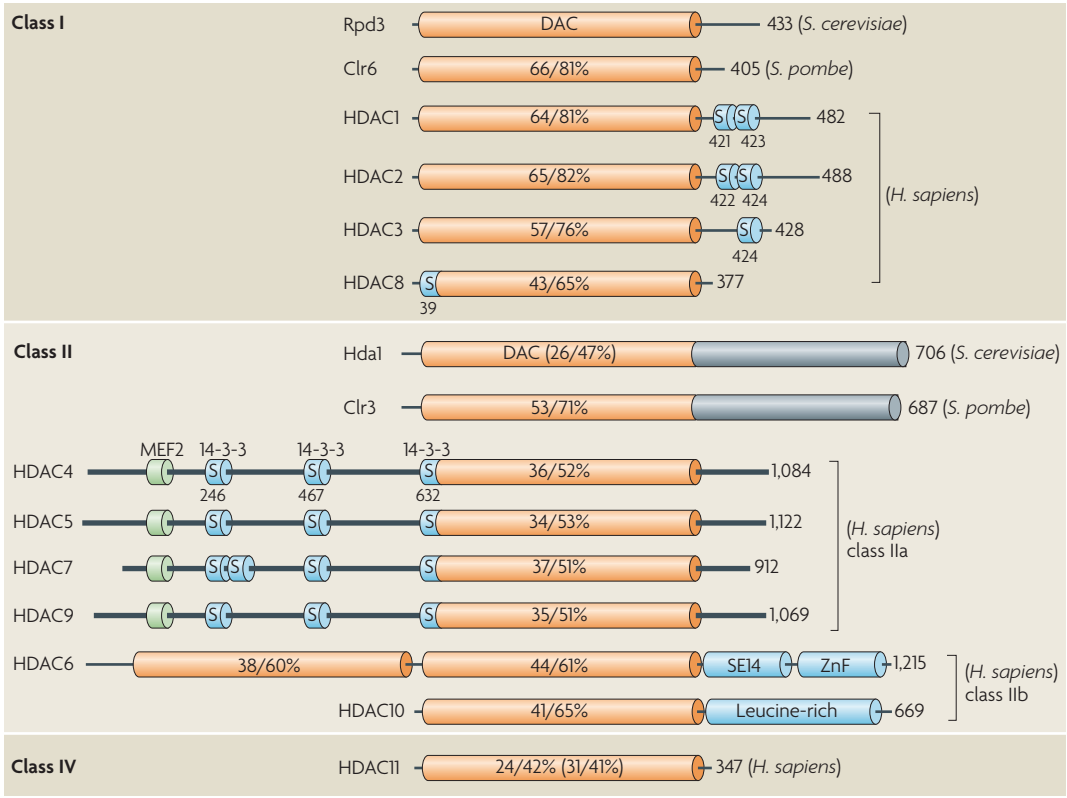


Figure 5 – Classification of the HDAC family
HDACs are grouped based on sequence homology to yeast proteins. Class I HDACs (a) are similar to yeast Rpd3 whereas class II HDACs (b) show homology to yeast Hda1. Binding motifs to MEF2 are represented in green and other motifs and phosphorylable serines are represented in blue. (DAC, deacetylase domain). Figure adapted from Yang and Seto, 2008.

Class I HDACs are ubiquitous nuclear enzymes with high deacetylase activity. They are recruited to gene promoters as part of the mSin3a and coREST complexes, and deacetylate target genes, altering chromatin structure to promote transcriptional repression. In contrast, class IIa HDACs (comprising HDACs -4, -5, -7 and -9) have a much more tissue-specific expression pattern (Grozinger et al., 1999). They are characterized by their long N-terminal domains, which contain multiple phosphorylation sites and intrinsic nuclear import and export signals that allow for dynamic nucleo-cytoplasmic trafficking. Shuttling between the cellular compartments is controlled by a wide variety of stimuli, implicating these molecules as potentially important signal transducers (Yang and Seto, 2008).

Human HDAC4 was first cloned in 1999 by Grozinger and colleagues, who described that it formed a complex with the class I histone deacetylase, HDAC3 (Grozinger et al., 1999). As mentioned previously, unlike class I HDACs, HDAC4 showed tissue-restricted expression patterns, with high levels of expression in neural tissues including the brain and skeletal muscle, hinting at a potential role in tissue differentiation. The first paper to describe HDAC4 function was published soon after and reported that HDAC4 could bind to and repress myocyte enhancer factor 2 (MEF2), a transcription factor involved in muscle development and neuronal survival (Heidenreich and Linseman, 2004; Miska et al., 1999). This group were also the first to demonstrate calcium-dependent HDAC4 nucleo-cytoplasmic shuttling, a mechanism that has since emerged as integral to class IIa HDAC function.

1.5.1 Molecular mechanisms of HDAC4

Since the first report of MEF2 binding, a conserved role for HDAC4 in transcriptional repression and transcription factor binding has emerged from reports in many different cell types and conditions (Li et al., 2012; Paroni et al., 2008; Salma and

McDermott, 2012; Sando Iii et al., 2012; Yang et al., 2011). In one dramatic example, global HDAC4 knockout revealed a role for HDAC4 in bone formation via runt-related transcription factor 2 (RUNX2) (Vega et al., 2004). In the absence of HDAC4, RUNX2-dependent transcription was activated too early in bone pregenitors: chondrocytes failed to differentiate, and ossified too soon, which was lethal in the early post-natal stage. Overexpression and knockdown studies have also revealed extensive transcriptional repercussions of HDAC4 manipulation (Kehat et al., 2011; Li et al., 2012; Sando Iii et al., 2012) although deletion of HDAC4 from the calcium/calmodulin-dependent protein kinase IIa (CaMKIIa) population of cortical neurons did not alter transcription in conditional knockouts (Kim et al., 2012), implying that other mechanisms of HDAC4 are likely to play a role in the learning and memory deficit observed in these mutant mice. Mechanisms other than transcriptional repression via deacetylation have also been reported, including a role as an E3 sumo-ligase (Zhao et al., 2005), and in histone methylation (Hohl et al., 2013) (Table 1).

Table 1 - HDAC4 interacting proteins

Protein	Cellular compartment	Function	References
MEF2	nucleus	Represses transcription of MEF2 target genes; in muscle this is partly through MEF2 sumoylation. May also occur through HDAC3/SMRT/NCoR deacetylation. Implications for myoblast differentiation, cell survival in neurons	Miska et al., 1999; Miska et al. 2001; Paroni et al. 2008; Zhao et al., 2005; Salma and McDermott, 2012; Li et al., 2012; Sando III et al., 2012
CREB	nucleus	Transcriptional repression; associated with cell death	Bolger and Yao, 2005; Li et al., 2012

p53	nucleus	Co-recruited to promoters following DNA damage, results in transcriptional repression	Berns et al., 2004; Basile, Montovani and Imbriano 2006
PPARγ	nucleus	Translocates to the nucleus after H_2O_2 stimulation, represses PPARγ transcription and makes neurons more vulnerable to oxidative stress	Yang et al., 2011
FOXO1/3	nucleus	Deacetylates FOXO transcription factors, enhancing transcription in the liver in response to glucagon signaling	Mihaylova et al., 2011
RUNX2	nucleus	Transcriptional repression; required for bone formation	Vega et al., 2004
HIF1 alpha	cytoplasm	Deacetylates HIF1alpha, enhancing its stability, protein expression and transcriptional activity. Improves retinal ganglion cell survival in development and disease.	Qian et al., 2006; Geng et al., 2011; Seo et al., 2009; Chen and Cepko, 2009
STAT1	cytoplasm	Activates and represses STAT1 via acetylation and sumoylation, respectively. Affects inflammatory transcriptional activation.	Sun et al., 2009; Yuan et al., 2005; Stronach et al., 2011
LXRa/ß	cytoplasm	Sumoylates LXRs, negatively regulates inflammatory responses in macrophages	Lee et al., 2009; Ghisletti et al., 2007; Stempelj et al., 2007
MEKK2	cytoplasm	Promotes deacetylation of MEKK2 after muscle denervation and contributes to muscle atrophy via AP1 induction	Choi et al., 2012
DNAJB8	cytoplasm	DNAJB8 promotes oxidized HDAC4 reduction by Trx1, leading to nuclear import and rescue from cardiac hypertrophy	Ago et al., 2008

The transcriptional repressor function of HDAC4 is independent of its deacetylase domain (Miska et al., 1999; Vega et al., 2004). Indeed, the deacetylase domain of HDAC4 is mysterious: on its own, HDAC4 has no endogenous deacetylase activity due to a conserved tyrosine to histidine substitution found in all class IIa enzymes (Lahm et al., 2007), and it is thought that most of the deacetylation activity ascribed to HDAC4 results from its partnership with HDAC3 (Fischle et al., 2002). However, HDAC3 is normally restricted to the nucleus, and studies have reported HDAC4-associated deaceylation activity in the cytoplasm (Choi et al., 2012; Qian et al., 2006; Seo et al., 2009; Stronach et al., 2011). Whether HDAC4 complexes with as-yet-unidentified binding partners to mediate this remains to be seen. Interestingly, global deletion of the HDAC4 deacetylase domain results in reduced thermosensitivity in knockout mice, in the absence of other gross morphological differences (Rajan et al., 2009). Although it is unclear which cell types are responsible for this phenotype, it is tempting to speculate that this may reflect a role for HDAC4 in DRG sensory neurons. Of note, a study in the nematode indicated that knockout of the HDAC4 homologue, *hda4,* led to reduced responses to a thermal gradient, something that normally elicits movement of the worms toward a preferred temperature (Wang et al., 2011), indicating that HDAC4 may have a conserved role in thermosensation.

The best characterized activity of HDAC4 is its dynamic nucleo-cytoplasmic shuttling, which relies on reversible phosphorylation and links the protein to several biochemical signaling pathways (Yang and Seto, 2008). Nuclear export of HDAC4 occurs in response to activation of calcium/calmodulin-dependent protein kinase (CaMK), which phosphorylates HDAC4 and allows it to associate with the chaperone 14-3-3 proteins (Grozinger and Schreiber, 2000; McKinsey et al., 2000). A recent report has also indicated that nuclear export of HDAC4 can be modulated directly by

nuclear calcium signaling (Schlumm et al., 2013), further strengthening the association of HDAC4 activity with calcium fluxes. Dephosphorylation by the protein phosphatase PP2A leads to nuclear accumulation of HDAC4 (Li et al., 2012; Paroni et al., 2008) and subsequent transcriptional repression. Nuclear localization has also been demonstrated following oxidation of HDAC4 and caspase-mediated cleavage events (Ago et al., 2008; Liu et al., 2004), implicating HDAC4 in apoptosis and oxidative stress signaling (Figure 6).

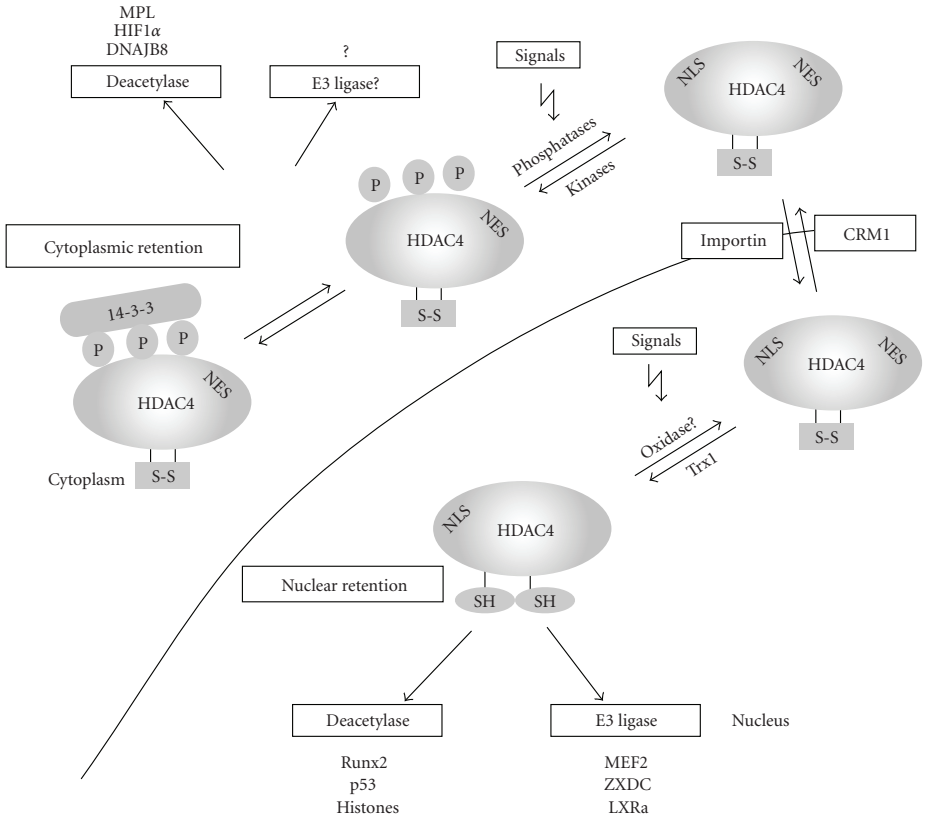


Figure 6 – Nucleo-cytoplasmic shuttling of HDAC4
Phosphorylation of HDAC4 leads to nuclear export and cytoplasmic retention by binding of the 14-3-3 proteins. The cytoplasmic form of HDAC4 may have protein deacetylase activity, though whether it also acts as an E3 SUMO-ligase in the cytoplasm is unclear. Dephosphorylation leads to HDAC4 nuclear accumulation, and reduction of sulfide bonds by Trx1 favours its retention. The identity of the oxidase responsible for HDAC4 oxidation is unknown. In the nucleus HDAC4 has E3 SUMO-ligase activity on the listed substrates, and also has deacetylase activity on RUNX2, p53 and histones, likely through complexing with HDAC3. Figure adapted from Yao and Yang 2011 (Yao and Yang, 2011).

1.5.2 HDAC4 in neurons

In cortical neurons, nuclear shuttling of HDAC4 has been shown to occur in both physiological and pathological conditions, with repercussions for cell survival and synaptic plasticity (Bolger and Yao, 2005; Li et al., 2012; Salma and McDermott, 2012; Sando Iii et al., 2012; Yang et al., 2011). Interestingly, three separate studies have shown HDAC4 shuttling in response to neuronal activity (Chawla et al., 2003; Sando Iii et al., 2012; Schlumm et al., 2013). The earliest of these, by Chawla *et al*, showed that spontaneous electrical activity was sufficient to cause nuclear export of HDAC4, which was dependent on CaMK. Sando *et al* showed that blocking glutamate receptors led to HDAC4 nuclear accumulation and subsequent downregulation of multiple genes associated with synaptic plasticity. Similarly, Schlumm *et al* indicated that blocking nuclear calcium using a targeted expression of CamBP4 led to accumulation of HDAC4 in the nucleus, which was relieved by bursts of action potentials. This poises HDAC4 as an activity-dependent signal transducer in neurons. Due to its transcriptional effects in the nucleus, this could have great implications for sensory neurons, for example, by de-repressing pro-inflammatory gene expression following injury. Indeed, HDAC4 has already been linked to the expression of genes that are involved in pain and regeneration, including *Ptgs2* that encodes COX2 and activating transcription factor 3 (*Atf3)*, a transcription factor that enhances sensory neuron regeneration after injury (Schlumm et al., 2013; Wang et al., 2008b). Interestingly, the role in COX2 transcription was linked to HDAC4 nuclear import following application of the epidermal growth factor (EGF). That HDAC4 is responsive to growth factor signaling, and has been linked to the transcription of pain-related genes may imply a role in sensory neuron transcriptional regulation. It will be of great interest to determine whether this may be the case.

Another interesting story that has emerged about HDAC4 regards its role in neuronal survival. The evidence here is conflicting, with some studies indicating that knockdown of HDAC4 can improve survival under toxic conditions (Bolger and Yao, 2005; Salma and McDermott, 2012; Yang et al., 2011) whereas others report that knockdown causes neuronal death, attributed to the loss of neuroprotective functions in the cytoplasm (Chen and Cepko, 2009; Li et al., 2012; Majdzadeh et al., 2008; Sando Iii et al., 2012). Evidence from knockout mice fail to support either hypothesis, as they do not display gross abnormalities in brain architecture, or neuronal viability (Kim et al., 2012; Price et al., 2012; Rajan et al., 2009), although this could be due to developmental compensation. One explanation that may account for this is that HDAC4 is maintained in a dynamic equilibrium between the cytoplasm and the nucleus, and it is the ratio of HDAC4 in each subcellular compartment that determines whether knockdown will be neuroprotective or pro-apoptotic. For example, when cells have only nuclear HDAC4, knockdown is beneficial because it reduces the nuclear:cytoplasmic ratio; when there is HDAC4 in both the nucleus and the cytoplasm, knockdown kills cells by reducing the overall levels of HDAC4. This is supported by over-expression studies that show a protective role of cytoplasmic-restricted HDAC4 (Chen and Cepko, 2009; Li et al., 2012; Liu et al., 2004) and a negative effect of nuclear-restricted HDAC4 over-expression (Bolger and Yao, 2005; Liu et al., 2004; Sando Iii et al., 2012).

Toxic agents, such as chemotherapeutic drugs and nucleoside analogue anti-retrovirals (NARTIs) can cause neuropathic pain in patients (Ferrier et al., 2013; Margolis et al., 2013). Due to its effect on cell survival, HDAC4 could play a role in mediating nociceptive responses to these stimuli.

1.6 Summary and aims

Transcriptional regulation is essential for appropriate development, and responses to injury. HDAC4 is a transcriptional corepressor which is required for physiological thermosensation, however the mechanisms underlying this remain unclear. In other tissues, HDAC4 has been shown to interact with proteins necessary for sensory neuron differentiation, for example the RUNX family transcription factors, as well as CREB that regulates injury responses. Whether HDAC4 regulates these proteins in sensory neurons to contribute to thermosensation is unknown. In addition, the capacity for HDAC4 to shuttle in and out of the nucleus in a calcium-dependent manner positions it as a molecular cue. One could postulate that the movement of HDAC4 after injury could have crucial implications for the transcriptional status of affected neurons, or may have an effect on cell survival following toxic insult.

To address these questions, I generated two novel strains of HDAC4 conditional knockout mice, and characterized their transcriptional and behavioural profiles across a variety of injury models. In the first data chapter I will describe the validation of the two conditional knockout strains, and the transcriptional and anatomical repercussions of HDAC4 deletion. In the second data chapter I will describe studies in which we explored whether HDAC4 is involved in peripheral nerve regeneration. The final data chapter will cover the role of HDAC4 in mediating nociception across a variety of pain models. In addition, Appendix I contains a bioinformatics analysis of HDAC4 expression and function.

HDAC inhibitors and other drugs that target chromatin modifying and transcriptional regulatory proteins are already being used clinically to treat cancer. Work to characterize the function of these molecules in diverse systems will provide a rational basis for broader application of these therapies.

2 Methods

2.1 Animals

All work performed conformed to United Kingdom Home Office legislation (Scientific Procedures Act 1986). All behaviour, surgery, and immunohistochemistry was performed on animals or tissue taken from 2-6 month old animals. When animals of both sexes were used, care was taken to ensure approximately equal numbers of males and females were used in each group (Table 2).

Table 2 - Sexes of animals used in each study

Study	Strain	# Males (wt/cKO)	# Females (wt/cKO)	Total (wt/cKO)
Naive - RNA for affy	Nav1.8	4/4	0/0	4/4
Naive - immunohistochemistry	Nav1.8	3/3	0/0	3/3
Carrageenan - behaviour	Nav1.8	6/6	0/0	6/6
CFA - behaviour	Nav1.8	6/6	0/0	6/6
PSL - behaviour	Nav1.8	8/8	0/0	8/8
PSL - RNA for array cards	Nav1.8	4/4	0/0	4/4
PSL - immunohistochemistry	Nav1.8	4/4	0/0	4/4
D4T - behaviour	Nav1.8	9/10	0/0	9/10
D4T - immunohistochemistry	Nav1.8	4/4	0/0	4/4
Crush 1	Nav1.8	2/4	5/3	7/7
Crush 2	Nav1.8	7/5	2/3	9/8
24h axotomy - immunohistochemistry	Nav1.8	3/3	0/0	3/3
Baseline sensitivity/acute nociception	Adv	3/4	7/3	10/7
24h Axotomy - RNA	Adv	4/4	0/0	4/4
CFA	Adv	5/1	7/5	12/6

2.1.1 Genotyping

Ear-derived DNA was analyzed by polymerase chain reaction (PCR) to identify HDAC4$^{fl/fl}$ and HDAC4 cKO mice. Ear clips were incubated between 3-12 hours at 55°C in lysis buffer (50 mM KCl, 25 mM $MgCl_2$, 10 mM Tris Base pH 8.5, 0.45% Tergitol, 0.45% Tween-20 and 0.1 mg/mL proteinase K in ddH_2O), then at 95°C for 20 minutes to inactivate proteinase K. 5 μL of this suspension was used for subsequent PCR reactions. All products were run on 2% agarose gels in 1X TAE stained with 0.5 mg/mL ethidium bromide.

Table 3 - Genotyping primers

	Forward (5' – 3')	**Reverse (5' – 3')**
HDAC4$^{fl/fl}$	ATCTGCCCACCAGACTATGTG	CTTGTTGAGAACAAACTCCTGCAGCT
HDAC4 recombined allele	AGGCTGAGGGCAAGTTAGAC	GATTGACCGTAATGGGATAGGTTACG
$Na_v1.8$-Cre	TGTAGATGGACTGCAGAGGATGGA	AAATGTTGCTGGATAGTTTTTACTGCC
Wildtype $Na_v1.8$	TGTAGATGGACTGCAGAGGATGGA	TTACCCGGTGTGTGCTGTAGAAAG
Advillin CreERT2	CCCTGTTCACTGTGAGTAGG	GCGATCCCTGAACATGTCCATC
Wildtype Advillin	CCCTGTTCACTGTGAGTAGG	AGTATCTGGTAGGTGCTTCCAG

To identify the HDAC4$^{fl/fl}$ allele, reactions were performed in a final volume of 25 μL using the GoTaq® DNA Polymerase kit from Promega according to manufacturer's instructions. Amplifications were performed as follows: heating at 94°C for 2 min, 35 cycles of 96°C for 15 s 58°C for 30 s and 72°C for 60 s, followed by a final extension at 72°C for 10 min. This yielded a wildtype band at 480 bp, and a floxed band at 620 bp. The HDAC4^{cKO} (recombined) allele was identified following the same protocol,

and resulted in a wildtype band at 1278 bp, a floxed band at 1343 bp and a recombined band at 290 bp.

To identify the $Na_v1.8$-Cre allele, reactions were performed in a final volume of 25 μL using the GoTaq® DNA Polymerase kit from Promega according to manufacturer's instructions. Amplifications were performed as follows: heating at 94°C for 2 min, 30 cycles of 94°C for 30 s, 60°C for 30 s and 72°C for 60 s, followed by a final extension at 72°C for 10 min. This yielded a Cre-positive band at 420 bp. The wildtype $Na_v1.8$ allele was identified following the same protocol, in a separate reaction and resulted in a 460 bp band.

To identify the Advillin-CreERT2 allele, reactions were performed in a final volume of 25 μL using the GoTaq® Flexi DNA Polymerase kit from Promega according to manufacturer's instructions, with a final concentration of 2.5 mM $MgCl_2$. Amplifications were performed as follows: heating at 96°C for 3 min, 30 cycles of 96°C for 30 s, 63°C for 30 s and 72°C for 60 s, followed by a final extension at 72°C for 10 min. This yielded a Cre-positive band at 180 bp. The wildtype Advillin allele was identified following the same protocol, in a separate reaction and resulted in a 480 bp band.

2.1.2 Tamoxifen Dosing

Tamoxifen (Sigma T5648) was prepared according to the protocol of Metzger and Chambon (Metzger and Chambon, 2001). Briefly, 10 mg tamoxifen were dissolved in 100 μL 100% ethanol, made up to 10 mg/mL in autoclaved sunflower oil, and placed on a shaker at room temperature for 2-3 hours. The drug was aliquoted and stored at -20°C prior to dosing. 8-10 week old mice received 2 mg tamoxifen/day i.p. over a five day period.

2.1.3 Inflammatory pain models

Acute inflammation was induced via intraplantar injection of lambda carrageenan (Sigma C3889). Carrageenan was made up to 2% in sterile saline, and 20 μL were injected into the right hindpaw.

To model chronic inflammatory pain, an intraplantar injection of 20 μL of Complete Freund's Adjuvant (CFA) (Sigma F5881) was made into the right hindpaw of affected animals.

2.1.4 Neuropathic pain models

To model neuropathic pain, the partial sciatic nerve ligation model (Seltzer et al., 1990) and the d4T model (Renn et al., 2011) were used. To ligate the sciatic nerve, animals were placed under isoflurane anaesthesia, the thigh area was shaved and the skin opened using a sterile scalpel (Swann-Morton). The thigh muscle was blunt dissected using surgical scissors (Fine Science Tools) and the sciatic nerve was located and held steady using curved forceps. A Vicryl suture was tied around approximately 60% of the nerve, then the nerve and muscle layers were gently repositioned and the skin was closed using sterile wound clips. Wound clips were removed ten days after surgery.

2′,3′-Didehydro-3′-deoxythymidine (stavudine; d4T) was received as a gift from Dr. Wenlong Huang and Dr. Andrew Rice from Imperial College London. It was reconstituted in 0.9% saline to 2.5 mg/mL and administered as a single 10 mg/kg intravenous (i.v.) dose by tail vein injection.

2.1.5 Sciatic crush model of peripheral nerve regeneration

Animals were placed under isoflurane anaesthesia, the thigh area was shaved and the skin opened using a sterile scalpel (Swann-Morton). The thigh muscle was blunt dissected using surgical scissors (Fine Science Tools) and the sciatic nerve was

exposed and crushed with fine forceps coated in lamp black to mark the crush site. The lesion site was kept a constant 37 mm from the tip of the third digit and the wound was closed with wound clips.

2.2 Behaviour

All behaviour testing was performed by an experimenter blind to genotype. On each day, animals were randomized into test boxes using the list randomizer function of http://www.random.org. Baselines were determined over three days.

2.2.1 Rotarod

The rotarod test was used to determine locomotor coordination. The rotarod (Ugo-Basile) was calibrated to accelerate from 4-38 RPM with a cut-off time of 295 seconds. Animals were allowed to habituate to the base speed for 20 seconds prior to the acceleration phase, and latency to fall was recorded. Three measurements were recorded on each test day, with at least 10 minutes between trials.

2.2.2 Von Frey Test

50% mechanical thresholds were determined using calibrated Von Frey filaments following the up-down method of Dixon (Dixon, 1965) and Chaplan (Chaplan et al., 1994). Animals were habituated to the testing environment for 60 minutes prior to testing. Filaments were applied to the plantar surface of the hindpaw for three seconds, and a bimodal (yes/no) response was recorded.

2.2.3 Hargreaves Test

Heat withdrawal thresholds were assessed using the Hargreaves apparatus (Ugo Basile), set to an infrared intensity of 40 and cut-off time of 32.5 seconds. Animals were habituated for at least 30 minutes prior to testing, and care was taken to ensure the glass base was kept clean, and that animals were not in deep sleep when

measurements were taken as this has been shown to greatly influence withdrawal latencies (Callahan et al., 2008). At least three measurements of withdrawal latency were taken per paw on each test day.

2.2.4 Tail flick

The tail flick response was measured at 49°C or 52°C to determine spinal reflex responses to innocuous warm and noxious heat stimuli respectively following the protocol of Ben Bassat (Ben Bassat et al., 1959). Briefly, mice were restrained, the tail immersed into a water bath and latency to respond recorded. Three measurements were recorded on the test day, with at least 5 minutes between trials.

2.2.5 Hot Plate

Two protocols were used to assess thermal sensitivity on the hot plate (IITC). In the first, animals were allowed to habituate for five minutes on a hot plate set to 40°C, and a temperature ramp of 2.5°C/minute was initiated. The temperature of the first response (flick, lick or jump) was recorded. In the second protocol, animals were habituated to the hot plate at room temperature for five minutes then returned to their home cage. Once all the animals had been habituated, animals were placed on the hot plate at either 52.5°C or 55°C and the latency to first response (flick, lick or jump) was recorded.

2.2.6 Randall-Selitto Test

The Randall-Selitto test was used to assess mechanical pain thresholds. Under light restraint, increasing pressure was applied to the hindpaw of each animal using a Ugo Basile Algesiometer. The pressure at which a withdrawal response was elicited was recorded, with a cut-off of 150 g. Scores represent the mean withdrawal threshold of both paws.

2.2.7 Sciatic Functional Index

The sciatic functional index is an integrated sensory motor function test designed to quantify re-innervation following sciatic nerve injury. Prior to surgery, animals were trained to run across a wooden plank toward a darkened home cage. Their hindpaws were inked and at least three paw prints per paw were measured on each day of testing. Measurements were: toe spread, first to fifth toes; intermediate toe spread, second to fourth toes; and print length end of the third toe to the bottom of the hind pad. These measurements were then used to calculate the sciatic functional index (Bain et al., 1989; Inserra et al., 1998).

2.2.8 Pinprick Assay

To assess sensory recovery following sciatic nerve crush, the pinprick test was used (Ma et al., 2011). Under light restraint, sixteen areas of the denervated paw were stimulated with a pin, and responses were scored on a three-point scale (0 – no response, 1 – light/inconsistent response, 2 – strong, consistent withdrawal response). Individual digit and composite scores were generated and compared using one-way repeated-measures analysis of variance (ANOVA) tests.

2.3 Molecular Biology

2.3.1 DRG dissections

Animals were killed by cervical dislocation, or by fatal overdose of sodium pentobarbital prior to transcardial perfusion with phosphate buffered saline (PBS). Dorsal laminectomy of the spinal cord was performed *in situ*. To identify L3-L5 DRGs, the sciatic nerve was traced up to the spinal cord, and the three ganglia attached were dissected, snap frozen in liquid nitrogen and stored at -80°C prior to RNA or protein extraction. For dissociated DRG culture experiments, cultures were washed twice with warm PBS prior to lysis.

2.3.2 RNA extraction

RNA extraction was performed with a two-step protocol consisting of phenol-chloroform extraction followed by clean-up and elution on Qiagen RNAeasy MinElute columns. Care was taken to avoid batch effects by processing samples in matched groups. Snap frozen tissues were transferred into 500 μL Trizol reagent (Invitrogen) in a fresh tube, and homogenized on ice in three 10 second bursts. Samples were lysed at room temperature for 10 minutes, then were transferred to Phase Lock Gel Heavy tubes (5 Prime), and 100 μL chloroform was added. Samples were shaken for 15 seconds and allowed to rest at room temperature for three minutes prior to centrifugation at 11300 RPM for 15 minutes at 4°C. The aqueous phase was transferred to an RNAse-free eppendorf tube, an equal volume of fresh 70% ethanol was added, and this was loaded onto columns for clean-up following the manufacturer's protocol. RNA concentration was measured using a Nanodrop Spectrophotometer (Thermo-Fisher Scientific) and 500 ng total RNA were used for subsequent first-strand cDNA synthesis reactions with SuperScript III according to manufacturer's protocol (Invitrogen).

2.3.3 Real-time quantitative PCR (RT-qPCR)

RT-qPCR was performed using the LightCycler FastStart DNA MasterPLUS SYBR Green I kit (Roche) according to manufacturer's protocol on a Roche LightCycler 480 machine. All primers used were exon-exon spanning and were tested both for efficiency using a standard curve and for specificity by melt curve analysis and gel electrophoresis of PCR products. All primers had an efficiency of 2.0 ± 0.2. Results were determined from plates where no template controls were used to ensure reagents were contamination free. Triplicate Ct values were averaged and results were analysed using the ΔΔCt method (Livak and Schmittgen, 2001).

Table 4 - RT-qPCR primers

	Forward (5' – 3')	**Reverse (5' – 3')**
Atf3	GTCACCAAGTCTGAGGCGGCC	TGACTCTTTCTGCAGGCACTCTGT
Camk2a	GCTGCCAAGATTATCAACACC	CACGCTCCAGCTTCTGGT
cJun	GGGACACAGCTTTCACCCTA	GAAAAGTAGCCCCCAACCTC
Hdac4 exon 1-2	TGAACTTAAGGCACTGACGC	AGGATTCAGCAGCTCCACAG
Hdac4 exon 6-7	CCAGCGATCCCCGCTACTGG	AGGCTGACACCCCACTCTGGG
Hdac4 exon 12-13	GCACCTCAGCAAGATAATCTC	GCTTCTTCCTCCTCACTCTC
Hdac5	TGTCACCGCCAGATGTTTTG	TGAGCAGAGCCGAGACACAG
Hdac7	CTGCTTTCAGGATAGTGGTG	ATTTGGCAGAAACATGGTGGTAGC
Hdac9	GCGAGACACAGATGCTCAGAC	TGGGTTTTCCTTCCATTGCT
Hsp27	TGTATTTCCGGGTGAAGCAC	CAGTGAAGACCAAGGAAGGC
Ntrk1	ATATCTAGCCAGCCTGCACTTTGT	GCTCATGCCAAAGTCTCCA
Snap25	GCTCCTCCACTCTTGCTACC	CAGCAAGTCAGTGGTGCTTC
Sprr1a	TGAGGAGGTACAGTGCAG GG	CAGAGAACCTGCTCTTCTCTG AGT
Sst	TTCTCTGTCTGGTTGGGCTC	CAGACTCCGTCAGTTTCTGC
Trpv1	AACCAGGGCAAAGTTCTTCC	CATCATCAACGAGGACCCAG
Vglut1	GTGCAATGACCAAGCACAAG	TAGTGCACCAGGGAGGCTAT
β-2-microglobulin	GCCTGTATGCTATCCAGAAAACCC	TGTGAGGCGGGTGGAACTGTG
Ywhaz	AGTCGTACAAAGACAGCACGCTAA	AGGCAGACAAAGGTTGGAAGG

2.3.4 TaqMan Low-Density RT-qPCR Array Cards

Custom TaqMan low-density RT-qPCR array cards were ordered from Life Technologies. On the day of the experiments, cDNA samples were diluted to 2 ng/μL in a final volume of 100 μL 1X PCR mastermix containing SYBR green in DNAse-free H2O. Samples were mixed by pipetting and loaded into wells, then cards were spun

at 1200 RPM for 2 minutes, sealed and run on an ABI 7900HT RT-qPCR machine (Applied Biosystems). Raw CT values were exported, and relative quantification was performed in Microsoft Excel using the ΔΔCT method. Multi-array express viewer (MeV) software was used to create data visualization tools.

2.3.5 Microarray

RNA was processed by UCL Genomics using an Ambion Whole transcript Expression Kit (Invitrogen) and hybridized to Affymetrix Mouse Gene Arrays (Mouse Gene 2.0ST) on a GeneChip Fluidics Station 450. Chips were scanned on an Affymetrix GeneChip Scanner. Quality control and analysis were carried out using the following bioconductor packages in R: oligo (Carvalho and Irizarry, 2010) for preprocessing, RMA normalization (Irizarry et al., 2003), and various quality controls (including MA plots, box plots, and principal component analysis) and limma (Smyth, 2005) for statistical analysis.

2.3.6 Protein extraction

Protein was extracted in lysis buffer (0.2% SDS in ddH20 with 1X protease inhibitor cocktail (Roche)) by shaking at room temperature for two hours with a Vortex at speed 4. Protein concentration was assessed by determining the absorbance at 280 nm on a Nanodrop Spectrophotometer (Thermo-Fisher Scientific). Protein lysates were stored at -80°C prior to reduction for 5 minutes at 100°C in 1X Laemmli buffer, after which they were stored at -20°C.

2.3.7 Western Blotting

20 μg of protein were run on NuPAGE® Novex® 10% Bis-Tris Gels (Invitrogen) then transferred onto 0.45-µM polyvinylidene fluoride membranes (Millipore). Membranes were blocked in 5% milk and incubated overnight at 4°C with an HDAC4 (H92, Santa Cruz) primary antibody at 1:500 dilution. After 3 washes in Tris-buffered saline and

0.1% Tween-20, a secondary antibody was used for 1 hour (1:5000, horseradish peroxidase–conjugated anti-rabbit; GE Healthcare). The signal was detected using an ECL prime kit (GE Healthcare) and visualized using a UVP GelDoc-It Imaging system (Ultraviolet products).

2.4 Tissue culture

2.4.1 Dissociated dorsal root ganglion culture

Following cervical dislocation and dorsal laminectomy, DRGs were dissected into F12 media (Gibco). Ganglia were digested for one hour at 37°C in a final concentration of 0.125% collagenase (Sigma) and 0.1 mg/mL DNAse I (Sigma), washed in 3 mL warm F12 and triturated in 2 mL F12 supplemented with 0.3% bovine serum albumin (Sigma), 1X N2 supplement (Gibco), and 1X penicillin/streptomycin (Sigma). The cell pellet was resuspended in supplemented F12 and plated onto coverslips pre-coated with poly-L-lysine (Invitrogen) and 0.01 mg/mL laminin (Sigma).

2.5 Fluorescence microscopy

2.5.1 Sample Preparation

Adult animals were transcardially perfused with freshly prepared 4% PFA in 0.1 M PB (pH 7.4-7.7) prior to dissection. Tissue was post-fixed at 4°C for 3 hours in 4% PFA in 0.1 M PB, followed by 24 hours at 4°C in 20% sucrose solution in 0.1 M PB. Samples were blocked in OCT medium (Tissue-Tek) and frozen in liquid nitrogen then stored at -80°C. Frozen sections were cut at 10 μM on a cryostat. Slides were dried for at least one hour and stored at -20°C until further processing. Slides were blocked for 30-60 minutes in 10% normal goat or donkey serum, incubated overnight at room temperature with primary antibodies, incubated for two hours in secondary

antibodies and mounted with Vectashield (Vector Labs). Antibodies used include anti-mouse NF200 (1:400, Millipore; MAB5266), anti-sheep CGRP (1:800, BioMol; CA1137), lectin-IB4 (1:50, Sigma-Aldrich), anti-rabbit TrkA (1:500, Biosensis; R152-200), anti-rabbit PGP9.5 (1:1000, Ultraclone), anti-rabbit Alexa 488 (1:1000, Invitrogen), anti-mouse Alexa 546 (1:1000, Invitrogen), anti-sheep Cy3 (1:400, Stratech; 713-166-147), anti-lectin AMCA (1:400; Vector Laboratories).

2.5.2 Immunocytochemistry

Cultured primary sensory neurons were washed three times with warm PBS, fixed with 4% PFA for twenty minutes at room temperature, washed three times in PBS and stored at 4C in PBS + 0.1% sodium azide until further processing, or blocked in 10% normal goat or donkey serum in PBS + 0.2% Triton X + 0.1% sodium azide for thirty minutes, incubated with 1:1000 anti-mouse β-3-tubulin (Promega) for one hour, washed and incubated in 1:1000 Alexa-Fluor 488 (Invitrogen) and 1:10000 DAPI (Life Technologies) for a further hour.

2.5.3 Microscopy and Image Analysis

For each experiment, a minimum of three sections, from three animals per group were used for analysis. To avoid bias, images were taken and processed in a blinded manner: animals were assigned randomized numbers at the time of dissection that were not revealed until analysis had been completed. Images of DRG tissue sections were taken using a Zeiss Axioplan 2 fluorescence microscope (Zeiss). Counting and cell size measurements were done using Image J and Axiovision software, respectively.

To assess neurite outgrowth in dissociated DRG cultures, neurons were imaged and analysed using the InCell Analyser 1000 and Developer Toolbox 1.0 software (GE Healthcare Life Sciences). The number of β-3-tubulin positive cells and the total

length of neurites per image were quantified in order to obtain a measurement of neurite length per neuron. Three wells from three independent experiments were averaged to determine the mean treatment effect.

Intraepidermal nerve fibre density was determined following the criteria of Lauria *et al.* (Lauria et al., 2005). Nerve fibres were counted at 40X magnification on a minimum of three sections per animal. The length of each section was measured in Image J, and the intraepidermal nerve fibre density was calculated as the average number of fibres counted/average section length.

2.5.4 Calcium Imaging

DRG neurons were used for Ca^{2+} imaging experiments after 18–24 h in culture. Cells were incubated in buffer (HBSS with 10 mM glucose, 10 mM HEPES, pH 7.4) with Fura-2-AM (2 µM) and probenecid (1 mM) for 60 min at 37°C, then coverslips were washed and mounted for imaging. Capsaicin was made up to 100 nM in buffer and applied to cells by continuous perfusion. Individual cell fluorescence was measured at 340 and 380 nm excitation, and 510 nm emission using a microscope-based imaging system (PTI, Ford, UK). At the end of each experiment, cells were challenged with KCl (50 mM) to provide a maximal Ca^{2+} signal against which to normalize responses. Neurons were identified morphologically and were excluded from analysis if they did not respond to KCl.

2.6 Statistical analysis and experimental design

In keeping with the 3Rs of animal testing (reduction, refinement and replacement), a large battery of behavioural tests was initially run in smaller groups to allow for the identification of any large effects (Cohen, 1988). Results that looked interesting were validated in a separate cohort of animals to decrease the chance of a false positive result.

Statistical analysis was performed with IBM SPSS v 21. Single behavioural measures, immunohistochemical counts and RT-qPCR data were analyzed using Welch's unpaired t-tests. Behavioural data with repeated measures were analyzed with repeated measures analysis of variance (RM ANOVA) tests with *day* and *paw* as within-subjects variables and genotype as the between-subjects factor. Data is presented as mean ± standard error (SEM).

For PCR array card studies, effects of injury were confirmed using multivariate ANOVAs with injury and genotype as independent variables and genes as dependent variables. To identify putative HDAC4 target genes, Welch's t-tests were used to compare similarly affected samples (e.g. cultured wt neurons vs cultured cKO neurons), followed by post-hoc false-discovery rate correction using the Benjamini-Hochberg test implemented in MS Excel. Genes that were not expressed in more than 2 samples/group were excluded from analysis. In cases where no genes passed false discovery criteria, genes were ranked by unadjusted p-value and manually inspected to investigate possible trends in the data.

3 Generation and characterization of HDAC4 mutant mice

3.1 Introduction

The creation of knock-in mouse strains is now commonly used to determine gene function *in vivo*. A number of technical advances, including recombinant DNA technology, embryonic stem cell biology and an understanding of the principles of homologous recombination allowed gene targeting to be applied to mice since the late 1980s (Capecchi, 1989). The procedure is done in two stages: first, DNA constructs are designed and inserted into embryonic stem cells (ES cells) (illustrated in Figure 7). By engineering DNA constructs that are homologous to a region of interest of the mouse chromosome and have positive and negative selection markers, only clones that have undergone correct targeting will grow under different conditions. The classical example is the use of the neomycin resistance gene (neo^r) and the HSV-tk cassette as the basis of positive-negative selection. The neo^r cassette is placed between the two homology arms so that upon recombination it will replace the targeted gene, allowing the clones to grow in neomycin. The HSV-tk cassette is placed downstream of the 3' homology arm. If a random integration has occurred, the clones will contain the HSV-tk cassette and will be sensitive to gancyclovir, an antiviral drug. Once positive clones have been identified, the ES cells will be injected into the blastocoel cavity of a 4.5 day embryo and then surgically implanted into pseudopregnant females. Commonly, the ES cells will come from a mouse strain with a different coat colour from that of the pseudopregnant female, so screening for mutations can be done on coat colour; those that are chimeric will be chosen for further breeding. If the mutation has made it into the germ cells, the progeny of a cross between a chimeric mouse and a wildtype mouse will be brown, and will have a 50% chance of carrying the mutated allele. This will be assessed

using PCR and heterozygous offspring will be mated to create homozygous mutant mice.

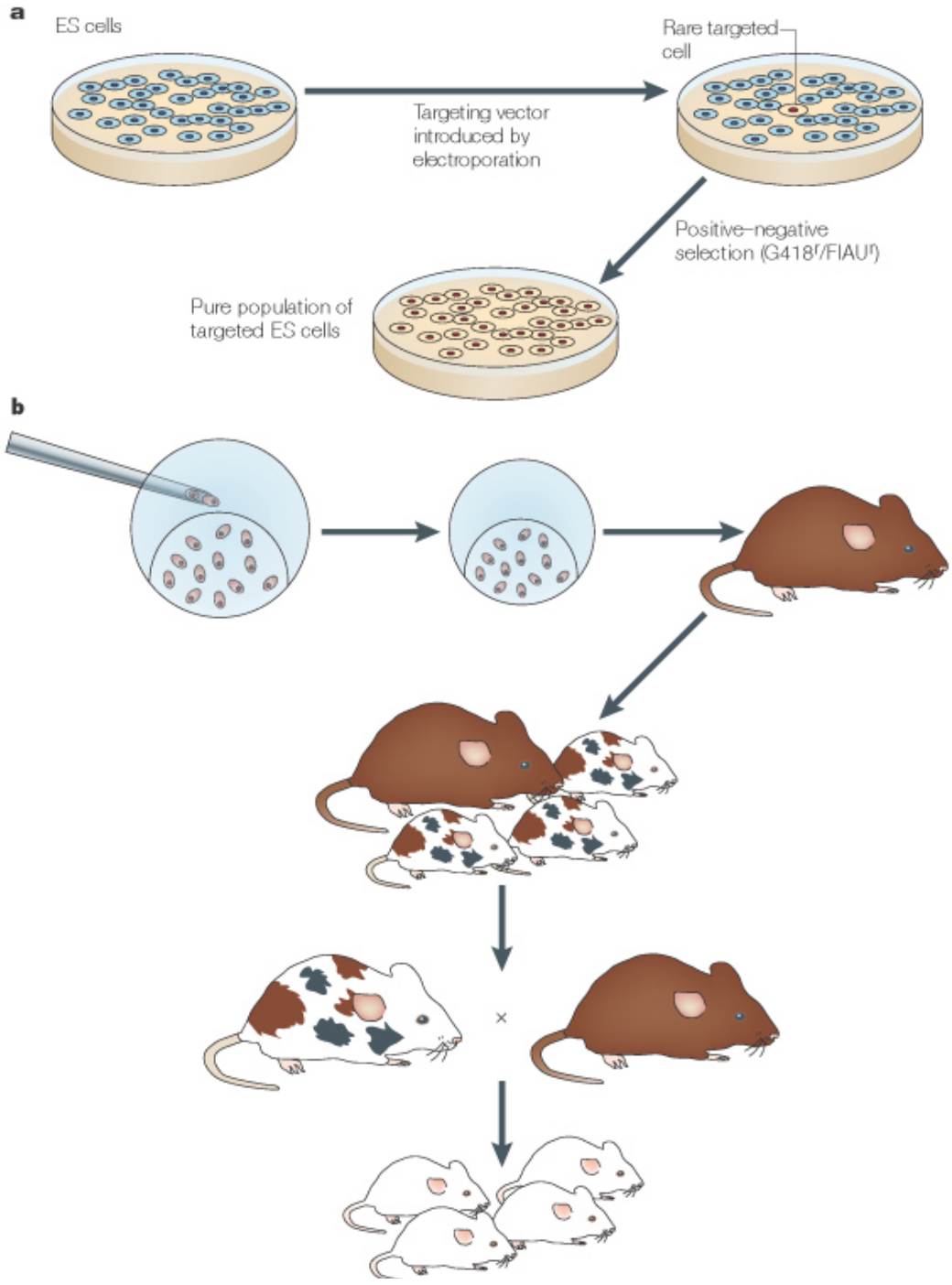


Figure 7 – General workflow to generate germline chimeras from gene-targeted embryonic stem cells, adapted from (Capecchi, 2005)

This strategy was used to produce global HDAC4 knockouts ($HDAC4^{-/-}$), first described by Vega *et al.* (Vega et al., 2004). Null HDAC4 mutants were found to have impairments in chondrocyte hypertrophy, an essential stage of bone development. Without this, ossification occurred far earlier than it should have, limiting mobility and leading to early postnatal lethality. The phenotypic abnormalities were seen as early as embryonic day 18 (E18) in $HDAC4^{-/-}$, and though the animals provided important information regarding the function of HDAC4, an alternative deletion strategy was required to determine the protein's function in adult tissues.

So-called 'conditional' deletion relies on tissue-specific promoters to cause selective mutation. One of the most commonly used methods of introducing conditional deletion is with the Cre-loxP system (Chu et al., 2008). Cre recombinase is a bacterial enzyme that recognizes particular DNA sequences (loxP sites). When it is expressed, it will snip out the area between two loxP sites and re-ligate the DNA. To create deletions in a cell population of interest, Cre recombinase is driven from a promoter that is selective for that population. When transgenic animals that express Cre are bred with animals carrying two copies of a gene with flanking loxP sites (floxed animals), heterozygous conditional knockout mice will be created. These will need to be backcrossed a further generation to produce homozygous conditional knockouts.

HDAC4 floxed mice were first described in 2007, by Eric Olson's group (Potthoff et al., 2007). In these animals, loxP sites were inserted into the introns on either side of exon 6, a region that contains the MEF binding domain which is required for HDAC4 to interact with RUNX2 and the MEF family transcription factors (Miska et al., 1999; Vega et al., 2004). Insertion of the loxP sites did not disrupt HDAC4 function and floxed animals were indistinguishable from wild-type littermates. Crossing $HDAC4^{fl/fl}$ mice with an animal carrying a globally expressed Cre resulted in global HDAC4

knockout. At the molecular level, HDAC4 protein could not be detected but an alternative transcript was clearly produced. Functionally, the mice phenocopied the global mutants, indicating that neither the alternative transcript, nor other class IIa HDACs could compensate for the loss of HDAC4.

One mouse line that has been developed to allow for conditional knockout in primary sensory neurons uses the promoter of the voltage gated sodium channel, $Na_v1.8$ (encoded by the gene *Scn9a*), to drive Cre expression (Nassar et al., 2004). $Na_v1.8$ is a member of the voltage gated sodium channel superfamily, and its expression is mainly limited to small, nociceptive sensory neurons, although recent evidence suggests that it is also expressed in a proportion of proprioceptive neurons as well (Shields et al., 2012). A targeted ablation study has indicated that this population is critical for cold, noxious mechanical and inflammatory pain sensation (Abrahamsen et al., 2008). In the $Na_v1.8$-Cre line, Cre recombinase has been knocked into the $Na_v1.8$ gene locus, downstream of the promoter. Heterozygotes display normal expression and function of the sodium channel, and consequently normal sensory and pain behaviours, whereas homozygotes phenocopy $Na_v1.8$ knockout mice.

Because $Na_v1.8$ is expressed during development, it is possible that knockout of HDAC4 at this time would affect development of the sensory neurons, particularly as known targets of HDAC4 are important in sensory neuron differentiation (Kobayashi et al., 2012; Yoshikawa et al., 2007). This is something we sought to investigate with these animals.

To avoid the complication of interpreting whether a behavioural phenotype is primary or secondary to developmental defects, an inducible knockout strategy can be employed (Wilson et al., 2008). One way to do this is to fuse Cre to a mutated form of the estrogen receptor (ERT2) that is insensitive to its endogenous ligand but is still

sensitive to tamoxifen, a competitive inhibitor of the estrogen receptor (Wang et al., 2008b). Under normal conditions, Cre is retained in the cytoplasm, chaperoned by heat-shock proteins. Upon tamoxifen administration, the drug binds the estrogen receptor and causes a conformational change that releases Cre from the chaperone proteins. Cre translocates to the nucleus and deletes floxed regions of the genome.

This can be combined with tissue-specific promoters that drive Cre to achieve inducible, tissue-specific knockout. Only very recently has this become available for sensory neuron targeting (Lau et al., 2011). Lau *et al.* made use of the bacterial artificial chromosome (BAC) transgenic approach to create animals that would express CreERT2 in all sensory neurons. BACs are used because they have a number of technical advantages over traditional methods. They can carry large amounts of information, up to several hundred kilobases of DNA, which means for any target gene they are likely to contain all of the required cis-regulatory elements for gene expression. This lends the strategy a high probability of success (Rong et al., 2010).

To target all sensory neurons, Cre is driven by the Advillin promoter. Advillin is an actin-binding protein of the gelsolin/villin family, which is expressed almost exclusively in peripheral sensory neurons (Gordon et al., 2009; Ontoria et al., 2009; Pan et al., 2010). Lau *et al.* fully characterized the transgenic mice, showing that introduction of the transgene does not affect pain or sensory behaviour, and also that tamoxifen dosing itself does not alter pain behaviour (Lau et al., 2011). With this in place, it is possible to use these mice to determine the effect of HDAC4 knockout in all adult sensory neurons.

HDAC4 is a transcriptional repressor, and has been shown to be involved in regulating genes that are important for sensory neuron differentiation and function. Interestingly, knockout mice that lack the deacetylase domain of HDAC4 reportedly have impaired thermosensation. The reason behind this is unclear, but it is tempting to speculate that this may be due to aberrant sensory neuron development. In addition, the capacity for HDAC4 to shuttle in and out of the nucleus in a calcium-dependent manner positions it as a molecular cue. The movement of HDAC4 after injury could have crucial implications for the transcriptional status of affected neurons.

3.2 Aims

The aims of this chapter are threefold:

- Validate HDAC4 knockout from both $Na_v1.8$ and Advillin positive populations of sensory neurons
- Investigate whether knockout of HDAC4 has consequences for sensory neuron development
- Characterize naïve sensory neuron transcription in the absence of HDAC4 and determine transcriptional effects of knockout in various injury models

3.3 Methods

All methods were performed as described in Chapter 2.

3.4 Results

3.4.1 Generation of HDAC4$^{Nav1.8}$ conditional knockouts

3.4.1.1 Breeding Scheme

Since the late 1990s it has been appreciated that different inbred strains of mice have varying sensitivity to nociceptive tests (Paroni et al., 2008). Because of this it has become clear that in order to understand effects of particular mutations, the background strain of the mutant mice must be considered, otherwise a nociceptive phenotype could be misattributed. The HDAC4$^{fl/fl}$ strain was initially bred onto a mixed SVz/129/Bl6 background, and at the time that we received them they had been backcrossed onto a C57/Bl6 (C57) background for two generations. We backcrossed them for two more generations. At N4, the animals should be >90% congenic, as according to Mendel's laws the amount of the donor strain is reduced by 50% with each generation (Figure 8). The $Na_v1.8$ line were backcrossed for many generations in Professor John Wood's lab (personal communication, Sam Gossage), meaning that the final cross between the N4 HDAC4$^{fl/fl}$ and the $Na_v1.8$s would yield N5 congenicity. At N5, approximately 97% of the genome should be derived from C57s. Due to time constraints, this was deemed an acceptable level of congenicity for our studies.

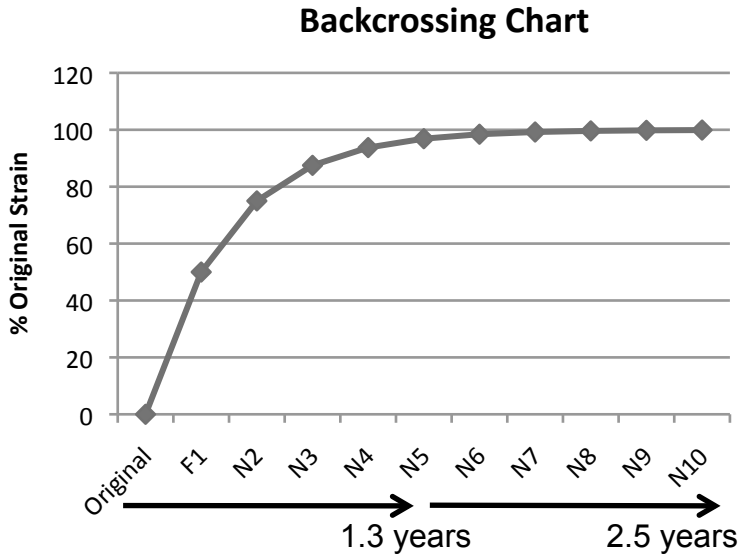


Figure 8 - By Mendel's laws, the original strain loses 50% of its genomic content with each cross to a pure inbred strain

A breeding plan was put in place to ensure that adequate numbers of experimental mice would be produced as early as possible. The breeding strategy for the experimental cohort ensured that all animals born would be used for the studies, as all were of one of the two desired genotypes, either HDAC4$^{fl/fl}$ or HDAC4$^{fl/fl}$;Na_v1.8-Cre (HDAC4 cKO). This meant that the first experimental cohort was ready to be phenotyped in February 2012 (Figure 9).

	F1 – N3 backcross		Date of cross: 7/2/2011 Date of birth: 28/2/2011
	Expected Ratio	Observed Ratio	
$HDAC4^{fl/+}$	19/19	19/19	
	F2 – N4 backcross		Date of cross: 11/4/2011 Date of birth: 2/5/2011
	Expected Ratio	Observed Ratio	
$HDAC4^{+/+}$	22.5/45	15/45	
$HDAC4^{fl/+}$	22.5/45	30/45	
	F3 – Generating $HDAC4^{fl/fl}$		Date of cross: 12/6/2011 Date of birth: 3/7/2011
	Expected Ratio	Observed Ratio	
$HDAC4^{+/+}$	10/40	11/40	
$HDAC4^{fl/+}$	20/40	19/40	
$HDAC4^{fl/fl}$	10/40	10/40	
	F4 – Generating $HDAC4^{-/+}$ cKOs ($HDAC4^{fl/fl}$ x $Na_v1.8$ $Cre^{-/-}$)		Date of cross: 14/8/2011 Date of birth: 4/9/2011
	Expected Ratio	Observed Ratio	
$HDAC4^{-/+}$ cKO	35/35	35/35	
	F5 – Generating $HDAC4_{cKO}$ ($HDAC4^{fl/fl}$ x $HDAC4^{-/+}$ cKO)		Date of cross: 16/10/2011 Date of birth: 6/11/2011
	Expected Ratio	Observed Ratio	
$HDAC4^{fl/+}$	7/28	N/A	
$HDAC4^{fl/fl}$	7/28	10/28	
$HDAC4^{-/+}$ cKO	7/28	N/A	
$HDAC4_{cKO}$	7/28	5/28	
	F6 – Generating $HDAC4_{cKO}$ and $HDAC4^{fl/fl}$ littermates		Date of cross: 18/12/2011 Date of birth: 8/1/2012
	Expected Ratio	Observed Ratio	
$HDAC4^{fl/fl}$	146.5/293	123/293	
$HDAC4_{cKO}$	146.5/293	166/293	

Figure 9 - Breeding Scheme, $HDAC4^{Nav1.8}$ cKO
$HDAC^{fl/fl}$ founders had been maintained on a mixed C57Bl/6 x CBA/1 (F1) background and required backcrossing. In each generation, animals were born in roughly Mendelian ratios. Note that in F5 Cre genotyping was only performed for $HDAC4^{fl/fl}$ animals, so the numbers of $HDAC4^{fl/+}$ and $HDAC4_{Nav1.8}$ were not assessed (N/A). Following this scheme, behavioural characterization of knockouts commenced in February 2012.

3.4.1.2 Genotyping and validation of HDAC4 knockout

To identify animals for breeding and experimental cohorts, PCR-based genotyping was used, following established protocols (Figure 10A and B). Each generation, animals were born in Mendelian ratios (Figure 9).

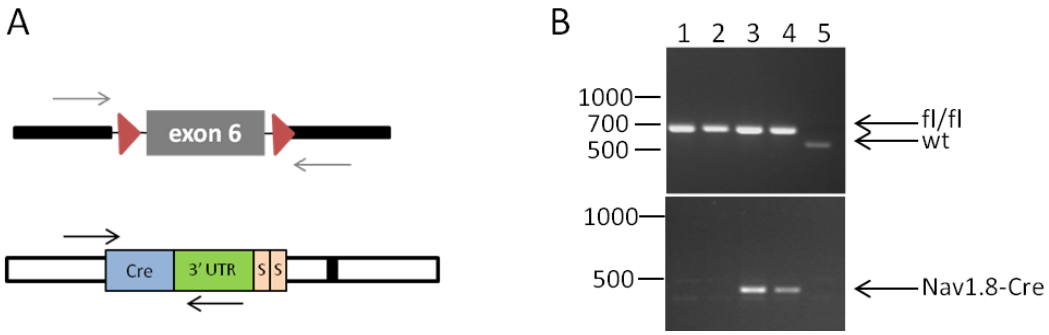


Figure 10 – Genotyping scheme and representative results
A – Schematic of primer locations for HDAC4 and $Na_v1.8$ Cre genotyping, respectively. **B** – Representative genotyping results from an F6 litter, with a wildtype negative control in lane 5.

Though both the $HDAC4^{fl/fl}$ strain and the $Na_v1.8$-Cre strain had been used independently, it was important to validate that recombination had occurred and caused successful knockout of HDAC4. This was first investigated at the genomic level, using DNA from DRG samples. The primers that were reported in the literature to detect the recombined allele did not work in my hands, so I endeavoured to design new primers that would be complementary to the intronic regions surrounding the deleted exon 6. The first sets of primers I tried failed to show a difference between the animals that were Cre positive and those that did not have Cre. Could it be that Cre was not able to access the loxP sites around HDAC4? Digging deeper, I double-checked the sequences of the primers, and that of the HDAC4 targeting construct. In the years since the mice had been first characterized, the gene had been re-annotated and a new exon had been described, making the targeted 'exon 6' called

'exon 7' on Ensembl. I designed a new set of primers and demonstrated the presence of the recombined allele (representative results Figure 16A).

The next steps were to confirm that the knockout had been successful at both the mRNA and protein levels. Cre expression in HDAC4$^{fl/fl}$ animals led to significant reduction of HDAC4 mRNA (Figure 11, n=3, $p<0.05$). Because it was reported that an alternative transcript was created in the HDAC4 cKOs, multiple sets of exon-spanning primers were designed to determine whether this could be detected using RT-qPCR. Primers spanning the targeted exon (exon 6-7) showed a statistically significant reduction in HDAC4 mRNA (fold change (FC)=0.43, n=3, p=0.04, Welch's t-test), and this was significantly less than the expression of exon 1-2 ($p<0.01$, student's t-test), but not significantly different from the expression of exon 11-12 (p=0.4, student's t-test), likely due to the high variability of exon 11-12 levels between individual samples. The expression of the other exons was also reduced in Cre positive animals compared to littermate controls (FC=0.57, =0.58, p=0.02, =0.07, Welch's t-test). This data indicates that an alternative transcript is likely to be present at lower levels than the endogenous transcript, possibly because it is less stable or subject to more degradation.

HDAC4 has a high structural homology with the three other Class IIa HDACs: HDAC5, HDAC7 and HDAC9. Because of this, there is a possibility that in the absence of HDAC4 there could be compensation for its function by one of these proteins. However, RT-qPCR analysis of the level of mRNA for each of these genes did not demonstrate a significant difference from HDAC4$^{fl/fl}$ controls (Figure 11). I interpret this to mean that compensation for HDAC4 loss was unlikely to have occurred in targeted cells.

A reduction in protein abundance was also observed using Western blotting, although this did not achieve statistical significance (FC=0.39, n=4-5, p=0.06). The residual expression of HDAC mRNA and protein is expected since there are many cells in the DRG that do not express Cre – both neurons not expressing $Na_v1.8$ and many non-neuronal cells. The combined genomic, transcriptional and protein evidence confirms that HDAC4 has been successfully deleted in this novel strain of conditional knockouts.

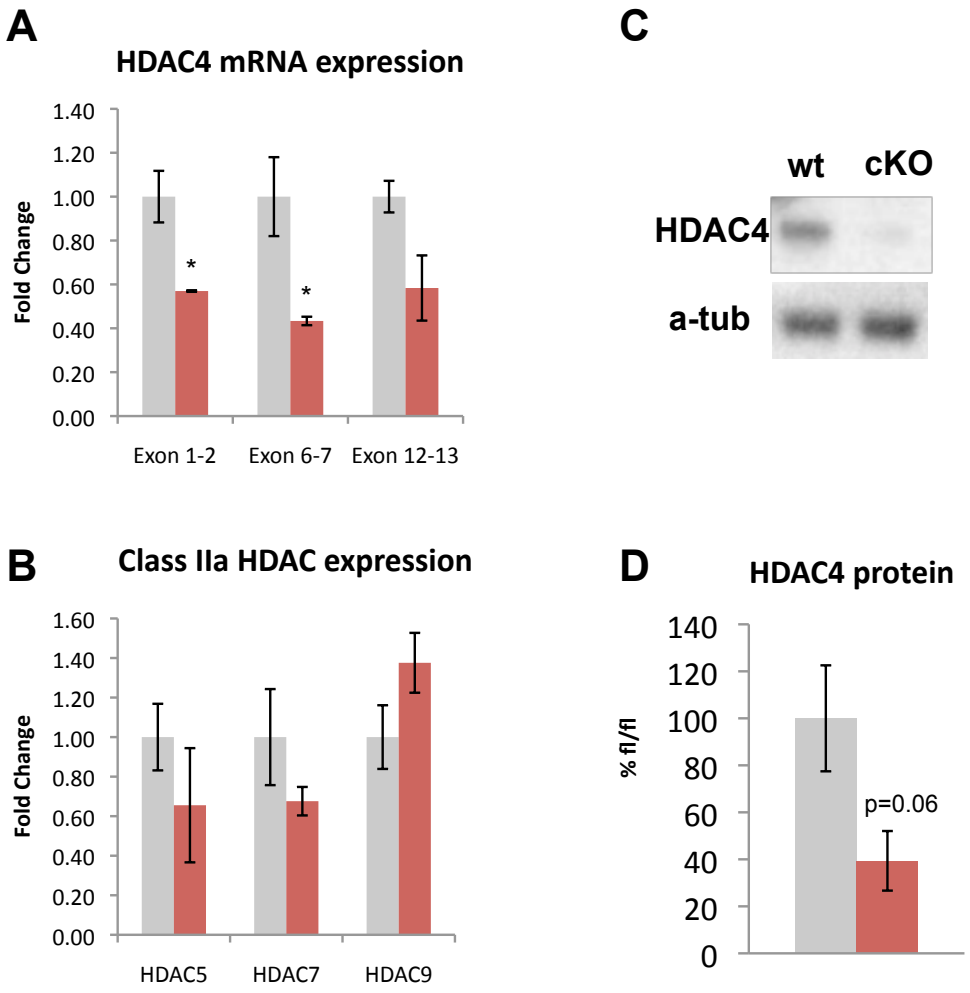


Figure 11 – Cre driven from the $Na_v1.8$ promoter successfully causes deletion of floxed HDAC4 in the DRG
A – *Hdac4* mRNA levels were measured using RT-qPCR. Both exons 1-2 and exons 6-7 were significantly less expressed in HDAC4 cKOs ($p<0.05$, n=3, Welch's t-test). **B –** Class IIa HDAC expression was measured by RT-qPCR. No significant differences were observed. **C** – Representative Western blot for HDAC4 with alpha-tubulin (a-tub) loading control **D** – Densitometric analysis indicates that HDAC4 cKO have reduced levels of HDAC4 protein but this did not achieve statistical significance (39%, n=4-5, p=0.06).

3.4.2 Functional effects of HDAC4 knockout in $Na_v1.8$-positive sensory neurons

3.4.2.1 Determining the effect of HDAC4 on sensory neuron development

Previous work on HDAC4 has implicated it in regulating the expression of the Runt family of transcription factors, which are critical for sensory neuron differentiation. For example, forced *Runx1* overexpression using the *Tau* promoter leads to a marked reduction of TrkA positive cells, and CGRP expression (Samad et al., 2010). Since the Cre used to generate these mutants is expressed during embryonic development, I sought to determine whether HDAC4 could play a role in sensory neuron differentiation by characterizing cell size distributions, and the proportion of cells expressing TrkA and the subtype markers CGRP, IB4 and neurofilament 200 (NF200) in adult L4 sensory ganglia using immunohistochemistry.

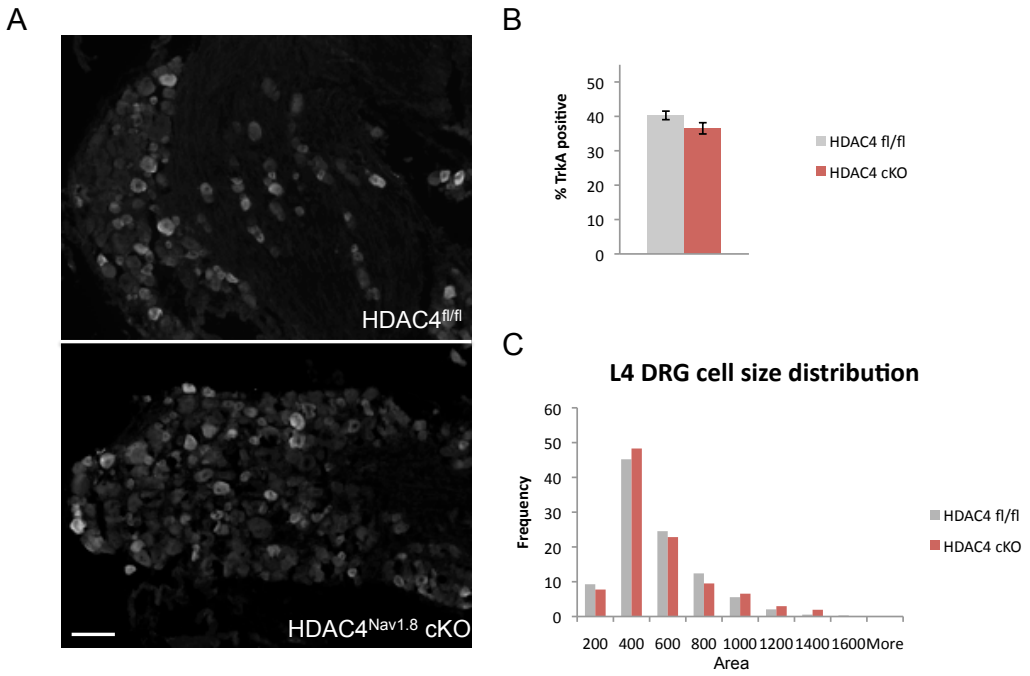


Figure 12 – There is no difference in the proportion of TrkA positive neurons or cell size in HDAC4$^{Nav1.8}$ cKOs compared to littermate controls
A – Whole L4 ganglia from HDAC4$^{Nav1.8}$ cKO and HDAC4$^{fl/fl}$ animals were stained for TrkA. Scale bar represents 100 μM. **B** – Quantification of immunofluorescence. Similar proportions of DRG cell profiles were found to be TrkA positive (40.3%, 36.5%). **C** – Similar cell size distributions were observed between the two genotypes

No difference in the proportion of TrkA positive cells was observed. Similarly, when we performed a size distribution of DRG profiles, we did not see a loss of small neurons. Furthermore, there were no differences in the proportion of cells expressing any of the three markers in HDAC4 cKOs (Table 5, Figure 13). From this analysis we could not find evidence for a role of HDAC4 in sensory neuron differentiation.

Table 5 - Quantification of subpopulation markers
Counting was done on 3-5 sections from at least 3 animals per genotype. No difference was observed in the proportion of profiles expressing the different population markers, suggesting that HDAC4 is dispensable for sensory neuron diversification (images next page)

	IB4			CGRP			NF200		
	#	total	%	#	total	%	#	total	%
HDAC4$^{fl/fl}$	711	1771	40.1	332	885	37.5	378	1186	31.9
HDAC4$^{Nav1.8}$ cKO	910	2229	40.8	263	689	38.2	302	1014	29.8

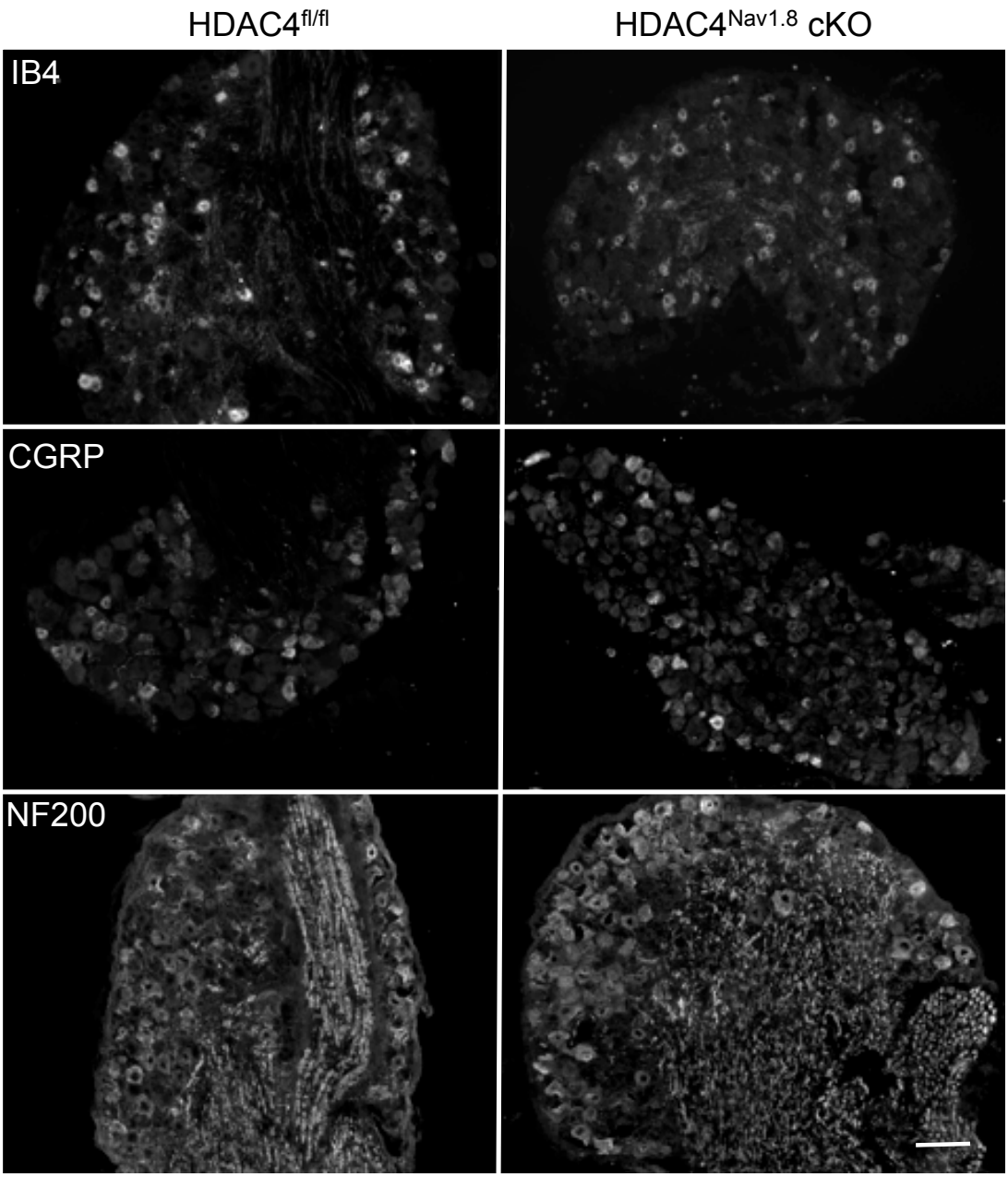


Figure 13 - HDAC4 is not required for sensory neuron differentiation
Images show representative naïve L4 DRG from HDAC4$^{fl/fl}$ animals on the left and HDAC4$^{Nav1.8}$ cKOs on the right; scale bar represents 100 μM. CGRP, IB4 and NF200 immunoreactivity can be used to classify the major subgroups of the DRG, namely the peptidergic unmyelinated/thinly myelinated neurons, the nonpeptidergic unmyelinated neurons, and the large myelinated neurons. Both HDAC4$^{fl/fl}$ and HDAC4$^{Nav1.8}$ cKOs showed equal proportions of these markers, indicating that HDAC4 does not play a role in sensory neuron diversification.

3.4.2.2 Transcriptional regulation in naïve animals

To determine the effect of HDAC4 on transcriptional regulation, I performed an affymetrix array on adult DRG samples from experimentally naïve HDAC4$^{fl/fl}$ and HDAC4 cKO animals. Analysis of this data proved that HDAC4 has little role in regulating transcription in naive sensory neurons. A principle component analysis (PCA) showed a high degree of overlap between the samples. The LIMMA algorithm was used to discover alternatively regulated transcripts. No genes passed this test (data not shown).

Similarly, medium-throughput analysis of mRNA levels using custom-designed Taq-Man low-density array cards yielded only four differentially regulated genes (from a pool of 48 genes on a 'pain card') at a statistical significance cut-off unadjusted $p<0.05$: *Ptgs2*, *Trpa1*, and the voltage-gated sodium channel genes *Scn11a* and *Scn10a* that encode for $Na_v1.9$ and $Na_v1.8$, respectively. The expression changes were small (<2 fold) and did not pass false-discovery testing using the Benjamini-Hochberg test (Figure 14), which may explain why they were not seen in the microarray. It is curious that the expression of these genes is lower than that observed in controls, as HDAC4 is thought to have a negative effect on transcription, so in its absence one would expect upregulation of target genes. This may imply that HDAC4 works to repress a negative transcriptional regulator, for example REST/NRSF. Interestingly, both *Trpa1* and *Scn10a* expression are regulated by REST knockdown (Uchida et al., 2010). Furthermore, HDAC4 has previously been linked to *Ptgs2* expression (Wang et al., 2008a). It may be interesting to follow up this finding using a protein expression assay, like an ELISA.

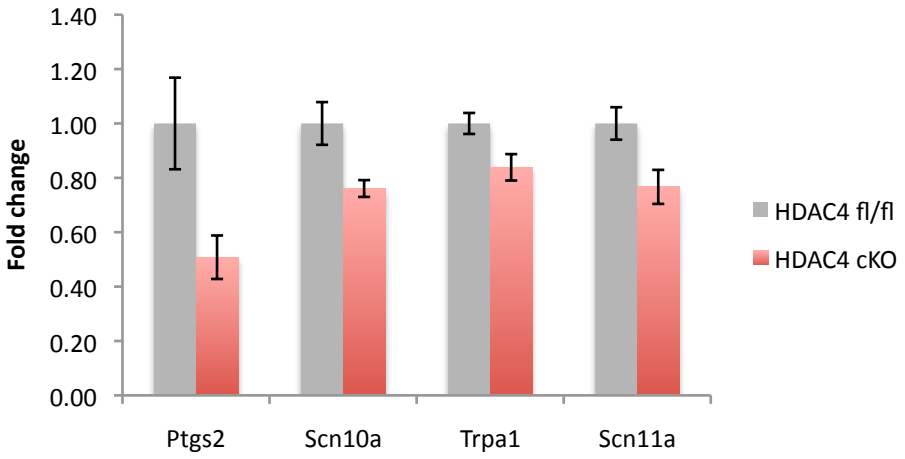


Figure 14 – HDAC4 has a limited effect on gene expression in naïve sensory neurons
Four genes were differentially expressed in naïve HDAC4$^{Nav1.8}$ cKO samples at a statistical cut-off of unadjusted p≤0.05: *Ptgs2* (FC=0.51, p=0.05); *Scn10a* (FC=0.76, p=0.05); *Trpa1* (FC=0.84, p=0.04) and *Scn11a* (FC=0.77, p=0.04). Although none of these survived false discovery testing, this may imply a role for HDAC4 in regulating the transcription of these genes.

3.4.2.3 Transcriptional regulation in a nerve injury model

Although robust transcriptional alterations were not observed in naïve DRG samples, I wondered whether the loss of HDAC4 would have implications for the transcriptional response to injury. Acute DRG dissociation and incubation in a high concentration of NGF (50 ng/mL) was used as an *in vitro* injury model. Putative HDAC4 targets were identified by comparing HDAC4$^{fl/fl}$ cultures with HDAC4$^{Nav1.8}$ cKO cultures. Using a cut-off value of unadjusted p<0.01, six genes were found to be differentially regulated: somatostatin (*Sst*), *Ngf,* the gene encoding TrkA (*Ntrk1*), calcitonin-related polypeptide alpha (*Calca*) that encodes for CGRP, *Trpv1* and the nerve growth factor inducible peptide *Vgf* (Figure 15). Of note, only *Ntrk1* passed false-discovery testing. To validate this analysis, a multivariate ANOVA was performed to compare gene expression after culturing with that of naïve adult DRGs, with injury and genotype as independent variables and genes as dependent variables. All genes discovered using unadjusted p-value criteria were also found to have significant interaction of *genotype x injury* (for details, see Table 6).

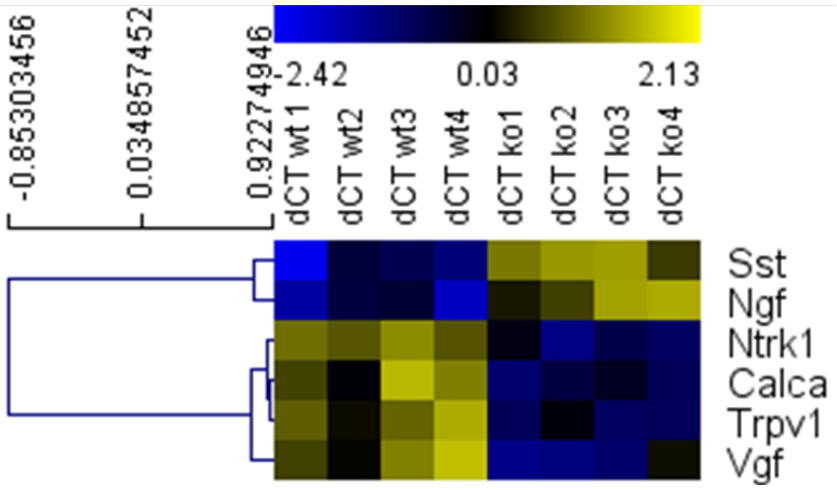


Figure 15 - Loss of HDAC4 results in altered transcriptional regulation following acute dissociation of DRG neurons
The heat map shows normalized individual expression values for six differentially regulated genes, with blue meaning lower expression and yellow meaning higher expression. Genes are arranged by hierarchical clustering, with those that were upregulated in the HDAC4 cKOs at the top, and downregulated genes below.

Interestingly, the majority of these genes are related to NGF signaling. *Ngf* itself was upregulated in the knockout, whereas its receptor, *Ntrk1*, and downstream target, *Vgf*, were both downregulated. TRPV1 activity is also known to be regulated by NGF (Ji et al., 2002), and has been shown to have implications for CGRP release (Meng et al., 2009; Nakanishi et al., 2010). This suggests that HDAC4$^{Nav1.8}$ cKOs may show reduced behavioural hypersensitivity, which will be discussed in Chapter 5.

Table 6 - Multivariate analysis confirms that HDAC4 is required for transcriptional regulation of NGF-associated genes
Genes are listed in the order that they appear in the heatmap in Figure 15. Analyses were performed against datasets from naïve adult DRG, with the factors *injury* (naïve vs cultured) and *genotype* (wildtype vs. HDAC4$^{Nav1.8}$ cKO). All genes discovered using t-tests were found to have significant genotype*injury interaction effects at p<0.02.

	Main effect of injury		**Main effect of genotype**		**Interaction genotype*injury**	
	p	**$F_{(1,12)}$**	**p**	**$F_{(1,12)}$**	**p**	**$F_{(1,12)}$**
Sst	<0.0001	26.32	0.001	21.37	0.019	7.26
Ngf	<0.0001	108.56	n.s	-	0.006	11.22
Ntrk1	0.001	20.92	<0.0001	27.48	0.002	15.13
Calca	n.s.	-	0.001	17.12	0.013	8.61
Trpv1	n.s.	-	0.017	7.64	0.002	15.92
Vgf	<0.0001	109.03	0.002	16.08	<0.0001	25.15

3.4.3 Advillin CreERT2 conditional knockout

The Advillin CreERT2 line was being developed and characterized early on in my PhD, and was made available for our use in mid-2012. A similar breeding strategy was adopted for the generation of HDAC4 Advillin CreERT2 cKOs ($HDAC4^{Adv}$ cKO). By the time the Advillin CreERT2 animals had been transferred to our animal house, I had already backcrossed $HDAC4^{fl/fl}$ twice to N4 C57 and could immediately cross the $HDAC4^{fl/fl}$ animals with the Cre line. Our first experimental cohort was ready to be dosed with tamoxifen in April 2013.

3.4.3.1 Genotyping and knockout validation

PCR based genotyping was used to inform breeding pair selection, following established protocols. Because BAC-derived genes can integrate at multiple sites in the chromosome, they may not follow Mendelian inheritance. However, if the transgene has integrated into one chromosome, there should be approximately 50% inheritance (Haruyama et al., 2009). We received four founders from Professor John Wood's lab, of which two successful litters were derived. One of these yielded 50% transgene expression, and this line was continued to produce HDAC4 cKOs. Cre positive animals were never crossed with one another to reduce the possibility of differing copy numbers between experimental animals.

Similarly to the $HDAC4^{Nav1.8}$ cKO line, it was necessary to validate the knockout of HDAC4 in this novel strain of conditional mutants. To do this, we analysed events at the DNA, RNA and protein level one week after the end of tamoxifen dosing. Using the same protocols and primers described above (see chapter 3.4.1.2), we successfully detected the recombined HDAC4 allele in DRG samples of Cre positive animals (Figure 16).

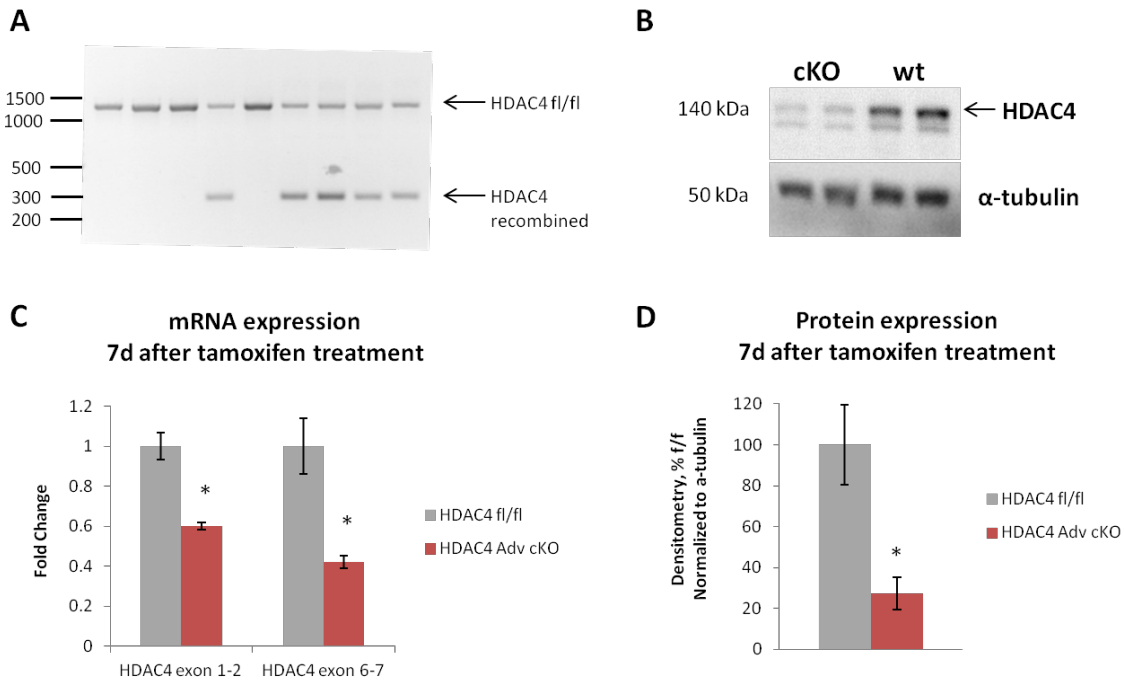


Figure 16 - Validation of HDAC4^{Adv} conditional deletion
HDAC4 conditional deletion was validated using PCR, RT-qPCR and Western blotting seven days after treatment with tamoxifen. **A –** PCR-based genotyping revealed the presence of the recombined (deleted) allele in Advillin-CreERT2 positive animals treated with tamoxifen. **B –** Western blot showing the loss of HDAC4 from Advillin-CreERT2 animals. The identity of the lower band is unknown. **C –** RT-qPCR revealed significant reduction in *Hdac4* mRNA in Advilin-CreERT2 animals (FC=0.6, =0.42, $p<0.05$) **D –** Quantification of the Western blot in B. Significant knockdown of HDAC4 protein was observed in tamoxifen-treated Advillin-CreERT2 animals (27.3% of controls, $p<0.05$). The remaining protein is possibly due to non-neuronal expression of HDAC4.

To determine whether reduced HDAC4 expression could be detected at the mRNA level, RT-qPCR against exons 1-2 and the targeted exon 6-7 was used. Results from RT-qPCR showed that, indeed, there was a significant reduction in the level of HDAC4 mRNA expression in Cre positive animals (Figure 16). Although both exons showed significantly reduced expression (n=3-4, p=0.021 exon 1-2, p=0.023 exon 6-7, Welch's t-test), the fold change between genotypes was greater for the targeted exon 6 (0.42 vs 0.60), possibly due to an alternate transcript that is maintained in the conditional knockout.

Protein levels of HDAC4 were assessed using western blotting. Cre positive animals had significantly less HDAC4 protein than Cre negative littermate controls (27.2% of control, n=3-4, p=0.047, Welch's t-test).

This evidence indicates that there has been successful targeting, tamoxifen administration and recombination of HDAC4 in the DRG, and that these animals can be used for further functional analysis.

3.4.4 Functional effects of HDAC4 deletion in adult sensory neurons

3.4.4.1 Transcriptional regulation in naïve animals

It was important to determine whether upregulation of other HDACs may compensate for the loss of HDAC4. RT-qPCR was used to look for the expression of HDAC5, HDAC7 and HDAC9, the other Class IIa HDACs. Interestingly, one week after tamoxifen administration, upregulation of both HDAC5 (1.7 fold, n=3, p=0.078) and HDAC9 was observed (1.4 fold, n=3, p=0.037), but HDAC7 expression was not affected (1.1 fold, n=3, p=0.5) (Figure 17).

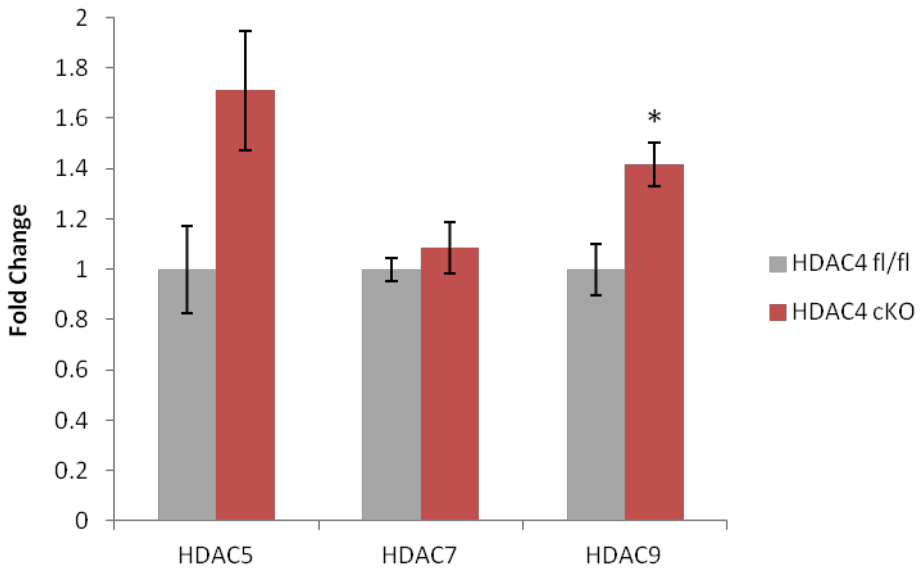


Figure 17 - Class IIa HDACs are upregulated following HDAC4 deletion
One week after tamoxifen treatment, RNA was extracted from HDAC4$^{fl/fl}$ and HDAC4^{Adv} cKO DRGs. A trend toward upregulation of other class IIa HDAC family members was observed in cKO samples, with *Hdac9* expression showing a statistically significant increase (FC=1.4, p=0.04). This suggests that class IIa HDAC expression is tightly regulated in adult sensory neurons, and may imply functional compensation for HDAC4 loss.

I further characterized the transcriptional differences between HDAC4^{Adv} cKOs and littermates using TaqMan PCR array cards as described previously. Interestingly,

Cacna2d1, Trpa1, the gene encoding the vaso-active intestinal protein (*Vip*), the mu-opioid receptor gene (*Oprm1)* and purinoreceptor 3 (*P2rx3*), were all differentially regulated in HDAC4^{Adv} cKOs at a statistical cut-off of unadjusted p<0.05 (Figure 18). However, it must be noted that none of these passed false-discovery criteria using the Benjamini-Hochberg test.

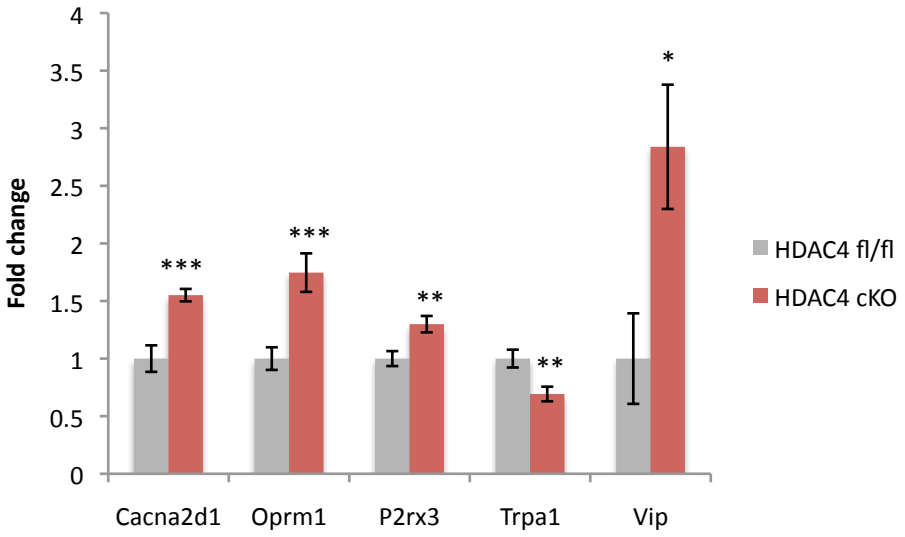


Figure 18 - Knockout of HDAC4 from adult DRG results in altered gene expression
Genes are arranged by unadjusted p-value. ***=p<0.01, **=p<0.02, *=p<0.05, n=4, Welch's t-test. N.B. No genes passed false-discovery testing. *Cacna2d1, Oprm1, P2rx3* and *Vip* were upregulated in HDAC4^{Adv} cKOs (FC=1.55, 1.75, 1.3, 2.84) and *Trpa1* was downregulated (FC=0.69).

3.4.4.2 Transcriptional regulation is altered in HDAC4^{Adv} cKOs after sciatic nerve transection

Having previously discovered that HDAC4$^{Nav1.8}$ cKO responded differently to an *in vitro* nerve injury model, we sought to determine whether HDAC4^{Adv} cKOs would also exhibit transcriptional dysregulation in response to nerve injury. The sciatic nerve transection model was used, and 24 hours after *in vivo* axotomy, L3 and L4 lumbar ganglia were harvested for RNA extraction and subsequent RT-qPCR analysis using TaqMan low-density array cards.

Comparison of wildtype (HDAC4$^{fl/fl}$) and HDAC4^{Adv} cKO ipsilateral gene expression revealed seven genes that were differentially expressed at an unadjusted p<0.05: *Ngf, Gad2, Scn10a*, *Calca, Cacna2d1, Trpa1* and *Vip1* (n=4, Welch's t-test) (Figure 19). Multivariate analysis of this data with the factors *injury* (sciatic nerve transection ipsi vs. contra) and *genotype* (wildtype vs. HDAC4^{Adv} cKO) confirmed significant main effects of *injury* for *Scn10a* ($F_{(1,12)}$=6.45, p=0.026), *Cacna2d1* ($F_{(1,12)}$=22.71, p<0.0001), *Gad2* ($F_{(1,12)}$=284.77, p<0.0001), and *Ngf* ($F_{(1,12)}$=56.23, p<0.0001). Significant main effects of *genotype* were observed for *Scn10a* ($F_{(1,12)}$=9.47, p=0.01), *Cacna2d1* ($F_{(1,12)}$=21.57, p=0.001), *Trpa1* ($F_{(1,12)}$=20.09, p=0.001), *Gad2* ($F_{(1,12)}$= 15.96, p=0.002), and *Vip* ($F_{(1,12)}$=11.30, p=0.006) and near significant *genotype x injury* interaction effects were observed for *Calca* ($F_{(1,12)}$=4.50, p=0.055) and *Ngf* ($F_{(1,12)}$=3.88, p=0.07).

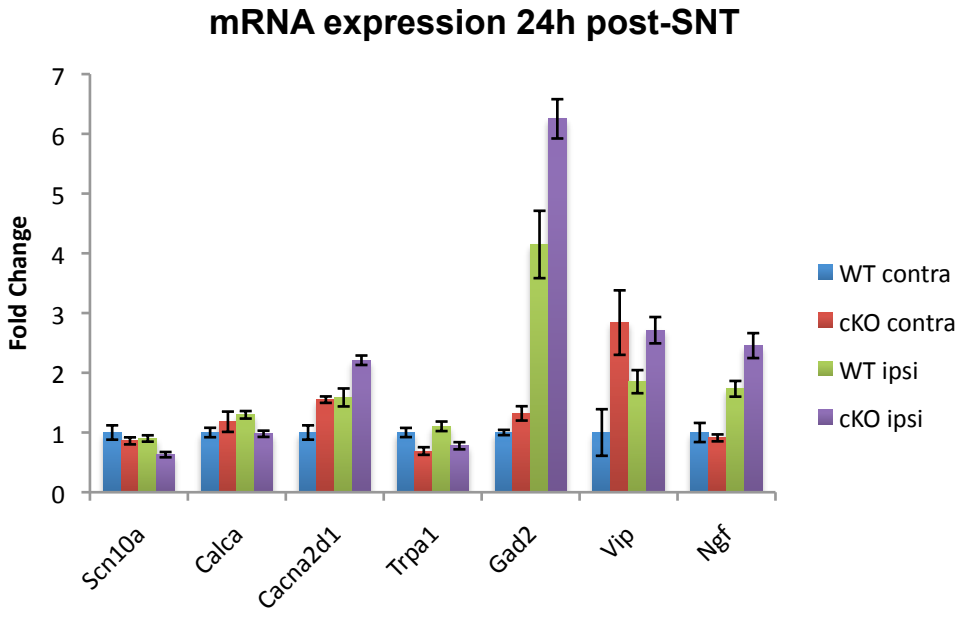


Figure 19 – After peripheral nerve injury multiple genes trend toward differential expression between HDAC4^{Adv} cKOs and littermates
Columns represent fold changes over uninjured wildtype controls (wt contra). Genes that were differentially regulated between injured wt and HDAC4^{Adv} cKO samples at unadjusted p<0.05 are shown. After correcting for multiple comparisons, no genes were statistically significant. Of note, *Calca* and *Ngf* expression trend in the same direction as changes observed in HDAC4$^{Nav1.8}$ cKOs.

After sciatic nerve transection *Scn10a, Calca* and *Trpa1* were expressed at lower levels in HDAC4^{Adv} cKOs compared to littermates, whereas *Ngf, Gad2, Cacna2d1* and *Vip* were expressed at higher levels. The overexpression of *Ngf* and downregulation of *Calca* were similar to what had been observed previously in the HDAC4$^{Nav1.8}$ cKOs (Figure 15), indicating that these might be conserved HDAC4 targets.

3.4.5 Is there a consistent effect of HDAC4 deletion on sensory neuron transcription? Comparing transcription data from HDAC4$^{Nav1.8}$ and HDAC4^{Adv} cKOs

HDAC4 has been shown to be critical for the regulation of a number of genes related to synaptic plasticity (Sando Iii et al., 2012), a key mechanism that underlies chronic pain. Conditional deletion of HDAC4 was associated with altered transcription in both strains of mice after injury. We hypothesized that true HDAC4 target genes would show consistent differences in both strains of conditional mutants. To investigate this we compared TaqMan low-density array card RT-qPCR data from four different models of injury: an *in vitro* inflammation model (dissociation + 50 ng/mL NGF), partial sciatic nerve ligation, sciatic nerve transection (SNT) and the Complete Freund's adjuvant (CFA) model of chronic inflammation (Table 7).

Table 7 - List of studies used for transcription 'meta-analysis'

	KO strain	Injury model	Tissue	Time point
Study 1	HDAC4$^{Nav1.8}$	dissociation (axotomy) + 50 ng/mL NGF (inflammation)	dissociated neurons	3 hours after plating
Study 2	HDAC4$^{Nav1.8}$	partial sciatic nerve ligation; naive control	L3-L5 DRG	D28 after injury
Study 3	HDAC4^{Adv}	sciatic nerve transection (axotomy)	L3-L5 DRG ipsi and contra	24 hours after injury
Study 4	HDAC4^{Adv}	Intraplantar injection of Complete Freund's Adjuvant (inflammation)	L3-L5 DRG ipsi	D15 after injury

3.4.5.1 Effect of HDAC4 deletion on uninjured sensory neuron transcription

To compare results from the different experiments, analysis was performed on normalized cycle time (CT) values (delta CT (dCT) = $CT_{gene\ of\ interest} - CT_{reference\ gene}$). Similar to previous results from the affymetrix array, comparison of naïve or uninjured samples (from studies 2 and 3) revealed no significant differences in gene expression between cKOs and littermate controls (n=8, $p>0.05$, Welch's t-test).

However, ranking the top ten gene expression changes by p-value in both datasets revealed that *Cacna2d1* was upregulated in both HDAC4$^{Nav1.8}$ cKOs and HDAC4^{Adv} cKOs (FC=1.32, 1.55; p=0.13, 0.01) and *Trpa1* was downregulated (FC=0.84, 0.69; p=0.04, 0.02) (Table 8, Figure 20), suggesting that HDAC4 is required to maintain transcript levels for these genes.

Table 8 - Top ranked gene expression changes, naïve and SNT contra

	HDAC4$^{Nav1.8}$ Naive	
	p	**Average FC cKO**
Scn11a	0.04	0.77
Trpa1	***0.04***	***0.84***
Scn10a	0.05	0.76
Ptgs2	0.05	0.51
Sgk1	0.08	0.69
Cacna2d1	***0.13***	***1.32***
Tacr1	0.15	1.67
Gabbr1	0.16	0.89
Ngf	0.20	0.44
Scn3a	0.23	1.50

	HDAC4^{Adv} Contra	
	p	**Average FC cKO**
Cacna2d1	***0.01***	***1.55***
Opmr1	0.01	1.75
P2rx3	0.02	1.30
Trpa1	***0.02***	***0.69***
Vip	0.04	2.84
Ntrk1	0.06	1.15
Vgf	0.07	1.48
Gad2	0.07	1.32
Kcns1	0.07	1.25
Bdnf	0.14	2.08

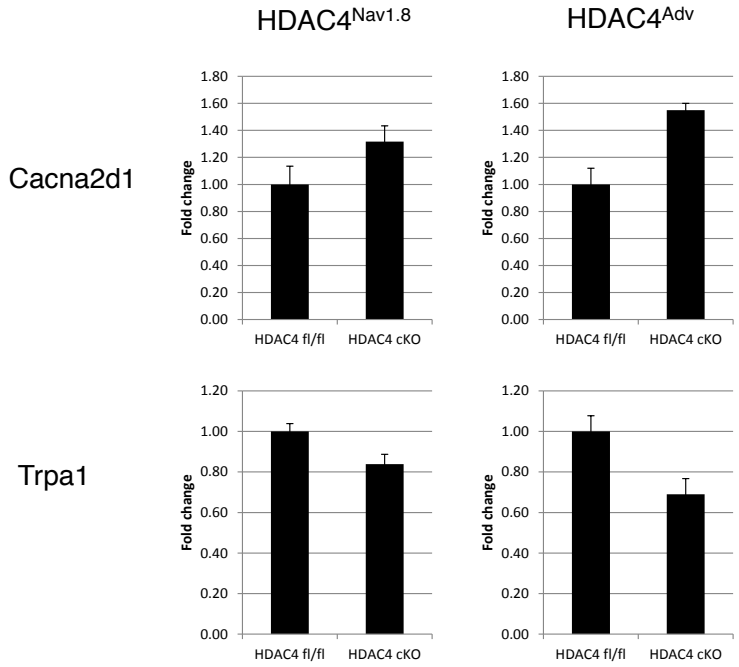


Figure 20 - *Cacna2d1* and *Trpa1* trend toward differential expression in both strains of HDAC4 cKOs.
Charts were generated from PCR array card data. FC and unadjusted p-values are as listed in Table 8. Interestingly, larger fold changes were observed in HDAC4^{Adv} cKOs, which is consistent with the deletion of HDAC4 from a larger population of sensory neurons.

3.4.5.2 Effect of HDAC4 deletion on sensory neuron transcription after injury

In contrast, comparison of gene expression after injury revealed three genes that were consistently differentially regulated in both strains of HDAC4 cKOs: *Calca, Ntrk1,* and *Trpv1* (Figure 21) (n=16, p<0.01, Welch's t-test). All genes were downregulated in HDAC4 cKOs compared to controls (average fold change =0.46, 0.54, 0.60, respectively). It must be noted that only *Calca* passed false discovery testing.

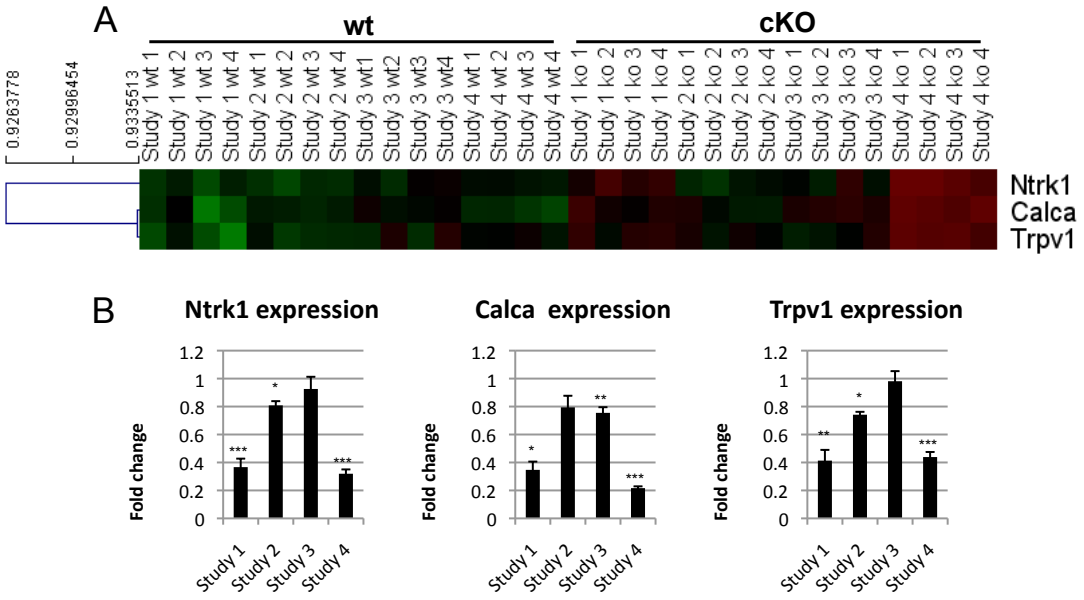


Figure 21 - HDAC4 cKO have altered transcriptional responses to injury
A transcription 'meta-analysis' indicated that *Ntrk1*, *Calca* and *Trpv1* were consistently downregulated in both strains of HDAC4 cKOs compared to similarly affected littermates after injury. NB Only *Calca* passed false discovery criteria. **A** – Heat map generated from dCT expression values. Each square comes from an individual sample, with HDAC4$^{fl/fl}$ samples on the left and HDAC4 cKO samples on the right. Genes are clustered hierarchically, with green representing higher expression, and red representing lower expression. Interestingly, *Trpv1* and *Calca* are very closely clustered, which is consistent with the known dependence of CGRP release on TRPV1 activity (Meng et al., 2009; Nakanishi et al., 2010). **B** – Fold change values from the individual experiments. Larger fold changes were observed in studies 1 and 4, which had a more direct inflammatory component. (***p<0.001, **p<0.01, *p<0.05, n=4, Welch's t-test).

3.5 Discussion

3.5.1 $Na_v1.8$ Cre and Advillin CreERT2 successfully recombine floxed HDAC4

Targeted deletion is a powerful tool to investigate gene function *in vivo,* leading to great advances in our understanding of biological systems. HDAC4 function has been linked to sensory processing: humans with mutations to HDAC4 exhibit signs of self-harm and have increased pain thresholds (Williams et al., 2010), and mice that lack the deacetylase domain of HDAC4 are less sensitive to noxious thermal stimuli (Rajan et al., 2009). Characterization of HDAC4 function in adults requires a conditional knockout strategy, as global knockout is lethal in the early post-natal stage (Vega et al., 2004). *Nav1.8* and *Advillin* are sensory neuron specific genes; Cre driven from their promoters allows for selective deletion of floxed alleles at different stages and in different sensory neuron populations (Lau et al., 2011; Nassar et al., 2004). These Cre lines have been validated for use in pain studies, as they have been shown not to interfere with normal sensory processing.

Crossing these Cre lines with the floxed *Hdac4* line resulted in recombination of *Hdac4*, such that mRNA and protein expression was significantly reduced. As expected, some message and protein did remain in the DRG in both strains of mice.

The remaining message in the $HDAC4^{Nav1.8}$ cKO is likely to arise from the $Na_v1.8$-negative cells of the DRG: Aβ and Aδ neurons and non-neuronal cells such as satellite glia. The remaining message and protein in the $HDAC4^{Adv}$ line could derive from non-neuronal cells, or may be due to incomplete tamoxifen-mediated Cre release. In the original paper that describes the Advillin CreERT2 line, a 90% recombination rate is reported using a flox-stop LacZ reporter line (Lau et al., 2011). The recombination efficiency cannot be directly translated because excision of floxed

regions is highly dependent on chromatin compaction, which is region specific. However, it indicates that the remaining message and protein could come from neurons that have not been exposed to tamoxifen. Staining for HDAC4 in sensory neurons after tamoxifen administration would illuminate this. One limitation has been finding reliable HDAC4 antibodies for immunohistochemistry. Although we have been able to validate antibodies for western blotting, these bind nonspecifically in frozen tissue sections under all conditions tested (data not shown). HDAC4-specific antibodies, or the use of epitope or GFP tagged mutants are required to address this.

3.5.2 HDAC4 is not required for sensory neuron development

HDAC4 is known to negatively regulate RUNX2 (Vega et al., 2004) and RUNX3 (Jin et al., 2004). Both RUNX1 and RUNX3 are required for sensory neuron differentiation (Chen et al., 2006; Kramer, 2006; Lopes et al., 2012; Lou et al., 2013; Marmigere et al., 2006; Nakamura et al., 2008; Samad et al., 2010). Due to the homology of RUNX1 with RUNX2 and RUNX3 we hypothesized that HDAC4 knockout from the $Na_v1.8$ population would phenocopy *Tau*-driven RUNX1 over-expressing animals, that have a characteristic pattern of altered sensory neuron development (Samad et al., 2010), including loss of TrkA positive neurons and reduced expression of CGRP. Immunohistochemical analysis of sensory neuron populations in adult DRG did not support this hypothesis, as $HDAC4^{Nav1.8}$ cKO animals had similar proportions of cells expressing markers for the three main neuronal subtypes, TrkA staining and cell size distribution. From this data we concluded that HDAC4 is not likely to repress RUNX1 in sensory neurons, possibly due to its subcellular localization in development. HDAC4 is normally cytoplasmic in neurons, but undergoes phosphorylation and activity-dependent shuttling to the nucleus (Sando Iii et al., 2012), where it would be able to interact with transcription factors like RUNX1. It is possible that at the stage in development when RUNX1 is active, HDAC4 is maintained in the cytoplasm. This

could be discerned using cellular fractionation and western blotting for RUNX1 and HDAC4, or through immunohistochemical analysis. HDAC4-specific antibodies, or the use of epitope or GFP-tagged HDAC4 mutants are required to investigate the subcellular localization of HDAC4 under different conditions and in development.

3.5.3 HDAC4 may be required for *Cacna2d1* and *Trpa1* expression in uninjured sensory neurons

HDAC4 has been shown to regulate the transcription of a number of genes associated with synaptic plasticity (Li et al., 2012; Sando Iii et al., 2012) and to interact with multiple transcription factors, such as CREB and MEF that are important for regulating neuronal function. We hypothesized that loss of HDAC4 would have consequences for the regulation of sensory neuron transcription.

Using a medium-throughput RT-qPCR screening method, four genes were found to be differentially regulated in experimentally naïve HDAC4$^{Nav1.8}$ cKO DRG: *Ptgs2*, *Trpa1, Scn10a* and *Scn11a*. All of these genes were less expressed in cKOs. In the HDAC4^{Adv} cKO animals, a few differences in gene expression were seen contralateral to nerve injury (considered in this case to reflect baseline transcriptional differences between genotypes). These included *Trpa1,* which was downregulated, as well as *Oprm1, P2rx3, Vip* and *Cacna2d1,* that were upregulated in cKOs. Further work to validate these changes with independent RT-qPCRs and Western blotting are required.

In contrast to the transcriptional differences observed with PCR array cards, microarray analysis of naïve adult HDAC4$^{Nav1.8}$ cKO and HDAC4$^{fl/fl}$ DRG yielded no significant differences between genotypes. This is in line with experiments from HDAC4^{CamKIIa} cKO, which lack HDAC4 in cortex, and which also do not exhibit altered transcription when compared to littermate controls (Kim et al., 2012). This is further

evidence that HDAC4 is not required for neuronal development, and does not alter baseline transcriptional programmes that lead to long-term changes in gene expression. However, technical limitations having to do with the analysis of microarray data (normalization) may also mask some of the transcriptional differences that do truly exist.

Microarray analysis relies on algorithms that normalize expression values across a chip, under the assumption that in most experiments, most genes will not be affected. However, the limitation of this assumption means that any intervention that causes global changes to gene expression, for example the use of a histone deacetylase inhibitor which will non-selectively increase gene expression across the entire genome, will be masked by the normalization process (Lovén et al., 2012). To get around this issue, it is necessary to either include samples with known RNA amounts as a kind of "standard" to correct against, or to use Next generation sequencing methods, or any other kind of direct quantification (such as the NanoString technology). These may reveal transcriptional differences that had previously been unrecognized using the LIMMA or SAM algorithms.

3.5.4 HDAC4 regulates transcriptional responses after injury

A key mechanism that underlies HDAC4 function is nucleo-cytoplasmic shuttling. This occurs in an activity-dependent manner. It is conceivable that injury could result in shuttling of HDAC4, allowing it to alter gene expression associated with synaptic plasticity or neuronal growth. Alternatively, it may interact with other factors in the cytoplasm that are required for altered transcription. Direct evidence of HDAC4 shuttling in the DRG is still lacking, and is a question that is important to resolve. Transcriptional regulation in the absence of HDAC4 provides some clues as to the role of HDAC4 after injury.

Across four different injury models, at different time points and in two HDAC4 knockout strains, there were consistent differences in gene expression between conditional knockouts and littermate controls. By analyzing all of this data together, as one dataset, the power of the analysis is increased, and it is possible to track down common HDAC4 target genes. In this manner I identified *Calca*, *Trpv1*, and *Ntrk1* as putative HDAC4 targets. These three transcripts were found to be less expressed in conditional knockouts than in littermate controls, which is curious considering that HDAC4 is a negative transcriptional regulator. This may suggest that HDAC4 does not directly alter the transcription of these genes. Indeed, published HDAC4 ChIP-Seq data from the cerebellum does not show enrichment for HDAC4 near these genes, although this may be due to cell-type specificity (Li et al., 2012). Interestingly, a recent study has shown that knockout of HDAC4 in cardiomyocytes results in altered chromatin dynamics, with knockout hearts exhibiting greater amounts of histone H3 lysine 9 (H3K9) di- and tri-methylation on the promoter region of a gene associated with stress-induced cardiac failure (Hohl et al., 2013). These marks are correlated to transcriptional repression (Kouzarides, 2007). Whether the 'paradoxical' downregulation of *Ntrk1*, *Calca* and *Trpv1* is associated with changes to these marks remains to be seen. Other possibilities for the mechanism underlying this transcriptional change are discussed in Appendix 1: Bioinformatics analysis of HDAC4 expression and function.

All of these genes are required for appropriate responses to inflammatory and heat stimuli, and are regulated by NGF (Ji et al., 2002; Lindsay and Harmar, 1989; McMahon, 1996). For example, NGF binding to TrkA sensitizes TRPV1 channels via the action of multiple intracellular signaling cascades (Bonnington and McNaughton, 2003; Chuang et al., 2001), and can increase protein expression in a p38-MAPK dependent manner (Ji et al., 2002). The increased expression and activity of TRPV1

leads to thermal hypersensitivity (Galoyan et al., 2003). In turn, NGF and TRPV1 signaling have also been shown to induce *Calca* mRNA expression (Lindsay and Harmar, 1989; Nakanishi et al., 2010). CGRP is an important signaling molecule at both the central and peripheral terminals of sensory neurons, and its expression levels have been shown to predict thermal hypersensitivity (Mogil, 2005). As all of these transcripts are reduced in HDAC4 cKOs, this may indicate that cKO animals would be less responsive to inflammatory mediators, and show reduced thermal hyperalgesia in models of inflammatory pain. This was investigated, and will be discussed in Chapter 5.

HDAC4 has been shown to interact with many different transcription factors, and is also capable of directly binding DNA. Further work to determine the mechanisms by which HDAC4 alters gene expression in sensory neurons is required.

4 HDAC4 and Regeneration

4.1 Introduction

In science, sometimes the most interesting findings are accidental. In the previous chapter, I reported that HDAC4 cKOs have lower relative mRNA expression of *Ntrk1*, the gene that encodes the high-affinity NGF receptor, TrkA. This finding was of interest to us as NGF signaling via TrkA is required for sensory neuron development, and in adults NGF is an important peripheral pain mediator (Pezet and McMahon, 2006). *Ntrk1* downregulation was initially observed three hours after culturing dissociated neurons in a high concentration of NGF (50 ng/mL). There were three hypotheses postulated to account for this: 1 – *Ntrk1* is constitutively expressed at lower levels in conditional knockouts, 2 – *Ntrk1* becomes downregulated as a result of nerve injury, 3 – *Ntrk1* becomes downregulated as a result of reduced NGF signaling. To test the first, I checked the level of *Ntrk1* in freshly dissected tissue; to test the second, I first performed an axotomy and then looked for *Ntrk1* expression levels; to test the third, I tried to validate an NGF application procedure, using *Bdnf* and *Hdac9* mRNA expression as a functional read-out, as they are known NGF targets (Guo et al., 2011; Michael et al., 1997).

As I was going through these experiments, I used the injury-induced transcription factor, *Atf3* as a positive control following axotomy. Interestingly, in cKO animals, *Atf3* showed a much lower expression level in this injury paradigm (Figure 22). When I compared this to data I had from HDAC4$^{Nav1.8}$ cKOs after partial sciatic nerve ligation, I discovered that *Atf3* was also less upregulated in this injury model. Intrigued, we began a series of experiments to explore the potential link between HDAC4 and ATF3.

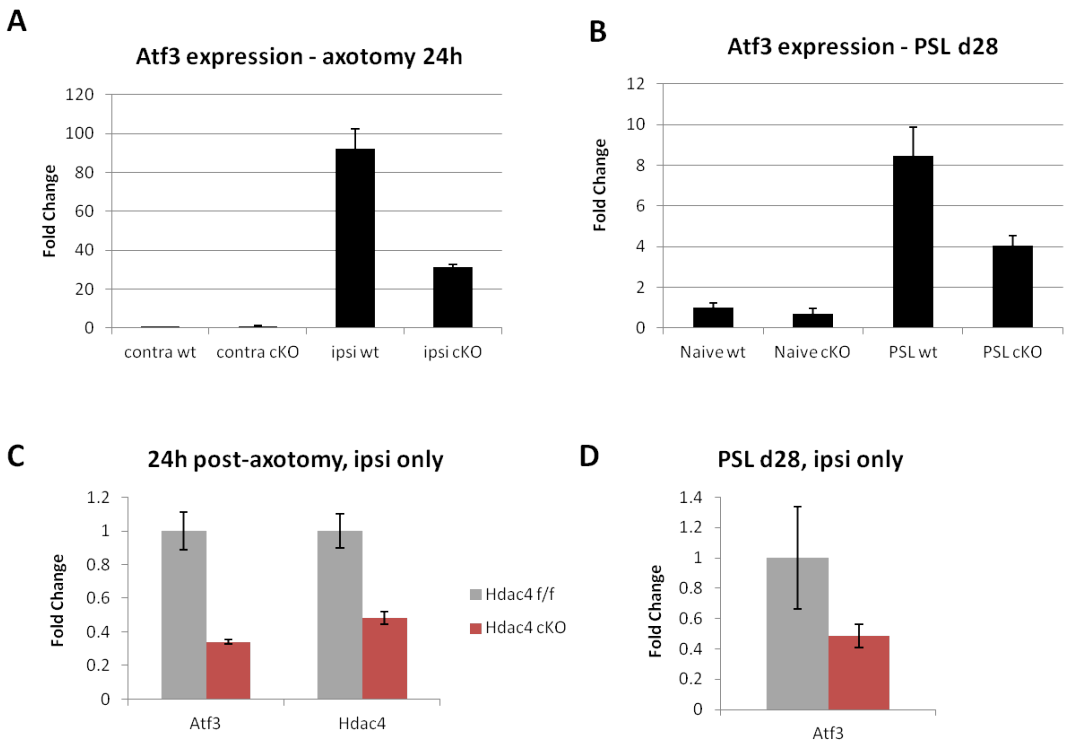


Figure 22 – After peripheral nerve injury, *Atf3* is less upregulated in HDAC4$^{Nav1.8}$ cKO DRG samples compared to littermate controls
A – RT-qPCR data from DRG 24 hours after sciatic nerve transection (axotomy). *Atf3* is upregulated after injury, however HDAC4 cKO induce *Atf3* to a lesser extent (wt FC=91.4, cKO FC=31.4, n=2). **B** – *Atf3* mRNA is upregulated after partial sciatic nerve ligation injury in both HDAC4 cKO and littermate controls ($p<0.01$, n=4), but HDAC4 cKOs show less upregulation (wt FC=8.5, cKO FC=4.1) **C** – Ipsilateral expression only, *Hdac4* shown as positive control. *Atf3* is less expressed in HDAC cKO (FC=0.34). **D** – Ipsilateral side only, PSL. *Atf3* is less expressed in HDAC4 cKO (FC=0.48, $p=0.05$, n=4)

ATF3 is a member of ATF/CREB subfamily of the basic region-leucine zipper (bZIP) family of transcription factors. Its expression is increased by multiple cell stress paradigms, a process that has been shown to rely on many different signaling pathways including JNK, p38, PKC and NFKB and the transcription factors Egr1, ATF2 and Fos/Jun (for review see (Hai et al., 2010)). In the DRG, ATF3 has been used as a marker of injury since 2000, when Tsujino *et al.* described its rapid induction in the nucleus following nerve injury (Tsujino et al., 2000). More recent work has indicated that supplementing growth factors can reduce ATF3 induction in a population-specific manner, suggesting that it is downstream of growth factor

receptor signaling pathways as well (Averill et al., 2004; Wang et al., 2003). This is supported by previous work showing robust ATF3 upregulation in growth factor deprived PC12 cells (Mayumi-Matsuda et al., 1999). Considering its interesting expression pattern, the function of ATF3 in the DRG is still less well-characterized than perhaps it deserves to be. One story that has emerged has implicated ATF3 in promoting nerve regeneration after injury. Delivery of ATF3 has been shown to enhance neurite outgrowth *in vitro* (Pearson et al., 2003; Seijffers et al., 2006) and increase the rate of regeneration *in vivo* (Seijffers et al., 2007).

HDAC4 nuclear accumulation has previously been linked to altered *Atf3* mRNA expression (Schlumm et al., 2013). Could HDAC4 be responsible for coordinating the expression of ATF3 in sensory neurons and play a role in peripheral nerve regeneration?

4.2 Aims

The aims of this chapter are to explore the observed transcriptional dysregulation of *Atf3* using the two sensory neuron-specific HDAC4 knockout lines established in Chapter 3 to determine whether HDAC4 is required for sensory neuron regeneration.

4.3 Methods

All experiments were performed as described in Chapter 2.

4.4 Results

4.4.1 Pilot data indicate that HDAC4 may be involved in functional recovery following peripheral nerve injury, via an ATF3-dependent transcriptional mechanism

Data from our pilot experiments demonstrated reduced expression of *Atf3* in HDAC4$^{Nav1.8}$ cKO DRGs following peripheral nerve injury. ATF3 has previously been reported to regulate the expression of regeneration-associated genes including the heat-shock protein 27 (*Hsp27),* the small proline-rich protein 1a (*Sprr1a)* and *cJun* (Seijffers et al., 2007), and it was hypothesized that in the HDAC4$^{Nav1.8}$ cKOs we may expect to see reduced expression of these genes compared to littermate controls. To test this hypothesis, I designed RT-qPCR primers for the three gene products and compared their expression in the DRG twenty-four hours after sciatic nerve transection injury (Figure 23). Once again, *Atf3* was less robustly induced in HDAC4$^{Nav1.8}$ conditional knockouts after this injury (wt FC=62.9, cKO FC=19.8, p=0.005 ipsi vs ipsi, n=3, Welch's t-test). In addition, the three injury-associated transcripts were upregulated, and *Sprr1a* expression achieved statistical significance in the ipsilateral DRG in both HDAC4 cKOs and littermate controls compared to the contralateral control samples ($p<0.01$, n=4, Welch's t-test). Although there was no statistically significant difference in gene expression between genotypes, a trend toward decreased induction in the conditional knockouts was observed for both *Hsp27* (FC 2.67 vs 2.17) and *Sprr1a* (FC 307.77 vs 240.87) compared to wildtype controls.

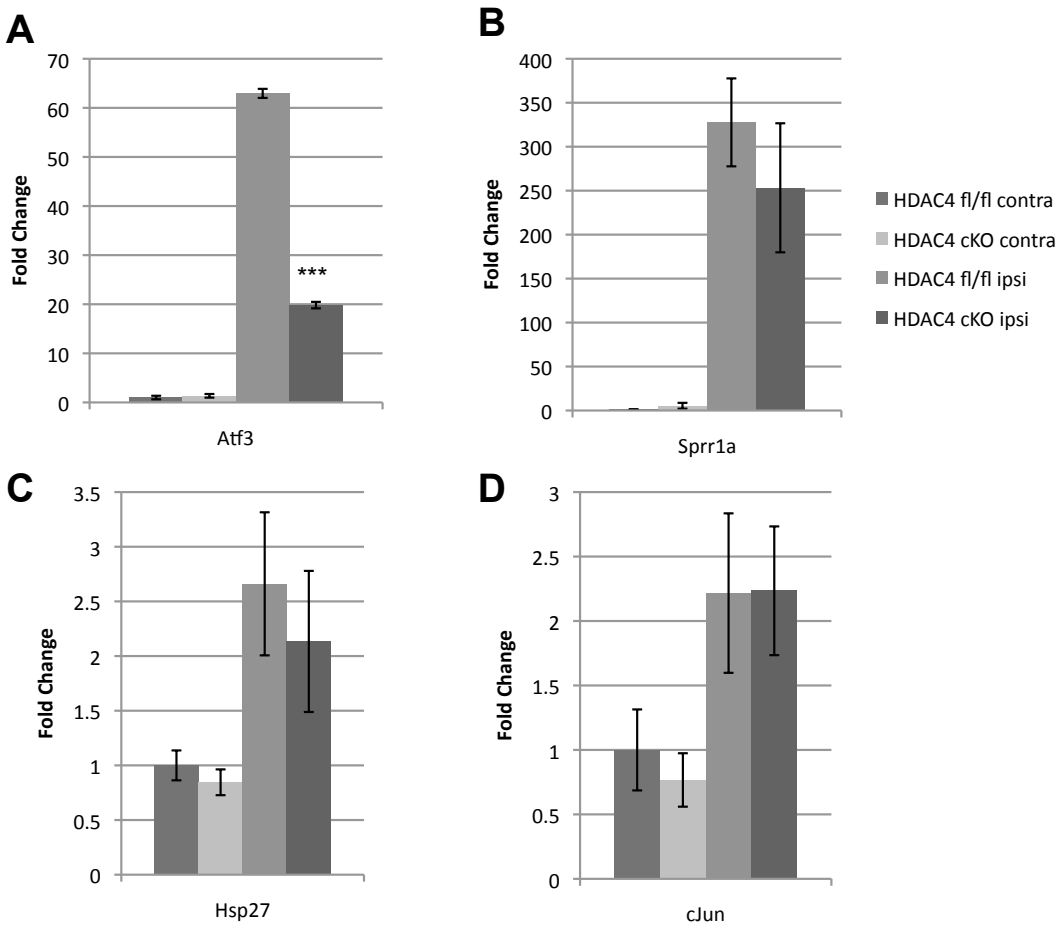


Figure 23 - Regeneration-associated genes are induced after sciatic nerve transection
RT-qPCR analysis of mRNA expression 24 hours after sciatic nerve transection. **A** – *Atf3* expression is upregulated more in wt littermates than in HDAC4 cKO (p=0.005, n=3) **B** – *Sprr1a* is significantly upregulated after injury (FC=327.7, =253.3, p<0.01 wt ipsi vs wt contra, n=4). A slight trend toward lower expression of *Sprr1a* is observed in HDAC4 cKO, however this is not statistically significant. **C** – *Hsp27* is induced after injury, with a slight trend toward lower expression in HDAC4 cKOs (FC=2.7, =2.1, p=0.07 wt ipsi vs wt contra, n=4) **D** – *cJun* is upregulated to a similar extent in both HDAC4 cKOs and littermate controls

Following from this data, we performed a pilot behavioural experiment and assessed motor and sensory recovery after sciatic nerve crush, using the sciatic functional index and pinprick tests, respectively. In the sciatic functional index test, paw placement while walking is compared between affected and unaffected paws. At baseline, the difference between the paws should be close to 0. After injury on the left side, the score becomes negative. This recovers over time. The pinprick test is a binary test of sensation. Under light restraint, the affected paw is poked with a pin in 16 different areas: on the 6 footpads and on distal and proximal areas of the digits.

The response is scored as yes (2 points), no (0 points) or inconsistent (1 point). After injury, animals do not respond on the affected side, but continue to respond on the unaffected side. This recovers over time, with animals first beginning to respond to more proximal stimulation and later responding to stimulation of the distal areas of the digits. Using these tests we observed no statistically significant difference between genotypes, however a trend toward delayed sensory recovery was observed at day 14 (Figure 24).

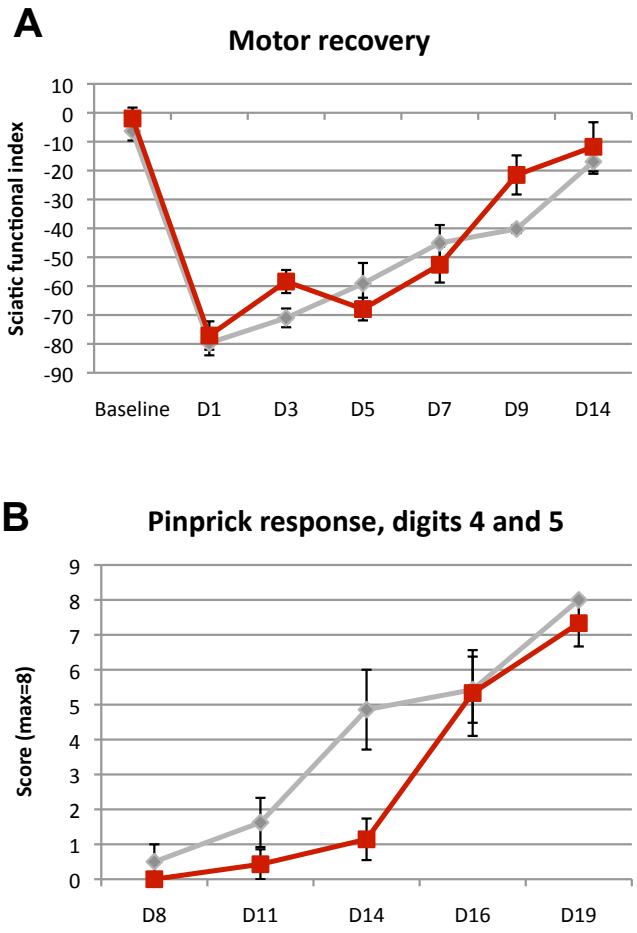


Figure 24 – A trend toward delayed sensory recovery was observed in HDAC4$^{Nav1.8}$ cKOs after sciatic nerve crush
The sciatic functional index and pinprick tests were used to assess motor and sensory recovery, respectively, after sciatic nerve crush. Red represents HDAC4$^{Nav1.8}$ cKO and grey lines represent HDAC4$^{fl/fl}$ controls **A** – Impairment in paw and digit placement was observed immediately following crush injury, which recovered nearly to baseline levels after two weeks. No difference was observed between genotypes. **B** – Pinprick responses were marked out of a maximum of 8 points. RM ANOVA revealed no statistically significant difference between groups over the entire recovery period, however lower responses were observed at D14 (n=6-7)

4.4.2 HDAC4 does not affect neurite outgrowth *in vitro*, or regeneration of epidermal nerve fibres after peripheral nerve injury

Unlike neurons of the central nervous system, peripheral sensory neurons have a high regenerative capacity, and readily grow neurites *in vitro*. This can be enhanced by the addition of growth factors, such as NGF. To determine whether HDAC4 is involved in mediating neurite outgrowth, a semi-automated image-analysis system was used to measure neurite length after twenty-four hours in culture. Cells from wildtype C57Bl/6 animals were incubated in different concentrations of NGF, and allowed to grow for twenty-four hours before being fixed and stained with beta-3-tubulin, a pan-neuronal marker. Eight images of each well were taken using the InCell Analyser, then this was processed using a semi-automated software program that allows the user to set parameters to select particular features within an image field. In this case, the cell body was identified separately from the neurites, which gave a quantification of both the number of neurons and the length of neurites in each well. For each condition, a measure of neurite length/neuron was assessed. Using these parameters, the program was capable of detecting an increasing neurite growth response with increasing NGF concentrations, that peaked at 10 ng/mL (Figure 25), however the effect sizes were small, with the maximum response only two-fold higher than the baseline. Following this, the same experiment was performed using cultures from HDAC4 cKO and wildtype controls. No difference in neurite outgrowth was observed between groups at any individual dose, however a comparison of the dose response curve indicated that HDAC4 cKOs responded much less to NGF (slope: wt = 45.3; cKO = 9.5). Contrary to our hypothesis, a trend toward increased neurite outgrowth was observed in HDAC4 cKOs at all but the highest dose of NGF.

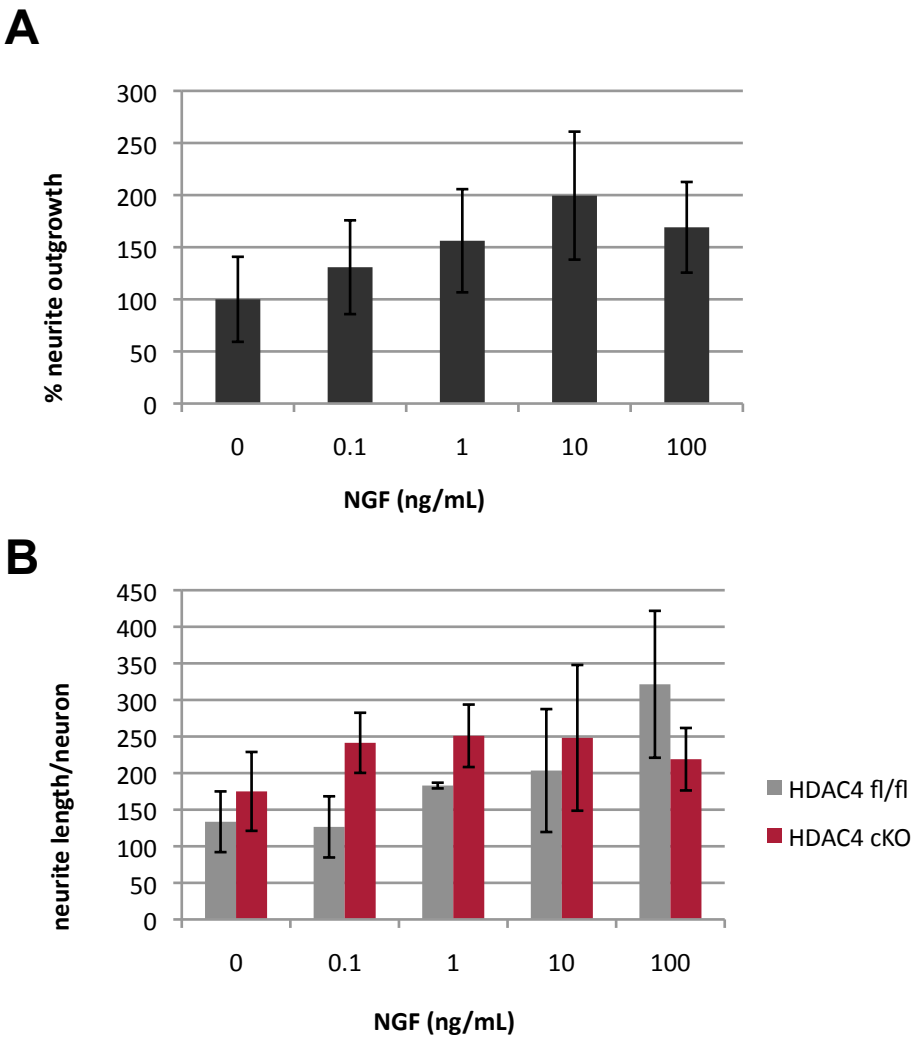


Figure 25 - Neurite outgrowth is not impaired in HDAC4$^{Nav1.8}$ cKOs
A – Bars represent average neurite length/neuron from three independent experiments, normalized to 0 ng/mL NGF control. Increasing concentrations of NGF increase the average neurite length, with a maximal response at 10 ng/mL. **B** – Using the same assay, a less robust NGF dose response was observed, and there was a high degree of variability between cultures. Though there appears to be a trend toward longer neurites in the HDAC$^{Nav1.8}$ cKO cultures across a range of doses, none of these were statistically significant (n=3).

I wondered whether the selective nature of the knockout may limit the capacity to visualize the differences in outgrowth. For example, it is possible that outgrowth from large sensory neurons, which are not $Na_v1.8$ positive, would obscure differences. We attempted to stain for CGRP and peripherin to get around this problem, but the high variability of staining meant that we could not use these to quantify outgrowth (data not shown).

Instead, I used a different measure of nerve regeneration - the density of innervation in the skin of the affected paw after sciatic crush injury. The advantage of this method is that it is specific for nociceptive Aδ and C-fibres, which are primarily $Na_v1.8$ positive. In this model, the sciatic nerve undergoes Wallerian degeneration distal to the crush injury, and epidermal nerve fibres are completely lost. As the nerve regenerates over time, the epidermis is re-innervated. PGP9.5 is a pan-neuronal marker and as expected, at twenty-one days after injury there was a significant loss of PGP9.5 staining on the affected side. This was not different between genotypes (Figure 26).

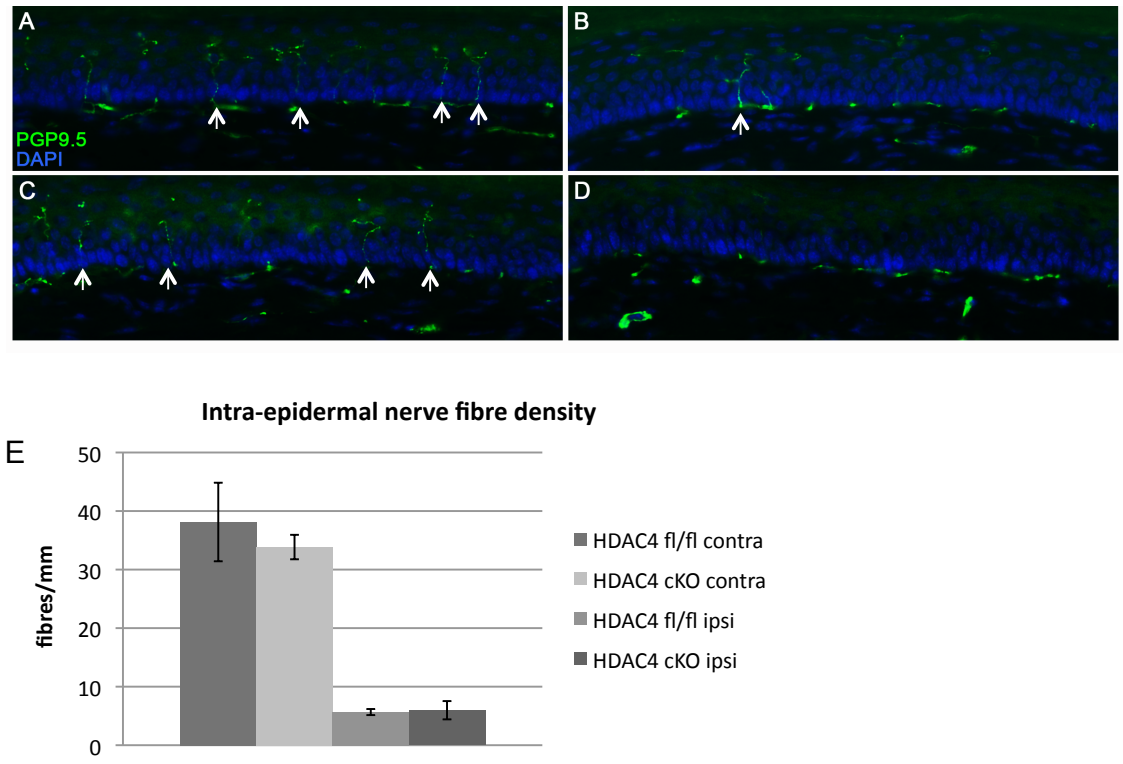


Figure 26 – HDAC4$^{Nav1.8}$ cKOs have similar epidermal innervation after sciatic nerve crush when compared to littermate controls
PGP9.5 was used to mark nerve fibres (green), and DAPI nuclear staining (blue) was used to visualize the epidermal border. Crossing fibres are indicated by arrows. All staining was performed 21 days after nerve injury. Scale bar represents 50 μM. **A** – HDAC4$^{fl/fl}$ contralateral to injury. **B** – HDAC4$^{fl/fl}$ ipsilateral to injury. **C** - HDAC4$^{Nav1.8}$ cKO contralateral to injury. **D** - HDAC4$^{Nav1.8}$ cKO ipsilateral to injury. **E** – Quantification of epidermal innervation is expressed as fibres/mm. A marked reduction in fibre density was observed ipsilateral to injury, however no difference was observed between groups (n=3-5)

Although more optimal experiments could be performed to have a definitive conclusion, from this evidence it appeared unlikely that HDAC4 has a significant role in mediating neurite outgrowth *in vitro* and for epidermal re-innervation *in vivo*.

4.4.3 HDAC4 cKOs have similar ATF3 protein expression after sciatic nerve transection

Atf3 mRNA expression was consistently dysregulated in a number of different experiments in HDAC4 cKOs (Figure 23). RNA levels are not always associated with protein expression, and the method of relative quantification used to assess mRNA expression means that variability in the reference sample can have implications for the interpretation of differences (Marguerat et al., 2012). To validate the RT-qPCR finding, immunohistochemistry for ATF3 protein was used.

Twenty-four hours after sciatic nerve transection, a similar proportion of DRG profiles were ATF3 positive in HDAC4 cKOs when compared to littermate controls (Figure 27 wt 83%, cKO 85%, n=3, p=0.3, Welch's t-test). Immunofluorescence intensity can be used as a surrogate for protein expression in sections that are the same thickness, stained at the same time and with images taken at the same exposure. Comparison of the immunofluorescence intensity distribution between cKOs and wildtype animals revealed no obvious difference in ATF3 intensity between groups (Figure 27).

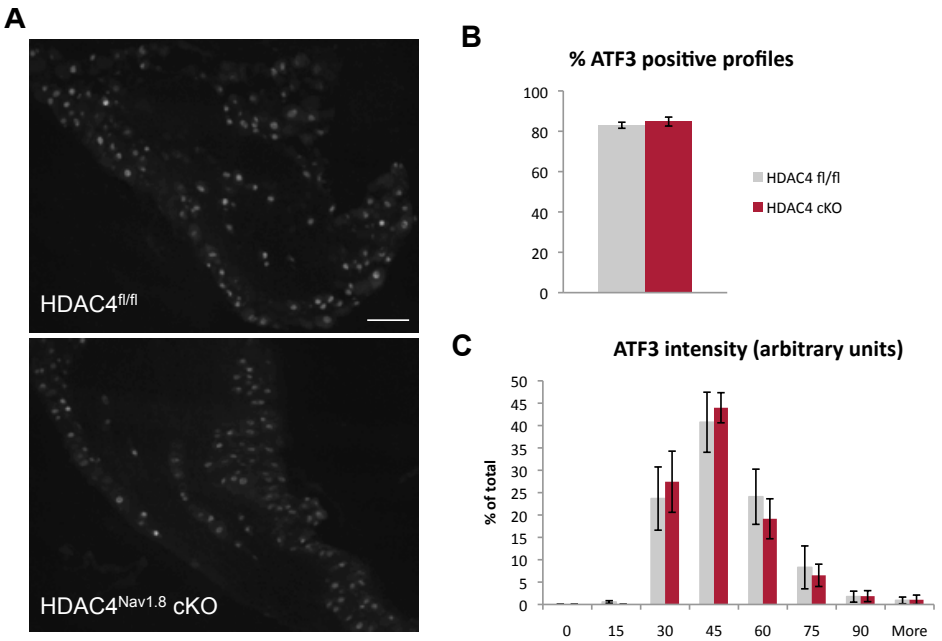


Figure 27 - ATF3 protein expression is not different between HDAC4$^{Nav1.8}$ cKOs and littermates 24 hours after nerve injury

A – L4 DRG sections stained for ATF3 24 hours after sciatic nerve transection. 10x overview image of HDAC4$^{fl/fl}$ on the top, HDAC4$^{Nav1.8}$ cKO below; scale bar represents 100 μM. No obvious difference in staining can be seen by eye. **B** – The proportion of ATF3 immunoreactive neuronal profiles is the same in both groups (n=3). **C** – Chart shows % of neurons with different levels of ATF3 staining intensity. Both groups show similar intensity distributions, suggesting similar expression levels of ATF3.

This data indicated that it was unlikely that ATF3 protein expression was different in HDAC4$^{Nav1.8}$ cKOs, despite the observed difference in mRNA expression.

4.4.4 *Atf3* mRNA is not differentially regulated in HDAC4^{Adv} cKO after sciatic nerve transection

To continue to explore the evidence for the role of HDAC4 in regulating *Atf3* expression, RNA was extracted from L3 and L4 lumbar DRGs twenty-four hours after sciatic nerve transection from tamoxifen-treated HDAC4^{Adv} cKOs and tamoxifen-treated littermate controls. In contrast to the results obtained from HDAC4$^{Nav1.8}$ cKOs, no difference in *Atf3* expression was observed between genotypes (Figure 28).

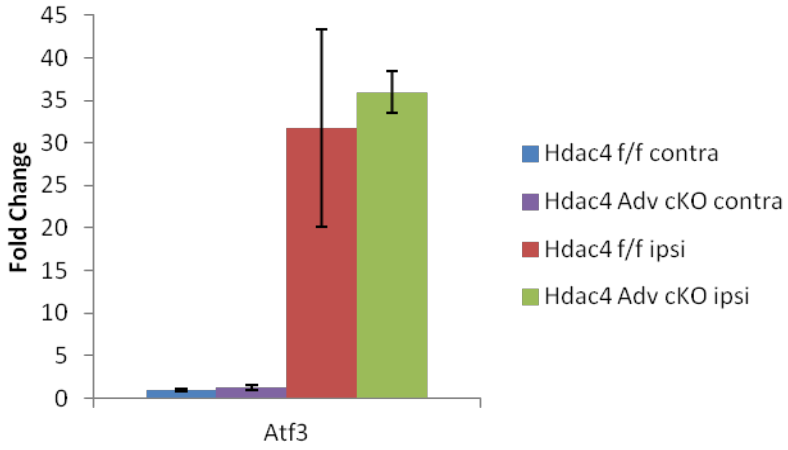


Figure 28 - *Atf3* is not differentially expressed in HDAC4^{Adv} cKOs after sciatic nerve injury
RT-qPCR analysis indicated that HDAC4^{Adv} cKO express similar levels of *Atf3* mRNA as littermate controls after sciatic nerve transection (n=4)

4.4.5 HDAC4 is not required for sensory recovery after peripheral nerve injury

Because we had failed to see differences in ATF3 protein expression, neurite outgrowth and epidermal re-innervation, it was deemed prudent to repeat the behavioural experiment. No difference in sensory recovery was observed in this second cohort (Figure 29).

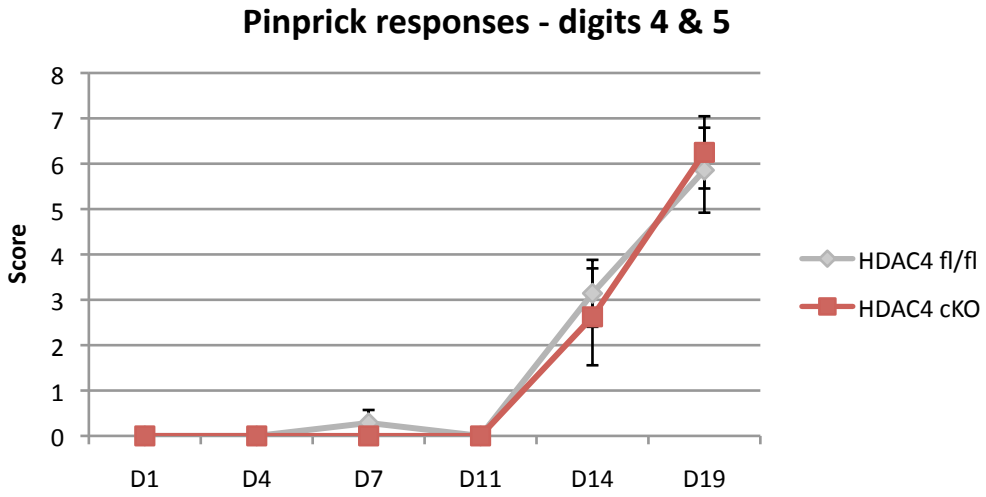


Figure 29 - No difference in sensory recovery was observed in a second behavioural experiment
Scores are out of a maximum of 8 points. In contrast to the first behavioural study, no difference in sensory recovery was observed between groups (n=7-8).

4.5 Discussion

Peripheral nerve regeneration is a complex tissue remodeling process that requires the coordination of both intrinsic and extrinsic signals (Chen et al., 2007). ATF3 is a transcription factor that is induced by nerve injury, and has previously been shown to promote regeneration and enhance the expression of growth-associated genes (Seijffers et al., 2006; Seijffers et al., 2007). The chance observation that *Atf3* mRNA expression was reduced in HDAC4$^{Nav1.8}$ cKOs after injury led us to investigate whether HDAC4 could play a role in peripheral nerve regeneration. Further experimental evidence failed to support the initial findings.

One of the key problems with RT-qPCR data analysis is that it is always relative to a reference sample. Other fields of research have long recognized that this poses a challenge for interpretation of results (Lovell et al., 2011), and recently this has been brought to the fore in the biological sciences (Lovén et al., 2012; Marguerat et al., 2012). In the case of *Atf3*, the perceived difference in expression could easily lie in simple arithmetic: dividing a large number over a small number can yield extremely different results. It is well-recognized that *Atf3* is induced after injury. By comparing the expression after injury to that before injury, we are essentially doing just that, and this can be misleading. The ability to look at the absolute expression of transcripts is becoming increasingly easy and more affordable, with the reducing costs of next-generation sequencing and medium-throughput technologies like the nCounter method. The adoption of these technologies over the more commonplace RT-qPCR will help to reduce some of the spurious correlations produced by relative quantification.

Regardless of the technique used to measure transcriptional differences, it is important to validate transcriptional effects with measurements of protein abundance,

as mRNA expression is not always correlated to protein expression (Gygi et al., 1999; Marguerat et al., 2012). Using immunohistochemistry, we determined that ATF3 staining was the same in both HDAC4$^{Nav1.8}$ cKOs and wildtype controls at 24 hours after sciatic nerve transection, suggesting that protein expression was equal. The use of a more quantitative technique, such as Western blotting, would provide further evidence for this. As discussed above, technical problems with relative quantification may account for the disparity between the mRNA and protein expression. Another possibility is that differences in post-transcriptional mechanisms such as mRNA decay or translation are involved.

Given that we did not see a difference in ATF3 protein expression, our inability to discern a difference in neurite outgrowth or skin re-innervation following injury are less surprising, but fairly significant technical limitations may also account for these results. The sensitivity of the *in vitro* neurite outgrowth assay could be improved by further technical optimization, for example by playing with plating density, serum and growth factor concentrations, and time in culture, which are all important factors in determining neurite outgrowth. However, the inability to differentiate between A- and C-fibre sprouting remains problematic, and the optimization of a C-fibre marker for immunocytochemical analysis is required. Ideally HDAC4$^{Nav1.8}$ cKOs and littermates would express GFP under the control of the $Na_v1.8$ promoter. With this tool, one could directly compare only the $Na_v1.8$-positive fibres from both groups.

One way I attempted to work around this problem was to investigate intra-epidermal fibre density after peripheral nerve injury, as only C- and Aδ-fibre nociceptors exist as free-nerve endings in the epidermis (McMahon, 2013). The inability to see a difference between genotypes may result from the time-point tested (twenty-one days after surgery), which may have been insufficient to allow for sufficient re-innervation. Indeed, it is possible that the fibres that were there may have been uninjured in the

first place, and this would therefore be more of a test of the lesion itself rather than the re-growth. Other groups have used neurogenic inflammation as a measure of re-innervation (Bester et al., 1998). This is something that we considered but did not pursue due to timing limitations.

Another possibility would be the use of pan-DRG knockout animals. We hypothesized that HDAC4 knockout would have a consistent effect on *Atf3* mRNA expression, and that the HDAC4^{Adv} cKOs would also demonstrate reduced induction of *Atf3* after injury. In this case, these animals could be used to investigate the role of HDAC4 in mediating neurite outgrowth without the need to optimize C-fibre specific markers. However, the transcriptional difference was not observed, and therefore the rationale to pursue neurite outgrowth and behavioural experiments was lacking. One interesting thing to note is that ATF3 has been shown to be regulated by estrogen-receptor signaling (Liu et al., 2007). The assessment of *Atf3* mRNA expression in the HDAC4^{Adv} cKOs and littermate controls was done only seven days after the animals received high doses of tamoxifen, an estrogen-receptor agonist. This is a potential confound to the direct interpretation of the results, which is that knockout of HDAC4 from adult sensory neurons does not affect *Atf3* expression. Analysis of *Atf3* expression at a later time may help to clear up this issue.

Behavioural data from our pilot study were consistent with the apparent reduction in *Atf3* mRNA that we measured, and suggested that sensory recovery could be delayed in HDAC4$^{Nav1.8}$ cKOs. However, we failed to replicate these findings in a second cohort. Every effort was made to ensure that animals in both groups received equal treatment, with surgeries performed as identically as possible, and all behavioural tests done blind to genotype. A power calculation using the experimentally determined means and population standard deviations at day fourteen, and the sample size of the different groups indicated that we had sufficient

power to detect this in both experiments (β = 0.9). Behavioural testing and interpretation is far from straightforward, and there are many variables in a test environment that may give rise to artefactual results (Crabbe et al., 1999). Whether the initial finding was true or a result of differences in animal husbandry or even slight variations in surgical procedures cannot be ruled out, nor can the lack of phenotype in the second group serve as a representative picture of what occurred. The conclusion that HDAC4 is unlikely to play a role in peripheral nerve regeneration has arisen from analysing evidence accumulated from multiple techniques. Further modification and optimization of outgrowth assays could be done, but in the absence of ATF3 protein differences and the inability to reproduce the behavioural findings, these experiments seem far from urgent.

5 HDAC4 and Nociception

5.1 Introduction

The impact of chronic pain is staggering. Affecting approximately one in five adults, chronic pain is associated with a significantly reduced quality of life, as well as a higher risk of depression and other mental health disorders (Breivik et al., 2006; Gureje O, 1998). The economic costs of chronic pain reflect this: for example in the UK, back pain alone is responsible for an estimated £5 billion of public funds each year (The British Pain Society, www.britishpainsociety.org/media_faq.htm). Critically, current therapies to treat pain often fall short of patient expectations. In a recent survey, 40% of sufferers reported inadequate pain control (Breivik et al., 2006). The need for improved treatment options is clear.

When we think about pain, it is often broken down into three different types: nociceptive or “good pain”, which arises from direct activation of nociceptors, like stepping on a piece of glass; inflammatory pain, which arises as a consequence to local inflammation and inflammatory mediators, and which can be treated by the use of steroids or non-steroidal anti-inflammatory drugs; and neuropathic pain, which is defined as “pain caused by a lesion or disease of the somatosensory nervous system” (McMahon, 2013). All of these different types of pain involve common anatomical substrates: primary nociceptors of the DRG, spinal dorsal horn interneurons and descending modulatory inputs from the brainstem and higher cortical centers.

Nociception is evolutionarily ancient and is critical for organisms to survive. For this reason, it is appropriate to model in lower species such as rodents. Tests of acute nociception, such as the hot plate test, have good face-, etiology- and construct-

validity and can be translated to human nociception, for example by comparing to heat pain threshold measurements from quantitative sensory testing (QST). Reflex withdrawal assays, such as the Hargreaves test and the Von Frey test, which measure thermal and mechanical withdrawal thresholds, respectively, can readily be employed in rodents to assess hypersensitivity associated with models of chronic pain, for example after the injection of an adjuvant which results in long-term inflammation, or after nerve injury. These measurements have been shown to be able to predict clinical efficacy of drugs for neuropathic pain (Kontinen and Meert, 2002) and are valuable tools which have led to the discovery of many novel therapeutic targets, for example the anti-NGF therapeutic, tanezumab (Lane et al., 2010; McMahon et al., 1995).

Over the past few years, the high attrition rate of novel analgesics has led to some backlash against some of the commonly used models of nociception in rodents, and emphasis has been placed on the development of new models that better mirror the clinical situation (Rice, 2008), as well as multifactorial behavioural analyses, rather than relying on reflex withdrawal alone (Mogil, 2009; Mogil and Crager, 2004). The stavudine (d4T) model belongs to this new category of neuropathic pain models. D4T is a thymidine analogue used to treat HIV, and painful peripheral neuropathy is a common side-effect in patients (Browne et al., 1993; Smyth et al., 2007; Winston et al., 2005). Intravenous injection of d4T has been shown to produce a long-lasting mechanical hypersensitivity in rodents (Huang et al., 2013; Renn et al., 2011) and can recapitulate other changes that are observed in patients, such as increased anxiety-like behaviours, as well as length-dependent changes to peripheral innervation (Huang et al., 2013). The molecular mechanisms underlying this remain unclear, with some groups citing a role for mitochondrial dysfunction, or BDNF

signaling (Cui et al., 1997; Renn et al., 2011; Robinson et al., 2007). This model has good face- and etiology-validity and is relatively under-explored.

Work to uncover the molecular mechanisms that contribute to chronic pain states may have great clinical relevance. Over the past few decades, it has become clear that widespread transcriptional dysregulation occurs throughout the pain neuraxis (LaCroix-Fralish et al., 2011), a process that is thought to contribute to the hyper-sensitized state of the system. Whether these changes may invoke epigenetic marks that allow for their persistence is a question that is only beginning to be answered (Denk and McMahon, 2012).

There is growing evidence to suggest that interfering with histone deacetylase activity can attenuate pain-related behaviour in a number of pre-clinical inflammatory pain models (Bai et al., 2010; Chiechio et al., 2009; Zhang et al., 2011). As HDAC inhibitors (HDACi) have been shown to have anti-inflammatory properties in other models (Shakespear et al., 2011) this is perhaps unsurprising. The first group to show efficacy of HDACi treatment in pain used repeated dosing with the HDACi MS-275 or SAHA and demonstrated that HDACi could reduce the nociceptive phenotype in the second phase of the formalin test. This was associated with increased acetylation of the NF-Kappa B subunit p65/RelA as well as increased expression of one of its target genes, mGlu2, in the spinal dorsal horn and DRG. The anti-nociceptive effect of MS-275 was blocked with a mGlu2/3 receptor antagonist (Chiechio et al., 2009). Another group, Bai *et al*., have shown that intrathecal pre-treatment of the HDAC inhibitors SAHA, TSA, LAQ824, VPA and 4-PB could be anti-nociceptive in the acute stages of a different inflammatory pain model, the Complete Freund's Adjuvant (CFA) model, though whether the effects are mediated at the chromatin level or by enhanced acetylation of non-histone proteins is not clear (Bai et al., 2010).

More recently, Zhang *et al.* determined that repeated TSA injection into the nucleus raphe magnus (NRM) was able to attenuate CFA-induced hypersensitivity. The effect was attributed to the drug's ability to increase acetylation at the hypoacetylated *Gad2* promoter, enhancing GAD65 expression and GABA inhibition, and thus altering descending pain modulation (Zhang et al., 2011). Intriguingly, this group also demonstrated hypoacetylation of *Gad2* in a model of neuropathic pain, indicating that this may be a common event in chronic pain states. It will be interesting to see whether HDAC inhibitor treatment in the NRM will be as effective in this, and other models of chronic pain. A paper from Tran *et al* reports analgesic efficacy of intracerebroventricular administration of the same HDAC inhibitor, TSA, in a stress-induced visceral pain model (Tran et al., 2012), and our group has recently shown that intrathecal HDAC inhibitor administration can partially prevent mechanical hypersensitivity associated with neuropathic pain (Denk et al., 2013). Whether this is mediated through the same GABAergic mechanism is not known, but this early evidence for the therapeutic potential of HDAC inhibitors warrants further investigation.

The most commonly used HDAC inhibitors are relatively "dirty" compounds, targeting multiple HDACs (Bradner et al., 2010). Investigating the role of individual HDACs using genetic tools may shed light on the mechanisms by which HDAC inhibitors work to alleviate pain, putting the groundwork in place to drive the development of novel inhibitors with improved specificity.

HDAC4 is a transcriptional co-repressor, known to bind to and modulate the activity of multiple transcription factors (Chauchereau et al., 2004; Miska et al., 1999; Ren et al., 2009; Stronach et al., 2011). In the adult nervous system, HDAC4 is primarily cytoplasmic (Darcy et al., 2010) but shows activity and NMDA-dependent shuttling in and out of the nucleus (Chawla et al., 2003; Sando Iii et al., 2012; Zhao et al., 2001).

In cortical neurons, nuclear localization of HDAC4 has been shown to regulate the transcription of genes associated with synaptic plasticity, including *Snap25* (Sando Iii et al., 2012). A recent 'meta-analysis' of pain-related transcriptional changes found that *Snap25*, *Vamp1* and *Sv2b*, genes associated with synaptic vesicle release and synaptic plasticity, were downregulated in multiple experiments (LaCroix-Fralish et al., 2011). Furthermore, our data suggest that HDAC4 is required for the expression of *Cacna2d1* and *Trpa1* in intact DRGs, as well as *Ntrk1, Calca* and *Trpv1* in injured ganglia. The dysregulation of these genes may have implications for the sensory behaviour of HDAC4 conditional knockouts.

Direct evidence for HDAC4's involvement in sensation comes from mutant mice in which the deacetylase domain of HDAC4 is deleted globally, as these animals displayed increased latency to respond to the hot plate test (Rajan et al., 2009). Our data indicate that this is unlikely to be due to developmental defects in the sensory nervous system, as $Na_v1.8$ cKOs display normal DRG cell size distribution and expression of subtype markers. Furthermore, HDAC4 has been linked to neuroprotection. Although the literature on this is somewhat contradictory, HDAC4 knockdown has been shown to be neuroprotective in neurons that are undergoing various types of cell stress, such as toxicity and oxidative stress (Bolger and Yao 2005, Yang 2011). Although sensory neuron death is not commonly seen in pain states, toxic agents such as d4T and chemotherapeutic drugs can produce painful neuropathies in patients. Could knockout of HDAC4 be protective in these models?

5.2 Aims

The aims of this chapter are to use the two sensory neuron-specific HDAC4 knockout lines established in Chapter 3 to determine whether HDAC4 is required for nociceptive behaviours in models of acute and chronic pain.

5.3 Methods

All experiments were performed as described in Chapter 2.

5.4 Results

5.4.1 Baseline sensory behaviour and acute nociception are unaffected by HDAC4 deletion

In Chapter 3 I described the effect of HDAC4 deletion on sensory neuron transcription. In the HDAC4$^{Nav1.8}$ cKO strain, the genes *Ptgs2*, *Scn10a, Trpa1* and *Scn11a* were downregulated and in the HDAC4^{Adv} cKO strain there was downregulation of *Trpa1* and upregulation of *Vip, Cacna2d1, Oprm1* and *P2rx3*. Only *Trpa1* and *Cacna2d1* were in the top ten dysregulated genes in both strains, which provides good evidence that these are true HDAC4 target genes. These genes have been implicated in sensory processing, and it is conceivable that the transcriptional differences observed may give rise to altered sensory behaviour: for example, the downregulation of *Trpa1* may imply a reduced sensitivity to TRPA1 ligands such as mustard oil; the upregulation of *Cacna2d1* may induce hyperexcitability by increasing synaptic calcium levels, leading to the prolonged release of peptides and glutamate from primary afferent terminals onto spinal dorsal horn interneurons. Behavioural testing was used to assess whether these transcriptional differences may have functional consequences.

Experimental bias in behavioural testing can greatly influence perceived outcomes (Rice, 2008). Blinding and randomization are required to enable unbiased assessment of behaviour. HDAC4$^{Nav1.8}$ cKO were indistinguishable from HDAC4$^{fl/fl}$ (aka wildtype (wt)) littermate controls by eye and grew to similar size and mass. This meant that blinding to genotype was completely effective. All comparisons were made between similarly affected littermates.

To begin to address the question of whether peripheral expression of HDAC4 is required for nociception, it was first necessary to ensure that the knockout had normal motor responses, as this can be a confound to interpreting withdrawal reflexes. The rotarod test is a measure of learned sensory-motor integration. To perform well, animals need to be able to coordinate their movements. HDAC4$^{Nav1.8}$ cKO were indistinguishable from littermates on this test (mean latency (s) wt = 213.2, cKO = 211.8; n =1 2; p > 0.05, Welch's t-test) (Figure 30).

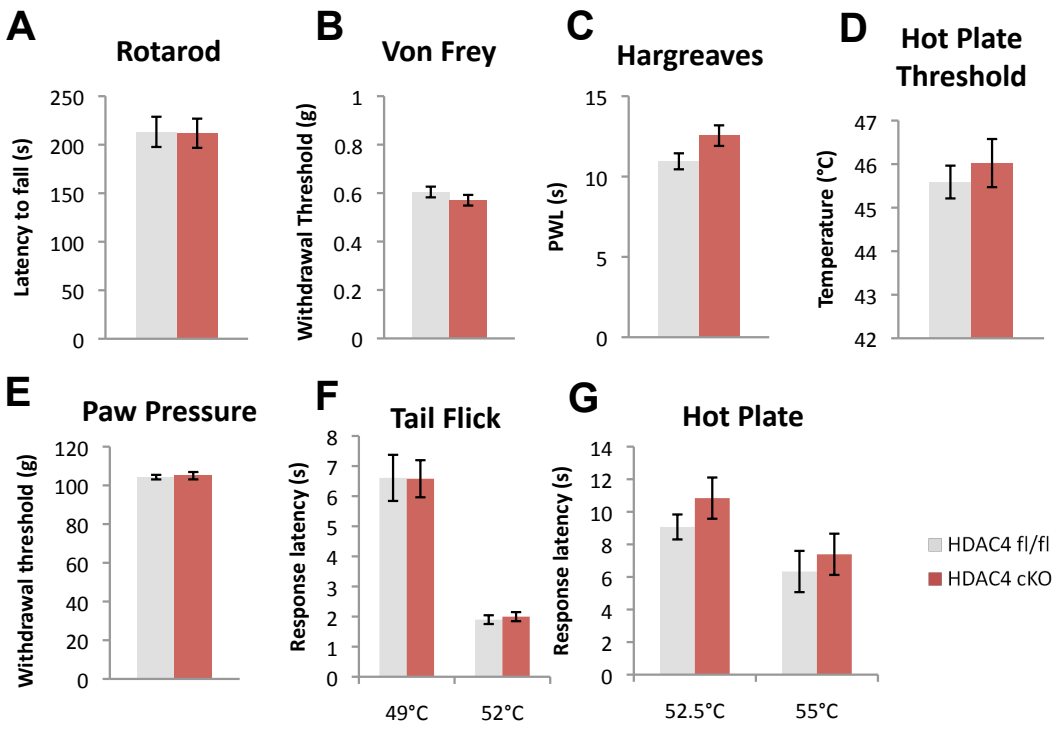


Figure 30 - HDAC4 expression in $Na_v1.8$ positive neurons is not required for baseline mechano- or thermo-sensation or acute nociception
A - The rotarod test is used as a measure of motor function. Animals are placed on a rotating bar that accelerates from 2-38 RPM and latency to fall is recorded. (n=12, p>0.05) **B** – Mechanical sensitivity was measured by the Von Frey test, no difference was observed between groups (n=30, p>0.05) **C** – In the Hargreaves test, animals are placed on a glass surface and latency to withdraw from a radiant heat source is recorded (latencies = 10.9, 12.5; p = 0.056 n = 20, Welch's t-test). **D** – To determine the hot plate response threshold, mice habituate for 5 minutes at 40°C, then the temperature is increased until the animal responds. (n=17/18, p>0.05) **E** – The Paw Pressure test (Randall Selitto test) is a measure of mechanical nociception. The force to elicit a withdrawal response is recorded (n=10, p>0.05) **F** - The tail flick response is used to test spinal reflex-mediated nociception. Under light restraint, 1 cm of the tail is immersed in a hot water bath and time to withdraw is recorded. (n=12, p>0.05) **G** – The hot plate test is used to determine thermal nociceptive responses. Animals are placed onto the hot plate and response latency is measured (n=10, p>0.05)

The Von Frey test was used to assess mechanosensation; no difference was observed between genotypes (mean threshold (g): wt = 0.60, cKO = 0.57; n = 30; $p > 0.05$). Threshold responses to thermal stimuli were assessed in two ways, using the Hargreaves test and using a variation of the hot plate test, in which animals are allowed to move freely on the hot plate while the temperature ramps at a constant rate of 2.5°C/minute. Because of the slow rate at which the temperature increases, this version of the hot plate test is thought to rely more on C-fibre than A-fibre function and has been shown to be sensitive to lower doses of analgesics than the traditional method (Hunskaar et al., 1986; Tjolsen et al., 1991). On both tests, there was a slight trend toward a greater latency to respond in the cKO group but this was not statistically significant (Hargreaves mean latency: wt = 10.9; cKO =12.6; n = 20; $p = 0.056$; hot plate threshold (ºC): wt = 45.6, cKO = 46.0; n = 17/18; $p > 0.05$).

The Randall-Sellitto test (Paw Pressure test) was used to determine threshold to respond to a noxious mechanical stimulus. No difference was observed between groups (mean response threshold (g): wt = 104.3, cKO = 105; n = 10; $p > 0.05$). The tail flick test and the hot plate tests were used to determine noxious thermosensitivity. A slight trend toward increased latency to respond to the hot plate was observed in cKOs but this was not statistically significant (mean 52.5ºC latency (s) wt = 9.1, cKO = 10.8; n = 10; $p > 0.05$; mean 55ºC latency (s) wt = 6.3, cKO = 7.4; n = 10; $p > 0.05$). No difference was observed in the tail flick test (mean 49ºC latency (s) wt = 6.6, cKO = 6.6; n = 12; mean 52ºC latency (s) wt = 1.9, cKO = 2.0; n = 12).

A similar battery of tests was performed on the $HDAC4^{Adv}$ cKOs and littermate controls. Due to time constraints the rotarod test was omitted. In keeping with the results from the $HDAC4^{Nav1.8}$ cKOs, $HDAC4^{Adv}$ cKOs were indistinguishable from littermate controls, and had no significant difference in adult body mass or general locomotor activity in the cage (Figure 3, personal observation). No differences

between genotypes were seen using the Von Frey test, or an adapted version of the Hargreaves test in which the animals are lightly restrained and a single paw is placed over a radiant heat source until the paw is withdrawn. The tail flick test similarly did not reveal any differences in thermosensation between genotypes. These results indicate that HDAC4 is not required for baseline sensory perception or acute nociception.

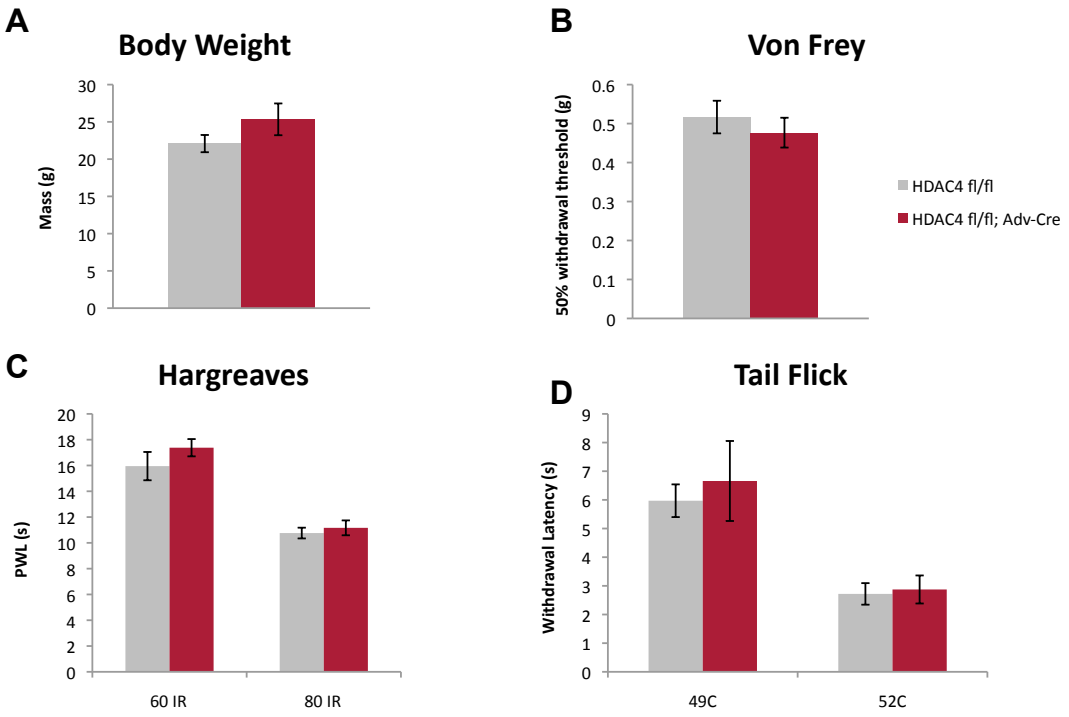


Figure 31 - HDAC4 cKO in adult sensory neurons does not affect acute nociception or sensory perception
A – HDAC4^{Adv} cKOs and littermates had no obvious morphological differences, and body weight was approximately equal in adult animals (n=7-10). **B** – Mechanical withdrawal thresholds were not different between groups (n=7-10). **C & D** – No difference in thermal withdrawal latency was observed on either the Hargreaves test or the Tail Flick test (n=7-10)

One strange result was observed in the Randall-Selitto test. This test was performed by a very experienced animal technician, and in his hands both the HDAC4^{Adv} cKOs and littermates were unresponsive and nearly all of them went to the cut-off value of 150 g (thresholds = 149, 148 g; n=7-10) (Figure 32). This was repeated in a second cohort of animals, and again none of the animals responded to either noxious

pressure or cold stimulation at 10ºC (n=9-11). Other animals from the colony that had not been treated with tamoxifen were tested and found to have responses in the normal range on these tests (withdrawal thresholds of 105.6 g and 12.8 s, n=4). Although preliminary, these experiments suggest that tamoxifen may be analgesic for noxious mechanical and cold sensing.

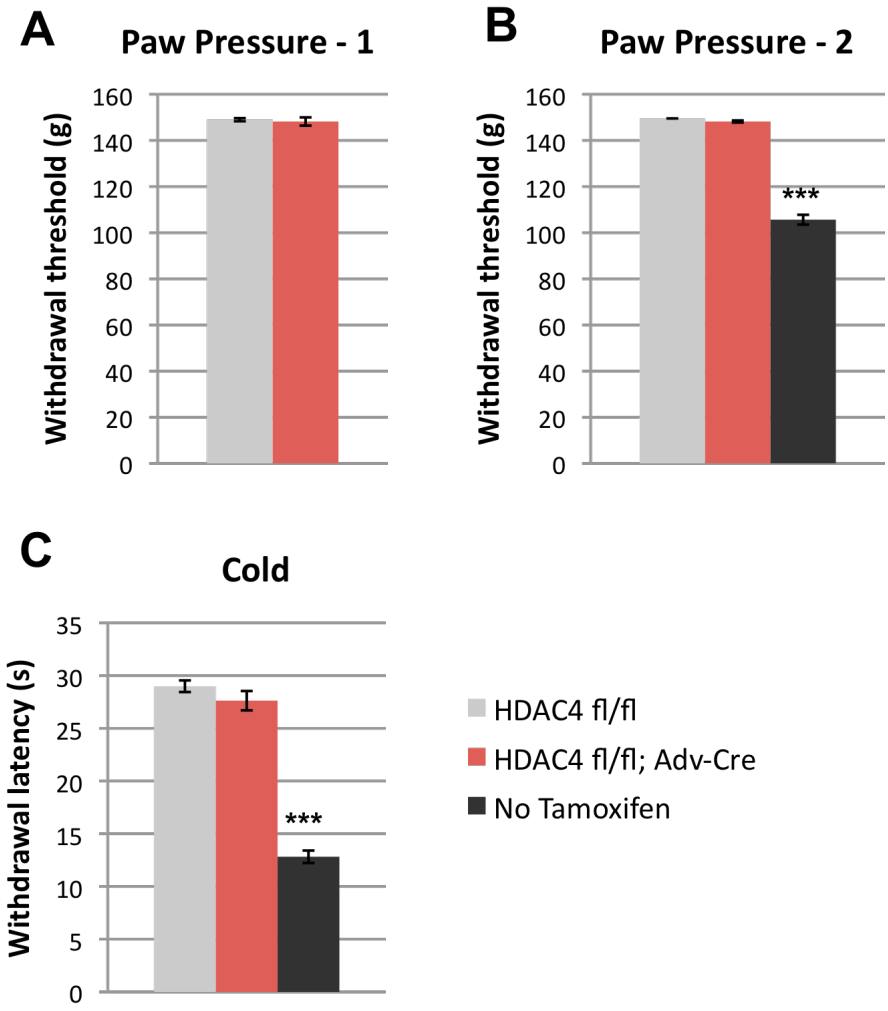


Figure 32 - Noxious mechanical and cold sensing are impaired after tamoxifen treatment
A – In the first behavioural cohort, almost all tamoxifen treated animals went to the cut-off value of 150 g (n=7-10) **B –** A second cohort of animals showed the same impairment (n=9-11). Interestingly, other animals from the colony that had not been treated with tamoxifen responded within the normal range ($p<0.01$, n=4). **C** – Cold sensing was also impaired in tamoxifen treated animals compared to untreated controls ($p<0.01$).

5.4.2 Mechanical hypersensitivity after nerve injury does not require HDAC4 expression from the $Na_v1.8$ population of sensory neurons

Transcriptional differences in the DRG were observed in both $HDAC4^{Nav1.8}$ cKO and $HDAC4^{Adv}$ cKO across a number of injury models, including the partial sciatic nerve ligation (PSL) model and sciatic nerve transection (SNT) model. By comparing these two studies directly, it emerged that two peptides that regulate behavioural sensitivity were differentially regulated in both models and in both strains of HDAC4 cKOs: *Sst*, the gene that encodes somatostatin and *Calca* that encodes CGRP. Interestingly, *Sst* was upregulated in both models ($HDAC4^{Nav1.8}$ FC = 2.64; $HDAC4^{Adv}$ FC = 3.08 both compared to WT ipsilateral controls), and *Calca* was downregulated ($HDAC4^{Nav1.8}$ FC = 0.79; $HDAC4^{Adv}$ FC = 0.75 compared to WT ipsilateral controls) (Figure 33). These changes would be consistent with reduced behavioural sensitivity, as SST administration in the spinal cord is analgesic (Chrubasik et al., 1984) and CGRP expression levels have been shown to associate tightly with responses to noxious thermal stimuli, with lower expression levels linked to reduced sensitivity (Mogil, 2005).

Table 9 - Top ranked gene expression changes after nerve injury, by unadjusted p-value. FC are calculated against $HDAC4^{fl/fl}$ ipsilateral controls.

	$HDAC4^{Nav1.8}$ PSL	
	p	**FC**
Sst	**0.00**	**2.64**
Trpv1	0.03	0.74
Gfap	0.03	0.36
Ntrk1	0.04	0.81
Atf3	0.05	0.48
Ccl2	0.05	0.69
Npy	0.05	0.33
Calca	**0.09**	**0.79**
Gabra5	0.10	0.82
Rest	0.12	0.74

	$HDAC4^{Adv}$ SNT	
	p	**FC**
Scn10a	0.01	0.70
Calca	**0.01**	**0.75**
Cacna2d1	0.02	1.39
Trpa1	0.02	0.71
Gad2	0.02	1.51
Vip	0.03	1.47
Ngf	0.03	1.42
Sst	**0.07**	**3.08**
Scn9a	0.08	0.89
Bdnf	0.11	1.55

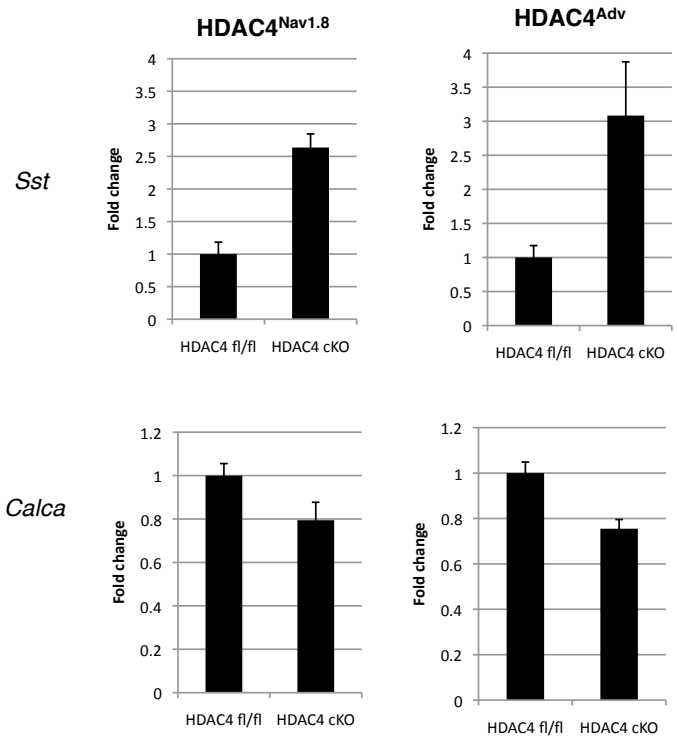


Figure 33 - *Sst* and *Calca* are differentially expressed in both strains of HDAC4 cKO after nerve injury
Charts were generated from PCR array card data and represent fold changes compared to similarly affected wildtype controls (either after PSL or SNT). Stats and fold changes as listed in Table 9.

The partial sciatic nerve ligation (PSL) model is a well-characterized model of neuropathic pain that is sensitive to drugs that show clinical efficacy such as gabapentin (Tanabe et al., 2005). The model consists of tying a suture around approximately one-third of the sciatic nerve, which results in long-lasting hypersensitivity to mechanical stimuli and is associated with transcriptional dysregulation (Kusuda et al., 2011). To test whether the transcriptional changes observed in HDAC4 cKOs may have consequences for nerve injury evoked hypersensitivity, the PSL model was induced in HDAC4$^{Nav1.8}$ cKOs. Although results from the control group were somewhat variable, PSL resulted in mechanical and thermal hypersensitivity to a similar extent in both HDAC4$^{Nav1.8}$ cKOs and littermates (Figure 34). A repeated measures ANOVA of Von Frey data confirmed significant main effects of both *day* ($F_{(4,48}$=11.65, p<0.0001, n=8) and *paw* ($F_{(1,70)}$=36.30, p<0.0001, n=8) as well as a significant interaction of *day x paw* ($F_{(5,70)}$=2.76, p=0.025,

n=8). A comparison of *day x paw x genotype* was not statistically significant, although a main effect of genotype was observed ($F_{(1,14)}$=8.22, p=0.012, n=8) likely due to the surprisingly high withdrawal thresholds in the wildtype group on days 7 and 14. Similarly, thermal hypersensitivity was observed in both groups with a significant main effect of *day* ($F_{(4,48)}$=11.65, p<0.0001, n=7) and a significant interaction of *day x paw* ($F_{(4,48)}$=3.19, p=0.021, n=7), but no significant effect of genotype. This indicates that despite altered transcriptional regulation, HDAC4 does not contribute to behavioural sensitization in this model of neuropathic pain.

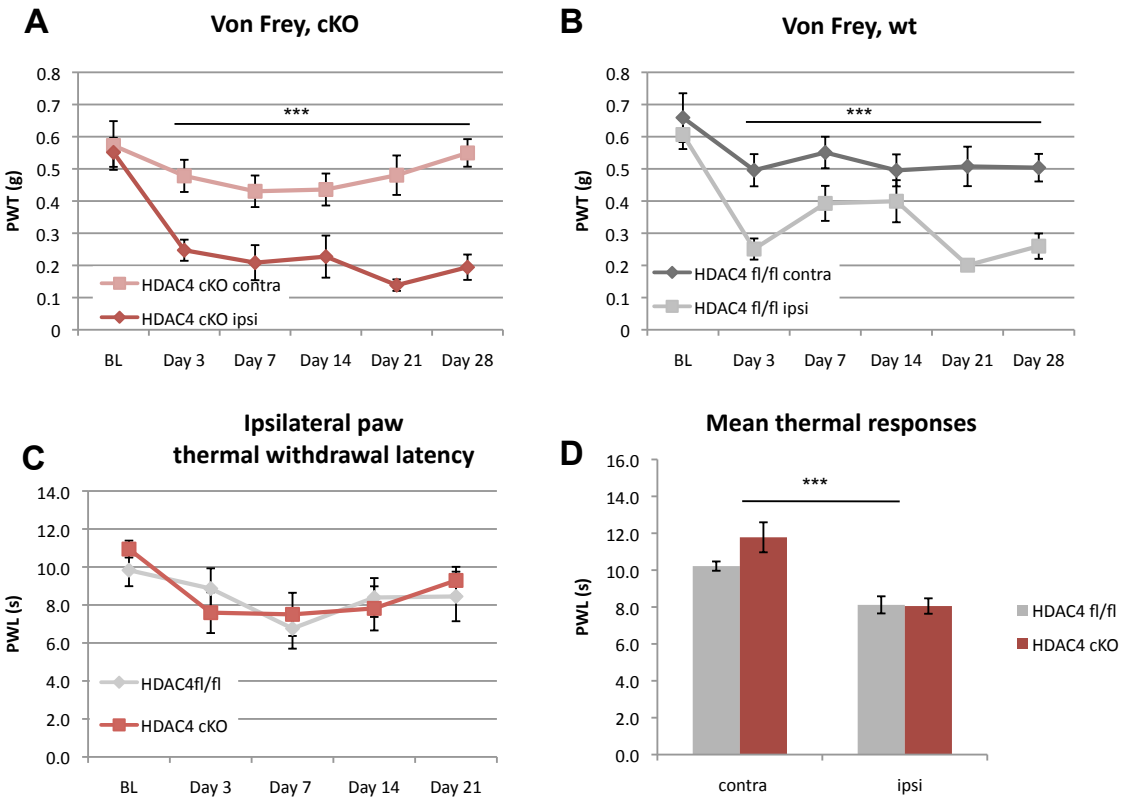


Figure 34 - HDAC4$^{Nav1.8}$ cKOs develop mechanical and thermal hypersensitivity after partial sciatic nerve ligation
Behavioural hypersensitivity after PSL was tested using the Von Frey and Hargreaves tests. **A & B –** HDAC4$^{Nav1.8}$ cKO (**A**) and HDAC$^{fl/fl}$ (**B**) show significant mechanical hypersensitivity after PSL; *** = main effect of *paw* (3-way RM ANOVA, $F_{(1,70)}$=36.3, p<0.0001, n=8). A significant main effect of genotype was observed ($F_{(1,14)}$=8.22, p=0.012) likely due to the surprisingly high PWTs in the wt group on days 7 and 14. **C** – Thermal hypersensitivity was not different between groups. **D** – Both groups developed mild but statistically significant thermal hypersensitivity; *** = main effect of *day* (RM ANOVA, $F_{(4,48)}$=11.65, p<0.0001, n=7).

5.4.3 HDAC4 is dispensable for the development of mechanical hypersensitivity in the d4T model

Stavudine, also known as d4T, is a thymidine analogue used to treat patients with HIV in the developing world. Its use has been associated with the development of painful peripheral neuropathy in patients (Browne et al., 1993; Smyth et al., 2007; Winston et al., 2005). Animal models recently been developed to unravel the mechanisms underlying this (Huang et al., 2013; Renn et al., 2011), and evidence from our lab indicates that prophylactic treatment with HDAC inhibitors can lessen the hypersensitivity associated with d4T treatment (Denk et al., 2013). D4T-associated neuropathy was initiated in mice via a single tail vein injection of the drug, and behaviour was assessed using the Von Frey test. Bilateral mechanical hypersensitivity was observed at day three and persisted throughout the testing period (Figure 35), but no difference in mechanical hypersensitivity was observed between genotypes. A repeated measures ANOVA of Von Frey data confirmed a significant main effect of *day* ($F_{(5,85)}=10.46$, $p<0.0001$, n=9-10), but no effect of genotype. D4T neuropathy has been shown to result in C-fibre loss from the epidermis (Huang et al., 2013). Twenty-eight days after D4T treatment, IENFD was assessed in cKOs and wildtype littermates, but no difference in epidermal innervation was observed (Figure 35). This indicates that HDAC4 is not required for D4T-associated neuropathy or mechanical hypersensitivity.

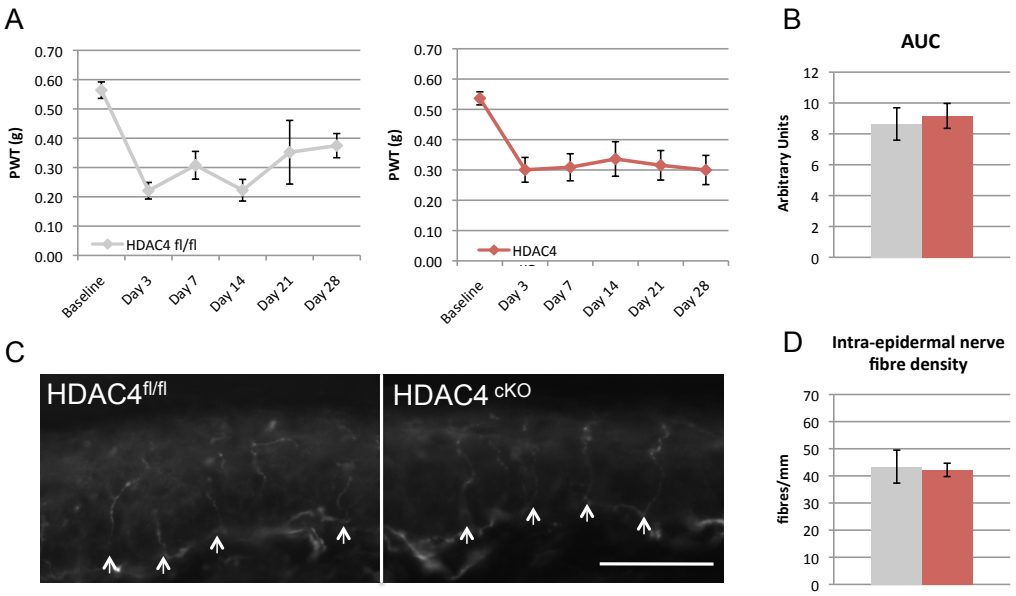


Figure 35 - D4T results in mechanical hypersensitivity that does not require peripheral expression of HDAC4
A – A single intravenous injection of 10 mg/kg d4T resulted in long-lasting mechanical hypersensitivity in HDAC4$^{fl/fl}$ and HDAC4$^{Nav1.8}$ cKO animals (RM ANOVA main effect of day, $F_{(5,85)}$=10.46, p<0.0001, n=9-10), but this was not different between groups. **B** – Area under the curve (AUC) analysis of withdrawal threshold data showed no significant difference between genotypes. **C** Skin sections stained for PGP9.5. Arrows indicate nerve fibres. Scale bar represents 50 µM. **D** - For each animal, intraepidermal nerve fibre density was calculated as the average number of fibres/average length of three sections. No significant difference was found between genotypes (n=3, Welch's t-test).

5.4.4 Loss of HDAC4 alters responses to inflammation

Some of the largest gene expression changes that we observed in HDAC4 cKOs came from experiments with an inflammatory component. For example, when dissociated sensory neurons from HDAC4$^{Nav1.8}$ cKOs were cultured with a high level of NGF, rapid downregulation of *Ntrk1, Calca, Trpv1* and *Vgf* was observed. Similarly, after Complete Freund's adjuvant injection into the hindpaw, HDAC4^{Adv} cKOs also had profoundly reduced expression of the majority these genes. Interestingly, analysis of the top dysregulated genes in the two inflammatory conditions revealed many other consistently differentially regulated transcripts, including the gene encoding the voltage-gated sodium channel, $Na_v1.8$ (*Scn9a*), the ATP-gated purinoreceptor 3 gene (*P2rx3),* GTP cyclohydrolase 1 (*Gch1), Atf3,* and

the voltage-gated potassium channel subunit *Kcns1* (Figure 36). With the exception of the differential regulation of the voltage-gated channels, the majority of these changes would predict reduced nociception. This suggested that HDAC4 may have a role in mediating peripheral sensitization.

	HDAC4$^{Nav1.8}$ NGF	
	p	**FC**
Ntrk1	**0.00**	**0.37**
P2rx3	**0.01**	**0.41**
Gch1	**0.01**	**0.37**
Trpv1	**0.01**	**0.41**
Ngf	0.01	2.04
Calca	**0.02**	**0.35**
Kcns1	**0.02**	**0.36**
Scn9a	**0.02**	**1.78**
Atf3	**0.02**	**0.72**
Sst	0.02	8.04
Reg3b	**0.03**	**31.11**
Vip	0.03	17.24
Gad2	0.05	4.76
Vgf	0.05	0.14

	HDAC4^{Adv} CFA	
	p	**FC**
Ntrk1	**0.00**	**0.32**
Trpv1	**0.00**	**0.44**
Trpa1	0.00	0.39
Calca	***0.00***	***0.22***
Gch1	**0.00**	**0.40**
Pdyn	0.00	2.51
Kcns1	**0.00**	**0.49**
P2rx3	**0.00**	**0.43**
P2rx4	0.00	0.57
Hcn2	0.00	0.60
Ctss	0.01	0.36
Oprm1	0.01	1.54
Scn3a	0.02	0.30
Scn9a	**0.02**	**1.70**
Nos1	0.03	0.51
Atf3	**0.03**	**0.54**
Ntrk2	0.03	2.00
Slco1a6	0.03	2.60
Reg3b	**0.04**	**0.52**
Gabbr1	0.05	1.42

Figure 36 - HDAC4 cKO have differential gene expression after inflammatory stimulation
Genes that were differentially expressed between wildtype and HDAC4 cKO after inflammatory stimulation are listed by unadjusted p-value (Welch's t-test, n=4). FC=fold change compared to similarly affected wildtype controls. Genes on both lists appear in bold. With the exception of *Reg3b*, all of the expression changes were consistent between the two experiments. *Reg3b* is not well expressed in the DRG, so the inconsistency between the experiments may be due to detection limits.

To begin to address this, we used calcium imaging to determine whether capsaicin responses may be reduced in HDAC4$^{Nav1.8}$ cKO sensory neurons after incubation with 50 ng/mL NGF overnight. Interestingly, fewer HDAC4$^{Nav1.8}$ cKO cells responded to capsaicin, although maximal responses were similar between genotypes (Figure 37). This suggests that the reduced *Trpv1* expression may be caused by selective

loss in a population of cells, rather than downregulation in all TRPV1 positive neurons. Immuocytochemical analysis of TRPV1 would help to verify this hypothesis.

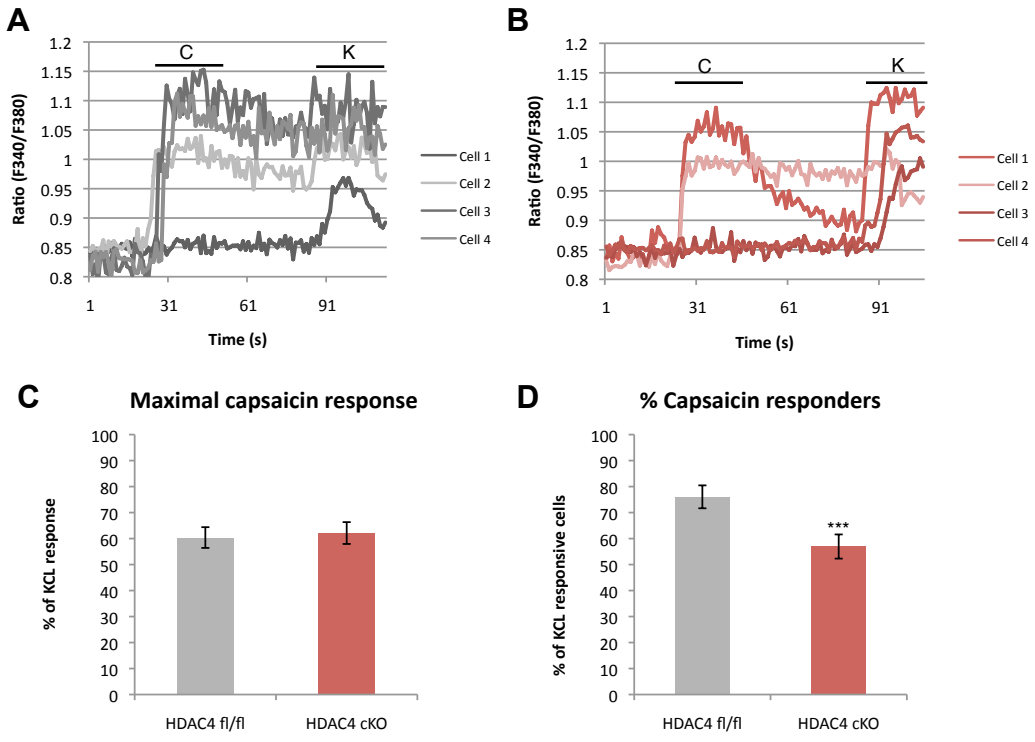


Figure 37 - Fewer HDAC4$^{Nav1.8}$ cKO DRG neurons respond to capsaicin
Representative fluorescence traces from calcium imaging experiments. C=100 nM capsaicin, K=50 mM KCl. **A** – HDAC4$^{fl/fl}$ neurons 18-24 hours after culturing with 50 ng/mL NGF **B** – HDAC4$^{Nav1.8}$ cKO neurons. Similar capsaicin and KCl responses were seen in both groups, however fewer HDAC4 cKO neurons respond to capsaicin. **C** – Mean peak capsaicin response is plotted as a percentage of the maximal response to KCl. No difference was observed between groups (n=5-6 coverslips). **D** – Cells were considered capsaicin responsive if their capsaicin peak was >20% of the KCl peak response. Significantly fewer HDAC4$^{Nav1.8}$ neurons responded to capsaicin treatment (n=5-6 coverslips, p=0.0001 Fisher's exact test, p=0.02 Welch's t-test)

To address whether this might also affect behavioural outcomes, the carrageenan model was used to model acute inflammation in HDAC4$^{Nav1.8}$ cKOs and littermates. Lambda-carrageenan was injected into the paw, and latency to respond to radiant heat was measured at various time points over a twenty-four hour period. In contrast to the marked differences in capsaicin sensitivity *in vitro*, no differences were observed on this test (RM ANOVA main effect of genotype, $F_{(1,10)}$=2.06, p=0.18, n=6) (Figure 38).

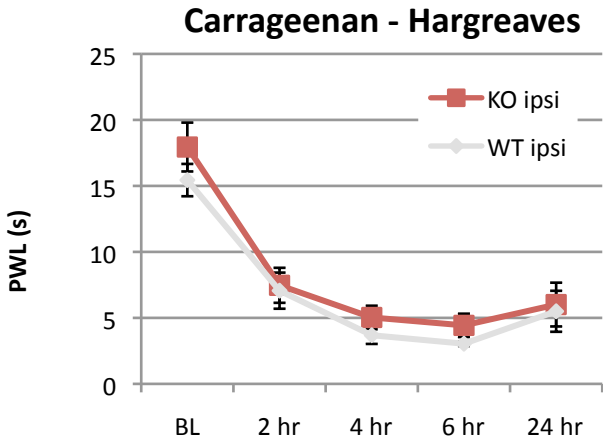


Figure 38 - HDAC4 is not required for thermal hypersensitivity in the carrageenan model of acute inflammatory pain
Withdrawal from a radiant heat source following intraplantar carrageenan injection does not require peripheral expression of HDAC4 (RM ANOVA main effect of genotype, $F_{(1,10)}$=2.06, p=0.18, n=6).

Because the onset of the behavioural changes occur rapidly, it is possible that this primarily reflects direct sensitization of nociceptors through post-translational modification. I hypothesized that a more long-term model may be more sensitive to transcriptional dysregulation and may reveal differences between the genotypes. The Complete Freund's Adjuvant (CFA) model is used to model arthritis pain. Injection of CFA into the plantar surface of the hindpaw leads to prolonged edema and hypersensitivity that recovers over a matter of weeks, and is associated with altered transcription in the DRG (Chang et al., 2010). Behavioural responses require the $Na_v1.8$ population of sensory neurons, as ablation of these neurons with diphtheria toxin leads to a marked absence of CFA-induced hypersensitivity (Abrahamsen et al., 2008). Comparison of CFA responses in $HDAC4^{Nav1.8}$ cKOs and littermates revealed a modest and statistically significant reduction in thermal hypersensitivity in the cKOs (Figure 39, RM ANOVA main effect of genotype, $F_{(1,8)}$=16.18, p=0.004, n=5).

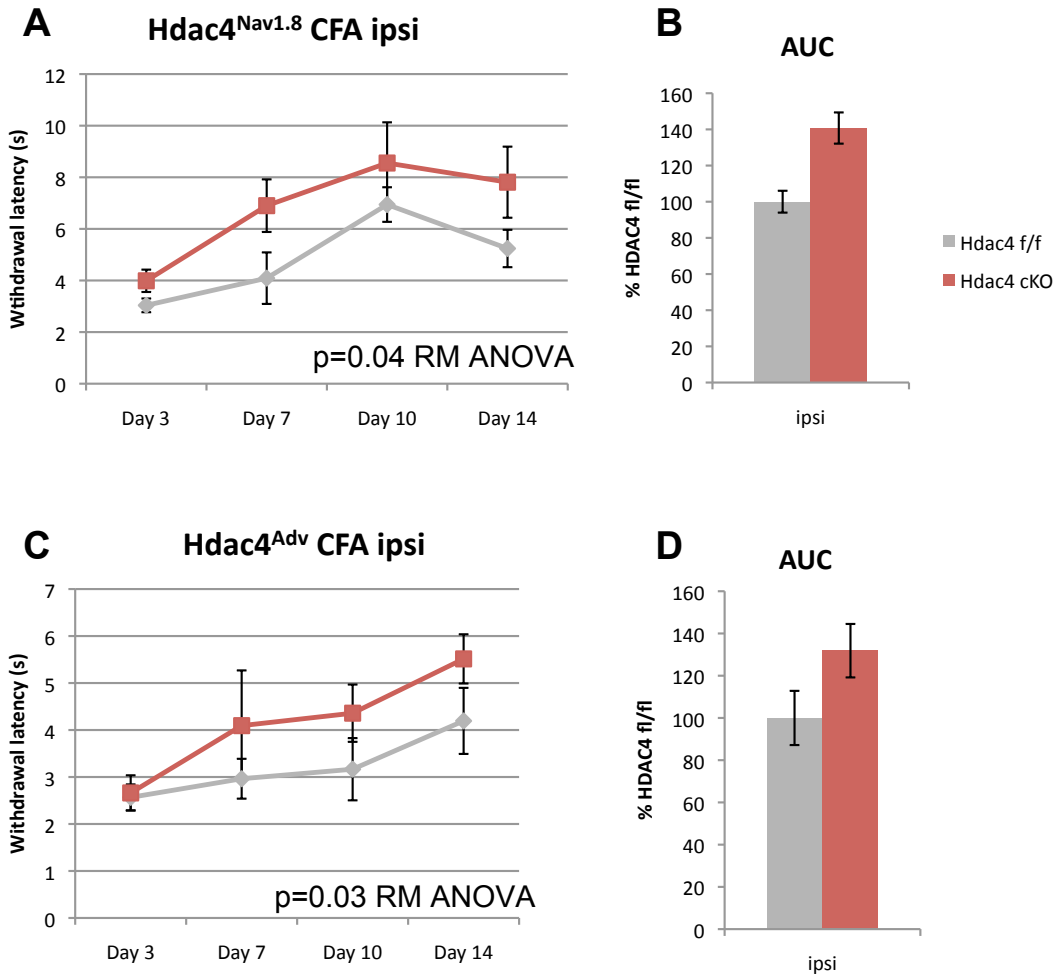


Figure 39 - HDAC4 is required for thermal hypersensitivity after CFA
A – Average thermal withdrawal thresholds from HDAC4$^{Nav1.8}$ cKO are represented in red and HDAC4$^{fl/fl}$ littermates are in grey. Thermal hypersensitivity after CFA injection is significantly attenuated in HDAC4$^{Nav1.8}$ cKO animals (RM ANOVA main effect of genotype, $F_{(1,8)}$ =16.18, p=0.004, n=5). **B** – Area under the curve (AUC) analysis of data in **A**. **C** – Similar to the results from HDAC4$^{Nav1.8}$ cKO, knockout of HDAC4 from adult sensory ganglia results in significantly attenuated thermal hypersensitivity after CFA (RM ANOVA main effect of genotype, $F_{(1,15)}$=5.56, p=0.03, n=6-12). **D** – AUC analysis of data in **C**

Similarly, CFA injection in HDAC4^{Adv} cKOs was also associated with attenuated thermal hypersensitivity (RM ANOVA, main effect of genotype $F_{(1,15)}$=5.56, p=0.032, n=6 cKOs, =12 littermates).

Interestingly, both HDAC4 cKO strains exhibited a similar degree of mechanical hypersensitivity when compared to littermate controls (Figure 40). A repeated measures ANOVA of Von Frey data from HDAC4$^{Nav1.8}$ cKOs and littermates

confirmed significant effects of both *day* ($F_{(5,45)}$=8.09, p<0.0001, n=5-6) and *paw* ($F_{(1,9)}$=45.61, p<0.0001, n=5-6) as well as a significant interaction of *day x paw* ($F_{(5,45)}$=3.23, p=0.014, n=5-6), but no effect of genotype was found. Similarly, repeated measures ANOVA analysis of Von Frey data from HDAC4^{Adv} cKOs and littermates confirmed significant effects of both *day* ($F_{(5,80)}$=8.79, p<0.0001, n=6-12) and *paw* ($F_{(1,16)}$=147.09, p<0.0001, n=6-12) as well as a significant interaction of *day x paw* ($F_{(5,80)}$=5.46, p<0.0001, n=6-12). No effect of genotype was observed. This provides evidence that HDAC4 may be involved specifically in mediating thermal sensitization following inflammation.

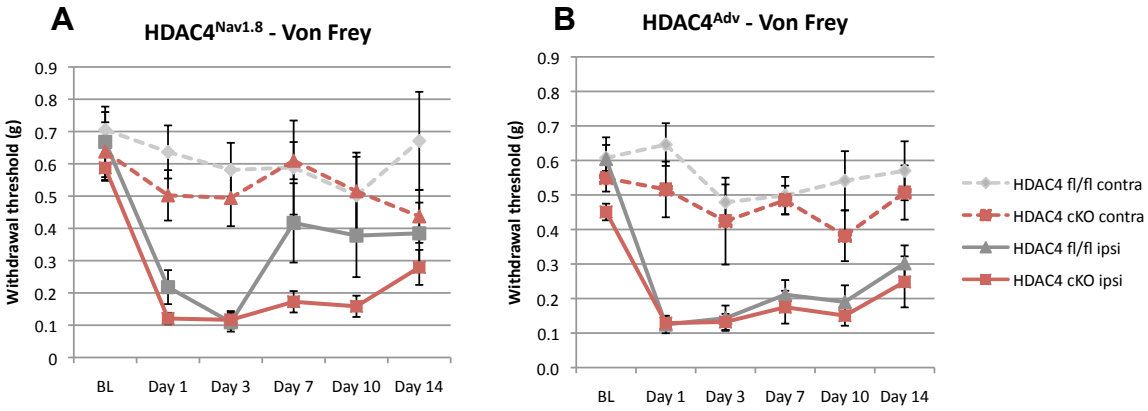


Figure 40 - HDAC4 is not required for mechanical hypersensitivity after CFA
Mechanical hypersensitivity was measured by the Von Frey test. **A** – Both HDAC4$^{Nav1.8}$ cKOs and littermates developed mechanical hypersensitivity after CFA injection (RM ANOVA significant effect of *day* ($F_{(5,45)}$=8.09, p<0.0001); *paw* ($F_{(1,9)}$=45.61, p<0.0001); significant interaction of *day x paw* ($F_{(5,45)}$=3.23, p=0.014, n=5-6). **B** – HDAC4^{Adv} cKOs and littermates developed mechanical hypersensitivity after CFA injection, which was not different between groups (RM ANOVA significant effect of *day* ($F_{(5,80)}$=8.79, p<0.0001); *paw* ($F_{(1,16)}$=147.09, p<0.0001); significant interaction of *day x paw* ($F_{(5,80)}$=5.46, p<0.0001, n=6-12).

Following these behavioural results, I looked at the regulation of other HDAC4 target genes to see whether they may also be differentially regulated after injury and in the HDAC4 cKO. Interestingly, wildtype animals showed downregulation of two known HDAC4 targets, *Hdac9* and *Snap25* after CFA injection (FC=0.74, =0.68, p=0.03, n=4, Welch's t-test between wt contra and wt ipsi). These genes were not downregulated in HDAC4^{Adv} cKOs (FC=1.51, =1.1, p>0.05, n=4, Welch's t-test, cKO

contra vs cKO ipsi) (Figure 41). No significant difference was observed in the expression of the HDAC4 target gene calcium/calmodulin kinase 2a (*Camk2a)* (FC=0.83, =0.66, n=4, p>0.05). Interestingly, validation of the previously characterized *Trpv1* expression changes revealed that *Trpv1* was not differentially regulated after injury in wildtype animals, however it was significantly downregulated in HDAC4^{Adv} cKOs (FC=0.95, =0.20, p<0.01 between wt ipsi and cKO ipsi). A similar trend was observed with the HDAC4 target gene, *Vglut1* (FC=0.74, =0.46, p>0.05 between wt ipsi and cKO ipsi, p=0.006 cKO contra vs cKO ipsi). Whether these changes may underlie the behavioural phenotype observed remains to be confirmed.

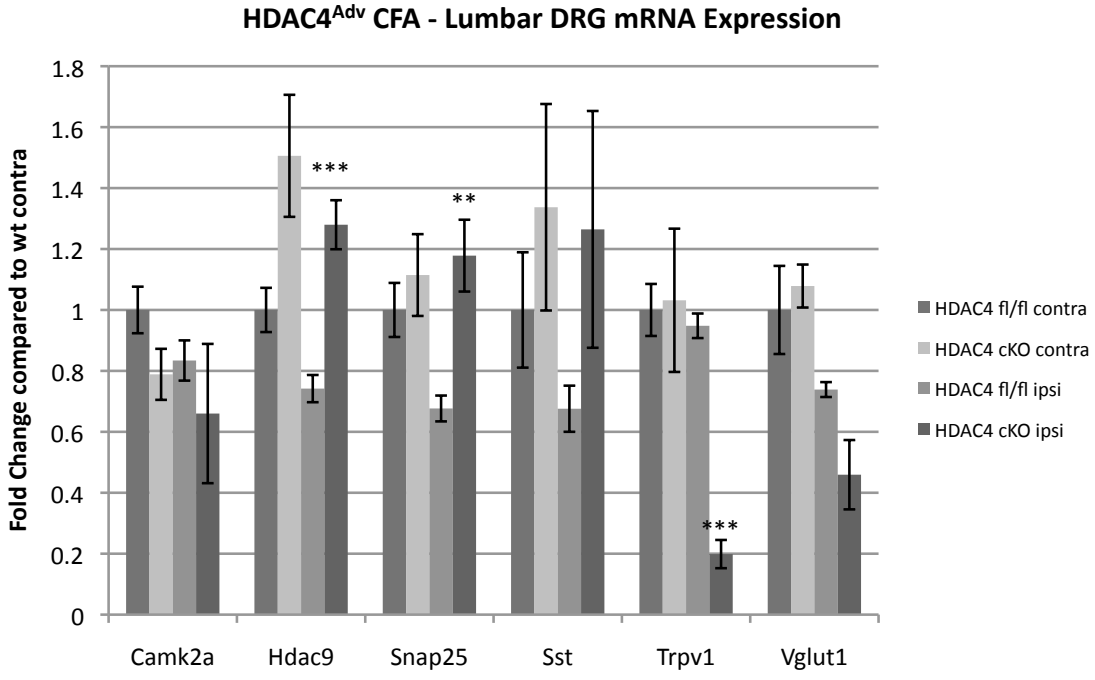


Figure 41 - Known HDAC4 targets are transcriptionally dysregulated after CFA
RT-qPCR analysis of previously described HDAC4 target genes. Significant differential regulation was observed for *Hdac9, Snap25*a and *Trpv1* in HDAC4^{Adv} cKO after CFA compared to HDAC4$^{fl/fl}$ littermates, but *Camk2a, Sst* and *Vglut1* were not significantly differentially regulated. ***p<0.001, **p<0.01, wildtype ipsi vs cKO ipsi, Welch's t-test, n-4.

5.4.5 Peripheral expression of HDAC4 is not required for most pain modalities

Histone deacetylase inhibitors are analgesic in a number of pre-clinical pain models, however the endogenous function of histone deacetylases in nociceptive pathways is far from clear (Denk and McMahon, 2012). Mutation of the deacetylase domain of HDAC4 affects thermosensation in the absence of obvious physiological defects (Rajan et al., 2009). Furthermore, knockdown of HDAC4 *in vitro* results in striking neurodegeneration and enhanced sensitivity to toxic insults (Li et al., 2012). Because of this we hypothesized that knockout of HDAC4 in sensory neurons, both in a subpopulation during development, and in all sensory neurons in adulthood, would alter sensitivity to noxious and innocuous stimuli. Interestingly, the phenotype of the conditional mutants was remarkably selective, indicating that HDAC4 is largely not required for innocuous sensation or nociception, with the exception of thermal hypersensitivity in a model of chronic inflammatory pain.

This suggests that the defect in thermosensation observed in HDAC4 deacetylase domain mutants does not depend on peripheral expression of HDAC4. Instead, this phenotype may arise as a consequence of defects in other areas of the nociceptive pathways, for example the interneurons of the spinal dorsal horn or the descending modulatory neurons of the midbrain. Conditional deletion of HDAC4 from these populations may provide evidence for this.

One of the hypotheses that I investigated was that HDAC4 could be neuroprotective in a model of toxic neuropathy, the d4T model. This was supported by evidence in the literature indicating that knockdown of HDAC4 could reduce sensitivity to oxidative and excitotoxic stress (Bolger and Yao, 2005; Yang et al., 2011). I failed to

see any difference in the mechanical hypersensitivity and skin innervation in HDAC4$^{Nav1.8}$ cKOs in this model, indicating that HDAC4 does not play a role in mediating the toxic effects of d4T and may not be important for oxidative stress signaling *in vivo*. Indeed, evidence for HDAC4 in mediating neuronal cell death has been conflicting. Although some studies claim HDAC4 knockdown is protective (Bolger and Yao, 2005; Yang et al., 2011), others indicate that knockdown causes neuronal cell death (Chen and Cepko, 2009; Li et al., 2012; Majdzadeh et al., 2008; Sando Iii et al., 2012). Neither of these claims have been substantiated by conditional knockout studies. In the past year, two studies have been published in which HDAC4 was knocked out of three different neuronal populations, none of which showed alterations to neuronal survival or gross brain morphology (Kim et al., 2012; Price et al., 2012). The absence of overt sensory behaviour differences after conditional ablation of HDAC4 in adult sensory neurons implies that developmental compensation cannot account for the lack of phenotype. Gross dissection, RNA and protein extraction also indicated that HDAC4^{Adv} cKOs were unlikely to have fewer neurons as DRGs were of a similar size and yielded similar amounts of RNA and protein (data not shown). Immunohistochemical analysis, for example staining for pro-apoptotic proteins such as caspases, alongside DRG cell counts would give a definitive answer to this question.

One surprising finding was that animals treated with tamoxifen were insensitive to cold and noxious mechanical stimulation, although heat and innocuous sensation were intact. This effect was independent of genotype, and a small group of animals that were not tamoxifen treated showed normal responses on these tests. Previous studies have indicated that tamoxifen treatment does not alter pain behaviour (Lau et al., 2011). However, sex-differences in pain behaviour are well-documented (Berkley, 1997), and estradiol and tamoxifen administration in ovariectomized rats has been

shown to reduce responses in the formalin test (Kuba et al., 2006). It is important to note that though the experimenter was blind to genotype, he was aware of the treatment status of all animals. The inclusion of a vehicle treatment group, and testing the same animals before and after treatment would clarify the role of tamoxifen in modulating noxious mechano- and cold sensation.

5.4.6 Loss of HDAC4 is associated with altered transcriptional regulation in inflammatory states, and reduced sensitivity to capsaicin *in vitro*

I previously reported that *Ntrk1, Calca* and *Trpv1* are consistently downregulated in both strains of HDAC4 cKOs after injury. Interestingly, the largest expression changes were seen in models with an inflammatory component, namely incubation with high levels of NGF and intraplantar CFA. Both *Calca* and *Trpv1* expression have been shown to be downstream of NGF signaling through the TrkA receptor (Amaya et al., 2004; Donnerer et al., 1992), and CGRP can also be influenced directly by TRPV1 activity (Nakanishi et al., 2010). Thus, altered intracellular signaling after TrkA activation may underlie the transcriptional change. Another possibility could be that HDAC4 interacts directly with the receptors, which is necessary for downstream activation of target genes. As discussed in Chapter 3, further work to explore the mechanism of this transcriptional change is required.

I hypothesized that *Trpv1* downregulation would affect responses to the TRPV1 ligand, capsaicin. Capsaicin binding to TRPV1 causes cation influx, which can be monitored using a calcium sensitive fluorescent dye. Interestingly, in knockout sensory neurons the response sizes were similar, but fewer neurons responded to capsaicin stimulation. This suggests that the reduced mRNA expression reflects the loss of TRPV1 from a subpopulation of neurons, rather than overall reduction of

message, which may be expected to produce smaller calcium responses in the same number of neurons. It will be necessary to validate this finding with immunocytochemistry. Another explanation for this finding could be loss of TRPV1 neurons due to cell death. Although no obvious difference in cell numbers or morphology was observed in DRG cultures, it will be important to investigate this as a potential mechanism because of the reported link between HDAC4 and neuronal survival in the literature.

Interestingly, a comparison of changes between the two inflammatory models indicated that there are more genes that are differentially expressed in both strains of HDAC4 cKOs. These included *P2rx3, Scn9a, Kcns1, Gch1* and *Atf3*. With the exception of *Atf3*, all of these genes have been shown to be important for pain processing, which is why they appear on the PCR array card. For example, single-nucleotide polymorphisms in the *Gch1* gene can predict pain sensitivity in some human populations, and inhibition of its activity has been shown to be analgesic in animal pain models (Latremoliere and Costigan, 2011). It will be interesting to determine whether these transcriptional changes give rise to functional differences in HDAC4 cKO sensory neurons, for example by testing the sensitivity of HDAC4 cKO neurons to P2xr3-selective ligands using calcium imaging. Further work to validate these targets is required.

5.4.7 Thermal hypersensitivity is attenuated in HDAC4 cKOs in a model of chronic inflammatory pain, but not after nerve injury or acute inflammation

Thermal hypersensitivity was attenuated in HDAC4 cKOs after intraplantar CFA injection, but not after carrageenan injection or in the partial sciatic nerve ligation (PSL) model of neuropathic pain. In the case of carrageenan, this may be due to the

requirement of de novo transcription for phenotypic differences. Carrageenan injection leads to an almost immediate decrease in withdrawal latencies, and responses are monitored in a short time frame after injection, from two to twenty-four hours. Transcriptional changes may occur on the order of hours, but protein turnover takes much longer, on the order of days, particularly if proteins need to be trafficked from distant cell bodies to nociceptor terminals (Djouhri et al., 2001). It is likely, therefore, that the nociceptor sensitization in this model is due to post-translational modification of receptors by inflammatory mediators, rather than transcriptional alterations. This would be consistent with the idea that transcriptional alterations resulting from HDAC4 loss are implicated in the conditional knockout phenotype.

It is somewhat surprising that no difference in thermal hypersensitivity was observed after PSL, particularly as expression changes, including reduced *Calca* expression and increased *Sst* expression in cKOs, would predict this (Chrubasik et al., 1984; Mogil, 2005). The small window afforded to observe differences (decreased latency of approximately two seconds compared to the contralateral paw) may have limited our capacity to detect behavioural differences in this model. The use of a model that exhibits a greater degree of thermal hypersensitivity, for example the chronic constriction injury, may reveal an additional role for HDAC4 in mediating thermal hypersensitivity after nerve injury.

It is important to note that it has been reported that the $Na_v1.8$ population of sensory neurons is dispensable for hypersensitivity in the partial sciatic nerve ligation model (Abrahamsen et al., 2008). In this study, Abrahamsen *et al* drove diphtheria toxin expression from the $Na_v1.8$ promoter to selectively ablate this population of neurons. However, it is now known that the expression of $Na_v1.8$ is much more wide-spread than was originally reported in this paper, which calls into question whether the diphtheria targeting in these animals was efficient (Shields et al., 2012). Additionally,

other studies employing the $Na_v1.8$-Cre line have shown differences in neuropathic pain behaviour using the PSL model (Emery et al., 2011; Samad et al., 2010). Further investigation of the mechanism through which HDAC4 contributes to thermal hypersensitivity, and possibly the use of other neuropathic pain models may help to clarify this.

The primary phenotypic change we observed in HDAC4 cKOs was reduced thermal hypersensitivity following CFA injection. This was seen in animals with HDAC4 deletion in a subset of primary neurons from embryonic stages, as well as in animals with targeted ablation in adulthood. This indicates that the difference is not likely to be due to a developmental process. Thermal hypersensitivity after inflammation has been shown to depend on TRPV1 activation, and indeed I demonstrated that HDAC4 cKOs express much lower levels of *Trpv1* mRNA, which may underlie the behavioural change. It is important to note, however, that a number of other pain-related transcripts were differentially expressed in HDAC4 cKOs after inflammation, some of which were not changed in the neuropathic pain models. Whether these genes may play a more important role than *Trpv1* in mediating this phenotype remains to be seen. Interestingly, previously described HDAC4 targets, *Snap25* and *Hdac9,* were downregulated in wildtype animals after CFA, and $HDAC4^{Adv}$ cKOs were spared from these changes. *Snap25* is required for neurotransmitter release, and is transcriptionally dysregulated in multiple tissues and pain models (LaCroix-Fralish et al., 2011) and *Hdac9* has been shown to be differentially regulated by NGF (Guo et al., 2011). It will be interesting to determine whether these genes may also be involved in peripheral sensitization.

Inflammation causes the release of many different inflammatory mediators that rely on intracellular signaling cascades to produce altered transcriptional regulation and peripheral sensitization. HDAC4 activity and subcellular localization is dependent on

many of the same signaling cascades, for example it can be trafficked from the nucleus in a calcium/calmodulin kinase-dependent manner. One of the main questions that remains regards the localization of HDAC4 in the sensory neurons of the DRG both before and after injury. Investigation of the subcellular localization could be done with immunohistochemistry, however given the lack of specific antibodies this remains a challenge. Instead, I have been attempting to optimize a subcellular fractionation protocol for Western blotting to look for the relative enrichment of HDAC4 in the cytoplasm or nucleus after CFA. Pilot data indicates that it may, indeed, be trafficked into the cytoplasm after injury, however further validation of this is required.

Alternatively, investigation of GFP-tagged HDAC4 in cell lines that are responsive to inflammatory mediators, for example PC12 cells, may provide a good model system to investigate HDAC4 shuttling. If this cell line can recapitulate some of the transcriptional differences observed after CFA, it may also be of use to investigate the mechanism of HDAC4 action through the introduction of mutated and/or tagged forms of HDAC4, and the use of luciferase constructs.

Finally, it may be interesting to try novel HDACi, for example MC1568 that targets the MEF2 binding site of class IIa HDACs and causes enforced repression of MEF2 activity (Nebbioso et al., 2009). Use of this drug would allow us to determine whether this domain of HDAC4 contributes to the cKO phenotype. Other pharmacological approaches, for example inhibition of ERK/MAPK to look for upstream signals regulating HDAC4 function, or inhibition of histone demethylation may also help to further elucidate the mechanism of HDAC4, potentially providing novel therapeutic approaches to modulate thermal hypersensitivity.

6 General Discussion

The role of histone deacetylases and other chromatin modifying proteins is a vast and largely unexplored area of sensory neuron biology. Evidence that HDACs are involved in pain and regeneration are accumulating (Geranton, 2011; Rivieccio et al., 2009). In this thesis I aimed to explore the function of HDAC4 using a conditional knockout approach. In the first data chapter, I reported the validation of two novel strains of HDAC4 knockouts with selective ablation of the enzyme in a subpopulation of sensory neurons during embryonic development and in all sensory neurons in adulthood. With these animals I established that HDAC4 was required for transcriptional regulation in response to injury and at rest.

In the second data chapter I investigated whether HDAC4 could play a role in peripheral nerve regeneration. I found that, despite regulating *Atf3* mRNA expression, it was not likely to be required for appropriate re-innervation.

In the final data chapter I determined that sensory neuron expression of HDAC4 was not required for innocuous or acutely noxious sensation, or for the development of mechanical hypersensitivity in a number of pain models. Interestingly, HDAC4 was required for full expression of thermal hypersensitivity in a model of chronic inflammatory pain. This was associated with reduced sensitivity to capsaicin *in vitro* and many transcriptional changes, including robust downregulation of the gene encoding the heat- and capsaicin-sensitive channel, TRPV1.

Many questions remain and many of these results require further validation. Throughout my project I used RT-qPCR array cards as a medium-throughput screening tool to determine whether HDAC4 loss may have implications for the transcriptional regulation of genes that we know are involved in innocuous and

noxious cutaneous sensation. This was a very productive experimental route, yielding many interesting results within each study. However, at times these results failed to hold up to closer scrutiny. For example, *Atf3* mRNA expression was found to be differentially regulated in conditional knockouts after nerve injury but protein expression appeared to be largely normal. There are many reasons that may account for this, which were discussed in more detail in Chapter 4; the take-home message is that transcriptional data cannot be used as a direct proxy for protein expression. In order to confidently determine the role of HDAC4 in sensory neurons, validation at the protein and functional levels are required.

That said, despite the negative data surrounding the *Atf3* and regeneration story there remain some interesting observations and questions. Although ATF3 protein expression did not appear to be different using immunohistochemistry, Western blotting would provide more robust evidence for this. In addition, the lack of observable differences on outgrowth measures could be due to technical limitations: the inability to differentiate small from large fibres in the culture study; and looking at an inappropriate time point for skin re-innervation. Further optimization of histological outcomes may help to answer whether HDAC4 does have an effect on neurite outgrowth. I attempted to inject a tracer distal to the crush site in order to trace neurons that had re-grown but this proved to be non-specific: almost every neuron picked up the tracer even when it was injected farther than the nerves could have been expected to regenerate. Direct imaging of C-fibre markers within the crushed nerve and through the lesion would provide the best evidence and could be achieved with some experimental optimization.

Another intriguing finding came from my attempt to repeat the sciatic nerve crush study in a cohort of HDAC4^{Adv} cKOs. I was required to terminate the study after one week because three out of five conditional knockouts autotomized. None of the seven

controls autotomized. This could be due to chance but it remains an odd observation and potentially interesting to explore further.

I have started to accumulate data on the role of HDAC4 in mediating responses to inflammation, and there is a hint that it may be due to altered regulation of TRPV1. Further experiments to elucidate the molecular mechanisms underlying this are required. *Trpv1* mRNA is highly downregulated in HDAC4 cKOs, which is curious because HDAC4 is thought to negatively regulate transcription, and thus, in its absence, one may expect enhanced transcription of target genes. This may imply that HDAC4 is required for the regulation of a negative transcription factor, such as REST or members of the NFKB subfamily. On the other hand, a cytoplasmic mechanism cannot be ruled out. It is possible that cytoplasmic HDAC4 is required to promote sumoylation or deacetylation of TRPV1 or other mediators that regulate its expression. In this case the loss of HDAC4 could alter the activity of these proteins. The first step to begin to address this will be to determine the subcellular localization of HDAC4 in inflammatory pain models. Dissociated DRG cultures treated with high levels of NGF mimicked many of the transcriptional changes observed after intraplantar CFA injection and were associated with reduced capsaicin sensitivity. This model system may provide a good starting point for uncovering the molecular mechanisms of HDAC4. Experiments to separate protein lysates into cytoplasmic and nuclear fractions have begun to be optimized and results look promising. Once this has been established, work to determine the expression and activity of putative nuclear or cytoplasmic targets can be investigated in more detail.

One interesting avenue that I did not discuss in my thesis was our attempt to deliver Cre intrathecally using adeno-associated viral vectors in order to target spinal cord neurons. Although this strategy was not successful in our first attempts, further optimization of this method, for example the use of higher titre vectors or a different

administration protocol, may provide new insights into the role of HDAC4 in other areas of the nervous system. This would also be a translatable strategy for other floxed mouse lines, streamlining some of the breeding time required for most experiments with transgenic animals.

Indeed, one of the key issues I encountered over the course of my project was the length of time required to prepare for animal experiments. The use of complementary strategies, for example pharmacological tools that interfere with HDAC4-MEF2 activity or other model systems to discern the function of HDAC4 e.g. cell lines that are easily transfected with tagged forms of the protein, may have sped up some of the progress. However, because my project was largely led by the behavioural phenotyping of conditional mutants, mechanistic studies were initiated only subsequent to validation of *in vivo* function. This is a high-risk, high-gain approach, although it is 'safe' in that the results are compelling and fairly definitive. Future studies to determine the role of novel targets would benefit from the use of higher-throughput screening methods.

HDAC inhibitors and other drugs that target chromatin modifying and transcriptional regulatory proteins are already being used clinically to treat cancer. Work to characterize the function of these molecules in diverse systems will provide a rational basis for the broader application of these therapies.

Appendix 1: Bioinformatics analysis of HDAC4 expression and function

6.1 Introduction

With the adoption of high-throughput technologies an increasing amount of data and resources have been made available online. Gene expression data, known and predicted protein-protein and protein-DNA interactions, motif finding algorithms – all of these can be accessed from the comfort of your own home (for example, while you are writing your thesis).

This chapter has its origins in curiosity about HDAC4 expression in the dorsal root ganglion, but the further I delved into the abyss of online bioinformatics tools, the more addicted I became to taking advantage of the mounds of data that have been produced to identify novel, conserved downstream targets. The power of this analysis comes from the use of genome-wide expression data, which allows for a completely unbiased approach to target identification, generating data-driven hypotheses that can be investigated experimentally.

6.2 Aims

The aims of this chapter are to describe HDAC4 expression in the dorsal root ganglion and spinal cord, and to explore its putative function using published data and online bioinformatics tools.

6.3 Results

6.3.1 Characterising *Hdac* mRNA expression in the DRG and spinal cord

From the earliest characterization of the class IIa HDACs (HDAC4, -5, -7 and -9), their expression has been shown to be tissue-specific, enriched in the brain, skeletal muscle and heart (Grozinger et al., 1999) and HDAC4 has been shown to have important roles in all of these tissues (Miska et al., 2001; Sando Iii et al., 2012; Vega et al., 2004). Darcy *et al* characterized the expression of HDAC4 in the brain, and showed that it was widely expressed across multiple areas and neuronal subtypes (Darcy et al., 2010). This suggests that HDAC4 is likely to be expressed in other neurons, such as spinal cord interneurons and primary sensory neurons of the dorsal root ganglia. To date, there has been no specific characterization of the HDAC expression profile in sensory neurons of the dorsal root ganglia or the spinal cord. To examine this, I made specific RT-qPCR primers for each of the HDACs and looked for their expression in naïve adult DRG and spinal cord. In addition, I obtained data from a next generation sequencing experiment that was performed by a post-doctoral fellow in our lab (Dr. Ana Antunes-Martins) to compare the expression profiles in mouse and rat tissue (Figure 1).

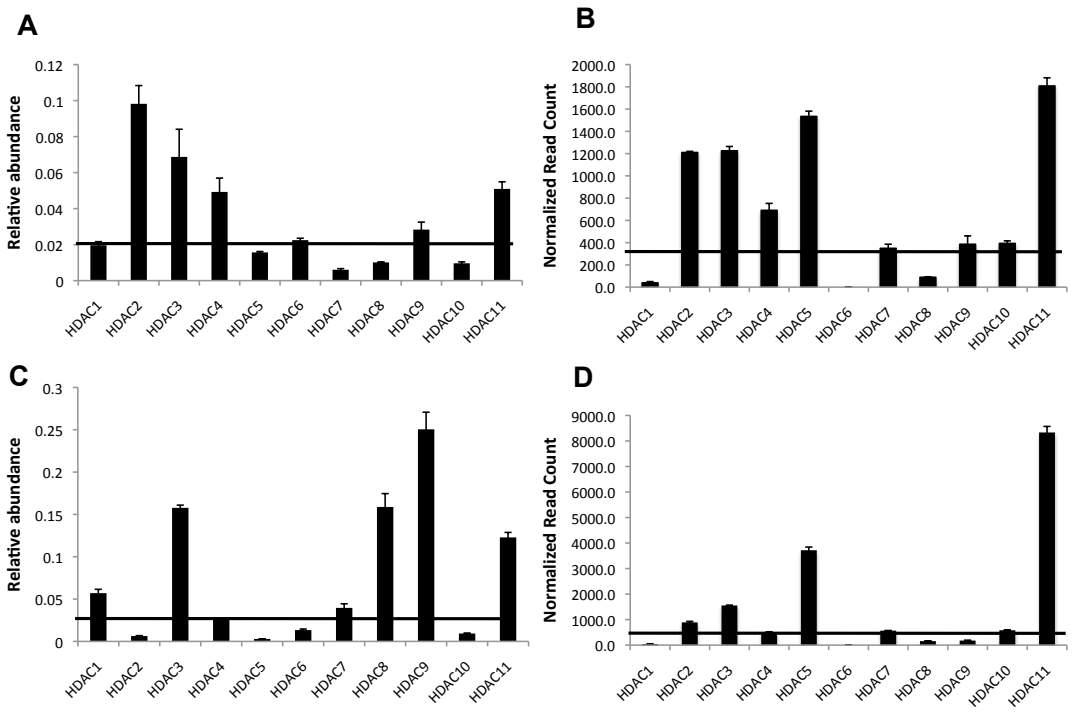


Figure 42 - HDAC mRNA expression profiles in mouse and rat DRG and spinal cord
Mouse expression data (**A** and **C**) comes from RT-qPCR experiments using HDAC specific primers. Abundance is relative to a housekeeping gene, Ywhaz. Rat expression data (**B** and **D**) are normalized read counts from next-generation sequencing (NGS) performed by Dr. Ana Antunes-Martins. Black lines represent median expression values (A=0.022, B=393, C=0.04, D=567). Interestingly, *Hdac4* expression is above the median value in both mouse (**A**) and rat (**B**) DRG, but not in spinal cord (**C** and **D**). Similar HDAC expression profiles are obtained in the DRG in both species, with HDAC2, -3, -4 and -11 showing the highest expression, though there is divergent expression of HDAC5. The spinal cord has a very different profile from the DRG in both species, with strong expression of HDAC3 and -11 in both mouse and rat, but some divergent patterns. These may represent true differences between the species, or may be attributed to the different techniques used to obtain data.

Interestingly, in adult mouse DRG, *Hdac4* was the most highly expressed class IIa HDAC, suggesting a primary role of HDAC4 in mediating class IIa HDAC activities in this tissue. It was also expressed above the median value for all HDACs in the rat, however, *Hdac5* was more expressed, which may represent a species difference in HDAC expression or may reflect differences in the techniques used to obtain data. For example, because of the high homology of HDAC4 and HDAC5 and because the rat genome is considerably less well-characterized than the mouse genome, it is possible that in the NGS experiment *Hdac4* sequencing reads were misaligned to

Hdac5. RT-qPCR and protein analysis would help to determine whether this is the case.

In the spinal cord, *Hdac4* was expressed below the median in both species. Surprisingly, the class IV HDAC, HDAC11, was highly expressed in both tissues in both species. Very little is known about this HDAC, and its strong expression in these tissues may indicate a role in neuronal function.

6.3.2 Localising *Hdac4* expression using the Allen Brain Atlas

The Allen Brain Atlas (**www.alleninstitute.org**) is an online resource that integrates gene expression and neuroanatomical data using RNA probe based *in situ* hybridization. Images of mouse spinal cord at post-natal day four (P4) are often accompanied by DRG sections, and allow for anatomical mapping of genes of interest within both structures (http://mousespinal.brain-map.org). Having established the expression of *Hdac4* mRNA in the mouse DRG, I sought to determine whether it might show subpopulation-specific expression, using the menthol-sensitive *Trpm8* as a positive control (Figure 43).

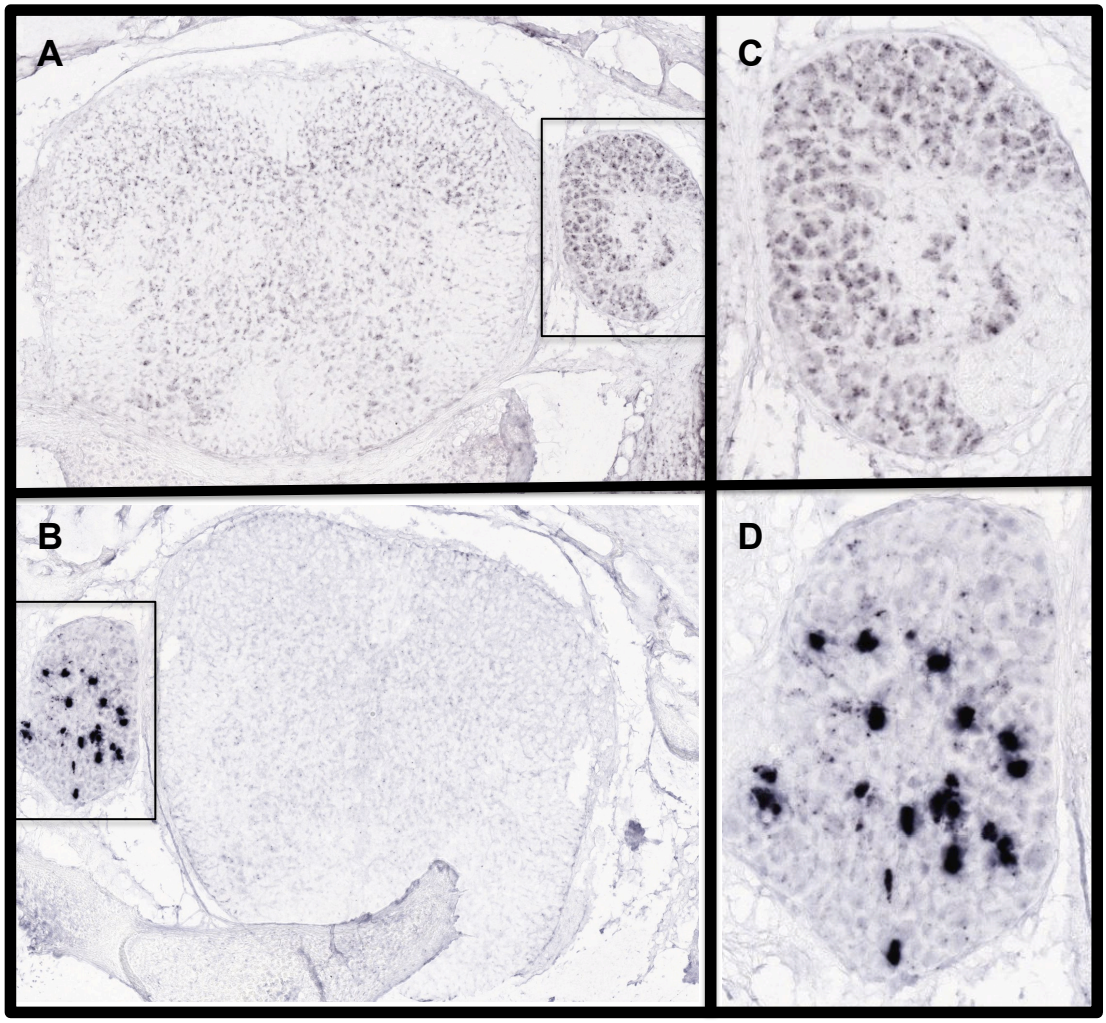


Figure 43 - *Hdac4* mRNA is expressed in all DRG sensory neurons at P4
Images from the Allen Brain Atlas. Top row, *Hdac4*, bottom row *Trpm8*. **C** and **D** are magnified views of the boxes in **A** and **B**. **A** – *Hdac4* has weak expression throughout the neuropil of the spinal cord, and is moderately expressed in the DRG. **B** – *Trpm8* shows strong, DRG specific expression, and no discernable expression in the spinal cord. **C –** No neuronal subtype-specificity is observed for *Hdac4* in the DRG. **D** – Sparse localization of *Trpm8* indicates subtype-specific expression

Hdac4 mRNA showed diffuse expression in both the DRG and neuropil of the spinal cord. In contrast, *Trpm8* was strongly localized to what appeared to be individual neurons of the DRG and could not be detected in the spinal cord. This is in line with the RT-qPCR and NGS data, indicating that HDAC4 is expressed in these tissues. (Mean *Trpm8* read count in spinal cord = 8.8 +- 3.5; in L4 DRG = 2503.4 +- 217.7; Mean *Hdac4* read count in spinal cord = 474.2 +- 51; in L4 DRG = 649.7 +- 13.5). In addition, this evidence suggests that HDAC4 is not preferentially expressed in particular DRG subtypes.

6.3.3 Using published chromatin immunoprecipitation and next generation sequencing data (ChIP-Seq) to investigate HDAC4 function

Chromatin immunoprecipitation in combination with next-generation sequencing (ChIP-Seq) allows for genome-wide characterization of transcription factor binding. To date, one group has published ChIP-Seq data of HDAC4 binding sites in the cerebellum (Li et al., 2012). In this paper, the authors compared HDAC4 occupancy between wildtype and ataxia telangiectasia knockout mice (*Atm*-/-) in which HDAC4 accumulates in the nucleus. To determine whether HDAC4 may be involved in mediating transcription through direct binding of genes known to be important for sensory neuron function, we performed a conservative bioinformatics analysis of this data, using tools on the Galaxy server (https://usegalaxy.org/). First, SoLID FASTQ files were uploaded to Galaxy from the European Nucleotide Archive (http://www.ebi.ac.uk/ena/) then converted to Sanger FASTQ files using the FASTQ Groomer tool (Blankenberg et al., 2010). Reads were mapped to the mm9 build of the mouse genome (Waterston et al., 2002) using the Bowtie tool (Langmead et al., 2009) which has recently been evaluated against other short-read mapping algorithms and consistently performed extremely well (Hatem et al., 2013). Following alignment, files were re-formatted into both BAM and BED formats for further analysis using SAM tools (Li et al., 2009). Peak calling was performed on BED files using the MACS peak calling algorithm, with wildtype input chromatin as the background control (Zhang et al., 2008). Finally, the Intersect tool was used to determine overlapping peaks between wildtype and *Atm*-/- samples. This yielded 1299 overlapping regions (Figure 44). Using the profile annotations tool, 294 of these regions were found to map to known UCSC genes. GPAT was used to annotate this

list (http://bips.u-strasbg.fr/GPAT/) (Krebs et al., 2008) and 212 genes were identified (Chromosome 10 results in Table 10, full list in Appendix 3: GPAT output file from ChIP-Seq analysis). Surprisingly, this list contained two genes that are essential for analgesia: the mu-opioid receptor, *Oprm1* and *Cacna2d1* that encodes the voltage-gated calcium channel subunit α2δ. Interestingly, *Cacna2d1* is upregulated in both strains of HDAC4 cKOs (FC=1.32, 1.55, Chapter 3), suggesting that HDAC4 may directly bind *Cacna2d1* in the DRG to regulate its expression. *Oprm1* was also upregulated in HDAC4^{Adv} cKOs (FC=1.75). This evidence suggests that HDAC4 may recognize similar targets in the brain and in the dorsal root ganglion. Although these transcriptional differences were not associated with overt behavioural differences at baseline, this suggests that HDAC4 cKOs would be more sensitive to gabapentinoids and morphine analgesia, indicating that modulation of HDAC4 could provide novel mechanisms of pain management.

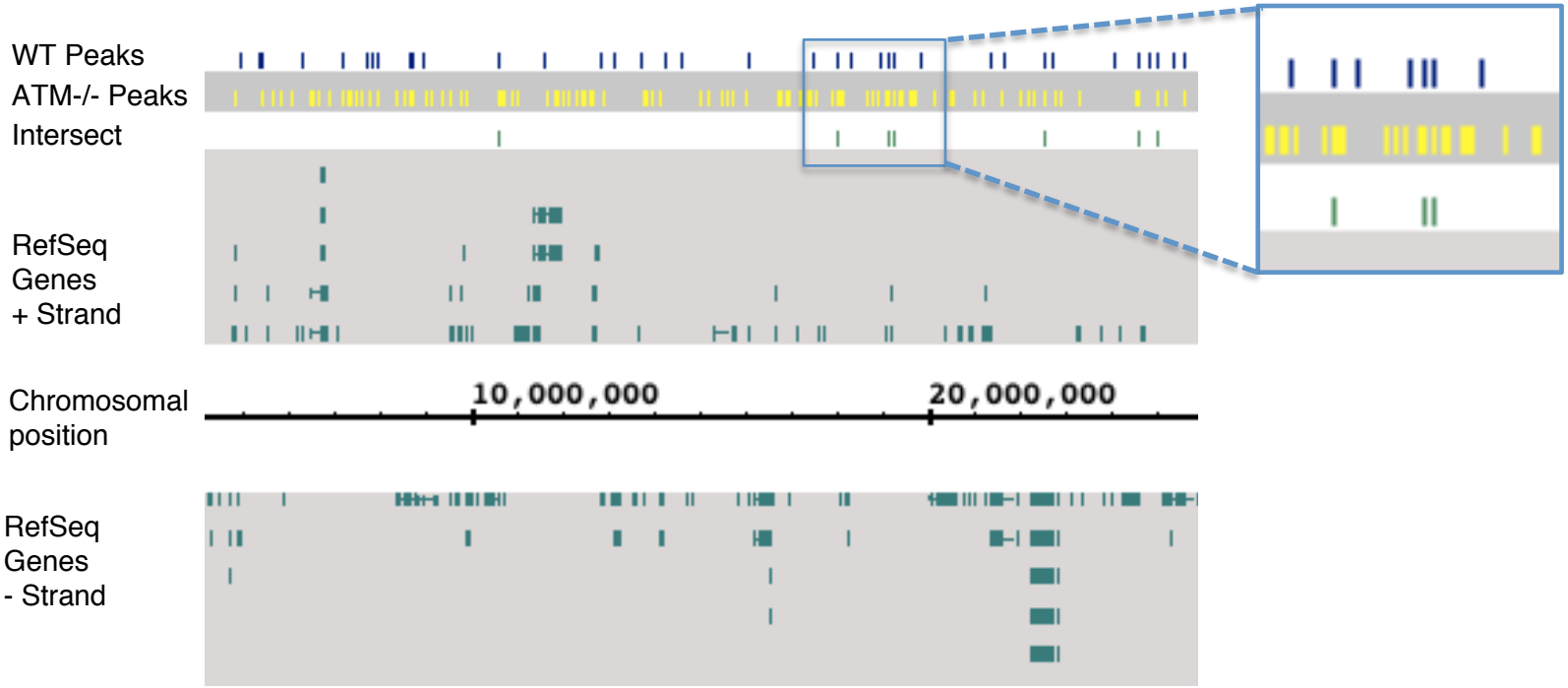


Figure 44 - Bioinformatics analysis of published HDAC4 ChIP-Seq data, partial chromosome 16 alignment
Figure from IGB viewer. Data from Li *et al* 2012. Peaks were discovered with the MACS algorithm, using 10% input chromatin as a control. The WT Peaks line shows the aligned HDAC4 peaks from wildtype cerebellum, in blue. ATM-/- Peaks are from ATM knockout cerebellum, shown in yellow on grey background. Many more peaks are found in the ATM knockout as HDAC4 accumulates in the nucleus. Intersect represents peaks that overlap between both datasets, shown in green. To reduce the number of false positive results, this was used to define putative HDAC4 binding sites.

Table 10 - Sample of GPAT output - Overlapping Peaks on Chromosome 10

feature_ID	chromosome	min_pos	max_pos	gene_ID	gene_name	strand	start_position	TSS_distance
MACS_peak_859	chr10	3527715	3527773	NM_001039652	Oprm1	-	3557940	30196
MACS_peak_870	chr10	4860285	4860320	NM_153399	Syne1	+	4795848	64454
MACS_peak_949	chr10	20179615	20179737	NM_013875	Pde7b	-	20444874	265198
MACS_peak_952	chr10	21977836	21977908	NM_009018	Raet1c	+	21893707	84165
MACS_peak_953	chr10	21977933	21978018	NM_009018	Raet1c	+	21893707	84268
MACS_peak_1005	chr10	31516009	31516040	NM_001013411	Nkain2	-	32609721	1093697
MACS_peak_1062	chr10	42242152	42242186	NM_017472	Snx3	+	42221859	20310
MACS_peak_1113	chr10	50686748	50686787	NM_011376	Sim1	+	50615456	71311
MACS_peak_1124	chr10	51864278	51864336	NM_011282	Ros1	-	51915050	50743
MACS_peak_1224	chr10	72841935	72841971	no_match				
MACS_peak_1289	chr10	94334776	94334830	NM_018797	Plxnc1	-	94407212	72409
MACS_peak_1365	chr10	107614275	107614309	NM_027892	Ppp1r12a	+	107599455	14837
MACS_peak_1369	chr10	107998262	107998296	NM_009306	Syt1	-	108448031	449752
MACS_peak_1402	chr10	114174430	114174494	NM_146241	Trhde	-	114238426	63964
MACS_peak_1403	chr10	114546341	114546392	NM_173391	Tph2	-	114622078	75712
MACS_peak_1429	chr10	123113356	123113391	NR_045514	Fam19a2	+	122701131	412242

6.3.4 Bioinformatics analysis of HDAC4 targets using publicly available microarray and ChIP-Seq data reveals three conserved HDAC4 target genes

To continue to explore the role of HDAC4 I looked for published microarray data from experiments in which HDAC4 had been overexpressed or knocked down on the GEO website. Two datasets were used for further analysis: one from overexpression of full-length HDAC4 in cardiomyocytes (Kehat et al., 2011) and a dataset from cultured embryonic cortical neurons that overexpressed a constitutively nuclear form of HDAC4 (Sando Iii et al., 2012). Using the GEO2R tool, I looked for differential regulation between controls and HDAC4 over-expressing samples. A list of differential genes was discovered for each study, and these three lists were input to a Venn Diagram making tool, genevenn.sourceforge.net. Three genes were found in all three lists: *Cacna2d1*, palmdelphin (*Palmd*), a lipid-raft associated protein involved in cell-shape control, and the adenylyl cyclase-associated protein 2 (*Cap2)* (Figure 45). Interestingly, all three genes show similar expression profiles to HDAC4, with overexpression in the brain, heart and skeletal muscle (Lattin et al., 2008; Wu et al., 2009) (Figure 46). CAP2 and CACNA2D1, like HDAC4, have both been linked to cardiac and skeletal muscle defects (Effendi et al., 2013; Fuller-Bicer et al., 2009; Peche et al., 2013), although the interaction of these proteins has never been tested experimentally. This evidence would suggest that HDAC4 may coordinate the appropriate expression of these genes through direct DNA binding.



Figure 45 – Venn Diagram from genevenn.sourceforge.net
Gene lists were generated from published microarray and annotated ChIP-Seq data (Figure 3). OE = over-expression. The dataset in red came from over-expression of full-length HDAC4 in cardiomyocytes (Kehat et al., 2011), green from over-expression of a constitutively nuclear form of HDAC4 in cultured cortical neurons. The three overlapping genes were *Cacna2d1,* known to be involved in pain signaling and a key target of analgesic drugs, as well as the lesser studied genes *Palmd* and *Cap2.*

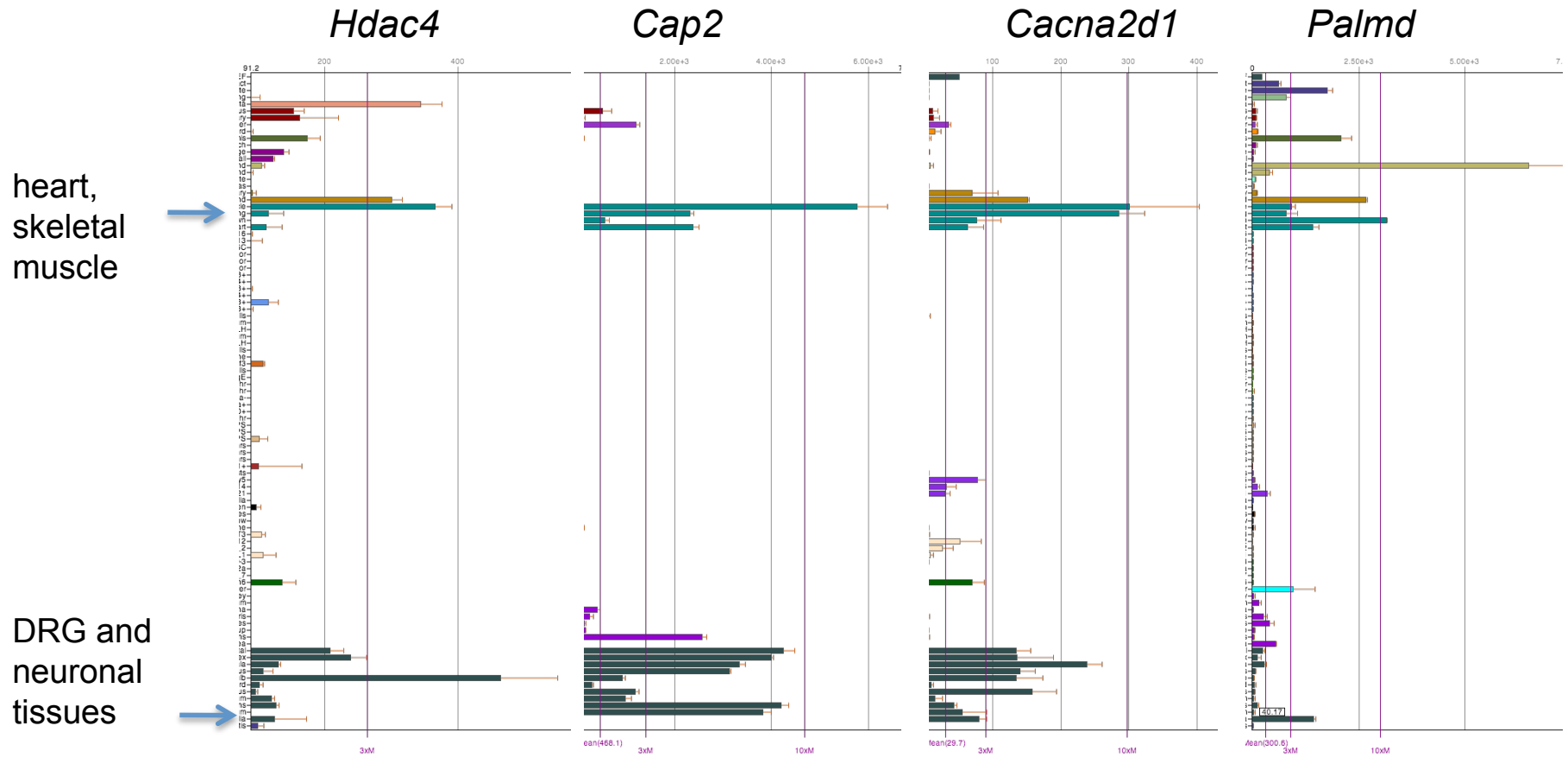


Figure 46 - HDAC4 and putative targets show similar tissue expression profiles, figure adapted from BioGPS.org
Tissue types are represented by individual bars, with tissues from similar origins represented in the same colour. The length of the bars indicates expression level.

6.3.5 Pathway analysis of putative HDAC4 targets confirms known functions of the protein

Pathway analysis programs make predictions about protein function by taking advantage of published data for example, yeast-two-hybrid protein-protein interaction studies, microarrays in various disease models, and literature searching for commonly co-published keywords.

To try to dig out new functions of HDAC4, I input the three gene lists into Ingenuity Pathway Analysis (Figure 47). Although this did not provide much new insight into the function of HDAC4, it did confirm current understanding of its function, for example highlighting enrichment for gene ontology (GO) terms such as development, morphology and cell-to-cell signaling, all of which have been shown to be affected by HDAC4 overexpression and knockout studies (Miska et al., 2001; Sando Iii et al., 2012; Vega et al., 2004), and gave me confidence that the gene lists that I generated were likely to be truly related to HDAC4.

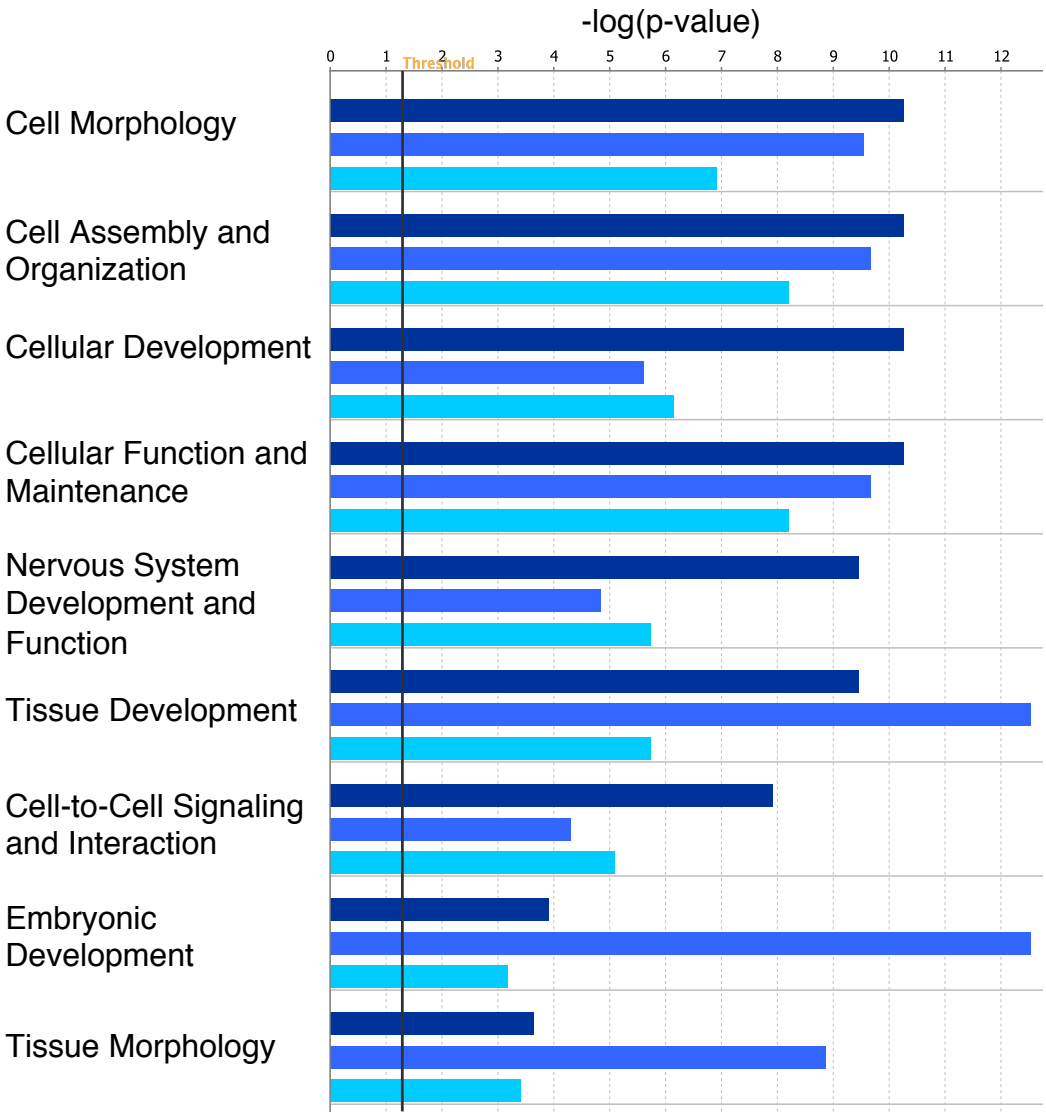


Figure 47 - Example of results from Ingenuity Pathway Analysis
Individual gene ontology terms are listed above, and adjusted p-values for each of the three datasets are charted. The expression gene lists are represented in darker blue, and the ChIP list is in light blue. The threshold p-value is in black. Gene lists show enrichment for GO annotations including development, cell assembly and cell signaling, which is in line with known HDAC4 functions from knockout and overexpression studies.

6.3.6 Network analysis of both experimentally validated and predicted HDAC4 targets identifies HDAC4 and NGF as upstream regulators and NF-Kappa B proteins as possible intermediaries

Ingenuity pathway analysis can also be used to identify whether genes of interest can be linked together in functional networks. Analysis of the three HDAC4 targets

identified from bioinformatics analysis (*Cap2, Palmd* and *Cacna2d1)* as well as the genes that were commonly dysregulated in the HDAC4 cKOs (*Trpa1, Ntrk1, Trpv1* and *Calca)* yielded a highly interconnected network associated with the GO terms Organismal Injury and Abnormalities, Neurological Disease, Cell Death and Survival. The top upstream regulators predicted were NGF (4/8 genes, p=3.9e-7) and HDAC4 (3/8 genes, p=5.84e-6). Interestingly, the NF-Kappa B (NFKB) complex was highly interconnected with the target genes, and had a central position in the network, indicating that it may be involved in mediating some of the expression differences observed (Figure 48).

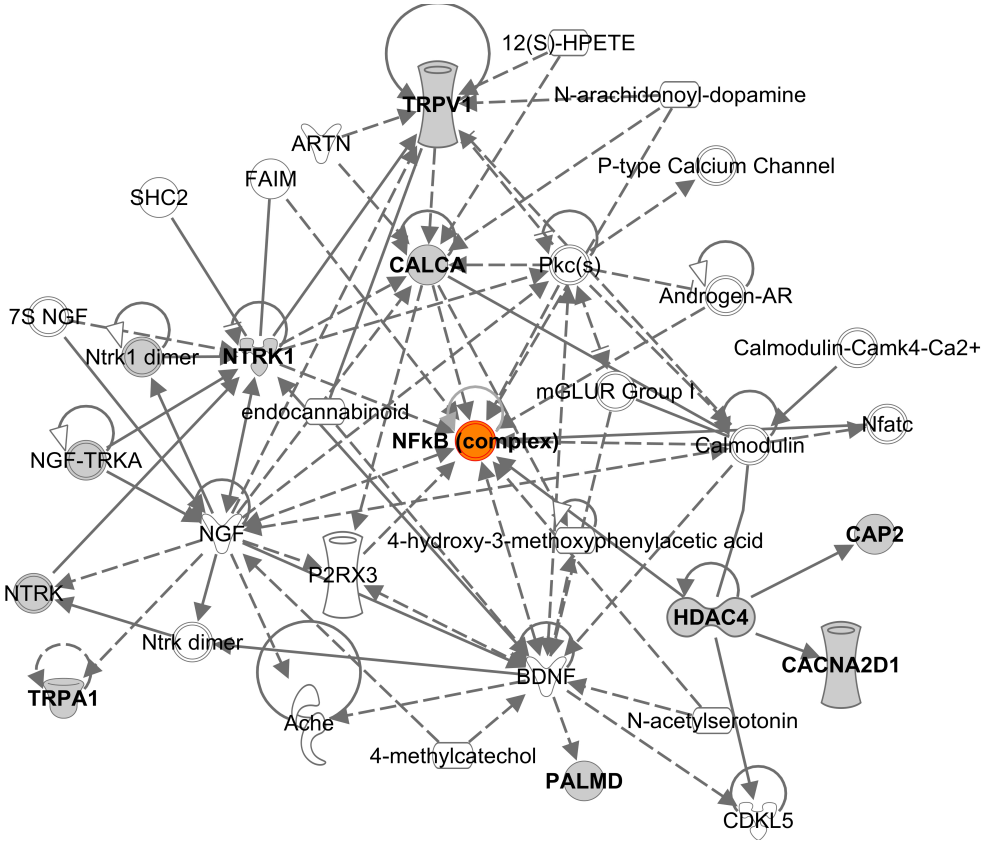


Figure 48 - Ingenuity Pathway Analysis Network
Target genes are in bold. Shapes are indicative of protein function. Solid lines represent direct interactions, dashed lines represent indirect interactions. Interestingly, the NF-Kappa B complex is quite central to the network, and interacts with most of the target genes. Whether HDAC4 exerts its transcriptional regulatory function in sensory neurons through interaction with NF-Kappa B proteins will be interesting to explore.

6.4 Discussion

The use of bioinformatics tools is straightforward, cheap and allows for rapid hypothesis generation. Further work to investigate the targets identified in this manner may provide novel insights into the role of HDAC4.

6.4.1 Expression data shows *Hdac4* mRNA in DRG and spinal cord

To my knowledge, there has been no direct characterization of HDAC isoform expression in the DRG and spinal cord, although a number of studies have investigated the analgesic potential of HDAC inhibitors. I used RT-qPCR and NGS sequencing data to look at the relative expression of these molecules, and discovered that in the mouse, HDAC4 is the most highly expressed class IIa HDAC in the DRG, which suggests that it may subserve most of the class IIa functions in this tissue. Interestingly, the relatively understudied class IV HDAC, HDAC11, is the most highly expressed HDAC in the rat DRG and spinal cord, and is very highly expressed in the mouse as well. Further investigation into the role of this HDAC may be warranted.

The Allen Brain Atlas is an excellent tool to determine mRNA localization in the developing and adult mouse spinal cord and brain. As an added bonus, P4 spinal cord sections often are flanked by DRGs, and can be investigated for sensory neuron expression of genes of interest. Using the Allen Brain Atlas, I determined that HDAC4 mRNA was expressed widely in the DRG though at a moderate level, compared to TRPM8, the menthol and cold-sensitive TRP channel that is known to have subtype specific expression. Confirmation of these findings at the protein level and in adult animals is required, however the lack of suitable antibodies for immunohistochemistry remains problematic.

6.4.2 "Conserved" HDAC4 targets include *Cacna2d1*, an important pain gene

The majority of published microarray data is now available through the GEO website, which has an incredibly easy-to-use analysis tool, GEO2R. Using these tools, along with a number of software tools in the Galaxy suite, I generated three lists of putative HDAC4 targets based on overexpression studies and an HDAC4 ChIP-Seq study.

Three genes overlapped between these datasets, *Cacna2d1, Palmd* and *Cap2*. Interestingly, all of them showed very similar tissue-specific expression patterns, providing further evidence for their coordinated expression, and suggests that HDAC4 may be involved in regulating the expression of these genes in all of these tissues.

Cacna2d1 is a voltage-gated calcium channel subunit that has repeatedly been linked to pain, and is the target of one of the most common drug classes for neuropathic pain, the gabapentinoids (Dickenson and Ghandehari, 2007). Interestingly, we observed upregulation of *Cacna2d1* in both strains of HDAC4 cKOs, although this was not associated with altered baseline sensory behaviour (Chapter 5). It would be interesting to determine whether this may alter the excitability of sensory neurons, or the sensitivity of the animals to gabapentinoids. Validation of this finding at the protein level would be required before undertaking this course of work.

CAP2 and PALMD are relatively underexplored proteins, although it was very surprising to discover that CAP2 mutations are associated with very similar pathologies as HDAC4 mutations. To date, no one has explored the possible link between these proteins. HDAC4 regulation of *Cap2* mRNA expression through direct association with chromatin represents a novel potential mechanism that could underlie cardiomyopathies and skeletal muscle defects.

This analysis was very conservative, reducing the amount of false positives as much as possible through the use of overlapping gene lists. However, it must be noted that 9788 HDAC4-positive peaks were discovered in the wildtype cerebellum using the MACS algorithm, which may represent true HDAC4 binding sites that simply are not shared with the ATM knockout.

Furthermore, our analysis was restricted to binding sites within annotated gene regions, but there may be true HDAC4 binding sites that do not lie within genes. Indeed, other studies that look for transcription binding sites can look as far as 100 kb away from transcription start sites for cis-regulatory regions (Bruce et al., 2009). Further investigation of these data may reveal other HDAC4 target genes.

6.4.3 Network analysis confirms known functions of HDAC4 in tissue development, morphology and cell-to-cell signaling, and suggests a role for NF-Kappa B interactions in mediating transcriptional effects

Pathway analysis and network generating tools are useful for making predictions about protein function and interactions. I used Ingenuity Pathway Analysis to search for novel functions of HDAC4 using the gene lists I generated from published microarray and ChIP-Seq studies. This provided a sanity check at the end of these investigations, confirming enrichment for genes in these lists for functions that are known to be associated with HDAC4 such as tissue and cellular morphology and development (Vega et al., 2004; Villavicencio-Lorini et al., 2013; Williams et al., 2010) as well as neuronal function and cell-to-cell signaling (Sando Iii et al., 2012).

Interestingly, analysis with a refined list of genes identified HDAC4 as an upstream regulator, and suggested that the NFKB complex may be involved in mediating some of these changes as it was highly interconnected with many HDAC4 targets. HDAC4

siRNA has previously been reported to reduce NFKB transcriptional activity (Usui et al., 2012), and a number of papers have shown that NFKB proteins can modulate behavioural hypersensitivity (Sun et al., 2006; Wei et al., 2007; Zang et al., 2010). Co-immunoprecipitation of HDAC4 with NFKB proteins, and measuring NFKB activity in both the wildtype and conditional knockout would provide evidence for this interaction.

This naïve bioinformatic analysis proves the utility of these freely available tools, and has provided good supporting evidence for the role of HDAC4 in mediating *Cacna2d1* transcription through direct chromatin association and repression, a result we could not have derived from our simple transcriptional expression study. It will be interesting to investigate this with ChIP-qPCR. Furthermore, this analysis has identified NF-Kappa B proteins as putative HDAC4 targets which may underlie the reduced transcription observed in HDAC4 cKOs after injury. Work to validate this may help to elucidate the mechanism through which HDAC4 modulates sensory neuron function.

References

Abrahamsen, B., Zhao, J., Asante, C., Cendan, C., Marsh, S., Martinez-Barbera, J., Nassar, M., Dickenson, A., and Wood, J. (2008). The cell and molecular basis of mechanical, cold, and inflammatory pain. Science (New York, NY) *321*, 702 - 705.

Ago, T., Liu, T., Zhai, P., Chen, W., Li, H., Molkentin, J.D., Vatner, S.F., and Sadoshima, J. (2008). A redox-dependent pathway for regulating class II HDACs and cardiac hypertrophy. Cell *133*, 978-993.

Allis, C.D., Jenuwein, T., and Reinberg, D. (2007). Epigenetics (Cold Spring Harbor, N.Y.: Cold Spring Harbor Laboratory Press).

Amaya, F., Shimosato, G., Nagano, M., Ueda, M., Hashimoto, S., Tanaka, Y., Suzuki, H., and Tanaka, M. (2004). NGF and GDNF differentially regulate TRPV1 expression that contributes to development of inflammatory thermal hyperalgesia. The European journal of neuroscience *20*, 2303-2310.

Arrowsmith, C.H., Bountra, C., Fish, P.V., Lee, K., and Schapira, M. (2012). Epigenetic protein families: a new frontier for drug discovery. Nature reviews Drug discovery *11*, 384-400.

Averill, S., Michael, G.J., Shortland, P.J., Leavesley, R.C., King, V.R., Bradbury, E.J., McMahon, S.B., and Priestley, J.V. (2004). NGF and GDNF ameliorate the increase in ATF3 expression which occurs in dorsal root ganglion cells in response to peripheral nerve injury. The European journal of neuroscience *19*, 1437-1445.

Bai, G., Wei, D., Zou, S., Ren, K., and Dubner, R. (2010). Inhibition of class II histone deacetylases in the spinal cord attenuates inflammatory hyperalgesia. Molecular pain *6*, 51.

Bain, J.R., Mackinnon, S.E., and Hunter, D.A. (1989). Functional evaluation of complete sciatic, peroneal, and posterior tibial nerve lesions in the rat. Plastic and reconstructive surgery *83*, 129-138.

Basbaum, A., Bautista, D., Scherrer, G., and Julius, D. (2009). Cellular and molecular mechanisms of pain. Cell *139*, 267 - 284.

Bautista, D.M., Jordt, S.E., Nikai, T., Tsuruda, P.R., Read, A.J., Poblete, J., Yamoah, E.N., Basbaum, A.I., and Julius, D. (2006). TRPA1 mediates the inflammatory actions of environmental irritants and proalgesic agents. Cell *124*, 1269-1282.

Bautista, D.M., Siemens, J., Glazer, J.M., Tsuruda, P.R., Basbaum, A.I., Stucky, C.L., Jordt, S.E., and Julius, D. (2007). The menthol receptor TRPM8 is the principal detector of environmental cold. Nature *448*, 204-208.

Ben Bassat, J., Peretz, E., and Sulman, F.G. (1959). Analgesimetry and ranking of analgesic drugs by the receptacle method. Arch Int Pharmacod *122*, 434-447.

Berkley, K.J. (1997). Sex differences in pain. Behav Brain Sci *20*, 371-380.

Bester, H., Allchorne, A.J., and Woolf, C.J. (1998). Recovery of C-fiber-induced extravasation following peripheral nerve injury in the rat. Experimental neurology *154*, 628-636.

Blankenberg, D., Gordon, A., Von Kuster, G., Coraor, N., Taylor, J., and Nekrutenko, A. (2010). Manipulation of FASTQ data with Galaxy. Bioinformatics *26*, 1783-1785.

Bolger, T.A., and Yao, T.P. (2005). Intracellular trafficking of histone deacetylase 4 regulates neuronal cell death. The Journal of neuroscience : the official journal of the Society for Neuroscience *25*, 9544-9553.

Bonilla, I.E., Tanabe, K., and Strittmatter, S.M. (2002). Small proline-rich repeat protein 1A is expressed by axotomized neurons and promotes axonal outgrowth. The Journal of neuroscience : the official journal of the Society for Neuroscience *22*, 1303-1315.

Bonnington, J.K., and McNaughton, P.A. (2003). Signalling pathways involved in the sensitisation of mouse nociceptive neurones by nerve growth factor. The Journal of physiology *551*, 433-446.

Bradner, J.E., West, N., Grachan, M.L., Greenberg, E.F., Haggarty, S.J., Warnow, T., and Mazitschek, R. (2010). Chemical phylogenetics of histone deacetylases. Nat Chem Biol *6*, 238-243.

Breivik, H., Collett, B., Ventafridda, V., Cohen, R., and Gallacher, D. (2006). Survey of chronic pain in Europe: Prevalence, impact on daily life, and treatment. European Journal of Pain *10*, 287-333.

Browne, M.J., Mayer, K.H., Chafee, S.B.D., Dudley, M.N., Posner, M.R., Steinberg, S.M., Graham, K.K., Geletko, S.M., Zinner, S.H., Denman, S.L.*, et al.* (1993). 2′,3′-Didehydro-3′-deoxythymidine (d4T) in Patients with AIDS or AIDS-Related Complex: A Phase I Trial. Journal of Infectious Diseases *167*, 21-29.

Brownell, J.E., Zhou, J., Ranalli, T., Kobayashi, R., Edmondson, D.G., Roth, S.Y., and Allis, C.D. (1996). Tetrahymena histone acetyltransferase A: a homolog to yeast Gcn5p linking histone acetylation to gene activation. Cell *84*, 843-851.

Bruce, A.W., Lopez-Contreras, A.J., Flicek, P., Down, T.A., Dhami, P., Dillon, S.C., Koch, C.M., Langford, C.F., Dunham, I., Andrews, R.M.*, et al.* (2009). Functional diversity for REST (NRSF) is defined by in vivo binding affinity hierarchies at the DNA sequence level. Genome Res *19*, 994-1005.

Callahan, B.L., Gil, A.S.C., Levesque, A., and Mogil, J.S. (2008). Modulation of mechanical and thermal nociceptive sensitivity in the laboratory mouse by behavioral state. J Pain *9*, 174-184.

Capecchi, M.R. (1989). Altering the genome by homologous recombination. Science (New York, NY) *244*, 1288-1292.

Capecchi, M.R. (2005). Gene targeting in mice: functional analysis of the mammalian genome for the twenty-first century. Nat Rev Genet *6*, 507-512.

Carvalho, B.S., and Irizarry, R.A. (2010). A framework for oligonucleotide microarray preprocessing. Bioinformatics *26*, 2363-2367.

Caterina, M.J. (1997). The capsaicin receptor: a heat-activated ion channel in the pain pathway. Nature *389*, 816-824.

Cervero, F., and Laird, J.M.A. (1999). Visceral pain. The Lancet *353*, 2145-2148.

Chang, M., Smith, S., Thorpe, A., Barratt, M., and Karim, F. (2010). Evaluation of phenoxybenzamine in the CFA model of pain following gene expression studies and connectivity mapping. Molecular pain *6*, 56.

Chaplan, S.R., Bach, F.W., Pogrel, J.W., Chung, J.M., and Yaksh, T.L. (1994). Quantitative assessment of tactile allodynia in the rat paw. Journal of neuroscience methods *53*, 55-63.

Chauchereau, A., Mathieu, M., de Saintignon, J., Ferreira, R., Pritchard, L.L., Mishal, Z., Dejean, A., and Harel-Bellan, A. (2004). HDAC4 mediates transcriptional repression by the acute promyelocytic leukaemia-associated protein PLZF. Oncogene *23*, 8777-8784.

Chawla, S., Vanhoutte, P., Arnold, F.J., Huang, C.L., and Bading, H. (2003). Neuronal activity-dependent nucleocytoplasmic shuttling of HDAC4 and HDAC5. Journal of neurochemistry *85*, 151-159.

Chen, B., and Cepko, C.L. (2009). HDAC4 regulates neuronal survival in normal and diseased retinas. Science (New York, NY) *323*, 256-259.

Chen, C., Broom, D., Liu, Y., de Nooij, J., Li, Z., Cen, C., Samad, O., Jessell, T., Woolf, C., and Ma, Q. (2006). Runx1 determines nociceptive sensory neuron phenotype and is required for thermal and neuropathic pain. Neuron *49*, 365 - 377.

Chen, Z.L., Yu, W.M., and Strickland, S. (2007). Peripheral regeneration. Annual review of neuroscience *30*, 209-233.

Chiechio, S., Zammataro, M., Morales, M.E., Busceti, C.L., Drago, F., Gereau, R.W.t., Copani, A., and Nicoletti, F. (2009). Epigenetic modulation of mGlu2

receptors by histone deacetylase inhibitors in the treatment of inflammatory pain. Mol Pharmacol *75*, 1014-1020.

Choi, M.C., Cohen, T.J., Barrientos, T., Wang, B., Li, M., Simmons, B.J., Yang, J.S., Cox, G.A., Zhao, Y., and Yao, T.P. (2012). A direct HDAC4-MAP kinase crosstalk activates muscle atrophy program. Molecular cell *47*, 122-132.

Chrubasik, J., Meynadier, J., Blond, S., Scherpereel, P., Ackerman, E., Weinstock, M., Bonath, K., Cramer, H., and Wunsch, E. (1984). SOMATOSTATIN, A POTENT ANALGESIC. The Lancet *324*, 1208-1209.

Chu, F., Chou, P., Mirkin, B.L., Mousa, S.A., and Rebbaa, A. (2008). Cellular conditioning with trichostatin A enhances the anti-stress response through up-regulation of HDAC4 and down-regulation of the IGF/Akt pathway. Aging Cell *7*, 516-525.

Chuang, H.H., Prescott, E.D., Kong, H., Shields, S., Jordt, S.E., Basbaum, A.I., Chao, M.V., and Julius, D. (2001). Bradykinin and nerve growth factor release the capsaicin receptor from PtdIns(4,5)P2-mediated inhibition. Nature *411*, 957-962.

Cohen, J. (1988) Statistical power analysis for the behavioral sciences (2nd ed.). Hillsdale, NJ: Erlbaum

Colburn, R.W., Lubin, M.L., Stone, D.J., Jr., Wang, Y., Lawrence, D., D'Andrea, M.R., Brandt, M.R., Liu, Y., Flores, C.M., and Qin, N. (2007). Attenuated cold sensitivity in TRPM8 null mice. Neuron *54*, 379-386.

Coste, B., Mathur, J., Schmidt, M., Earley, T.J., Ranade, S., Petrus, M.J., Dubin, A.E., and Patapoutian, A. (2010). Piezo1 and Piezo2 are essential components of distinct mechanically activated cation channels. Science (New York, NY) *330*, 55-60.

Costigan, M., Befort, K., Karchewski, L., Griffin, R., D'Urso, D., Allchorne, A., Sitarski, J., Mannion, J., Pratt, R., and Woolf, C. (2002). Replicate high-density rat genome oligonucleotide microarrays reveal hundreds of regulated genes in the dorsal root ganglion after peripheral nerve injury. BMC Neuroscience *3*, 16.

Crabbe, J.C., Wahlsten, D., and Dudek, B.C. (1999). Genetics of mouse behavior: interactions with laboratory environment. Science (New York, NY) *284*, 1670-1672.

Crow, M., Denk, F., and McMahon, S.B. (2013). Genes and epigenetic processes as prospective pain targets. Genome medicine *5*, 12.

Cui, L., Locatelli, L., Xie, M.Y., and Sommadossi, J.P. (1997). Effect of nucleoside analogs on neurite regeneration and mitochondrial DNA synthesis

in PC-12 cells. The Journal of pharmacology and experimental therapeutics *280*, 1228-1234.

Dai, Y., Iwata, K., Fukuoka, T., Kondo, E., Tokunaga, A., Yamanaka, H., Tachibana, T., Liu, Y., and Noguchi, K. (2002). Phosphorylation of extracellular signal-regulated kinase in primary afferent neurons by noxious stimuli and its involvement in peripheral sensitization. The Journal of neuroscience : the official journal of the Society for Neuroscience *22*, 7737-7745.

Darcy, M.J., Calvin, K., Cavnar, K., and Ouimet, C.C. (2010). Regional and subcellular distribution of HDAC4 in mouse brain. The Journal of comparative neurology *518*, 722-740.

Day, J.J., and Sweatt, J.D. (2011). Epigenetic mechanisms in cognition. Neuron *70*, 813-829.

Delmas, P., Hao, J., and Rodat-Despoix, L. (2011). Molecular mechanisms of mechanotransduction in mammalian sensory neurons. Nature reviews Neuroscience *12*, 139-153.

Denk, F., Huang, W., Sidders, B., Bithell, A., Crow, M., Grist, J., Sharma, S., Ziemek, D., Rice, A.S., Buckley, N.J*., et al.* (2013). HDAC inhibitors attenuate the development of hypersensitivity in models of neuropathic pain. Pain *154*, 1668-1679.

Denk, F., and McMahon, S.B. (2012). Chronic pain: emerging evidence for the involvement of epigenetics. Neuron *73*, 435-444.

Dhaka, A., Murray, A.N., Mathur, J., Earley, T.J., Petrus, M.J., and Patapoutian, A. (2007). TRPM8 is required for cold sensation in mice. Neuron *54*, 371-378.

Dickenson, A.H., and Ghandehari, J. (2007). Anti-convulsants and anti-depressants. Handb Exp Pharmacol, 145-177.

Dickson, B.J. (2002). Molecular mechanisms of axon guidance. Science (New York, NY) *298*, 1959-1964.

Dixon, W.J. (1965). The Up-and-Down Method for Small Samples. Journal of the American Statistical Association *60*, 967-978.

Djouhri, L., Dawbarn, D., Robertson, A., Newton, R., and Lawson, S.N. (2001). Time course and nerve growth factor dependence of inflammation-induced alterations in electrophysiological membrane properties in nociceptive primary afferent neurons. The Journal of neuroscience : the official journal of the Society for Neuroscience *21*, 8722-8733.

Donate, P.B., Fornari, T.A., Macedo, C., Cunha, T.M., Nascimento, D.C.B., Sakamoto-Hojo, E.T., Donadi, E.A., Cunha, F.Q., and Passos, G.A. (2013). T

Cell Post-Transcriptional miRNA-mRNA Interaction Networks Identify Targets Associated with Susceptibility/Resistance to Collagen-induced Arthritis. PLoS ONE *8*, e54803.

Donnerer, J., Schuligoi, R., and Stein, C. (1992). Increased content and transport of substance P and calcitonin gene-related peptide in sensory nerves innervating inflamed tissue: evidence for a regulatory function of nerve growth factor in vivo. Neuroscience *49*, 693-698.

Effendi, K., Yamazaki, K., Mori, T., Masugi, Y., Makino, S., and Sakamoto, M. (2013). Involvement of hepatocellular carcinoma biomarker, cyclase-associated protein 2 in zebrafish body development and cancer progression. Experimental cell research *319*, 35-44.

Emery, E.C., Young, G.T., Berrocoso, E.M., Chen, L., and McNaughton, P.A. (2011). HCN2 ion channels play a central role in inflammatory and neuropathic pain. Science (New York, NY) *333*, 1462-1466.

FDA (2012). Tanezumab: Arthritis advisory committee briefing document.

Ferrier, J., Pereira, V., Busserolles, J., Authier, N., and Balayssac, D. (2013). Emerging trends in understanding chemotherapy-induced peripheral neuropathy. Current pain and headache reports *17*, 364.

Field, M.J., Cox, P.J., Stott, E., Melrose, H., Offord, J., Su, T.-Z., Bramwell, S., Corradini, L., England, S., Winks, J.*, et al.* (2006). Identification of the α2-δ-1 subunit of voltage-dependent calcium channels as a molecular target for pain mediating the analgesic actions of pregabalin. Proceedings of the National Academy of Sciences *103*, 17537-17542.

Fischle, W., Dequiedt, F., Hendzel, M.J., Guenther, M.G., Lazar, M.A., Voelter, W., and Verdin, E. (2002). Enzymatic activity associated with class II HDACs is dependent on a multiprotein complex containing HDAC3 and SMRT/N-CoR. Molecular cell *9*, 45-57.

Fischle, W., Wang, Y., and Allis, C.D. (2003). Histone and chromatin cross-talk. Current opinion in cell biology *15*, 172-183.

Frank, E., and Sanes, J.R. (1991). Lineage of neurons and glia in chick dorsal root ganglia: analysis in vivo with a recombinant retrovirus. Development (Cambridge, England) *111*, 895-908.

Fuller-Bicer, G.A., Varadi, G., Koch, S.E., Ishii, M., Bodi, I., Kadeer, N., Muth, J.N., Mikala, G., Petrashevskaya, N.N., Jordan, M.A.*, et al.* (2009). Targeted disruption of the voltage-dependent calcium channel alpha2/delta-1-subunit. American journal of physiology Heart and circulatory physiology *297*, H117-124.

Galoyan, S.M., Petruska, J.C., and Mendell, L.M. (2003). Mechanisms of sensitization of the response of single dorsal root ganglion cells from adult rat to noxious heat. The European journal of neuroscience *18*, 535-541.

Gascon, E., Gaillard, S., Malapert, P., Liu, Y., Rodat-Despoix, L., Samokhvalov, I.M., Delmas, P., Helmbacher, F., Maina, F., and Moqrich, A. (2010). Hepatocyte Growth Factor-Met Signaling Is Required for Runx1 Extinction and Peptidergic Differentiation in Primary Nociceptive Neurons. The Journal of Neuroscience *30*, 12414-12423.

Geranton, S.M. (2011). Targeting epigenetic mechanisms for pain relief. Curr Opin Pharmacol.

Geranton, S.M., Morenilla-Palao, C., and Hunt, S.P. (2007). A role for transcriptional repressor methyl-CpG-binding protein 2 and plasticity-related gene serum- and glucocorticoid-inducible kinase 1 in the induction of inflammatory pain states. The Journal of neuroscience : the official journal of the Society for Neuroscience *27*, 6163-6173.

Glozak, M.A., Sengupta, N., Zhang, X., and Seto, E. (2005). Acetylation and deacetylation of non-histone proteins. Gene *363*, 15-23.

Gold, M.S., Levine, J.D., and Correa, A.M. (1998). Modulation of TTX-R I Na by PKC and PKA and Their Role in PGE2-Induced Sensitization of Rat Sensory Neurons In Vitro. The Journal of Neuroscience *18*, 10345-10355.

Gordon, J.W., Pagiatakis, C., Salma, J., Du, M., Andreucci, J.J., Zhao, J., Hou, G., Perry, R.L., Dan, Q., Courtman, D.*, et al.* (2009). Protein kinase A-regulated assembly of a MEF2{middle dot}HDAC4 repressor complex controls c-Jun expression in vascular smooth muscle cells. The Journal of biological chemistry *284*, 19027-19042.

Grozinger, C.M., Hassig, C.A., and Schreiber, S.L. (1999). Three proteins define a class of human histone deacetylases related to yeast Hda1p. Proceedings of the National Academy of Sciences of the United States of America *96*, 4868-4873.

Grozinger, C.M., and Schreiber, S.L. (2000). Regulation of histone deacetylase 4 and 5 and transcriptional activity by 14-3- 3-dependent cellular localization. Proceedings of the National Academy of Sciences *97*, 7835-7840.

Guo, T., Mandai, K., Condie, B.G., Wickramasinghe, S.R., Capecchi, M.R., and Ginty, D.D. (2011). An evolving NGF-Hoxd1 signaling pathway mediates development of divergent neural circuits in vertebrates. Nat Neurosci *14*, 31-36.

Gureje O, V.K.M.S.G.E.G.R. (1998). Persistent pain and well-being: A world health organization study in primary care. JAMA: The Journal of the American Medical Association *280*, 147-151.

Gygi, S.P., Rochon, Y., Franza, B.R., and Aebersold, R. (1999). Correlation between protein and mRNA abundance in yeast. Mol Cell Biol *19*, 1720-1730.

Haberland, M., Montgomery, R.L., and Olson, E.N. (2009). The many roles of histone deacetylases in development and physiology: implications for disease and therapy. Nat Rev Genet *10*, 32-42.

Hai, T., Wolford, C.C., and Chang, Y.S. (2010). ATF3, a hub of the cellular adaptive-response network, in the pathogenesis of diseases: is modulation of inflammation a unifying component? Gene expression *15*, 1-11.

Haig, D. (2004). The (dual) origin of epigenetics. Cold Spring Harbor symposia on quantitative biology *69*, 67-70.

Hammer, P., Banck, M., Amberg, R., Wang, C., Petznick, G., Luo, S., Khrebtukova, I., Schroth, G., Beyerlein, P., and Beutler, A. (2010). mRNA-seq with agnostic splice site discovery for nervous system transcriptomics tested in chronic pain. Genome Res *20*, 847 - 860.

Han, Z., Boyle, D.L., Chang, L., Bennett, B., Karin, M., Yang, L., Manning, A.M., and Firestein, G.S. (2001). c-Jun N-terminal kinase is required for metalloproteinase expression and joint destruction in inflammatory arthritis. The Journal of clinical investigation *108*, 73-81.

Hao, J., Padilla, F., Dandonneau, M., Lavebratt, C., Lesage, F., Noel, J., and Delmas, P. (2013). Kv1.1 channels act as mechanical brake in the senses of touch and pain. Neuron *77*, 899-914.

Haruyama, N., Cho, A., and Kulkarni, A.B. (2009). Overview: engineering transgenic constructs and mice. Current protocols in cell biology / editorial board, Juan S Bonifacino [et al] *Chapter 19*, Unit 19 10.

Hatem, A., Bozdag, D., Toland, A., and Catalyurek, U. (2013). Benchmarking short sequence mapping tools. BMC Bioinformatics *14*, 184.

Heidenreich, K.A., and Linseman, D.A. (2004). Myocyte enhancer factor-2 transcription factors in neuronal differentiation and survival. Molecular neurobiology *29*, 155-166.

Hohl, M., Wagner, M., Reil, J.C., Muller, S.A., Tauchnitz, M., Zimmer, A.M., Lehmann, L.H., Thiel, G., Bohm, M., Backs, J.*, et al.* (2013). HDAC4 controls histone methylation in response to elevated cardiac load. The Journal of clinical investigation *123*, 1359-1370.

Huang, W., Calvo, M., Karu, K., Olausen, H.R., Bathgate, G., Okuse, K., Bennett, D.L.H., and Rice, A.S.C. (2013). A clinically relevant rodent model of the HIV antiretroviral drug stavudine induced painful peripheral neuropathy. PAIN *154*, 560-575.

Hunskaar, S., Berge, O.G., and Hole, K. (1986). A modified hot-plate test sensitive to mild analgesics. Behavioural brain research *21*, 101-108.

Igwe, O.J. (2005). Modulation of peripheral inflammation in sensory ganglia by nuclear factor (kappa)B decoy oligodeoxynucleotide: involvement of SRC kinase pathway. Neuroscience letters *381*, 114-119.

Inoue, G., Ochiai, N., Ohtori, S., Nakagawa, K., Gemba, T., Doya, H., Ito, T., Koshi, T., Moriya, H., and Takahashi, K. (2006). Injection of nuclear factor-kappa B decoy into the sciatic nerve suppresses mechanical allodynia and thermal hyperalgesia in a rat inflammatory pain model. Spine (Phila Pa 1976) *31*, 2904-2908.

Inserra, M.M., Bloch, D.A., and Terris, D.J. (1998). Functional indices for sciatic, peroneal, and posterior tibial nerve lesions in the mouse. Microsurgery *18*, 119-124.

Irizarry, R.A., Hobbs, B., Collin, F., Beazer-Barclay, Y.D., Antonellis, K.J., Scherf, U., and Speed, T.P. (2003). Exploration, normalization, and summaries of high density oligonucleotide array probe level data. Biostatistics *4*, 249-264.

Ji, R.R., Samad, T.A., Jin, S.X., Schmoll, R., and Woolf, C.J. (2002). p38 MAPK activation by NGF in primary sensory neurons after inflammation increases TRPV1 levels and maintains heat hyperalgesia. Neuron *36*, 57-68.

Jin, Y.-H., Jeon, E.-J., Li, Q.-L., Lee, Y.H., Choi, J.-K., Kim, W.-J., Lee, K.-Y., and Bae, S.-C. (2004). Transforming Growth Factor-β Stimulates p300-dependent RUNX3 Acetylation, Which Inhibits Ubiquitination-mediated Degradation. Journal of Biological Chemistry *279*, 29409-29417.

Kandel, E., Schwartz, J.H., and Jessell, T. (2000). Principles of Neural Science (McGraw-Hill Medical).

Kehat, I., Accornero, F., Aronow, B.J., and Molkentin, J.D. (2011). Modulation of chromatin position and gene expression by HDAC4 interaction with nucleoporins. The Journal of cell biology *193*, 21-29.

Khasar, S.G., Lin, Y.H., Martin, A., Dadgar, J., McMahon, T., Wang, D., Hundle, B., Aley, K.O., Isenberg, W., McCarter, G.*, et al.* (1999). A novel nociceptor signaling pathway revealed in protein kinase C epsilon mutant mice. Neuron *24*, 253-260.

Kim, M.S., Akhtar, M.W., Adachi, M., Mahgoub, M., Bassel-Duby, R., Kavalali, E.T., Olson, E.N., and Monteggia, L.M. (2012). An essential role for histone deacetylase 4 in synaptic plasticity and memory formation. The Journal of neuroscience : the official journal of the Society for Neuroscience *32*, 10879-10886.

Kobayashi, A., Senzaki, K., Ozaki, S., Yoshikawa, M., and Shiga, T. (2012). Runx1 promotes neuronal differentiation in dorsal root ganglion. Molecular and Cellular Neuroscience *49*, 23-31.

Kontinen, V.K., and Meert, T.F. (2002). Proceedings of the 10th World Congress on Pain (Nature Publishing Group), pp. 489-498.

Kouzarides, T. (2007). Chromatin modifications and their function. Cell *128*, 693-705.

Kramer, I. (2006). A role for Runx transcription factor signaling in dorsal root ganglion sensory neuron diversification. Neuron *49*, 379-393.

Krebs, A., Frontini, M., and Tora, L. (2008). GPAT: Retrieval of genomic annotation from large genomic position datasets. BMC Bioinformatics *9*, 533.

Kuba, T., Wu, H.B., Nazarian, A., Festa, E.D., Barr, G.A., Jenab, S., Inturrisi, C.E., and Quinones-Jenab, V. (2006). Estradiol and progesterone differentially regulate formalin-induced nociception in ovariectomized female rats. Horm Behav *49*, 441-449.

Kusuda, R., Cadetti, F., Ravanelli, M.I., Sousa, T.A., Zanon, S., De Lucca, F.L., and Lucas, G. (2011). Differential expression of microRNAs in mouse pain models. Molecular pain *7*, 17.

LaCroix-Fralish, M.L., Austin, J.S., Zheng, F.Y., Levitin, D.J., and Mogil, J.S. (2011). Patterns of pain: meta-analysis of microarray studies of pain. Pain *152*, 1888-1898.

Lahm, A., Paolini, C., Pallaoro, M., Nardi, M.C., Jones, P., Neddermann, P., Sambucini, S., Bottomley, M.J., Lo Surdo, P., Carfı, A.*, et al.* (2007). Unraveling the hidden catalytic activity of vertebrate class IIa histone deacetylases. Proceedings of the National Academy of Sciences *104*, 17335-17340.

Lallemend, F., and Ernfors, P. (2012). Molecular interactions underlying the specification of sensory neurons. Trends in Neurosciences *35*, 373-381.

Lane, N.E., Schnitzer, T.J., Birbara, C.A., Mokhtarani, M., Shelton, D.L., Smith, M.D., and Brown, M.T. (2010). Tanezumab for the treatment of pain from osteoarthritis of the knee. N Engl J Med *363*, 1521-1531.

Langmead, B., Trapnell, C., Pop, M., and Salzberg, S.L. (2009). Ultrafast and memory-efficient alignment of short DNA sequences to the human genome. Genome biology *10*, R25.

Latremoliere, A., and Costigan, M. (2011). GCH1, BH4 and pain. Current pharmaceutical biotechnology *12*, 1728-1741.

Lattin, J.E., Schroder, K., Su, A.I., Walker, J.R., Zhang, J., Wiltshire, T., Saijo, K., Glass, C.K., Hume, D.A., Kellie, S.*, et al.* (2008). Expression analysis of G Protein-Coupled Receptors in mouse macrophages. Immunome research *4*, 5.

Lau, J., Minett, M.S., Zhao, J., Dennehy, U., Wang, F., Wood, J.N., and Bogdanov, Y.D. (2011). Temporal control of gene deletion in sensory ganglia using a tamoxifen-inducible Advillin-Cre-ERT2 recombinase mouse. Molecular pain *7*, 100.

Lauria, G., Cornblath, D.R., Johansson, O., McArthur, J.C., Mellgren, S.I., Nolano, M., Rosenberg, N., Sommer, C., and European Federation of Neurological, S. (2005). EFNS guidelines on the use of skin biopsy in the diagnosis of peripheral neuropathy. European journal of neurology : the official journal of the European Federation of Neurological Societies *12*, 747-758.

Lawson, S.N., and Biscoe, T.J. (1979). Development of mouse dorsal root ganglia: an autoradiographic and quantitative study. Journal of neurocytology *8*, 265-274.

Lee, J.S., Smith, E., and Shilatifard, A. (2010). The language of histone crosstalk. Cell *142*, 682-685.

Levi-Montalcini, R., and Cohen, S. (1956). IN VITRO AND IN VIVO EFFECTS OF A NERVE GROWTH-STIMULATING AGENT ISOLATED FROM SNAKE VENOM. Proceedings of the National Academy of Sciences of the United States of America *42*, 695-699.

Levin, M.E., Jin, J.G., Ji, R.R., Tong, J., Pomonis, J.D., Lavery, D.J., Miller, S.W., and Chiang, L.W. (2008). Complement activation in the peripheral nervous system following the spinal nerve ligation model of neuropathic pain. Pain *137*, 182-201.

Li, H., Handsaker, B., Wysoker, A., Fennell, T., Ruan, J., Homer, N., Marth, G., Abecasis, G., and Durbin, R. (2009). The Sequence Alignment/Map format and SAMtools. Bioinformatics *25*, 2078-2079.

Li, J., Chen, J., Ricupero, C.L., Hart, R.P., Schwartz, M.S., Kusnecov, A., and Herrup, K. (2012). Nuclear accumulation of HDAC4 in ATM deficiency promotes neurodegeneration in ataxia telangiectasia. Nat Med *18*, 783-790.

Lindsay, R.M., and Harmar, A.J. (1989). Nerve growth factor regulates expression of neuropeptide genes in adult sensory neurons. Nature *337*, 362-364.

Liu, B., Lin, G., Willingham, E., Ning, H., Lin, C.S., Lue, T.F., and Baskin, L.S. (2007). Estradiol upregulates activating transcription factor 3, a candidate gene in the etiology of hypospadias. Pediatric and developmental pathology : the official journal of the Society for Pediatric Pathology and the Paediatric Pathology Society *10*, 446-454.

Liu, F., Dowling, M., Yang, X.J., and Kao, G.D. (2004). Caspase-mediated specific cleavage of human histone deacetylase 4. The Journal of biological chemistry *279*, 34537-34546.

Liu, Q., Tang, Z., Surdenikova, L., Kim, S., Patel, K., Kim, A., Ru, F., Guan, Y., Weng, H., and Geng, Y. (2009). Sensory neuron-specific GPCR Mrgprs are itch receptors mediating chloroquine-induced pruritus. Cell *139*, 1353 - 1365.

Liu, Y., Yang, F., Okuda, T., Dong, X., Zylka, M., Chen, C., Anderson, D., Kuner, R., and Ma, Q. (2008). Mechanisms of compartmentalized expression of Mrg class G-protein-coupled sensory receptors. The Journal of neuroscience : the official journal of the Society for Neuroscience *28*, 125 - 132.

Livak, K.J., and Schmittgen, T.D. (2001). Analysis of relative gene expression data using real-time quantitative PCR and the 2(-Delta Delta C(T)) Method. Methods (San Diego, Calif) *25*, 402-408.

Lopes, C., Liu, Z., Xu, Y., and Ma, Q. (2012). Tlx3 and Runx1 Act in Combination to Coordinate the Development of a Cohort of Nociceptors, Thermoceptors, and Pruriceptors. The Journal of Neuroscience *32*, 9706-9715.

Lou, S., Duan, B., Vong, L., Lowell, B.B., and Ma, Q. (2013). Runx1 Controls Terminal Morphology and Mechanosensitivity of VGLUT3-expressing C-Mechanoreceptors. The Journal of Neuroscience *33*, 870-882.

Lovell, D., Müller, W., Taylor, J., Zwart, A., and Helliwell, C. (2011). Proportions, Percentages, PPM: Do the Molecular Biosciences Treat Compositional Data Right? In Compositional Data Analysis (John Wiley & Sons, Ltd), pp. 191-207.

Lovén, J., Orlando, David A., Sigova, Alla A., Lin, Charles Y., Rahl, Peter B., Burge, Christopher B., Levens, David L., Lee, Tong I., and Young, Richard A. (2012). Revisiting Global Gene Expression Analysis. Cell *151*, 476-482.

Luo, W., Wickramasinghe, S.R., Savitt, J.M., Griffin, J.W., Dawson, T.M., and Ginty, D.D. (2007). A Hierarchical NGF Signaling Cascade Controls Ret-Dependent and Ret-Independent Events during Development of Nonpeptidergic DRG Neurons. Neuron *54*, 739-754.

Ma, C.H.E., Omura, T., Cobos, E.J., Latr, xE, moli, xE, re, A., Ghasemlou, N., Brenner, G.J.*, et al.* (2011). Accelerating axonal growth promotes motor recovery after peripheral nerve injury in mice. The Journal of clinical investigation *121*, 4332-4347.

Ma, Q. (2012). Population coding of somatic sensations. Neurosci Bull *28*, 91-99.

Ma, Q., Fode, C., Guillemot, F., and Anderson, D.J. (1999). Neurogenin1 and neurogenin2 control two distinct waves of neurogenesis in developing dorsal root ganglia. Genes & development *13*, 1717-1728.

Majdzadeh, N., Wang, L., Morrison, B.E., Bassel-Duby, R., Olson, E.N., and D'Mello, S.R. (2008). HDAC4 inhibits cell-cycle progression and protects neurons from cell death. Developmental neurobiology *68*, 1076-1092.

Makwana, M., and Raivich, G. (2005). Molecular mechanisms in successful peripheral regeneration. The FEBS journal *272*, 2628-2638.

Margolis, A.M., Heverling, H., Pham, P.A., and Stolbach, A. (2013). A Review of the Toxicity of HIV Medications. Journal of medical toxicology : official journal of the American College of Medical Toxicology.

Marguerat, S., Schmidt, A., Codlin, S., Chen, W., Aebersold, R., and Bahler, J. (2012). Quantitative analysis of fission yeast transcriptomes and proteomes in proliferating and quiescent cells. Cell *151*, 671-683.

Marmigere, F., and Ernfors, P. (2007). Specification and connectivity of neuronal subtypes in the sensory lineage. Nature reviews Neuroscience *8*, 114-127.

Marmigere, F., Montelius, A., Wegner, M., Groner, Y., Reichardt, L., and Ernfors, P. (2006). The Runx1/AML1 transcription factor selectively regulates development and survival of TrkA nociceptive sensory neurons. Nat Neurosci *9*, 180 - 187.

Mayumi-Matsuda, K., Kojima, S., Nakayama, T., Suzuki, H., and Sakata, T. (1999). Scanning gene expression during neuronal cell death evoked by nerve growth factor depletion. Biochimica et biophysica acta *1489*, 293-302.

Maze, I., Noh, K.M., and Allis, C.D. (2013). Histone regulation in the CNS: basic principles of epigenetic plasticity. Neuropsychopharmacology *38*, 3-22.

McKinsey, T.A., Zhang, C.L., and Olson, E.N. (2000). Activation of the myocyte enhancer factor-2 transcription factor by calcium/calmodulin-dependent protein kinase-stimulated binding of 14-3-3 to histone deacetylase 5. Proceedings of the National Academy of Sciences *97*, 14400-14405.

McMahon, S.B. (1996). NGF as a mediator of inflammatory pain. Philosophical transactions of the Royal Society of London Series B, Biological sciences *351*, 431-440.

McMahon, S.B. (2013). Wall and Melzack's textbook of pain, 6th edn (Philadelphia, PA: Elsevier/Saunders).

McMahon, S.B., Armanini, M.P., Ling, L.H., and Phillips, H.S. (1994). Expression and coexpression of Trk receptors in subpopulations of adult

primary sensory neurons projecting to identified peripheral targets. Neuron *12*, 1161-1171.

McMahon, S.B., Bennett, D.L., Priestley, J.V., and Shelton, D.L. (1995). The biological effects of endogenous nerve growth factor on adult sensory neurons revealed by a trkA-IgG fusion molecule. Nat Med *1*, 774-780.

Meng, J., Ovsepian, S.V., Wang, J., Pickering, M., Sasse, A., Aoki, K.R., Lawrence, G.W., and Dolly, J.O. (2009). Activation of TRPV1 mediates calcitonin gene-related peptide release, which excites trigeminal sensory neurons and is attenuated by a retargeted botulinum toxin with anti-nociceptive potential. The Journal of neuroscience : the official journal of the Society for Neuroscience *29*, 4981-4992.

Metzger, D., and Chambon, P. (2001). Site- and time-specific gene targeting in the mouse. Methods (San Diego, Calif) *24*, 71-80.

Michael, G.J., Averill, S., Nitkunan, A., Rattray, M., Bennett, D.L.H., Yan, Q., and Priestley, J.V. (1997). Nerve Growth Factor Treatment Increases Brain-Derived Neurotrophic Factor Selectively in TrkA-Expressing Dorsal Root Ganglion Cells and in Their Central Terminations within the Spinal Cord. The Journal of Neuroscience *17*, 8476-8490.

Miska, E.A., Karlsson, C., Langley, E., Nielsen, S.J., Pines, J., and Kouzarides, T. (1999). HDAC4 deacetylase associates with and represses the MEF2 transcription factor. The EMBO journal *18*, 5099-5107.

Miska, E.A., Langley, E., Wolf, D., Karlsson, C., Pines, J., and Kouzarides, T. (2001). Differential localization of HDAC4 orchestrates muscle differentiation. Nucleic acids research *29*, 3439-3447.

Mogil, J.S. (2005). Variable sensitivity to noxious heat is mediated by differential expression of the CGRP gene. Proc Natl Acad Sci USA *102*, 12938-12943.

Mogil, J.S. (2009). Animal models of pain: progress and challenges. Nature reviews Neuroscience *10*, 283-294.

Mogil, J.S., and Crager, S.E. (2004). What should we be measuring in behavioral studies of chronic pain in animals? Pain *112*, 12-15.

Molliver, D.C. (1997). IB4-binding DRG neurons switch from NGF to GDNF dependence in early postnatal life. Neuron *19*, 849-861.

Nahin, R.L., and Byers, M.R. (1994). Adjuvant-induced inflammation of rat paw is associated with altered calcitonin gene-related peptide immunoreactivity within cell bodies and peripheral endings of primary afferent neurons. The Journal of comparative neurology *349*, 475-485.

Nakamura, S., Senzaki, K., Yoshikawa, M., Nishimura, M., Inoue, K., Ito, Y., Ozaki, S., and Shiga, T. (2008). Dynamic regulation of the expression of neurotrophin receptors by Runx3. Development (Cambridge, England) *135*, 1703-1711.

Nakanishi, M., Hata, K., Nagayama, T., Sakurai, T., Nishisho, T., Wakabayashi, H., Hiraga, T., Ebisu, S., and Yoneda, T. (2010). Acid activation of Trpv1 leads to an up-regulation of calcitonin gene-related peptide expression in dorsal root ganglion neurons via the CaMK-CREB cascade: a potential mechanism of inflammatory pain. Molecular biology of the cell *21*, 2568-2577.

Nassar, M.A., Stirling, L.C., Forlani, G., Baker, M.D., Matthews, E.A., Dickenson, A.H., and Wood, J.N. (2004). Nociceptor-specific gene deletion reveals a major role for Nav1.7 (PN1) in acute and inflammatory pain. Proceedings of the National Academy of Sciences of the United States of America *101*, 12706-12711.

Nebbioso, A., Manzo, F., Miceli, M., Conte, M., Manente, L., Baldi, A., De Luca, A., Rotili, D., Valente, S., Mai, A.*, et al.* (2009). Selective class II HDAC inhibitors impair myogenesis by modulating the stability and activity of HDAC-MEF2 complexes. EMBO Rep *10*, 776-782.

Obata, K., Yamanaka, H., Dai, Y., Mizushima, T., Fukuoka, T., Tokunaga, A., and Noguchi, K. (2004). Differential activation of MAPK in injured and uninjured DRG neurons following chronic constriction injury of the sciatic nerve in rats. The European journal of neuroscience *20*, 2881-2895.

Ontoria, J.M., Altamura, S., Di Marco, A., Ferrigno, F., Laufer, R., Muraglia, E., Palumbi, M.C., Rowley, M., Scarpelli, R., Schultz-Fademrecht, C.*, et al.* (2009). Identification of novel, selective, and stable inhibitors of class II histone deacetylases. Validation studies of the inhibition of the enzymatic activity of HDAC4 by small molecules as a novel approach for cancer therapy. J Med Chem *52*, 6782-6789.

Pan, L., Pan, H., Jiang, H., Du, J., Wang, X., Huang, B., and Lu, J. (2010). HDAC4 inhibits the transcriptional activation of mda-7/IL-24 induced by Sp1. Cell Mol Immunol *7*, 221-226.

Paroni, G., Cernotta, N., Dello Russo, C., Gallinari, P., Pallaoro, M., Foti, C., Talamo, F., Orsatti, L., Steinkuhler, C., and Brancolini, C. (2008). PP2A regulates HDAC4 nuclear import. Molecular biology of the cell *19*, 655-667.

Patodia, S., and Raivich, G. (2012). Role of transcription factors in peripheral nerve regeneration. Frontiers in molecular neuroscience *5*, 8.

Pearson, A.G., Gray, C.W., Pearson, J.F., Greenwood, J.M., During, M.J., and Dragunow, M. (2003). ATF3 enhances c-Jun-mediated neurite sprouting. Molecular Brain Research *120*, 38-45.

Peche, V.S., Holak, T.A., Burgute, B.D., Kosmas, K., Kale, S.P., Wunderlich, F.T., Elhamine, F., Stehle, R., Pfitzer, G., Nohroudi, K.*, et al.* (2013). Ablation of cyclase-associated protein 2 (CAP2) leads to cardiomyopathy. Cellular and molecular life sciences : CMLS *70*, 527-543.

Pezet, S., and McMahon, S. (2006). Neurotrophins: mediators and modulators of pain. Annual review of neuroscience *29*, 507 - 538.

Potthoff, M.J., Wu, H., Arnold, M.A., Shelton, J.M., Backs, J., McAnally, J., Richardson, J.A., Bassel-Duby, R., and Olson, E.N. (2007). Histone deacetylase degradation and MEF2 activation promote the formation of slow-twitch myofibers. The Journal of clinical investigation *117*, 2459-2467.

Price, V., Wang, L., and D'Mello, S.R. (2012). Conditional deletion of histone deacetylase-4 in the central nervous system has no major effect on brain architecture or neuronal viability. Journal of Neuroscience Research, n/a-n/a.

Qian, D.Z., Kachhap, S.K., Collis, S.J., Verheul, H.M., Carducci, M.A., Atadja, P., and Pili, R. (2006). Class II histone deacetylases are associated with VHL-independent regulation of hypoxia-inducible factor 1 alpha. Cancer Res *66*, 8814-8821.

Rajan, I., Savelieva, K.V., Ye, G.L., Wang, C.Y., Malbari, M.M., Friddle, C., Lanthorn, T.H., and Zhang, W. (2009). Loss of the putative catalytic domain of HDAC4 leads to reduced thermal nociception and seizures while allowing normal bone development. PLoS One *4*, e6612.

Ren, G., Zhang, G., Dong, Z., Liu, Z., Li, L., Feng, Y., Su, D., Zhang, Y., Huang, B., and Lu, J. (2009). Recruitment of HDAC4 by transcription factor YY1 represses HOXB13 to affect cell growth in AR-negative prostate cancers. Int J Biochem Cell Biol *41*, 1094-1101.

Ren, K., Novikova, S., He, F., Dubner, R., and Lidow, M. (2005). Neonatal local noxious insult affects gene expression in the spinal dorsal horn of adult rats. Molecular pain *1*, 27.

Renn, C.L., Leitch, C.C., Lessans, S., Rhee, P., McGuire, W.C., Smith, B.A., Traub, R.J., and Dorsey, S.G. (2011). Brain-derived neurotrophic factor modulates antiretroviral-induced mechanical allodynia in the mouse. Journal of Neuroscience Research *89*, 1551-1565.

Rice, A.S.C. (2008). Animal models and the prediction of efficacy in clinical trials of analgesic drugs: a critical appraisal and call for uniform reporting standards. Pain *139*, 241-245.

Rivieccio, M.A., Brochier, C., Willis, D.E., Walker, B.A., D'Annibale, M.A., McLaughlin, K., Siddiq, A., Kozikowski, A.P., Jaffrey, S.R., Twiss, J.L.*, et al.* (2009). HDAC6 is a target for protection and regeneration following injury in the nervous system. Proceedings of the National Academy of Sciences of the United States of America *106*, 19599-19604.

Robinson, B., Li, Z., and Nath, A. (2007). Nucleoside reverse transcriptase inhibitors and human immunodeficiency virus proteins cause axonal injury in human dorsal root ganglia cultures. Journal of neurovirology *13*, 160-167.

Rodriguez Parkitna, J., Kaminska-Chowaniec, D., Obara, I., Mika, J., Przewlocka, B., and Przewlocki, R. (2006). Comparison of gene expression profiles in neuropathic and inflammatory pain. J Physiol Pharmacol *57*, 14.

Rong, Y., Zhang, M., Zhang, L., Wang, X.L., and Shen, Y.H. (2010). JNK-ATF-2 inhibits thrombomodulin (TM) expression by recruiting histone deacetylase4 (HDAC4) and forming a transcriptional repression complex in the TM promoter. FEBS letters *584*, 852-858.

Rundlett, S.E., Carmen, A.A., Kobayashi, R., Bavykin, S., Turner, B.M., and Grunstein, M. (1996). HDA1 and RPD3 are members of distinct yeast histone deacetylase complexes that regulate silencing and transcription. Proceedings of the National Academy of Sciences of the United States of America *93*, 14503-14508.

Salma, J., and McDermott, J.C. (2012). Suppression of a MEF2-KLF6 Survival Pathway by PKA Signaling Promotes Apoptosis in Embryonic Hippocampal Neurons. The Journal of Neuroscience *32*, 2790-2803.

Samad, O., Liu, Y., Yang, F.-C., Kramer, I., Arber, S., and Ma, Q. (2010). Characterization of two Runx1-dependent nociceptor differentiation programs necessary for inflammatory versus neuropathic pain. Molecular pain *6*, 45.

Sando Iii, R., Gounko, N., Pieraut, S., Liao, L., Yates Iii, J., and Maximov, A. (2012). HDAC4 Governs a Transcriptional Program Essential for Synaptic Plasticity and Memory. Cell *151*, 821-834.

Schlumm, F., Mauceri, D., Freitag, H.E., and Bading, H. (2013). Nuclear Calcium Signaling Regulates Nuclear Export of a Subset of Class IIa Histone Deacetylases following Synaptic Activity. Journal of Biological Chemistry *288*, 8074-8084.

Seijffers, R., Allchorne, A.J., and Woolf, C.J. (2006). The transcription factor ATF-3 promotes neurite outgrowth. Molecular and Cellular Neuroscience *32*, 143-154.

Seijffers, R., Mills, C.D., and Woolf, C.J. (2007). ATF3 Increases the Intrinsic Growth State of DRG Neurons to Enhance Peripheral Nerve Regeneration. The Journal of Neuroscience *27*, 7911-7920.

Seltzer, Z., Dubner, R., and Shir, Y. (1990). A novel behavioral model of causalgiform pain produced by partial sciatic nerve injury in rats. Pain *43*, 205-218.

Seo, H.W., Kim, E.J., Na, H., and Lee, M.O. (2009). Transcriptional activation of hypoxia-inducible factor-1alpha by HDAC4 and HDAC5 involves differential recruitment of p300 and FIH-1. FEBS letters *583*, 55-60.

Shakespear, M.R., Halili, M.A., Irvine, K.M., Fairlie, D.P., and Sweet, M.J. (2011). Histone deacetylases as regulators of inflammation and immunity. Trends in Immunology *32*, 335-343.

Shields, S.D., Ahn, H.S., Yang, Y., Han, C., Seal, R.P., Wood, J.N., Waxman, S.G., and Dib-Hajj, S.D. (2012). Nav1.8 expression is not restricted to nociceptors in mouse peripheral nervous system. Pain *153*, 2017-2030.

Smith, M.D. (2001). Brn-3a activates the expression of Bcl-xL and promotes neuronal survival in vivo as well as in vitro. Mol Cell Neurosci *17*, 460-470.

Smyth, G.K. (2005). limma: Linear Models for Microarray Data. In Bioinformatics and Computational Biology Solutions Using R and Bioconductor, R. Gentleman, V. Carey, W. Huber, R. Irizarry, and S. Dudoit, eds. (Springer New York), pp. 397-420.

Smyth, K., Affandi, J.S., McArthur, J.C., Bowtell-Harris, C., Mijch, A.M., Watson, K., Costello, K., Woolley, I.J., Price, P., Wesselingh, S.L.*, et al.* (2007). Prevalence of and risk factors for HIV-associated neuropathy in Melbourne, Australia 1993–2006. HIV Medicine *8*, 367-373.

Snider, W.D. (1994). Functions of the neurotrophins during nervous system development: what the knockouts are teaching us. Cell *77*, 627-638.

Snider, W.D., and McMahon, S.B. (1998). Tackling pain at the source: new ideas about nociceptors. Neuron *20*, 629-632.

Society, T.B.P. The British Pain Society - FAQs.

Srinivasan, R., Wolfe, D., Goss, J., Watkins, S., de Groat, W.C., Sculptoreanu, A., and Glorioso, J.C. (2008). Protein kinase C epsilon contributes to basal and sensitizing responses of TRPV1 to capsaicin in rat dorsal root ganglion neurons. The European journal of neuroscience *28*, 1241-1254.

Stronach, E.A., Alfraidi, A., Rama, N., Datler, C., Studd, J.B., Agarwal, R., Guney, T.G., Gourley, C., Hennessy, B.T., Mills, G.B.*, et al.* (2011). HDAC4-regulated STAT1 activation mediates platinum resistance in ovarian cancer. Cancer Res *71*, 4412-4422.

Sun, T., Song, W.G., Fu, Z.J., Liu, Z.H., Liu, Y.M., and Yao, S.L. (2006). Alleviation of neuropathic pain by intrathecal injection of antisense oligonucleotides to p65 subunit of NF-kappaB. British journal of anaesthesia *97*, 553-558.

Szyf, M. (2009). Epigenetics, DNA methylation, and chromatin modifying drugs. Annu Rev Pharmacol Toxicol *49*, 243-263.

Tamura, S., Morikawa, Y., and Senba, E. (2005). Up-regulated phosphorylation of signal transducer and activator of transcription 3 and cyclic AMP-responsive element binding protein by peripheral inflammation in primary afferent neurons possibly through oncostatin M receptor. Neuroscience *133*, 797-806.

Tanabe, M., Takasu, K., Kasuya, N., Shimizu, S., Honda, M., and Ono, H. (2005). Role of descending noradrenergic system and spinal alpha2-adrenergic receptors in the effects of gabapentin on thermal and mechanical nociception after partial nerve injury in the mouse. Br J Pharmacol *144*, 703-714.

Tjolsen, A., Rosland, J.H., Berge, O.G., and Hole, K. (1991). The increasing-temperature hot-plate test: an improved test of nociception in mice and rats. Journal of pharmacological methods *25*, 241-250.

Tran, L., Chaloner, A., Sawalha, A.H., and Greenwood Van-Meerveld, B. (2012). Importance of epigenetic mechanisms in visceral pain induced by chronic water avoidance stress. Psychoneuroendocrinology.

Tsujino, H., Kondo, E., Fukuoka, T., Dai, Y., Tokunaga, A., Miki, K., Yonenobu, K., Ochi, T., and Noguchi, K. (2000). Activating Transcription Factor 3 (ATF3) Induction by Axotomy in Sensory and Motoneurons: A Novel Neuronal Marker of Nerve Injury. Molecular and Cellular Neuroscience *15*, 170-182.

Uchida, H., Ma, L., and Ueda, H. (2010). Epigenetic gene silencing underlies C-fiber dysfunctions in neuropathic pain. The Journal of neuroscience : the official journal of the Society for Neuroscience *30*, 4806-4814.

Usui, T., Okada, M., Mizuno, W., Oda, M., Ide, N., Morita, T., Hara, Y., and Yamawaki, H. (2012). HDAC4 mediates development of hypertension via vascular inflammation in spontaneous hypertensive rats. American journal of physiology Heart and circulatory physiology *302*, H1894-1904.

Valder, C.R., Liu, J.J., Song, Y.H., and Luo, Z.D. (2003). Coupling gene chip analyses and rat genetic variances in identifying potential target genes that may contribute to neuropathic allodynia development. Journal of neurochemistry *87*, 560-573.

Vega, R.B., Matsuda, K., Oh, J., Barbosa, A.C., Yang, X., Meadows, E., McAnally, J., Pomajzl, C., Shelton, J.M., Richardson, J.A.*, et al.* (2004). Histone deacetylase 4 controls chondrocyte hypertrophy during skeletogenesis. Cell *119*, 555-566.

Vega-Avelaira, D., Geranton, S., and Fitzgerald, M. (2009). Differential regulation of immune responses and macrophage/neuron interactions in the dorsal root ganglion in young and adult rats following nerve injury. Molecular pain *5*, 70.

Victoratos, P., Yiangou, M., Avramidis, N., and Hadjipetrou, L. (1997). Regulation of cytokine gene expression by adjuvants in vivo. Clinical & Experimental Immunology *109*, 569-578.

Villavicencio-Lorini, P., Klopocki, E., Trimborn, M., Koll, R., Mundlos, S., and Horn, D. (2013). Phenotypic variant of Brachydactyly-mental retardation syndrome in a family with an inherited interstitial 2q37.3 microdeletion including HDAC4. Eur J Hum Genet *21*, 743-748.

Wang, H., Sun, H., Della Penna, K., Benz, R.J., Xu, J., Gerhold, D.L., Holder, D.J., and Koblan, K.S. (2002). Chronic neuropathic pain is accompanied by global changes in gene expression and shares pathobiology with neurodegenerative diseases. Neuroscience *114*, 529-546.

Wang, R., Guo, W., Ossipov, M.H., Vanderah, T.W., Porreca, F., and Lai, J. (2003). Glial cell line-derived neurotrophic factor normalizes neurochemical changes in injured dorsal root ganglion neurons and prevents the expression of experimental neuropathic pain. Neuroscience *121*, 815-824.

Wang, W.-H., Cheng, L.-C., Pan, F.-Y., Xue, B., Wang, D.-Y., Chen, Z., and Li, C.-J. (2011). Intracellular Trafficking of Histone Deacetylase 4 Regulates Long-Term Memory Formation. The Anatomical Record: Advances in Integrative Anatomy and Evolutionary Biology *294*, 1025-1034.

Wang, W.-L., Lee, Y.-C., Yang, W.-M., Chang, W.-C., and Wang, J.-M. (2008a). Sumoylation of LAP1 is involved in the HDAC4-mediated repression of COX-2 transcription. Nucleic acids research *36*, 6066-6079.

Wang, W.L., Lee, Y.C., Yang, W.M., Chang, W.C., and Wang, J.M. (2008b). Sumoylation of LAP1 is involved in the HDAC4-mediated repression of COX-2 transcription. Nucleic acids research *36*, 6066-6079.

Waterston, R.H., Lindblad-Toh, K., Birney, E., Rogers, J., Abril, J.F., Agarwal, P., Agarwala, R., Ainscough, R., Alexandersson, M., An, P.*, et al.* (2002). Initial sequencing and comparative analysis of the mouse genome. Nature *420*, 520-562.

Wei, X.-H., Zang, Y., Wu, C.-Y., Xu, J.-T., Xin, W.-J., and Liu, X.-G. (2007). Peri-sciatic administration of recombinant rat TNF-α induces mechanical allodynia via upregulation of TNF-α in dorsal root ganglia and in spinal dorsal horn: The role of NF-kappa B pathway. Experimental neurology *205*, 471-484.

Williams, S.R., Aldred, M.A., Der Kaloustian, V.M., Halal, F., Gowans, G., McLeod, D.R., Zondag, S., Toriello, H.V., Magenis, R.E., and Elsea, S.H. (2010). Haploinsufficiency of HDAC4 causes brachydactyly mental retardation syndrome, with brachydactyly type E, developmental delays, and behavioral problems. Am J Hum Genet *87*, 219-228.

Wilson, A.J., Byun, D.S., Nasser, S., Murray, L.B., Ayyanar, K., Arango, D., Figueroa, M., Melnick, A., Kao, G.D., Augenlicht, L.H.*, et al.* (2008). HDAC4

promotes growth of colon cancer cells via repression of p21. Molecular biology of the cell *19*, 4062-4075.

Winston, A., McAllister, J., Amin, J., Cooper, D.A., and Carr, A. (2005). The use of a triple nucleoside-nucleotide regimen for nonoccupational HIV post-exposure prophylaxis. HIV Medicine *6*, 191-197.

Wood, J.N., and Eijkelkamp, N. (2012). Noxious mechanosensation – molecules and circuits. Current Opinion in Pharmacology *12*, 4-8.

Wu, C., Orozco, C., Boyer, J., Leglise, M., Goodale, J., Batalov, S., Hodge, C., Haase, J., Janes, J., Huss, J.*, et al.* (2009). BioGPS: an extensible and customizable portal for querying and organizing gene annotation resources. Genome biology *10*, R130.

Xiao, H.S., Huang, Q.H., Zhang, F.X., Bao, L., Lu, Y.J., Guo, C., Yang, L., Huang, W.J., Fu, G., Xu, S.H.*, et al.* (2002). Identification of gene expression profile of dorsal root ganglion in the rat peripheral axotomy model of neuropathic pain. Proceedings of the National Academy of Sciences of the United States of America *99*, 8360-8365.

Yang, H., Mitchell, K., Keller, J., and Iadarola, M. (2007). Peripheral inflammation increases Scya2 expression in sensory ganglia and cytokine and endothelial related gene expression in inflamed tissue. Journal of neurochemistry *103*, 1628 - 1643.

Yang, X.J., and Seto, E. (2008). The Rpd3/Hda1 family of lysine deacetylases: from bacteria and yeast to mice and men. Nature reviews Molecular cell biology *9*, 206-218.

Yang, Y., Qin, X., Liu, S., Li, J., Zhu, X., Gao, T., and Wang, X. (2011). Peroxisome proliferator-activated receptor gamma is inhibited by histone deacetylase 4 in cortical neurons under oxidative stress. Journal of neurochemistry *118*, 429-439.

Yao, Y.L., and Yang, W.M. (2011). Beyond histone and deacetylase: an overview of cytoplasmic histone deacetylases and their nonhistone substrates. Journal of biomedicine & biotechnology *2011*, 146493.

Yoshikawa, M., Senzaki, K., Yokomizo, T., Takahashi, S., Ozaki, S., and Shiga, T. (2007). Runx1 selectively regulates cell fate specification and axonal projections of dorsal root ganglion neurons. Developmental Biology *303*, 663-674.

Yukhananov, R., and Kissin, I. (2008). Persistent changes in spinal cord gene expression after recovery from inflammatory hyperalgesia: A preliminary study on pain memory. BMC Neuroscience *9*, 32.

Zang, Y., He, X.H., Xin, W.J., Pang, R.P., Wei, X.H., Zhou, L.J., Li, Y.Y., and Liu, X.G. (2010). Inhibition of NF-kappaB prevents mechanical allodynia

induced by spinal ventral root transection and suppresses the re-expression of Nav1.3 in DRG neurons in vivo and in vitro. Brain Res *1363*, 151-158.

Zhang, Y., Liu, T., Meyer, C.A., Eeckhoute, J., Johnson, D.S., Bernstein, B.E., Nusbaum, C., Myers, R.M., Brown, M., Li, W.*, et al.* (2008). Model-based analysis of ChIP-Seq (MACS). Genome biology *9*, R137.

Zhang, Z., Cai, Y.Q., Zou, F., Bie, B., and Pan, Z.Z. (2011). Epigenetic suppression of GAD65 expression mediates persistent pain. Nat Med.

Zhao, X., Ito, A., Kane, C.D., Liao, T.S., Bolger, T.A., Lemrow, S.M., Means, A.R., and Yao, T.P. (2001). The modular nature of histone deacetylase HDAC4 confers phosphorylation-dependent intracellular trafficking. The Journal of biological chemistry *276*, 35042-35048.

Zhao, X., Sternsdorf, T., Bolger, T.A., Evans, R.M., and Yao, T.-P. (2005). Regulation of MEF2 by Histone Deacetylase 4- and SIRT1 Deacetylase-Mediated Lysine Modifications. Molecular and Cellular Biology *25*, 8456-8464.

Appendix 2: Bioinformatics analysis parameters

Table 11 - Bowtie Alignment Parameters

Input Parameter	Value
Will you select a reference genome from your history or use a built-in index?	indexed
Select a reference genome	/galaxy/data/mm9/bowtie_index/mm9
Is this library mate-paired?	single
FASTQ file	27: FASTQ Groomer on data 7
Bowtie settings to use	full
Skip the first n reads (-s)	0
Only align the first n reads (-u)	-1
Trim n bases from high-quality (left) end of each read before alignment (-5)	0
Trim n bases from low-quality (right) end of each read before alignment (-3)	5
Maximum number of mismatches permitted in the seed (-n)	0
Maximum permitted total of quality values at mismatched read positions (-e)	70
Seed length (-l)	28
Whether or not to round to the nearest 10 and saturating at 30 (--nomaqround)	Round to nearest 10
Number of mismatches for SOAP-like alignment policy (-v)	-1
Whether or not to try as hard as possible to find valid alignments when they exist (-y)	Do not try hard

Report up to n valid alignments per read (-k)	1
Whether or not to report all valid alignments per read (-a)	Do not report all valid alignments
Suppress all alignments for a read if more than n reportable alignments exist (-m)	-1
Write all reads with a number of valid alignments exceeding the limit set with the -m option to a file (--max)	False
Write all reads that could not be aligned to a file (--un)	False
Whether or not to make Bowtie guarantee that reported singleton alignments are 'best' in terms of stratum and in terms of the quality values at the mismatched positions (--best)	doBest
Maximum number of backtracks permitted when aligning a read (--maxbts)	800
Whether or not to report only those alignments that fall in the best stratum if many valid alignments exist and are reportable (--strata)	Do not use strata option
Override the offrate of the index to n (-o)	-1
Seed for pseudo-random number generator (--seed)	-1
Suppress the header in the output SAM file	False

Table 12 - MACS peak-finding parameters

Experiment Name	MACS in Galaxy
Paired End Sequencing	single_end
ChIP-Seq Tag File	30: SAM-to-BAM on data 26: converted BAM
ChIP-Seq Control File	42: SAM-to-BAM on data 40: converted BAM
Effective genome size	2700000000.0
Tag size	25
Band width	300
Pvalue cutoff for peak detection	1e-05
Select the regions with MFOLD high-confidence enrichment ratio against background to build model	32
Parse xls files into into distinct interval files	False
Save shifted raw tag count at every bp into a wiggle file	no_wig
Use fixed background lambda as local lambda for every peak region	False
3 levels of regions around the peak region to calculate the maximum lambda as local lambda	1000,5000,10000
Build Model	create_model
Diagnosis report	no_diag
Perform the new peak detection method (futurefdr)	False

Appendix 3: GPAT output file from ChIP-Seq analysis

feature_ID	chromosome	min_pos	max_pos	gene_ID	gene_name	strand	start_position	TSS_distance
MACS_peak_41	chr1	10592022	10592094	NM_177834	Cpa6	-	10710024	117966
MACS_peak_114	chr1	22562733	22562819	NM_183018	Rims1	-	22812563	249787
MACS_peak_119	chr1	24618337	24623028	no_match				
MACS_peak_244	chr1	53298693	53298724	NM_153556	Pms1	-	53353840	55132
MACS_peak_296	chr1	66451937	66451980	NM_008632	Mtap2	+	66221902	230056
MACS_peak_300	chr1	67366481	67366517	no_match				
MACS_peak_311	chr1	70605410	70605476	NM_025728	Spag16	+	69998188	607255
MACS_peak_314	chr1	71125910	71125974	NM_007525	Bard1	-	71149546	23604
MACS_peak_319	chr1	72742935	72742972	NM_176980	Ankar	-	72747138	4185
MACS_peak_320	chr1	72743061	72743095	NM_176980	Ankar	-	72747138	4060
MACS_peak_324	chr1	73900119	73900166	NR_045311	6030407O03Rik	-	73911040	10898
MACS_peak_337	chr1	78511600	78511643	NM_026713	Mogat1	+	78507634	3987
MACS_peak_358	chr1	82744083	82744119	NM_029409	Mff	+	82721492	22609
MACS_peak_389	chr1	93116722	93116761	NM_016894	Ramp1	+	93076398	40343
MACS_peak_609	chr1	133333857	133333914	NM_001081011	Srgap2	-	133423938	90053

MACS_peak_621	chr1	138115036	138115070	NM_028872	5730559C18Rik	-	138130857	15804
MACS_peak_742	chr1	162958354	162958390	NM_173424	Zbtb37	-	162964390	6018
MACS_peak_778	chr1	172504407	172504445	NM_001109985	Nos1ap	-	172519980	15554
MACS_peak_811	chr1	182866962	182866997	NM_010094	Lefty1	+	182865169	1810
MACS_peak_830	chr1	190802224	190802300	NM_172650	Kctd3	-	190831719	29457
MACS_peak_842	chr1	195054003	195054111	NM_001044751	Hsd11b1	-	195068554	14497
MACS_peak_859	chr10	3527715	3527773	NM_001039652	Oprm1	-	3557940	30196
MACS_peak_870	chr10	4860285	4860320	NM_153399	Syne1	+	4795848	64454
MACS_peak_949	chr10	20179615	20179737	NM_013875	Pde7b	-	20444874	265198
MACS_peak_952	chr10	21977836	21977908	NM_009018	Raet1c	+	21893707	84165
MACS_peak_953	chr10	21977933	21978018	NM_009018	Raet1c	+	21893707	84268
MACS_peak_1005	chr10	31516009	31516040	NM_001013411	Nkain2	-	32609721	1093697
MACS_peak_1062	chr10	42242152	42242186	NM_017472	Snx3	+	42221859	20310
MACS_peak_1113	chr10	50686748	50686787	NM_011376	Sim1	+	50615456	71311
MACS_peak_1124	chr10	51864278	51864336	NM_011282	Ros1	-	51915050	50743
MACS_peak_1224	chr10	72841935	72841971	no_match				
MACS_peak_1287	chr10	92363657	92363691	no_match				
MACS_peak_1289	chr10	94334776	94334830	NM_018797	Plxnc1	-	94407212	72409
MACS_peak_1365	chr10	107614275	107614309	NM_027892	Ppp1r12a	+	107599455	14837

MACS_peak_1369	chr10	107998262	107998296	NM_009306	Syt1	-	108448031	449752
MACS_peak_1402	chr10	114174430	114174494	NM_146241	Trhde	-	114238426	63964
MACS_peak_1403	chr10	114546341	114546392	NM_173391	Tph2	-	114622078	75712
MACS_peak_1429	chr10	123113356	123113391	NR_045514	Fam19a2	+	122701131	412242
MACS_peak_1471	chr11	3547495	3547533	NR_002322	Tug1	-	3547536	22
MACS_peak_1475	chr11	5127047	5127079	NM_032396	Kremen1	-	5161613	34550
MACS_peak_1489	chr11	9252974	9253008	NM_178259	Abca13	+	9091944	161047
MACS_peak_1596	chr11	34440916	34440951	NM_033374	Dock2	-	34597325	156392
MACS_peak_1609	chr11	39125133	39125187	no_match				
MACS_peak_1613	chr11	40551695	40551732	NM_026023	Nudcd2	+	40547143	4570
MACS_peak_1652	chr11	51269256	51269290	NM_153393	Col23a1	+	51103421	165852
MACS_peak_1673	chr11	57116144	57116235	NM_001252403	Gria1	+	56826547	289642
MACS_peak_1719	chr11	70794600	70794639	NM_007573	C1qbp	-	70796528	1909
MACS_peak_1785	chr11	90400104	90400242	NM_011505	Stxbp4	-	90499422	99249
MACS_peak_1786	chr11	90400305	90400381	NM_011505	Stxbp4	-	90499422	99079
MACS_peak_1787	chr11	90400408	90400451	NM_011505	Stxbp4	-	90499422	98993
MACS_peak_1807	chr11	94443982	94444020	NM_153807	Acsf2	-	94463100	19099
MACS_peak_1826	chr11	100668946	100668979	NM_011489	Stat5b	-	100683884	14922
MACS_peak_1841	chr11	103044907	103044948	NM_019679	Fmnl1	+	103032451	12476

MACS_peak_1842	chr11	104393573	104393611	NM_145436	Cdc27	-	104411934	18342
MACS_peak_1848	chr11	105267800	105267837	NM_172568	Mar-10	-	105318049	50231
MACS_peak_1885	chr11	114560471	114560517	NM_053273	Ttyh2	+	114536781	23713
MACS_peak_1893	chr11	119327933	119327965	no_match				
MACS_peak_1937	chr12	7933008	7933052	no_match				
MACS_peak_1979	chr12	16754618	16754711	NM_001252071	Greb1	-	16764045	9381
MACS_peak_1989	chr12	20923166	20923204	no_match				
MACS_peak_2076	chr12	42241697	42241756	NM_053122	Immp2l	+	41750676	491050
MACS_peak_2090	chr12	46034622	46034665	NM_144552	Stxbp6	-	46175470	140827
MACS_peak_2186	chr12	68160152	68160209	NM_207010	Mdga2	-	68323536	163356
MACS_peak_2188	chr12	68160332	68160532	NM_207010	Mdga2	-	68323536	163104
MACS_peak_2190	chr12	68160850	68160937	NM_207010	Mdga2	-	68323536	162643
MACS_peak_2227	chr12	82217935	82218007	NM_022316	Smoc1	+	82127794	90177
MACS_peak_2303	chr12	103576125	103576163	NM_001161365	Rin3	+	103521850	54294
MACS_peak_2340	chr12	115059591	115059622	no_match				
MACS_peak_2347	chr12	116472701	116472735	no_match				
MACS_peak_2410	chr13	12410921	12410962	NM_033268	Actn2	-	12432999	22058
MACS_peak_2424	chr13	15091904	15091945	no_match				
MACS_peak_2543	chr13	46017910	46017945	NM_009124	Atxn1	-	46060360	42433

MACS_peak_2544	chr13	46042013	46042045	NM_009124	Atxn1	-	46060360	18331
MACS_peak_2545	chr13	46622579	46622615	NM_026056	Cap2	+	46597271	25326
MACS_peak_2547	chr13	47009683	47009715	NM_010617	Kif13a	-	47025087	15388
MACS_peak_2551	chr13	49012998	49013037	NM_001033268	Fam120a	-	49063197	50180
MACS_peak_2566	chr13	53365271	53365354	NM_013846	Ror2	-	53381478	16166
MACS_peak_2579	chr13	60777947	60778038	NM_134062	Dapk1	+	60703571	74421
MACS_peak_2588	chr13	62583854	62583884	no_match				
MACS_peak_2595	chr13	63142897	63142932	NM_028079	2010111I01Rik	+	63116293	26621
MACS_peak_2664	chr13	77444222	77444276	NM_001145676	2210408I21Rik	+	77274796	169453
MACS_peak_2668	chr13	77578162	77578320	NM_001145676	2210408I21Rik	+	77274796	303445
MACS_peak_2674	chr13	78139588	78139623	NM_001163420	Fam172a	+	77847950	291655
MACS_peak_2675	chr13	78159832	78159943	NM_001163420	Fam172a	+	77847950	311937
MACS_peak_2676	chr13	78217440	78217475	NM_001163420	Fam172a	+	77847950	369507
MACS_peak_2762	chr13	97921248	97921282	NM_177266	Gfm2	+	97907891	13374
MACS_peak_2817	chr13	113643535	113643568	NM_008903	Ppap2a	+	113591130	52421
MACS_peak_2837	chr13	120151364	120151394	NM_008710	Nnt	-	120197818	46439
MACS_peak_2839	chr13	120276600	120276641	NR_027974	3110070M22Rik	-	120277191	571
MACS_peak_2888	chr14	11727973	11728027	NM_010210	Fhit	-	11994546	266546
MACS_peak_2890	chr14	11825648	11825724	NM_010210	Fhit	-	11994546	168860

MACS_peak_2892	chr14	13370194	13370258	NM_012061	Cadps	-	13655593	285367
MACS_peak_2968	chr14	35154586	35154620	NM_008133	Glud1	+	35123912	30691
MACS_peak_3067	chr14	53420088	53420152	no_match				
MACS_peak_3088	chr14	58051162	58051222	NM_009376	Ift88	+	58042907	8285
MACS_peak_3139	chr14	77836070	77836123	NM_001253759	Enox1	+	77556569	279527
MACS_peak_3335	chr14	115612244	115612279	NM_175500	Gpc5	+	115491436	120825
MACS_peak_3368	chr14	123850814	123850897	NM_177393	Nalcn	-	124026366	175511
MACS_peak_3508	chr15	31434664	31434694	NM_172606	37315	-	31460792	26113
MACS_peak_3536	chr15	37183389	37183424	NM_026496	Grhl2	+	37162790	20616
MACS_peak_3563	chr15	44304155	44304226	NM_138674	Pkhd1l1	+	44289098	15092
MACS_peak_3583	chr15	47905751	47905788	NM_001081391	Csmd3	-	48623535	717766
MACS_peak_3638	chr15	59288130	59288167	NM_001164604	Nsmce2	+	59205752	82396
MACS_peak_3656	chr15	63890297	63890378	NM_144846	Fam49b	-	63892010	1673
MACS_peak_3740	chr15	85372595	85372669	NM_001163634	Wnt7b	-	85408500	35868
MACS_peak_3781	chr15	100243296	100243331	NM_008732	Slc11a2	-	100253486	10173
MACS_peak_3827	chr16	10975160	10975272	NM_019980	Litaf	-	10993214	17998
MACS_peak_3850	chr16	18511270	18511303	NM_023120	Gnb1l	+	18498963	12323
MACS_peak_3851	chr16	19117281	19117317	no_match				
MACS_peak_3871	chr16	22560593	22560632	NM_138650	Dgkg	-	22657304	96692

MACS_peak_3903	chr16	32236284	32236316	NM_173439	Fbxo45	-	32247111	10811
MACS_peak_3935	chr16	41705086	41705124	NM_175548	Lsamp	+	41533454	171651
MACS_peak_3994	chr16	56755742	56755775	NM_172825	Gpr128	-	56795971	40213
MACS_peak_4129	chr16	88239233	88239265	NM_146072	Grik1	-	88290503	51254
MACS_peak_4177	chr17	12195749	12195783	NM_016694	Park2	+	11033249	1162517
MACS_peak_4183	chr17	13743882	13744007	NR_045437	2700054A10Rik	-	13746960	3016
MACS_peak_4186	chr17	13744420	13744533	NR_045437	2700054A10Rik	-	13746960	2484
MACS_peak_4187	chr17	13744590	13744862	NR_045437	2700054A10Rik	-	13746960	2234
MACS_peak_4188	chr17	13744975	13745591	NR_045437	2700054A10Rik	-	13746960	1677
MACS_peak_4189	chr17	13745604	13746081	NR_045437	2700054A10Rik	-	13746960	1118
MACS_peak_4250	chr17	26114174	26114205	no_match				
MACS_peak_4253	chr17	27064710	27064740	NM_053173	Kifc5b	+	27054035	10690
MACS_peak_4260	chr17	29413077	29413116	NM_030561	BC004004	+	29405732	7364
MACS_peak_4265	chr17	30309378	30309416	NM_148926	Zfand3	+	30142031	167366
MACS_peak_4278	chr17	34706666	34706699	NM_010929	Notch4	+	34701239	5443
MACS_peak_4284	chr17	36028987	36029027	NM_026987	Dhx16	+	36016722	12285
MACS_peak_4328	chr17	42939260	42939317	NM_009847	Cd2ap	-	43013373	74085
MACS_peak_4332	chr17	43457759	43457822	NM_133776	Gpr110	+	43407295	50495
MACS_peak_4372	chr17	51890542	51890577	NM_001163630	Satb1	-	51951379	60820

MACS_peak_4469	chr17	68090697	68090735	NM_008480	Lama1	+	68046604	44112
MACS_peak_4470	chr17	68090802	68090842	NM_008480	Lama1	+	68046604	44218
MACS_peak_4494	chr17	71896979	71897016	no_match				
MACS_peak_4497	chr17	72427434	72427475	NM_007439	Alk	-	72953647	526193
MACS_peak_4499	chr17	73492973	73493010	NM_001177968	Lclat1	+	73457324	35667
MACS_peak_4500	chr17	73515938	73515991	NM_001177968	Lclat1	+	73457324	58640
MACS_peak_4501	chr17	73548076	73548113	NM_001177968	Lclat1	+	73457324	90770
MACS_peak_4663	chr18	11995310	11995344	NR_045421	Gm6277	-	11997886	2559
MACS_peak_4700	chr18	22531712	22531756	NM_001167777	Asxl3	+	22503589	28145
MACS_peak_4702	chr18	22978430	22978461	NM_001161483	Nol4	-	23197164	218719
MACS_peak_4703	chr18	22997222	22997257	NM_001161483	Nol4	-	23197164	199925
MACS_peak_4705	chr18	23664013	23664054	NM_207650	Dtna	+	23573915	90118
MACS_peak_4707	chr18	25335360	25335405	NM_001033532	AW554918	+	25327520	7862
MACS_peak_4781	chr18	43073577	43073650	NM_028392	Ppp2r2b	-	43219125	145512
MACS_peak_4782	chr18	43733449	43733489	NM_001163637	Jakmip2	-	43847427	113958
MACS_peak_4882	chr18	65263659	65263715	NM_031881	Nedd4l	+	65183180	80507
MACS_peak_4884	chr18	65279469	65279644	NM_031881	Nedd4l	+	65183180	96376
MACS_peak_4943	chr18	78394983	78395032	NM_001110274	Slc14a2	-	78403179	8172
MACS_peak_4944	chr18	78395088	78395149	NM_001110274	Slc14a2	-	78403179	8061

MACS_peak_4985	chr18	89200748	89200791	NM_175542	Rttn	+	89141181	59588
MACS_peak_4986	chr18	89645076	89645113	NM_001039173	Dok6	-	89938528	293434
MACS_peak_5052	chr19	18752719	18752790	NM_026120	2410127L17Rik	+	18745269	7485
MACS_peak_5071	chr19	23431916	23431993	NM_174857	Mamdc2	-	23522812	90858
MACS_peak_5097	chr19	30809409	30809448	NM_011160	Prkg1	-	31738860	929432
MACS_peak_5099	chr19	32018778	32018811	NM_001081074	A1cf	+	31943250	75544
MACS_peak_5100	chr19	32018885	32018933	NM_001081074	A1cf	+	31943250	75659
MACS_peak_5124	chr19	36497198	36497233	NM_029508	Pcgf5	+	36453556	43659
MACS_peak_5126	chr19	36777943	36777979	no_match				
MACS_peak_5164	chr19	50385115	50385194	NM_001252501	Sorcs1	-	50753136	367982
MACS_peak_5216	chr2	5082897	5082932	NM_028804	Ccdc3	+	5058821	24093
MACS_peak_5217	chr2	5455951	5455990	NM_177343	Camk1d	-	5635710	179740
MACS_peak_5305	chr2	22442807	22442990	NM_148413	Myo3a	+	22149129	293769
MACS_peak_5306	chr2	22443049	22446054	NM_148413	Myo3a	+	22149129	295422
MACS_peak_5374	chr2	41751717	41751790	NM_053011	Lrp1b	-	42509118	757365
MACS_peak_5383	chr2	43518346	43518383	NM_027552	Kynu	+	43410848	107516
MACS_peak_5401	chr2	49644585	49644622	NM_027990	Lypd6b	+	49643205	1398
MACS_peak_5478	chr2	62466752	62466794	NM_001164477	Ifih1	-	62484312	17539
MACS_peak_5499	chr2	68436980	68437063	NM_177651	4933409G03Rik	+	68420469	16552

MACS_peak_5666	chr2	105466045	105466081	NR_002867	Pax6os1	-	105510487	44424
MACS_peak_5691	chr2	110133770	110133849	NM_130452	Bbox1	-	110145882	12073
MACS_peak_5710	chr2	112983268	112983300	no_match				
MACS_peak_5731	chr2	120762337	120762412	NM_009461	Ubr1	-	120796451	34077
MACS_peak_5734	chr2	121348240	121348274	NM_030234	Wdr76	+	121332458	15799
MACS_peak_5740	chr2	122536223	122536261	no_match				
MACS_peak_6336	chr3	75754176	75754212	NM_175193	Golim4	-	75760753	6559
MACS_peak_6376	chr3	87241592	87241635	NM_183222	Fcrl5	+	87239703	1910
MACS_peak_6430	chr3	98971413	98971447	NM_027462	Wars2	+	98945012	26418
MACS_peak_6440	chr3	99785195	99785251	NM_028892	Spag17	+	99689339	95884
MACS_peak_6441	chr3	99785290	99785323	NM_028892	Spag17	+	99689339	95967
MACS_peak_6464	chr3	104756200	104756243	NM_009520	Wnt2b	-	104764627	8406
MACS_peak_6532	chr3	116666552	116666596	NM_023245	Palmd	-	116671870	5296
MACS_peak_6535	chr3	117040253	117040289	NM_177664	D3Bwg0562e	-	117063794	23523
MACS_peak_6551	chr3	120925849	120925913	NM_178936	Tmem56	-	120966234	40353
MACS_peak_6609	chr3	135125098	135125135	NM_025356	Ube2d3	+	135101722	23394
MACS_peak_6707	chr3	158111997	158112033	NM_001081358	Lrrc7	-	158225185	113170
MACS_peak_6739	chr4	5765020	5765061	no_match				
MACS_peak_6749	chr4	6778838	6778879	NM_145711	Tox	-	6917870	139012

MACS_peak_6827	chr4	19572532	19572611	NM_177327	Wwp1	-	19636147	63576
MACS_peak_6991	chr4	56866312	56866372	NM_018761	Ctnnal1	-	56878083	11741
MACS_peak_7073	chr4	70039154	70039288	NM_145990	Cdk5rap2	-	70071401	32180
MACS_peak_7232	chr4	97315407	97315441	NM_001122952	Nfia	+	97248633	66791
MACS_peak_7268	chr4	110966433	110966465	NM_030231	Agbl4	+	110070395	896054
MACS_peak_7287	chr4	113667574	113667617	NM_001167878	Skint5	-	113672108	4513
MACS_peak_7311	chr4	120174330	120174368	NM_013883	Scmh1	+	120077885	96464
MACS_peak_7407	chr4	154252264	154252349	NM_013783	Mmel1	+	154243693	8613
MACS_peak_7409	chr4	154891898	154891961	NM_001160017	Gnb1	+	154865469	26460
MACS_peak_7450	chr5	9328616	9328691	NM_172706	9330182L06Rik	+	9266192	62461
MACS_peak_7495	chr5	15606949	15606986	NM_001110843	Cacna2d1	+	15440508	166459
MACS_peak_7531	chr5	22105725	22105759	no_match				
MACS_peak_7563	chr5	31952587	31952622	NM_153196	Rbks	-	31999983	47379
MACS_peak_7569	chr5	34420761	34420804	NM_181857	Poln	-	34512097	91315
MACS_peak_7750	chr5	73131805	73131839	NM_001122754	Txk	-	73144012	12190
MACS_peak_7825	chr5	86480418	86480454	NM_007683	Cenpc1	-	86494608	14172
MACS_peak_7888	chr5	103293219	103293252	NM_029270	Arhgap24	+	102910409	382826
MACS_peak_7897	chr5	106010419	106010460	NM_133897	Lrrc8c	+	105948489	61950
MACS_peak_7924	chr5	113185591	113185626	NM_028901	Myo18b	-	113325382	139774

MACS_peak_7926	chr5	113662469	113662534	NM_001033428	Tmem211	+	113655928	6573
MACS_peak_7962	chr5	128014781	128014825	NM_175432	Tmem132c	+	127722195	292608
MACS_peak_7974	chr5	132568314	132568353	NM_177047	Auts2	-	133018213	449880
MACS_peak_7994	chr5	136837356	136837398	NM_198602	Cux1	-	137043275	205898
MACS_peak_8001	chr5	138482217	138482248	NM_001039889	Smok3b	+	138478451	3781
MACS_peak_8013	chr5	141818269	141818304	NM_177879	Sdk1	+	141717487	100799
MACS_peak_8025	chr5	144263582	144263614	NM_144915	Daglb	+	144225360	38238
MACS_peak_8026	chr5	144404009	144404091	NM_011182	Cyth3	+	144383315	20735
MACS_peak_8050	chr5	148423005	148423155	NM_010228	Flt1	-	148537564	114484
MACS_peak_8072	chr6	4873768	4873876	NM_181595	Ppp1r9a	+	4853319	20503
MACS_peak_8073	chr6	4874140	4874176	NM_181595	Ppp1r9a	+	4853319	20839
MACS_peak_8074	chr6	4929320	4929372	NM_181595	Ppp1r9a	+	4853319	76027
MACS_peak_8194	chr6	27982346	27982382	NM_008174	Grm8	-	28084369	102005
MACS_peak_8201	chr6	29698349	29698691	NM_176996	Smo	+	29685496	13024
MACS_peak_8202	chr6	29698765	29698948	NM_176996	Smo	+	29685496	13360
MACS_peak_8203	chr6	29698976	29699059	NM_176996	Smo	+	29685496	13521
MACS_peak_8214	chr6	33727952	33727987	NM_009148	Exoc4	+	33199149	528820
MACS_peak_8224	chr6	37314886	37314918	NM_178661	Creb3l2	-	37392148	77246
MACS_peak_8238	chr6	41074097	41074158	no_match				

MACS_peak_8281	chr6	47605196	47605276	no_match				
MACS_peak_8285	chr6	47609466	47609612	no_match				
MACS_peak_8286	chr6	47613766	47613952	no_match				
MACS_peak_8287	chr6	47618143	47618261	no_match				
MACS_peak_8288	chr6	47622501	47622583	no_match				
MACS_peak_8295	chr6	47635427	47635545	no_match				
MACS_peak_8296	chr6	47636057	47636197	no_match				
MACS_peak_8298	chr6	47689999	47690223	no_match				
MACS_peak_8302	chr6	47698642	47698788	no_match				
MACS_peak_8384	chr6	62123479	62123549	NM_001164316	Fam190a	+	61130318	993196
MACS_peak_8418	chr6	67961891	67961960	no_match				
MACS_peak_8487	chr6	82711256	82711309	NM_013820	Hk2	-	82724448	13166
MACS_peak_8489	chr6	83090519	83090558	NM_133641	Rtkn	+	83087077	3461
MACS_peak_8502	chr6	88211729	88211759	NM_023060	Eefsec	-	88396533	184789
MACS_peak_8531	chr6	100529278	100529325	NM_181590	Shq1	-	100621151	91850
MACS_peak_8542	chr6	103599041	103599289	NM_007697	Chl1	+	103460869	138296
MACS_peak_8554	chr6	105744443	105744474	NM_001109749	Cntn4	+	105627738	116720
MACS_peak_8617	chr6	119940739	119940828	NM_001185021	Wnk1	-	119988673	47890
MACS_peak_8709	chr6	142906337	142906397	NM_011374	St8sia1	-	142912972	6605

MACS_peak_8713	chr6	144174729	144174782	no_match				
MACS_peak_8829	chr7	19618910	19618972	NM_026605	Sympk	+	19609725	9216
MACS_peak_8902	chr7	35743189	35743244	NM_008820	Pepd	+	35697425	45791
MACS_peak_8913	chr7	38157254	38157286	no_match				
MACS_peak_9020	chr7	66021157	66021205	NM_009728	Atp10a	+	65913571	107610
MACS_peak_9087	chr7	71752092	71752130	NM_007461	Apba2	+	71646591	105520
MACS_peak_9148	chr7	89050992	89051024	NM_013886	Hdgfrp3	-	89079345	28337
MACS_peak_9157	chr7	90759371	90759406	NM_177695	Tmc3	+	90733440	25948
MACS_peak_9209	chr7	101433469	101433504	no_match				
MACS_peak_9272	chr7	119818511	119818545	no_match				
MACS_peak_9415	chr8	17290635	17290684	NM_053171	Csmd1	-	17535385	244726
MACS_peak_9437	chr8	24205944	24206174	NM_031158	Ank1	+	24168746	37313
MACS_peak_9438	chr8	24206235	24206280	NM_031158	Ank1	+	24168746	37511
MACS_peak_9451	chr8	28220148	28220183	NM_054044	Gpr124	+	28196312	23853
MACS_peak_9496	chr8	40449077	40449129	NR_044988	Gm6213	+	40383333	65770
MACS_peak_9572	chr8	58454287	58454347	NM_080438	Glra3	+	58419621	34696
MACS_peak_9645	chr8	73543979	73544018	NR_045487	1700026F02Rik	-	73550654	6656
MACS_peak_9649	chr8	74932251	74932291	NM_007944	Eps15l1	-	74945373	13102
MACS_peak_9705	chr8	90282778	90282818	NM_033327	Zfp423	-	90483494	200696

MACS_peak_9708	chr8	91111252	91111289	NM_001163660	Nkd1	+	91051531	59739
MACS_peak_9805	chr8	119893178	119893218	NM_028941	Cmip	+	119873069	20129
MACS_peak_9806	chr8	120193924	120193972	NM_028725	Sdr42e1	-	120195415	1467
MACS_peak_9826	chr8	126485381	126485458	NM_019552	Abcb10	-	126507022	21603
MACS_peak_9853	chr9	3590942	3590978	NM_001033322	Gucy1a2	+	3532348	58612
MACS_peak_9899	chr9	10186515	10186578	NM_001033359	Cntn5	-	10904726	718180
MACS_peak_9922	chr9	15124219	15124268	NM_176976	5830418K08Rik	-	15162232	37989
MACS_peak_9924	chr9	15126016	15126055	NM_176976	5830418K08Rik	-	15162232	36197
MACS_peak_9973	chr9	24549530	24549669	NM_194263	Tbx20	-	24578747	29148
MACS_peak_9993	chr9	31700236	31700319	NM_013800	Barx2	-	31720870	20593
MACS_peak_10006	chr9	35444874	35444931	no_match				
MACS_peak_10007	chr9	35489188	35489246	no_match				
MACS_peak_10097	chr9	64584698	64584731	NM_017382	Rab11a	-	64585563	849
MACS_peak_10131	chr9	78559796	78559829	NM_153098	Cd109	+	78463352	96460
MACS_peak_10138	chr9	79931764	79931833	NM_146003	Senp6	+	79914709	17089
MACS_peak_10155	chr9	83452812	83452858	NM_172507	Sh3bgrl2	+	83441944	10891
MACS_peak_10215	chr9	96753566	96753607	NM_153420	Acpl2	-	96789841	36255
MACS_peak_10240	chr9	107750112	107750169	NM_029169	Rbm6	-	107775150	25010
MACS_peak_10259	chr9	113779357	113779391	NM_029633	Clasp2	+	113721703	57671

MACS_peak_10285	chr9	123016478	123016532	NM_026917	Zdhhc3	-	123022323	5818
MACS_peak_11142	chrX	34989842	34989880	NM_001085356	Rhox2f	+	34985927	3934
MACS_peak_11148	chrX	36165249	36165286	NM_183126	6030498E09Rik	+	36125956	39311
MACS_peak_11360	chrX	68640647	68640683	NM_016985	Mtmr1	+	68617934	22731
MACS_peak_11463	chrX	84127738	84127768	NM_001160403	Il1rapl1	-	85360962	1233209
MACS_peak_11521	chrX	93297952	93297983	NM_010833	Msn	+	93291383	6584
MACS_peak_11558	chrX	100917600	100917635	NM_009197	Slc16a2	-	101017327	99710
MACS_peak_11570	chrX	103060192	103060222	NM_009530	Atrx	-	103124711	64504
MACS_peak_11745	chrX	126917888	126917942	NM_172493	Diap2	+	126284277	633638
MACS_peak_11768	chrX	130684595	130684650	NM_183319	Xkrx	-	130696467	11845
MACS_peak_11921	chrX	163813503	163813544	NM_026662	Prps2	-	163820631	7108
MACS_peak_11924	chrX	164425136	164425168	NM_001033330	Frmpd4	-	165015165	590013
MACS_peak_11936	chrX	166427377	166427446	NM_183151	Mid1	+	166317553	109858

Appendix 4: Gene expression data

All values are expressed as fold changes, and genes are listed alphabetically. wt=wildtype (HDAC4$^{fl/fl}$); ko = HDAC4 cKO; sem = standard error of the mean. #VALUE! indicates the transcript was not detected. If #VALUE! appears across an entire row, it was not expressed in one or more of the control samples and a fold change could not be determined. These were excluded from analysis. P-values represent t-tests of FC values.

Table 13 – HDAC4$^{Nav1.8}$ *in vitro* injury model, 50 ng/mL NGF (Study 1)

ID	wt 3h1	wt 3h2	wt 3h3	wt 3h4	ko 3h 1	ko 3h 2	ko 3h 3	ko 3h 4	p	wt average	wt sem	ko average	ko sem
Adcyap	1.21	1.07	0.77	0.95	1.05	0.92	0.63	0.95	0.43	1.00	0.09	0.89	0.09
Aif1	0.55	0.87	1.51	1.07	1.08	1.24	2.16	3.20	0.16	1.00	0.20	1.92	0.49
Atf3	1.06	0.88	0.89	1.17	0.64	0.66	0.80	0.76	0.02	1.00	0.07	0.72	0.04
Bdnf	0.58	0.52	1.31	1.58	0.17	0.91	1.76	2.73	0.55	1.00	0.26	1.39	0.55
Cacna2d1	1.33	0.92	0.58	1.17	0.78	1.00	0.39	0.16	0.15	1.00	0.16	0.58	0.19
Calca	0.99	0.61	1.34	1.06	0.28	0.45	0.45	0.21	0.02	1.00	0.15	0.35	0.06
Ccl2	0.75	0.60	1.49	1.16	0.33	1.10	0.58	0.99	0.39	1.00	0.20	0.75	0.18
Ccr2	1.91	0.98	0.47	0.65	7.65	25.46	2.50	3.71	0.20	1.00	0.32	9.83	5.33
Ctss	0.49	0.01	1.02	2.48	0.11	0.13	0.22	0.32	0.23	1.00	0.53	0.19	0.05
Egfr	0.95	1.47	0.85	0.73	1.12	0.17	0.30	0.44	0.12	1.00	0.16	0.51	0.21
Gabbr1	1.18	1.02	0.82	0.97	0.90	0.90	1.11	0.98	0.76	1.00	0.07	0.97	0.05
Gabra5	1.39	0.88	0.87	0.87	1.19	2.30	1.41	0.07	0.64	1.00	0.13	1.24	0.46
Gad2	0.61	0.29	2.92	0.18	2.67	3.08	5.36	7.95	0.05	1.00	0.65	4.76	1.21

ID	wt 3h1	wt 3h2	wt 3h3	wt 3h4	ko 3h 1	ko 3h 2	ko 3h 3	ko 3h 4	p	wt average	wt sem	ko average	ko sem
Gal	0.78	0.53	1.34	1.35	0.26	0.43	0.70	1.58	0.51	1.00	0.20	0.75	0.29
Gapdh	1.24	1.27	0.75	0.74	1.61	1.38	1.50	0.91	0.15	1.00	0.15	1.35	0.16
Gch1	1.18	0.90	0.86	1.06	0.46	0.27	0.68	0.06	0.01	1.00	0.07	0.37	0.13
Gfap	1.46	0.62	1.45	0.47	1.48	1.04	0.19	0.28	0.55	1.00	0.26	0.74	0.31
Hcn2	1.12	1.14	0.94	0.79	1.33	0.92	1.08	0.81	0.82	1.00	0.08	1.03	0.11
Hprt	0.69	0.68	1.32	1.31	0.52	0.64	0.58	1.11	0.26	1.00	0.18	0.71	0.13
Kcns1	0.98	0.96	1.03	1.03	0.66	0.50	0.24	0.02	0.02	1.00	0.02	0.36	0.14
Ngf	1.03	1.24	1.07	0.67	1.51	1.80	2.37	2.49	0.01	1.00	0.12	2.04	0.23
Ngfr	0.66	0.96	1.45	0.93	1.58	1.29	0.72	0.39	0.99	1.00	0.16	0.99	0.27
Nos1	1.11	1.58	0.52	0.79	0.79	0.78	0.26	0.27	0.14	1.00	0.23	0.53	0.15
Npy	3.52	0.17	0.04	0.27	0.77	0.33	0.49	4.44	0.71	1.00	0.84	1.51	0.98
Ntrk1	1.17	0.89	1.07	0.87	0.52	0.35	0.38	0.22	0.00	1.00	0.07	0.37	0.06
Ntrk2	1.27	1.45	0.55	0.72	1.77	1.81	1.55	0.54	0.30	1.00	0.22	1.42	0.30
Ntrk3	1.33	1.27	0.71	0.69	1.93	1.44	1.67	0.36	0.41	1.00	0.17	1.35	0.34
Oprm1	2.48	0.16	1.13	0.22	1.53	1.76	3.06	4.54	0.10	1.00	0.54	2.72	0.69
P2rx3	1.27	1.10	0.71	0.92	0.59	0.48	0.34	0.24	0.01	1.00	0.12	0.41	0.08
P2rx4	0.92	0.88	0.98	1.22	1.12	0.60	0.55	0.05	0.15	1.00	0.08	0.58	0.22

ID	wt 3h1	wt 3h2	wt 3h3	wt 3h4	ko 3h 1	ko 3h 2	ko 3h 3	ko 3h 4	p	wt average	wt sem	ko average	ko sem
Pdyn	0.96	0.79	1.26	1.00	1.56	0.21	0.37	0.54	0.37	1.00	0.10	0.67	0.30
Ptgs2	1.20	0.77	1.13	0.90	0.88	0.67	1.49	0.77	0.83	1.00	0.10	0.95	0.18
Reg3b	0.86	1.88	0.31	0.96	17.44	20.10	35.00	51.89	0.03	1.00	0.33	31.11	7.93
Rest	1.24	1.40	0.68	0.68	0.23	1.00	0.25	0.78	0.16	1.00	0.19	0.56	0.19
Scn10a	1.23	1.32	0.58	0.87	0.83	0.93	0.68	0.30	0.21	1.00	0.17	0.69	0.14
Scn11a	1.22	1.40	0.55	0.82	1.31	1.47	1.13	1.30	0.22	1.00	0.19	1.30	0.07
Scn3a	1.38	1.06	0.59	0.97	0.95	1.14	0.27	0.40	0.29	1.00	0.16	0.69	0.21
Scn9a	1.14	1.21	0.62	1.03	1.75	1.94	2.16	1.26	0.02	1.00	0.13	1.78	0.19
Sgk1	1.47	0.84	0.76	0.92	0.80	1.19	0.96	1.40	0.68	1.00	0.16	1.09	0.13
Slco1a6	0.58	1.26	0.21	1.95	11.74	13.53	23.57	34.94	0.03	1.00	0.39	20.95	5.34
Sst	0.55	1.89	0.84	0.72	8.17	10.31	10.56	3.13	0.02	1.00	0.30	8.04	1.72
Tac1	1.07	0.84	0.87	1.21	0.74	1.05	1.31	1.54	0.45	1.00	0.09	1.16	0.17
Tacr1	2.56	0.11	0.52	0.80	1.04	1.20	2.10	3.11	0.28	1.00	0.54	1.86	0.48
Trpa1	0.97	1.13	0.78	1.12	0.91	0.89	0.85	0.50	0.14	1.00	0.08	0.79	0.10
Trpv1	1.10	0.71	0.90	1.28	0.39	0.63	0.37	0.27	0.01	1.00	0.12	0.41	0.08
Vgf	0.90	0.42	0.95	1.73	0.08	0.13	0.10	0.24	0.05	1.00	0.27	0.14	0.04
Vip	0.48	1.04	1.03	1.45	9.66	11.14	19.40	28.76	0.03	1.00	0.20	17.24	4.40

Table 14 - HDAC4$^{Nav1.8}$ naive gene expression (Study 2)

ID	naive wt1	naive wt2	naive wt3	naive wt4	naive cko1	naive cko2	naive cko3	naive cko4	p	wt average	wt sem	ko average	ko sem
Adcyap	0.79	0.97	1.12	1.13	0.88	0.87	1.46	1.02	0.73	1.00	0.08	1.06	0.14
Aif1	0.53	1.08	0.86	1.53	1.25	0.80	1.59	1.68	0.30	1.00	0.21	1.33	0.20
Atf3	1.37	1.27	0.97	0.40	1.42	0.67	0.34	0.36	0.40	1.00	0.22	0.70	0.25
Bdnf	0.98	0.38	1.65	0.98	0.88	0.83	1.39	1.17	0.83	1.00	0.26	1.07	0.13
Cacna2d1	0.94	0.74	1.38	0.94	1.15	1.11	1.41	1.60	0.13	1.00	0.14	1.32	0.12
Calca	0.90	0.92	1.30	0.89	0.68	0.68	1.27	0.79	0.43	1.00	0.10	0.85	0.14
Ccl2	0.88	1.15	0.50	1.46	0.74	0.59	1.07	0.85	0.45	1.00	0.20	0.81	0.10
Ccr2	1.00	0.83	0.91	1.26	1.05	1.08	1.45	0.95	0.39	1.00	0.09	1.13	0.11
Ctss	1.43	1.00	0.95	0.61	0.92	0.97	1.45	0.61	0.96	1.00	0.17	0.99	0.18
Egfr	0.77	1.04	0.78	1.40	0.71	0.94	1.20	0.97	0.82	1.00	0.15	0.96	0.10
Gabbr1	0.85	1.12	1.02	1.01	0.85	0.84	0.90	0.98	0.16	1.00	0.06	0.89	0.03
Gabra5	0.96	0.93	1.01	1.11	0.89	1.25	1.06	1.12	0.39	1.00	0.04	1.08	0.08
Gad2	#VALUE!	#VALUE!	#VALUE!	#VALUE!	#VALUE!	#VALUE!	#VALUE!	#VALUE!	#VALUE!	#VALUE!	#VALUE!	#VALUE!	#VALUE!

ID	naive wt1	naive wt2	naive wt3	naive wt4	naive cko1	naive cko2	naive cko3	naive cko4	p	wt average	wt sem	ko average	ko sem
Gal	0.97	0.69	1.05	1.29	0.61	0.53	1.94	0.92	0.99	1.00	0.13	1.00	0.33
Gapdh	0.91	1.12	0.95	1.02	1.03	1.10	1.05	1.08	0.27	1.00	0.05	1.06	0.01
Gch1	1.16	1.07	1.04	0.73	1.06	0.68	1.01	0.76	0.38	1.00	0.09	0.88	0.09
Gfap	1.52	1.02	1.01	0.46	0.54	0.71	0.90	1.78	0.95	1.00	0.22	0.98	0.28
Hcn2	0.91	1.12	1.08	0.89	0.98	0.94	1.02	1.20	0.67	1.00	0.06	1.04	0.06
Hprt	1.13	0.85	1.06	0.96	0.95	0.87	0.93	0.89	0.24	1.00	0.06	0.91	0.02
Kcns1	0.82	1.16	1.00	1.02	1.10	0.83	0.81	1.06	0.64	1.00	0.07	0.95	0.07
Ngf	1.14	1.92	0.51	0.43	0.39	0.33	0.60	0.45	0.20	1.00	0.34	0.44	0.06
Ngfr	0.75	1.36	0.92	0.97	0.64	0.79	0.81	1.00	0.26	1.00	0.13	0.81	0.07
Nos1	0.78	1.25	1.05	0.92	0.64	0.85	1.35	0.64	0.53	1.00	0.10	0.87	0.17
Npy	1.15	0.77	1.43	0.65	0.29	1.84	0.08	3.88	0.60	1.00	0.18	1.52	0.88
Ntrk1	0.76	1.01	1.08	1.16	0.72	0.74	0.94	1.02	0.26	1.00	0.09	0.86	0.07
Ntrk2	0.85	1.11	1.05	0.99	0.97	0.90	1.18	1.22	0.51	1.00	0.06	1.07	0.08
Ntrk3	0.79	1.12	1.06	1.03	1.04	0.80	1.17	1.04	0.94	1.00	0.07	1.01	0.08
Oprm1	#VALUE!	#VALUE!	#VALUE!	#VALUE!	#VALUE!	#VALUE!	#VALUE!	#VALUE!	#VALUE!	#VALUE!	#VALUE!	#VALUE!	#VALUE!

ID	naive wt1	naive wt2	naive wt3	naive wt4	naive cko1	naive cko2	naive cko3	naive cko4	p	wt average	wt sem	ko average	ko sem
P2rx3	0.88	1.10	1.04	0.98	0.91	0.86	1.05	1.07	0.68	1.00	0.05	0.97	0.05
P2rx4	1.00	1.06	1.12	0.81	0.85	0.72	0.99	1.02	0.31	1.00	0.07	0.89	0.07
Pdyn	0.22	2.63	0.58	0.57	1.79	1.35	#VALUE!	1.60	#VALUE!	1.00	0.55	#VALUE!	#VALUE!
Ptgs2	0.74	1.49	0.81	0.96	0.47	0.52	0.33	0.71	0.05	1.00	0.17	0.51	0.08
Reg3b	#VALUE!	#VALUE!	#VALUE!	#VALUE!	#VALUE!	#VALUE!	#VALUE!	#VALUE!	#VALUE!	#VALUE!	#VALUE!	#VALUE!	#VALUE!
Rest	0.75	1.16	0.72	1.38	0.93	0.71	1.23	1.27	0.88	1.00	0.16	1.03	0.13
Scn10a	0.79	1.12	1.12	0.97	0.72	0.76	0.72	0.85	0.05	1.00	0.08	0.76	0.03
Scn11a	0.84	1.12	1.01	1.03	0.61	0.89	0.85	0.73	0.04	1.00	0.06	0.77	0.06
Scn3a	0.83	0.77	1.17	1.23	1.58	0.67	1.48	2.26	0.23	1.00	0.12	1.50	0.33
Scn9a	0.85	0.80	1.24	1.10	0.91	0.93	1.09	1.11	0.94	1.00	0.10	1.01	0.05
Sgk1	1.00	1.17	1.14	0.69	0.86	0.62	0.84	0.43	0.08	1.00	0.11	0.69	0.10
Slco1a6	#VALUE!	#VALUE!	#VALUE!	#VALUE!	#VALUE!	#VALUE!	#VALUE!	#VALUE!	#VALUE!	#VALUE!	#VALUE!	#VALUE!	#VALUE!
Sst	0.70	0.79	0.55	1.96	0.85	0.93	2.45	2.83	0.26	1.00	0.32	1.76	0.51
Tac1	0.90	0.95	1.10	1.05	0.84	0.82	1.37	0.77	0.75	1.00	0.05	0.95	0.14

ID	naive wt1	naive wt2	naive wt3	naive wt4	naive cko1	naive cko2	naive cko3	naive cko4	p	wt average	wt sem	ko average	ko sem
Tacr1	1.48	0.47	1.59	0.46	2.30	1.33	1.92	1.12	0.15	1.00	0.31	1.67	0.27
Trpa1	0.95	1.03	1.09	0.92	0.79	0.81	0.98	0.77	0.04	1.00	0.04	0.84	0.05
Trpv1	0.94	0.95	1.09	1.03	1.20	0.93	1.80	0.96	0.36	1.00	0.04	1.22	0.20
Vgf	0.83	0.74	1.23	1.20	0.77	1.38	1.19	1.71	0.31	1.00	0.12	1.26	0.20
Vip	#VALUE!	#VALUE!	#VALUE!	#VALUE!	#VALUE!	#VALUE!	#VALUE!	#VALUE!	#VALUE!	#VALUE!	#VALUE!	#VALUE!	#VALUE!

Table 15 - HDAC4$^{Nav1.8}$ D28 partial sciatic nerve ligation (Study 2). Expression values are normalized to wildtype naïve controls

ID	PSL wt1	PSL wt2	PSL wt3	PSL wt4	PSL cko1	PSL cko2	PSL cko3	PSL cko4	p	wt average	wt sem	ko average	ko sem
Adcyap	1.68	1.88	1.78	1.78	1.52	1.28	1.15	1.97	0.19	1.78	0.04	1.48	0.18
Aif1	1.71	2.96	1.97	1.91	3.22	2.21	1.77	1.53	0.92	2.14	0.28	2.18	0.37
Atf3	7.40	7.08	11.51	6.57	3.98	3.31	3.96	4.91	0.03	8.14	1.14	4.04	0.33
Bdnf	1.48	1.55	1.70	1.71	1.33	1.08	2.02	2.43	0.76	1.61	0.06	1.71	0.31
Cacna2d1	1.36	1.99	2.14	2.30	1.65	0.99	1.72	1.87	0.22	1.95	0.21	1.56	0.19
Calca	0.80	1.09	1.02	1.10	0.69	0.74	0.92	0.89	0.08	1.00	0.07	0.81	0.06
Ccl2	1.11	1.13	1.19	1.20	0.60	0.80	0.82	1.06	0.03	1.16	0.02	0.82	0.10
Ccr2	2.49	1.67	1.10	0.61	1.66	1.63	1.07	1.25	0.88	1.47	0.40	1.40	0.15
Ctss	2.81	2.40	3.60	1.64	2.39	2.24	1.68	1.51	0.22	2.61	0.41	1.95	0.21
Egfr	1.90	1.34	1.52	0.81	1.47	1.43	0.77	1.18	0.55	1.39	0.23	1.21	0.16
Gabbr1	0.70	1.04	0.82	1.01	0.95	0.90	0.88	0.83	0.99	0.89	0.08	0.89	0.02
Gabra5	1.47	1.42	1.45	1.54	1.35	1.23	0.95	1.44	0.12	1.47	0.03	1.24	0.11
Gad2	#VALUE!	#VALUE!	#VALUE!	#VALUE!	#VALUE!	#VALUE!	#VALUE!	#VALUE!	#VALUE!	#VALUE!	#VALUE!	#VALUE!	#VALUE!
Gal	2.01	2.99	7.93	3.69	1.67	1.61	2.64	2.40	0.21	4.16	1.30	2.08	0.26
Gapdh	0.82	1.09	0.78	1.11	1.09	1.20	0.82	0.91	0.66	0.95	0.09	1.01	0.08

ID	PSL wt1	PSL wt2	PSL wt3	PSL wt4	PSL cko1	PSL cko2	PSL cko3	PSL cko4	p	wt average	wt sem	ko average	ko sem
Gch1	1.40	1.35	1.27	1.12	1.20	0.57	0.93	1.23	0.14	1.29	0.06	0.98	0.15
Gfap	2.83	2.63	4.35	2.22	1.66	0.43	0.97	1.43	0.02	3.01	0.47	1.12	0.27
Hcn2	0.85	0.98	0.81	0.93	1.12	0.98	1.06	0.66	0.62	0.89	0.04	0.95	0.10
Hprt	1.14	1.09	1.19	0.89	1.05	1.01	1.18	1.00	0.87	1.08	0.07	1.06	0.04
Kcns1	0.63	0.68	0.61	0.68	0.88	0.70	0.81	0.58	0.26	0.65	0.02	0.74	0.07
Ngf	0.52	0.71	0.69	0.68	0.59	0.68	0.47	0.70	0.57	0.65	0.04	0.61	0.05
Ngfr	0.93	0.99	0.77	1.22	1.24	1.12	1.04	1.05	0.26	0.98	0.09	1.11	0.05
Nos1	0.86	1.33	1.14	1.14	1.38	1.30	1.44	0.93	0.37	1.12	0.10	1.26	0.11
Npy	215.93	202.48	384.07	180.23	89.81	77.57	85.75	86.19	0.04	245.68	46.72	84.83	2.59
Ntrk1	0.73	1.10	0.80	0.95	0.85	0.78	0.71	0.64	0.17	0.89	0.08	0.74	0.05
Ntrk2	1.06	1.19	0.92	1.06	1.25	1.08	1.01	0.91	0.96	1.06	0.06	1.06	0.07
Ntrk3	1.46	1.46	1.28	1.71	1.93	1.27	1.53	1.10	0.93	1.48	0.09	1.46	0.18
Oprm1	#VALUE!	#VALUE!	#VALUE!	#VALUE!	#VALUE!	#VALUE!	#VALUE!	#VALUE!	#VALUE!	#VALUE!	#VALUE!	#VALUE!	#VALUE!
P2rx3	0.53	1.11	0.79	1.01	1.03	0.96	0.95	0.85	0.55	0.86	0.13	0.95	0.04
P2rx4	1.03	1.17	0.93	1.06	1.31	0.98	1.16	0.91	0.71	1.05	0.05	1.09	0.09
Pdyn	#VALUE!	2.50	0.48	#VALUE!	#VALUE!	1.19	#VALUE!	0.20	#VALUE!	#VALUE!	#VALUE!	#VALUE!	#VALUE!
Ptgs2	1.32	0.70	0.31	0.31	0.78	0.97	0.41	0.22	0.83	0.66	0.24	0.60	0.17

ID	PSL wt1	PSL wt2	PSL wt3	PSL wt4	PSL cko1	PSL cko2	PSL cko3	PSL cko4	p	wt average	wt sem	ko average	ko sem
Reg3b	#VALUE!	#VALUE!	#VALUE!	#VALUE!	#VALUE!	#VALUE!	#VALUE!	#VALUE!	#VALUE!	#VALUE!	#VALUE!	#VALUE!	#VALUE!
Rest	1.68	1.30	1.41	1.05	1.03	1.14	1.00	1.01	0.09	1.36	0.13	1.04	0.03
Scn10a	0.50	1.20	0.74	1.20	0.65	0.69	0.62	0.73	0.27	0.91	0.17	0.67	0.02
Scn11a	0.42	1.15	0.63	1.12	0.74	0.84	0.80	0.65	0.71	0.83	0.18	0.76	0.04
Scn3a	0.84	1.93	1.35	2.57	2.01	0.90	1.63	1.75	0.83	1.67	0.37	1.58	0.24
Scn9a	0.78	1.02	0.95	1.26	1.32	0.67	1.29	1.11	0.62	1.00	0.10	1.10	0.15
Sgk1	0.81	0.44	0.66	0.37	0.97	0.48	0.59	0.60	0.58	0.57	0.10	0.66	0.11
Slco1a6	#VALUE!	#VALUE!	#VALUE!	#VALUE!	#VALUE!	#VALUE!	#VALUE!	#VALUE!	#VALUE!	#VALUE!	#VALUE!	#VALUE!	#VALUE!
Sst	0.27	0.73	0.71	0.76	1.41	2.01	1.80	1.43	0.00	0.62	0.12	1.66	0.15
Tac1	0.84	1.36	0.97	1.19	1.19	1.18	1.14	1.08	0.67	1.09	0.11	1.15	0.02
Tacr1	#VALUE!	0.78	0.53	1.16	0.46	0.67	0.36	0.81	#VALUE!	#VALUE!	#VALUE!	0.58	0.10
Trpa1	0.50	0.74	0.68	1.04	0.53	0.44	0.65	0.89	0.49	0.74	0.11	0.63	0.10
Trpv1	0.95	1.51	1.23	1.38	0.94	1.04	0.90	0.96	0.08	1.27	0.12	0.96	0.03
Vgf	1.24	1.64	2.07	1.76	2.19	1.19	1.88	2.44	0.47	1.68	0.17	1.93	0.27
Vip	#VALUE!	#VALUE!	#VALUE!	#VALUE!	#VALUE!	#VALUE!	#VALUE!	#VALUE!	#VALUE!	#VALUE!	#VALUE!	#VALUE!	#VALUE!

Table 16 - HDAC4^{Adv} naive gene expression (Study 3)

ID	wt 1	wt 2	wt 3	wt 4	cKO 1	cKO 2	cKO 3	cKO 4	p	wt average	wt sem	ko average	ko sem
Adcyap	#VALUE!	#VALUE!	#VALUE!	#VALUE!	#VALUE!	#VALUE!	#VALUE!	#VALUE!	#VALUE!	#VALUE!	#VALUE!	#VALUE!	#VALUE!
Aif1	1.38	0.52	1.13	0.97	1.62	0.65	1.75	1.85	0.22	1.00	0.18	1.47	0.28
Atf3	0.46	0.87	0.48	2.19	0.78	0.58	1.57	4.44	0.44	1.00	0.41	1.84	0.89
Bdnf	0.56	1.15	1.24	1.06	1.43	0.88	3.08	2.95	0.14	1.00	0.15	2.08	0.55
Cacna2d1	1.15	1.15	1.04	0.66	1.60	1.50	1.67	1.43	0.01	1.00	0.12	1.55	0.05
Calca	0.92	0.83	1.05	1.20	1.40	0.71	1.43	1.17	0.39	1.00	0.08	1.18	0.17
Ccl2	#VALUE!	#VALUE!	#VALUE!	#VALUE!	#VALUE!	#VALUE!	#VALUE!	#VALUE!	#VALUE!	#VALUE!	#VALUE!	#VALUE!	#VALUE!
Ccr2	#VALUE!	#VALUE!	#VALUE!	#VALUE!	#VALUE!	#VALUE!	#VALUE!	#VALUE!	#VALUE!	#VALUE!	#VALUE!	#VALUE!	#VALUE!
Ctss	2.08	0.81	0.28	0.83	1.02	0.74	0.59	0.74	0.60	1.00	0.38	0.77	0.09
Egfr	1.20	1.43	0.79	0.58	1.62	1.20	0.63	0.44	0.94	1.00	0.19	0.97	0.27
Gabbr1	1.07	1.25	1.06	0.62	1.12	1.03	1.17	0.96	0.64	1.00	0.13	1.07	0.05
Gabra5	#VALUE!	#VALUE!	#VALUE!	#VALUE!	#VALUE!	#VALUE!	#VALUE!	#VALUE!	#VALUE!	#VALUE!	#VALUE!	#VALUE!	#VALUE!
Gad2	0.89	1.10	0.99	1.03	1.43	0.96	1.45	1.45	0.07	1.00	0.04	1.32	0.12
Gal	1.33	1.25	0.89	0.53	1.43	0.40	1.01	0.29	0.53	1.00	0.18	0.78	0.27
Gapdh	1.12	1.04	0.93	0.92	1.24	1.18	1.09	0.99	0.14	1.00	0.05	1.12	0.05
Gch1	1.07	1.12	0.88	0.93	1.39	1.21	0.86	1.08	0.33	1.00	0.05	1.14	0.11

ID	wt 1	wt 2	wt 3	wt 4	cKO 1	cKO 2	cKO 3	cKO 4	p	wt average	wt sem	ko average	ko sem
Gfap	#VALUE!	#VALUE!	#VALUE!	#VALUE!	#VALUE!	#VALUE!	#VALUE!	#VALUE!	#VALUE!	#VALUE!	#VALUE!	#VALUE!	#VALUE!
Hcn2	1.23	0.81	1.00	0.96	0.99	1.00	1.03	0.99	0.98	1.00	0.09	1.00	0.01
Hprt	0.91	0.97	1.06	1.06	0.83	0.86	0.93	1.00	0.13	1.00	0.04	0.91	0.04
Kcns1	1.07	1.06	1.03	0.84	1.53	1.13	1.22	1.12	0.07	1.00	0.05	1.25	0.10
Ngf	0.68	0.79	1.31	1.23	1.03	0.80	0.83	0.98	0.62	1.00	0.16	0.91	0.06
Ngfr	1.17	0.80	1.02	1.01	1.74	0.78	1.20	1.12	0.38	1.00	0.08	1.21	0.20
Nos1	0.90	1.20	0.94	0.96	1.03	1.08	1.44	0.79	0.60	1.00	0.07	1.08	0.13
Npy	#VALUE!	#VALUE!	#VALUE!	#VALUE!	#VALUE!	#VALUE!	#VALUE!	#VALUE!	#VALUE!	#VALUE!	#VALUE!	#VALUE!	#VALUE!
Ntrk1	1.08	0.84	1.02	1.05	1.23	1.16	1.09	1.14	0.06	1.00	0.06	1.15	0.03
Ntrk2	1.13	0.86	1.15	0.86	1.07	0.82	1.37	1.02	0.64	1.00	0.08	1.07	0.11
Ntrk3	0.92	1.25	1.10	0.72	1.55	0.96	1.36	1.14	0.20	1.00	0.12	1.25	0.13
Oprm1	1.13	1.18	0.94	0.75	1.96	1.34	2.07	1.62	0.01	1.00	0.10	1.75	0.17
P2rx3	0.87	1.16	1.04	0.92	1.45	1.13	1.38	1.24	0.02	1.00	0.06	1.30	0.07
P2rx4	1.02	1.16	0.92	0.89	2.02	0.88	1.01	0.75	0.62	1.00	0.06	1.16	0.29
Pdyn	1.14	1.54	0.73	0.60	0.71	0.88	1.02	0.77	0.53	1.00	0.21	0.84	0.07
Ptgs2	#VALUE!	#VALUE!	#VALUE!	#VALUE!	#VALUE!	#VALUE!	#VALUE!	#VALUE!	#VALUE!	#VALUE!	#VALUE!	#VALUE!	#VALUE!
Reg3b	0.91	1.19	1.03	0.88	1.23	0.85	1.34	0.83	0.69	1.00	0.07	1.06	0.13

ID	wt 1	wt 2	wt 3	wt 4	cKO 1	cKO 2	cKO 3	cKO 4	p	wt average	wt sem	ko average	ko sem
Rest	0.86	1.04	1.15	0.95	2.10	0.74	1.31	1.37	0.27	1.00	0.06	1.38	0.28
Scn10a	1.34	0.90	0.96	0.80	0.93	0.73	0.99	0.80	0.35	1.00	0.12	0.86	0.06
Scn11a	1.04	0.91	1.18	0.86	0.64	0.62	1.21	0.91	0.37	1.00	0.07	0.85	0.14
Scn3a	0.84	1.06	1.59	0.52	2.50	0.81	1.61	0.39	0.56	1.00	0.22	1.33	0.47
Scn9a	1.12	1.21	1.13	0.54	1.45	1.17	1.60	1.02	0.18	1.00	0.16	1.31	0.13
Sgk1	0.56	0.42	1.62	1.40	1.60	0.93	0.98	1.36	0.55	1.00	0.30	1.22	0.16
Slco1a6	#VALUE!	#VALUE!	#VALUE!	#VALUE!	#VALUE!	#VALUE!	#VALUE!	#VALUE!	#VALUE!	#VALUE!	#VALUE!	#VALUE!	#VALUE!
Sst	0.87	1.31	0.87	0.95	0.36	0.47	0.89	2.68	0.86	1.00	0.11	1.10	0.54
Tac1	1.31	1.17	0.71	0.82	0.96	0.74	1.17	0.87	0.72	1.00	0.14	0.94	0.09
Tacr1	0.85	1.13	1.21	0.81	2.71	0.92	1.43	1.11	0.27	1.00	0.10	1.54	0.40
Trpa1	1.07	1.08	1.08	0.77	0.77	0.59	0.83	0.58	0.02	1.00	0.08	0.69	0.06
Trpv1	1.32	0.88	0.76	1.04	1.15	0.90	1.23	0.94	0.72	1.00	0.12	1.06	0.08
Vgf	0.66	1.06	0.82	1.46	1.39	1.43	1.42	1.67	0.07	1.00	0.17	1.48	0.07
Vip	0.34	2.13	0.90	0.63	3.76	1.34	3.47	2.78	0.04	1.00	0.39	2.84	0.54

Table 17 - HDAC4^{Adv} 24 hours after sciatic nerve transection (Study 3). Values are normalized to wildtype naïve controls.

ID	wt i 1	wt i 2	wt i 3	wt i 4	ko i 1	ko i 2	ko i 3	ko i 4	p	wt average	wt sem	ko average	ko sem
Adcyap	#VALUE!	#VALUE!	#VALUE!	#VALUE!	#VALUE!	#VALUE!	#VALUE!	#VALUE!	#VALUE!	#VALUE!	#VALUE!	#VALUE!	#VALUE!
Aif1	2.57	3.17	1.57	2.29	4.89	1.82	3.53	4.26	0.17	2.40	0.33	3.63	0.66
Atf3	18.18	18.70	31.61	50.15	22.15	23.44	51.51	73.87	0.41	29.66	7.50	42.74	12.39
Bdnf	1.26	1.20	2.12	3.25	2.78	2.88	3.14	3.36	0.11	1.96	0.48	3.04	0.13
Cacna2d1	1.63	1.60	1.19	1.93	2.26	1.98	2.35	2.25	0.02	1.59	0.15	2.21	0.08
Calca	1.13	1.42	1.26	1.37	1.10	0.87	0.91	1.03	0.01	1.30	0.06	0.98	0.05
Ccl2	#VALUE!	#VALUE!	#VALUE!	#VALUE!	#VALUE!	#VALUE!	#VALUE!	#VALUE!	#VALUE!	#VALUE!	#VALUE!	#VALUE!	#VALUE!
Ccr2	#VALUE!	#VALUE!	#VALUE!	#VALUE!	#VALUE!	#VALUE!	#VALUE!	#VALUE!	#VALUE!	#VALUE!	#VALUE!	#VALUE!	#VALUE!
Ctss	4.34	3.76	1.15	2.17	2.21	4.41	2.45	3.33	0.79	2.85	0.73	3.10	0.50
Egfr	1.19	1.12	1.07	1.34	1.40	1.37	0.91	1.49	0.46	1.18	0.06	1.29	0.13
Gabbr1	1.30	2.14	1.08	1.82	1.56	1.38	1.26	1.24	0.42	1.59	0.24	1.36	0.07
Gabra5	#VALUE!	#VALUE!	#VALUE!	#VALUE!	#VALUE!	#VALUE!	#VALUE!	#VALUE!	#VALUE!	#VALUE!	#VALUE!	#VALUE!	#VALUE!
Gad2	3.23	3.90	3.67	5.79	5.59	6.11	6.15	7.16	0.02	4.15	0.56	6.25	0.33
Gal	1.61	1.58	0.59	1.51	1.99	0.95	1.05	1.20	0.94	1.32	0.24	1.30	0.24
Gapdh	1.09	1.15	1.01	1.24	1.23	1.25	0.98	1.00	0.93	1.12	0.05	1.11	0.07

ID	wt i 1	wt i 2	wt i 3	wt i 4	ko i 1	ko i 2	ko i 3	ko i 4	p	wt average	wt sem	ko average	ko sem
Gch1	0.57	0.98	0.80	0.62	0.78	0.81	0.37	0.77	0.67	0.74	0.09	0.68	0.10
Gfap	#VALUE!	#VALUE!	#VALUE!	#VALUE!	#VALUE!	#VALUE!	#VALUE!	#VALUE!	#VALUE!	#VALUE!	#VALUE!	#VALUE!	#VALUE!
Hcn2	0.89	0.72	0.95	0.71	0.91	0.68	0.92	0.92	0.66	0.82	0.06	0.86	0.06
Hprt	0.92	0.88	0.98	0.83	0.84	0.82	1.01	1.00	0.86	0.91	0.03	0.92	0.05
Kcns1	1.05	1.15	0.89	1.20	1.25	1.19	0.95	1.15	0.53	1.07	0.07	1.14	0.06
Ngf	1.92	1.46	1.56	1.99	3.02	2.48	2.04	2.28	0.03	1.73	0.13	2.45	0.21
Ngfr	1.00	0.95	1.06	0.85	0.99	0.78	0.97	0.95	0.54	0.97	0.04	0.93	0.05
Nos1	1.02	1.35	0.78	0.92	1.34	0.63	1.26	0.80	0.96	1.02	0.12	1.01	0.17
Npy	#VALUE!	#VALUE!	#VALUE!	#VALUE!	#VALUE!	#VALUE!	#VALUE!	#VALUE!	#VALUE!	#VALUE!	#VALUE!	#VALUE!	#VALUE!
Ntrk1	1.02	1.27	0.88	0.99	1.02	1.06	0.69	1.08	0.55	1.04	0.08	0.96	0.09
Ntrk2	0.88	0.84	0.88	0.87	1.03	0.82	1.11	0.98	0.15	0.87	0.01	0.98	0.06
Ntrk3	0.92	1.04	1.02	1.17	1.03	0.76	0.99	1.02	0.35	1.04	0.05	0.95	0.06
Oprm1	1.25	1.06	0.94	0.92	1.26	0.83	1.20	1.29	0.46	1.04	0.08	1.15	0.11
P2rx3	1.17	1.42	0.96	1.47	1.20	1.07	1.18	1.30	0.63	1.25	0.12	1.19	0.05
P2rx4	1.12	1.49	1.02	0.87	1.02	1.00	0.73	0.98	0.25	1.13	0.13	0.93	0.07
Pdyn	0.76	1.32	0.73	0.72	0.60	0.70	0.67	0.84	0.31	0.88	0.14	0.70	0.05
Ptgs2	#VALUE!	#VALUE!	#VALUE!	#VALUE!	#VALUE!	#VALUE!	#VALUE!	#VALUE!	#VALUE!	#VALUE!	#VALUE!	#VALUE!	#VALUE!

ID	wt i 1	wt i 2	wt i 3	wt i 4	ko i 1	ko i 2	ko i 3	ko i 4	p	wt average	wt sem	ko average	ko sem
Reg3b	1.67	1.24	0.79	0.85	0.94	1.59	1.02	1.35	0.74	1.14	0.20	1.23	0.15
Rest	1.80	1.30	1.11	1.88	1.74	1.38	1.19	1.44	0.71	1.52	0.19	1.44	0.11
Scn10a	0.83	1.06	0.84	0.87	0.71	0.67	0.62	0.51	0.01	0.90	0.05	0.63	0.04
Scn11a	0.66	0.94	1.02	1.35	0.65	0.62	0.76	0.75	0.12	0.99	0.14	0.69	0.03
Scn3a	1.96	1.36	0.93	1.75	1.35	0.93	1.92	0.71	0.47	1.50	0.23	1.23	0.27
Scn9a	1.11	0.92	1.11	1.02	0.97	0.91	0.96	0.85	0.08	1.04	0.05	0.92	0.03
Sgk1	0.74	0.42	1.12	1.23	0.88	1.06	0.58	1.51	0.64	0.88	0.18	1.01	0.20
Slco1a6	#VALUE!	#VALUE!	#VALUE!	#VALUE!	#VALUE!	#VALUE!	#VALUE!	#VALUE!	#VALUE!	#VALUE!	#VALUE!	#VALUE!	#VALUE!
Sst	3.90	4.31	1.73	3.10	5.96	5.29	13.75	15.21	0.07	3.26	0.57	10.05	2.58
Tac1	1.06	0.83	0.82	1.13	0.97	0.85	1.08	0.76	0.70	0.96	0.08	0.92	0.07
Tacr1	1.61	1.25	0.83	1.07	1.76	0.82	1.06	1.22	0.92	1.19	0.16	1.22	0.20
Trpa1	0.98	1.16	0.98	1.31	0.95	0.75	0.71	0.69	0.02	1.10	0.08	0.78	0.06
Trpv1	1.29	0.92	1.29	0.99	1.30	1.12	1.08	0.90	0.87	1.12	0.10	1.10	0.08
Vgf	3.94	2.86	2.37	2.52	4.44	4.52	2.68	3.54	0.17	2.92	0.35	3.79	0.43
Vip	1.37	1.90	1.83	2.31	2.72	2.89	3.14	2.10	0.03	1.85	0.19	2.71	0.22

Table 18 - HDAC4^{Adv} D15 CFA gene expression (Study 4)

ID	wt 1	wt 2	wt 3	wt 4	ko 1	ko 2	ko 3	ko 4	p	wt average	wt sem	ko average	ko sem
Adcyap	#VALUE!	#VALUE!	#VALUE!	#VALUE!	#VALUE!	#VALUE!	#VALUE!	#VALUE!	#VALUE!	#VALUE!	#VALUE!	#VALUE!	#VALUE!
Aif1	1.18	1.09	0.97	0.75	3.00	0.68	1.09	1.47	0.35	1.00	0.09	1.56	0.51
Atf3	0.68	0.98	1.14	1.20	0.69	0.33	0.32	0.80	0.03	1.00	0.12	0.54	0.12
Bdnf	1.07	0.81	1.24	0.88	1.70	0.71	1.10	0.49	0.99	1.00	0.09	1.00	0.26
Cacna2d1	0.81	0.99	1.29	0.91	0.94	1.09	0.91	0.95	0.84	1.00	0.10	0.98	0.04
Calca	0.93	0.87	1.06	1.13	0.23	0.23	0.18	0.23	0.00	1.00	0.06	0.22	0.01
Ccl2	#VALUE!	#VALUE!	#VALUE!	#VALUE!	#VALUE!	#VALUE!	#VALUE!	#VALUE!	#VALUE!	#VALUE!	#VALUE!	#VALUE!	#VALUE!
Ccr2	0.80	1.20	1.17	0.83	1.95	#VALUE!	#VALUE!	#VALUE!	#VALUE!	1.00	0.11	#VALUE!	#VALUE!
Ctss	0.68	1.25	1.01	1.05	0.27	0.43	0.62	0.13	0.01	1.00	0.12	0.36	0.10
Egfr	0.81	1.44	1.11	0.64	#VALUE!	#VALUE!	0.16	0.12	#VALUE!	1.00	0.18	#VALUE!	#VALUE!
Gabbr1	1.03	0.87	1.15	0.96	1.18	1.61	1.70	1.17	0.05	1.00	0.06	1.42	0.14
Gabra5	#VALUE!	#VALUE!	#VALUE!	#VALUE!	#VALUE!	#VALUE!	#VALUE!	#VALUE!	#VALUE!	#VALUE!	#VALUE!	#VALUE!	#VALUE!
Gad2	0.83	0.98	1.14	1.04	0.54	0.67	0.61	1.00	0.06	1.00	0.06	0.71	0.10
Gal	0.85	1.47	0.92	0.75	1.14	1.57	1.61	2.67	0.10	1.00	0.16	1.75	0.33
Gapdh	0.96	0.91	1.07	1.05	0.86	0.72	1.00	0.80	0.08	1.00	0.04	0.85	0.06
Gch1	1.17	0.81	1.05	0.97	0.46	0.41	0.19	0.54	0.00	1.00	0.08	0.40	0.07

ID	wt 1	wt 2	wt 3	wt 4	ko 1	ko 2	ko 3	ko 4	p	wt average	wt sem	ko average	ko sem
Gfap	0.41	0.94	1.10	1.56	#VALUE!	#VALUE!	0.59	0.29	#VALUE!	1.00	0.24	#VALUE!	#VALUE!
Hcn2	1.19	0.89	0.99	0.93	0.53	0.48	0.66	0.74	0.00	1.00	0.07	0.60	0.06
Hprt	1.03	1.07	0.94	0.96	1.16	1.34	1.02	1.22	0.06	1.00	0.03	1.18	0.07
Kcns1	0.90	1.04	0.90	1.16	0.48	0.54	0.44	0.51	0.00	1.00	0.06	0.49	0.02
Ngf	0.92	1.14	0.92	1.03	0.66	1.03	0.17	0.77	0.15	1.00	0.05	0.66	0.18
Ngfr	0.77	0.82	1.46	0.95	1.65	1.23	1.27	1.23	0.13	1.00	0.16	1.34	0.10
Nos1	0.97	0.74	0.98	1.32	0.75	0.33	0.31	0.67	0.03	1.00	0.12	0.51	0.11
Npy	#VALUE!	#VALUE!	#VALUE!	#VALUE!	#VALUE!	#VALUE!	#VALUE!	#VALUE!	#VALUE!	#VALUE!	#VALUE!	#VALUE!	#VALUE!
Ntrk1	0.95	0.93	1.07	1.06	0.32	0.32	0.25	0.40	0.00	1.00	0.04	0.32	0.03
Ntrk2	1.23	0.85	0.99	0.93	2.66	1.63	2.29	1.43	0.03	1.00	0.08	2.00	0.29
Ntrk3	0.98	0.99	1.06	0.97	1.01	0.77	0.95	0.92	0.19	1.00	0.02	0.91	0.05
Oprm1	0.78	1.05	1.11	1.06	1.77	1.72	1.28	1.37	0.01	1.00	0.07	1.54	0.12
P2rx3	0.85	0.89	1.04	1.22	0.49	0.41	0.34	0.48	0.00	1.00	0.08	0.43	0.04
P2rx4	1.08	0.83	1.01	1.08	0.70	0.37	0.59	0.63	0.00	1.00	0.06	0.57	0.07
Pdyn	0.79	1.24	0.85	1.12	2.27	2.95	2.76	2.07	0.00	1.00	0.11	2.51	0.21
Ptgs2	0.70	1.85	0.99	0.46	#VALUE!	3.41	1.91	1.91	#VALUE!	1.00	0.30	#VALUE!	#VALUE!
Reg3b	0.84	1.24	1.00	0.92	0.73	0.14	0.44	0.76	0.04	1.00	0.09	0.52	0.15

ID	wt 1	wt 2	wt 3	wt 4	ko 1	ko 2	ko 3	ko 4	p	wt average	wt sem	ko average	ko sem
Rest	2.61	0.62	0.46	0.31	0.24	0.08	0.01	0.23	0.21	1.00	0.54	0.14	0.06
Scn10a	0.96	0.86	1.19	0.99	1.09	0.76	0.68	0.68	0.15	1.00	0.07	0.80	0.10
Scn11a	0.79	1.03	0.96	1.21	1.05	0.72	0.71	0.77	0.17	1.00	0.09	0.81	0.08
Scn3a	0.94	1.35	1.12	0.59	0.74	0.32	0.06	0.10	0.02	1.00	0.16	0.30	0.16
Scn9a	0.75	0.86	1.36	1.02	2.09	1.34	1.89	1.48	0.02	1.00	0.13	1.70	0.18
Sgk1	0.98	1.31	0.91	0.80	0.87	1.00	0.60	0.88	0.29	1.00	0.11	0.84	0.08
Slco1a6	0.65	0.68	1.65	1.02	2.61	3.89	2.22	1.66	0.03	1.00	0.23	2.60	0.47
Sst	1.22	0.91	1.13	0.74	6.19	10.59	#VALUE!	3.14	#VALUE!	1.00	0.11	#VALUE!	#VALUE!
Tac1	0.72	0.98	1.25	1.04	0.85	0.73	0.73	0.98	0.22	1.00	0.11	0.82	0.06
Tacr1	0.70	1.73	1.04	0.53	0.81	0.47	0.32	0.73	0.22	1.00	0.26	0.58	0.11
Trpa1	0.87	1.10	1.08	0.94	0.31	0.50	0.28	0.46	0.00	1.00	0.06	0.39	0.06
Trpv1	0.98	0.97	0.95	1.10	0.44	0.45	0.34	0.52	0.00	1.00	0.03	0.44	0.04
Vgf	1.13	0.94	0.98	0.95	#VALUE!	0.12	0.15	0.25	#VALUE!	1.00	0.04	#VALUE!	#VALUE!
Vip	1.08	0.88	0.94	1.09	0.37	0.33	0.89	1.35	0.35	1.00	0.05	0.73	0.24